Challenging mysteries of the Universe with gravity beyond general relativity

Paul Martens

Doctoral thesis, July the 31st, 2023

京都大学
KYOTO UNIVERSITY

YITP
YUKAWA INSTITUTE FOR
THEORETICAL PHYSICS

CGPQI
Center for Gravitational Physics and
Quantum Information
Yukawa Institute for Theoretical Physics, Kyoto University

Abstract

While general relativity (GR) has certainly proven a formidable framework via which we understand the past history and current dynamics of our Universe, modern observations are also suggesting there could exist a more complete theory of gravity. First, GR is infamously non-renormalizable, and there is currently no accepted extension of GR in the high energy regimes. Furthermore, modern cosmology faces the mysteries of dark matter as well as dark energy, both of which could be framed as limitation of GR. Last but not least, probing beyond GR also helps us gain a deeper insight into the theory itself.

In a first part, we briefly review GR along the common tools invoked in cosmology, before painting an overview of some modified gravity theories, with a focus on the ones used thereafter. This work indeed aims at demonstrating how these alternative theories can help us answer the aforementioned puzzles.

In a second part, we first establish the Wheeler-DeWitt equation in the formalism of Hořava-Lifshitz (HL) gravity in $d + 1$ dimensions. We also show that the DeWitt wave function for tensor perturbation is indeed well-defined around the classical Big Bang singularity, unlike GR. HL gravity is a recent quantum gravity candidate that aims at addressing the non-renormalizability of GR by treating time and space separately at higher energies. Incidentally, this theory also incorporates dark matter as an integration constant. Subsequently, we consider a previously proposed relaxation mechanism for the cosmological constant (CC) that provides a dynamical explanation to the small value of the CC. While this would address the CC problem, and thus dark energy as well, the process simultaneously empties the Universe of its content. Using a Horndeski class model, we then build a proof-of-concept model that incorporates a reheating phase to resolve this last issue.

In a last part, the focus is put on a type-II minimally modified gravity denominated as "VCDM". Similarly to HL gravity, this class of theory is not invariant under four-dimensional diffeomorphism as time is treated as physically different than space, and, like GR, only propagates two degrees of freedom. We start by numerically investigating the collapse of a scalar field in VCDM and verify the sane creation of an apparent horizon, thusly bringing an extra validation of the theory. Finally, we construct a bouncing Universe scenario by exploiting the specificities of VCDM. Such a scenario has the advantage of avoiding any initial singularity altogether, but has often proven difficult to implement in a stable way. The setup built here satisfies the near scale invariant scalar perturbation power spectrum and the small tensor-to-scalar ratio. Additionally, a possibly observable signature of the model is found in its blue-tilted tensor perturbation power spectrum.

Throughout this work, all analytical computations are supplemented by numerical simulations that produce a qualitative and perhaps more instinctive understanding of this work.

Acknowledgements

I wish to express my most sincere and deepest gratitude to my advisor, Shinji Mukohyama, who has guided me throughout this thesis and always fully supported me whatever path I followed. I must extend my thanks to all the colleagues from the Yukawa Institute of Theoretical Physics and elsewhere, with whom I may have collaborated, but whose company I have always enjoyed. Their smiles, jokes and ideas have made my stay and research all the better. In particular, I would like to thank Antonio De Felice for always taking the time to answer to my questions.

I am also very appreciative of all the researchers who took the time to welcome me both in Japan and abroad. If not for their motivating exchanges and sharing their interesting perspectives, my motivation to learn more about so many aspects of physics would surely not be as strong as today. Truly, Kyoto has proven to be a fantastic opportunity for me to learn a lot and grew as a researcher.

But more than an academic experience, Kyoto has also proven to be a formidable human adventure. Friends at my dormitory, my shared house, from Japanese language courses and other horizons have certainly enlightened my days in ways impossible otherwise. My gratitude also goes to the support given by my friends abroad, particularly of Michele Oliosi, and by all my family. I was very lucky and appreciative of having both my parents and my sister coming here in Japan. And I would like to also thank my kind, loving and patient girlfriend, Wenfeng, who has unconditionnaly supported me.

Finally, this thesis was made possible thanks to my collaborators Ryo Namba, Alexander Ganz, Hiroki Matsui and Atabak Fathe Jalali. While this text does not exploit our common work, I am equally grateful to Francesco Di Fillipo. Without the help of each of them, this work and all that I learned would certainly have been much diminished. Thanks also to Josef Seitz and my advisor for helping me adjust this thesis until the very end.

I admit I find difficult to encapsulate in such a short text the expression of my gratitude. There may be no words, but “thank you”. I am wishing everyone the best.

Contents

List of Figures

List of Tables

Acronyms

ADM Arnowitt, Deser and Misner

AH apparent horizon

BH black hole

CC cosmological constant

CMB cosmic microwave background

DE dark energy

DM dark matter

DoF degrees of freedom

EoM equations of motion

FLRW Friedmann-Lemaître-Robertson-Walker

GR general relativity

GWs gravitational waves

HL Hořava-Lifshitz

IR infrared

MMG minimally modified gravity

MTBG minimal theory of bigravity

NEC null energy condition

RG renormalization group

UV ultraviolet

WDW Wheeler-DeWitt

Introduction

Physics starts with the familiar. The mass of an apple, the speed of a falling apple, the temperature of an apple or an apple rolling down a hill are all concepts that are as well-known to Newton as they are to all. And, through the ages, we learned to model and describe these in rigorous mathematical terms. In so doing, physics expanded into new territories. As of today, while some familiar phenomena still require their own formulation, such as the dynamics of sand, many physicists have now trouble to sleep because of other observations, far from life's everyday's scales, observations that bring deeply puzzling mysteries. These apparently come in two flavors. On the one end, considering larger and larger distances, there is realm of astrophysics and cosmology. On the other end, diving into smaller and smaller objects, stands the quantum land and the standard model of particles.

It is fair to say that both fields have undergone revolutionary developments in the XX^{th} century, when their unintuitive yet highly successful frameworks were formulated. In particular, relevant for the present text, gravity, whose dynamics seemed long settled by the inverse square law Newton wrote, was famously reformulated under the *equivalence principle* by Einstein in circa 1916 into what is called *general relativity* [1]. First a curiosity that only accounted for Mercury's perhelion's advance [2], it soon got further comforted when light was observed to be deflected by the Sun's gravitational imprint in the *Eddington experiment* in 1920 [3]. The third test proposed by Einstein at the time, the *redshift* of light, was only observed and confirmed much later, in 1954 [4]. Since the early days of its genesis, general relativity has demonstrated time and time again to be a brilliantly successful framework to talk about gravity. And yet...

At about the same time, the seeds of quantum mechanics also sprouted into the successful framework describing much smaller length scales that is now called the *standard model*. The two formalisms could have remained distant and forever estranged worlds, but, in some peculiar cases, both must somehow cohabite and collaborate. How? By which operation? Quantum theory had established a common procedure —*renormalization*— to regularize its inhabitants. Unfortunately, and now infamously, the approach is unapplicable to general relativity: the latter theory is *non-renormalizable* [5, 6]. While the fault may lie on the side of quantum field theory, the opposite is just as likely. Squaring this circle and matching the two ends into an all-encompassing theory of quantum gravity has proven a formidable challenge, which does not have yet any admitted answer. The most commonly explored path to that aim is probably superstring theory [7, 8, 9, 10], but others are also under consideration, such as loop quantum gravity [11, 12]. A fairly recently proposed path in this field —and one that we shall work with in chapter III— is Hořava-Lifshitz gravity [13], which assumes a fundamental and physical difference between time and space to achieve renormalizability, in principle.

While this issue alone is already a strong enough motivation to explore the landscape beyond general relativity, modern astrophysics has hit on other tenacious mysteries for which a new theory of gravity could be a possible answer. The two main ones are surely *dark matter* and *dark energy*, sometimes bundled together under *dark sector*. This "dark" naturally does not stem from any "dark arts" or mystical fantasies.

Dark matter comes from the significant discrepancy between the observed luminous mass populating our Universe and the gravitating one inferred from the observed dynamics of astrophysical entities [14, 15, 15, 16]. The latter being much larger, the name is logically referring to that non-luminous and unobserved mass. As numerical simulations tend to support, this missing puzzle piece behaves very much as a pressureless fluid; some even say a *superfluid*[17, 18]. It is therefore only natural research turned towards a possible missing particle that the standard model had not accounted for[19]. Yet, one by one, candidates for dark matter seem to be ruled out and the search space is shrinking as ice melts in Kyoto's summer. Some alternative candidates still stand, such as primordial black holes [20], and new, more powerful search experiments are being devised and built as these lines are being written [21, 22]. But could there not be any other explanation? Actually, early on already, it was suggested to modify Newtonian dynamics to account for the first imprints of dark matter on the galaxy's rotational curves [23, 24, 25, 26].

These were abbreviated MOND theories and, while the underlying idea is not entirely ruled out, other candidates have also been devised[27], and dark matter's deep nature still remains more elusive than ever. Nevertheless, unsettling as may be, there remains the very tangible possibility that dark matter survives our scrutiny as a mathematical artifact mimicking matter, but with no apparent manifestation outside of gravity.

Dark energy is a more subtle, yet possibly deeper problem. Again, invisible by itself, dark energy is the conjectured culprit for driving the recently observed acceleration of the Universe's expansion [28, 29]. But its *raison d'être* is fundamentally the underlying cosmological constant problem. The latter reveals itself when physicists coming from high-energy physics confront their computations of the vacuum expectation value (which should amounts to the cosmological constant) with cosmological observations. The two simply do not match. Not only do they not match, they mismatch spectacularly as the value inferred from observations is about sixty orders of magnitude lower. Rarely, if ever, physics has had two values so strongly differ.

It turns out all these three problems, non-renormalizability, dark matter and dark energy, can each be approached by assuming a more general theory of gravity. However, as if these were not enough incentives to investigate whether a more general theory of gravity exists, there is at least one more motivation worth mentioning. Modelling and understanding deviations from general relativity also helps us deconstruct the latter and better understand its numerous ramifications and rich structure. Under the assumptions of Lovelock's theorem, general relativity is the most general theory in four dimensions[30]. Being so tightly constrained also explicitly spells for us which paths can be taken to write a new extended gravity.

In this thesis, we will consider through different and somewhat independent case studies what modifying gravity can allow us to achieve and how it can answer the aforementioned mysteries of the Universe. A probably obvious start would be to consider the simple, yet fruitful formalism of scalar-tensor theories (see section II.1). These take general relativity (the tensor) and add a single field (the scalar). This can be done in different ways, but a frequent starting point would be the class of Horndeski theories [31, 32, 33], and we shall do so in chapter IV. Even more general, one could consider the DHOST[34, 35, 36, 37, 38, 39] or even the U-DHOST framework[40, 41, 42]. Many more exist and are being investigated and exploited everyday. Nowadays, numerical simulations can also be used to explore where a pen and paper get bogged down, and we shall take advantage of these in this work as well.

But all attempt always has to eventually bridge and match with observations to represent an admissible and healthy option to consider. And observations tell us deviations from general relativity, if truly there are any, must be incredibily small[43]. In part because of that, invoking Occam's razor, we shall, in this work, argue for minimalism. General relativity is equipped with only two degrees of freedom. Minimally modified gravity thus aim for no more, despite invoking an auxiliary scalar field. Indeed, this recently formulated class of theories has been trying to do more with no more degree of freedom. Its similarity will be verified in chapter V. And, while there is still much to be developed, its formalism has managed to explore areas inaccessible to general relativity, as a bouncing Universe presented at the end of this work, in chapter VI, shall show.

On a bright last note, we shall end this introductory body by noticing that important observations for gravity are planned in the upcoming years. Since the detection of the long yearned for observations of gravitational waves, physicists have started to unravel that rich and new window on our Universe. Just as the cinema was first silent before acquiring a sound and music, gravitational waves being intrisically associated with gravity appear as a promising mine of information for the years to come. Among the new observatories that should be established in the near future, we find LiteBIRD[44, 45], KAGRA[46] or LISA[47], to name only these. In parallel, more traditionnal channels of observations are also significantly improving as the recent "photo" of a black hole shadow can testify [48]. While general relativity is still proving to extremely difficult champion to dethrone, very wise, or a fool, would be the physicist betting all on the upcoming observations disproving or comforting Einstein's gravity.

Structure This text fundamentally bundles and contextualize into a cohesive whole three works that have now been published [49, 50, 51]. The fourth one, also here included, should hopefully soon be submitted to a journal as well. We also mention that, in parallel to these studies, another work was not included here [52]. It is true that it may have frayed its way in, but, unlike all the other works gathered here, it is not resorting to any modified gravity theories. Nonetheless, while we decided not to include it, any curious reader is naturally welcome to independently consult it.

The current work is articulated around three distinctive parts, each coincidentally split into two chapters. The overall aim is first to contextualize modifiying gravity, then to illustrate possible venues that this opens, before finally focusing on minimally modified gravity theories. We would thus like to

argue that, without ruling out any paths yet, minimally modified gravity theories can represent a potent alternative to general relativity, whose framework, while minimal, has enough room to accommodate phenomena general relativity cannot.

Part I In a first part, we have decided to provide a review of general relativity and its candidate extensions. The first chapter is thus focused on the former, where we start by formally formulating general relativity (section I.1), talking of the deep symmetries it calls, before spelling Lovelock's theorem to lead us into its mathematical definition. We shall also spend time to introduce the ADM decomposition (section I.2). The latter is indeed of particular importance to this work, as the alternative theories of gravity that are subsequently studied hypothesize a physical differentation between time and space, a feature that is conveniently expressed in the ADM formalism. As general relativity would not be of much interest if it had remained just a theory, it is also relevant to recall its predictions under the "cosmological principle" and its implications on the history of the Universe (section I.3). Last but certainly not least in the context of this text, we review three important shortcomings of general relativity (section I.4), namely: the non-renormalizability of general relativity, the cosmological constant problem and dark matter.

Once general relativity and commonly used theoretical tools are well-established, chapter II turns to different possible theories of gravity and attempts to present them in brief terms. The list does not aim to be exhaustive, but simply to give some reference points to the reader. We start with scalar-tensor theories (section II.1) and continue with vector-tensor (section II.2) and scalar-vector-tensor theories (section II.3), before talking of bimetric and massive gravity (section II.4). We mention the maybe more agnostic effective field approach (section II.7), before introducing two of the theories we work with in the subsequent chapters: Hořava-Lifshitz gravity (section II.5) and minimally modified gravity (section II.6).

Part II In the second part, we shall concretely apply, and thus illustrate, two different modified gravity frameworks. Firstly, in chapter III, we work with Hořava-Lifshitz gravity and establish, in its $d+1$ dimensional formalism, the Wheeler-DeWitt equation. Hořava-Lifshitz gravity is a recent attempt to fit the observational constraints that restrict modifying gravity to stay in the vicinity of general relativity. Incidentally, Hořava-Lifshitz also brings along a component that could account as dark matter. After its presentation in section II.5, we establish the working setup in section III.1 and exhibit the Wheeler-DeWitt equation, along with a numerical realization, in the following section III.2.

Secondly, we turn our attention towards the cosmological constant problem that underlies dark energy (chapter IV). A previous mechanism was set up to phenomenologically explain the small value of the cosmological constant by invoking a dynamical relaxation mechanism, but in so doing also emptied the Universe of its content [53, 54]. We therefore here exploit the framework of Horndeski theories, presented in section II.1.3, to build a subsequent reheating phase to repopulate the Universe. We first establish what is the cosmic evolution we wish to achieve (section IV.1) before writing down the perturbative expansion of the model and deriving stability conditions (section IV.2). From there, we explicitly define all the components of the model (section IV.3) and numerically verify its well-behavior (section IV.4).

The first chapter in this part was aiming to find a known result is a new formalism, while the second consisted in building up an early Universe scenario. And now, with these two case studies under our belt, we then turn our attention to minimally modified gravity in the next part, and we will essentially go through two case studies of the same kind.

Part III The third and last part of delves into applications of one particular (type-II) minimally modified gravity theory called VCDM. In the first chapter of the part, we investigate the spherical collapse of a scalar field in VCDM (chapter V). Whether a theory can accommodate a healthy black hole solution or not has often acted as a litmus test to determine the validity of a new theory. We know general relativity does predict the existence of black holes. A new contender for the title of theory of gravity must thus also if not admit a black hole solution, at the very least incorporate some mechanism or entity that closely mimic a black hole.

After this satisfying health check of VCDM, we take advantage of VCDM to go beyond general relativity. Similarly to before, we build an early Universe scenario within the formalism of VCDM. We construct a healthy bouncing Universe scenario (chapter VI). This option implies doing away with any initial cosmic singularity in the distant past. While the idea is not new, its stable implementation has proven to be not impossible, but a challenge. Again, after working out the equations of motion (section VI.1), we carry out a perturbative analysis of the system (section VI.2). This will guide the concrete implementation subsequently presented and finally numerically supported (section VI.3).

This brings us to the end of this work. In a last chapter, chapter VII, we conclude with a brief summary of the achievements given in this text and a discussion of their importance and possible future expansions. Some appendices are collected afterwards, before the list of references.

Conventions and notations We hereafter list some of the conventions and notations we shall adopt in this text.

- The metric has the signature $(-,+,+,+)$.
- We adopt natural units, where both the speed of light c and the reduced Planck constant $\hbar$ are set to 1, *i.e.* $c = \hbar = 1$.
- Unless explicitly stated otherwise we adopt Einstein's convention of summing over repeated indices. That is to say that an expression such as: $A_i B_i$ would be implicitly strictly equivalent to writing $\sum_i A_i B_i$.
- Spacetime indices are written using greek characters (*e.g.* μ, ν, ρ, σ,...) and spatial only indices are written using latin characters (*e.g.* i, j, k, ℓ,...).
- We recall that the reduced Planck mass $M_{\rm Pl}$ is related to Newton's gravitational constant G by the relation
$$M_{\rm Pl}^2 = \frac{1}{8\pi G} \,. \tag{1}$$

General relativity and beyond

Chapter I

Gravity in general relativity

We shall start with a chapter that gives a short —but helpful— review of *general relativity* (GR), along the recall of well-known results and common manipulations. This will enable us to clearly frame the mathematical apparatus that is exploited in the subsequent chapters and allow us to refer to it whenever needed. Shall any further interest arise, we also indicate for the more curious readers thorough reviews of the topics discussed in this text. In so assuming minimal knowledge of the reader, we hope to ease the reading and understanding of the current the work. However, we assume a working knowledge of the mathematical foundations of GR

I.1 Formulation of General relativity

As a first and essential stepping stone, this section naturally formulates GR. While most of the work subsequently presented will stray away from it, GR today probably represents the central pillar in cosmology around which research is carried on, and the results of this text are no exceptions. It is not to say that GR is the final theory of gravitation: modern cosmological observations do show its predictions are insufficient to account for *e.g. dark energy* (DE) and *dark matter* (DM). After giving its mathematical expression in this section I.1, we briefly review some of its predictions in section I.3. Finally, we list some of the main mysteries yet unsolved that GR alone seems unable to elucidate in section I.4.

I.1.1 Symmetries

Often, enunciating the symmetries a theory must respect allows to pin down in part or in full the underlying theory itself. It is again the case for GR through Lovelock's theorem, given in section I.1.2.

That is however not the initial path Einstein followed when formulating GR. The *weak equivalence principle* can be simply formulated as "all bodies fall in a gravitational field with the same acceleration regardless of their mass or their internal structure". An equivalent mathematical formulation would be to say that the intertial mass m_{I}, appearing in Newton's second law $\boldsymbol{F} = m_{\mathrm{I}}\boldsymbol{a}$, is equal to the passive gravitational mass m_{P}, the mass in Newton's law of gravity $\boldsymbol{F} = m_{\mathrm{P}}\boldsymbol{g}$. In other words, as long as tidal effects can be neglected, a free-falling apparatus behaves as if the embedding gravitational field was absent altogether.

Einstein extended the idea from mechanical laws to all the laws of physics paving the way to the formulation of GR. This latter reformulation of the equivalence principle is commonly referred to as the *Einstein equivalence principle*. Diffeomorphism invariance or general covariance, the idea that physics is completely independent of any choice of coordinates, transpires from there into an intrinsic property of GR.

I.1.2 Lovelock's theorem

We now state Lovelock's theorem closely to how it was initially stated in ref. [30]. Consider a rank two tensor $A^{\mu\nu}$ in such that it is

$$\begin{cases} A^{\mu\nu}(g_{\mu\nu}; \partial_\rho g_{\mu\nu}, \partial_{\rho\sigma} g_{\mu\nu}) & \text{concomitants of } g_{\mu\nu} \text{ and its first two derivatives} \quad \text{(I.1a)} \\ \nabla_\nu A^{\mu\nu} = 0 & \text{divergence free} \quad \text{(I.1b)} \end{cases}$$

then it can be written as

$$A^{\mu\nu} = a\, G^{\mu\nu} + b\, g^{\mu\nu} \tag{I.2}$$

where a and b are constants and $G^{\mu\nu}$ is the Einstein tensor defined in eq. (I.7).

The same assumptions also imply that $A^{\mu\nu}$ is both symmetric and at most linear in the second derivatives of the metric tensor g. Moreover, in four dimensions, the only admissible equations of motion are the Einstein field equations (given in eq. (I.8)) [55]. This sets the basis for GR, but also reveals how to depart from GR: at least one of the hypotheses must be relaxed. This can be achieved in different ways, by *e.g.*

- considering extra (or fewer) dimensions,
- adding extra fields,
- going beyond the second order derivatives of the metric,
- Non-locality
- assuming the field equations do not come from an action.

I.1.3 Formal definition

Lovelock's theorem and discussion now clearly restricted the building blocks for building GR. Not any action can yields eq. (I.2) as its *equations of motion* (EoM). The action that describe GR, called the Einstein-Hilbert action, must actually read

$$S_{\mathrm{EH}} \coloneqq \frac{M_{\mathrm{Pl}}^2}{2} \int \sqrt{-g}\, (R + \Lambda)\, \mathrm{d}^4x \tag{I.3}$$

where M_{Pl} is Planck's mass, g is the determinant of the metric $g_{\mu\nu}$, R is the scalar curvature and Λ denotes the CC. At this stage, this action only describes spacetime itself, without any matter. If one adds matter, we would simply write

$$S_{\mathrm{total}} \coloneqq S_{\mathrm{EH}} + S_{\mathrm{matter}} \,. \tag{I.4}$$

The natural following steps, now that an action is defined, would be to derive the corresponding equations of motions. These are the Einstein field equations and are usually defined along with the two following quantities. Firstly, we shall define the stress-energy-momentum tensor, that is going to essentially encapsulate the role of matter, by

$$T^{\mu\nu} \coloneqq \frac{2}{\sqrt{-g}} \cdot \frac{\delta S_{\mathrm{matter}}}{\delta g^{\mu\nu}} \,. \tag{I.5}$$

The conservation of the stress-energy-momentum tensor can be expressed as

$$\nabla_\mu T^{\mu\nu} \,. \tag{I.6}$$

Secondly, we introduce the Einstein tensor $G_{\mu\nu}$ as

$$G_{\mu\nu} \coloneqq R_{\mu\nu} - \frac{1}{2} R g_{\mu\nu} \tag{I.7}$$

where $R_{\mu\nu}$ denotes the Ricci curvature tensor.

Using these eqs. (I.5) and (I.7), we write the Einstein field equations compactly as

$$G_{\mu\nu} + \Lambda g_{\mu\nu} = 8\pi G T_{\mu\nu} \,. \tag{I.8}$$

These equations are very general and should encompass all the gravitational phenomena GR describes. Unfortunately, they can also easily turn out very difficult or impossible to solve analytically.

Now, before looking into particular solutions, in section I.3, we shall first describe the *ADM decomposition* and what is called the *null energy condition*.

I.2 The ADM decomposition

The ADM decomposition, named after Arnowitt, Deser and Misner who first suggested it [56], could be seen as a simple re-writing of terms to separate temporal and spatial contributions in equations. To this aim, the main idea is to slice spacetime into three dimensional manifolds and isolate hypersurfaces at constant times. In doing so, we only mathematically treat space and time independently. Most notably perhaps, this approach enables us to easily adopt a Hamiltonian perspective, the point-of-view traditionally favored in quantum field theory. Both HL gravity and the VCDM model, both of which we detail in sections II.5 and II.6.1, take advantage of it for their formulation.

We here give a working introduction to its formalism and ideas [57, 58], but the curious reader is invited to consult more thorough summaries such as refs. [56, 59, 60, 58].

I.2.1 Formalism

To realize the ADM decomposition, we thus decide to cut spacetime at constant t (non-intersecting) hypersurfaces. While we call it t as we will often choose this parameter to coincide with the time, it does not necessarily have to be so and another parameter may be chosen without altering any of the following derivations. Moreover, some considerations in the current development will be given for three spatial dimensions. However, the overall formalism can be easily generalized to higher (or lower) dimensions as well.

Let us consider one particular hypersurface defined by the position function X^μ. We can describe the tangent space of any point with the basis $(e_i)^\mu \coloneqq \nabla_i X^\mu$ where ∇_i stands for the covariant derivative. There is then a unique perpendicular vector n^μ that satisfies the two conditions

$$\begin{cases} g_{\mu\nu} e_i^\mu n^\nu = 0 \,, & \text{(I.9a)} \\ g_{\mu\nu} n^\mu n^\nu = -1 \,. & \text{(I.9b)} \end{cases}$$

If we are now to make our hypersurface "evolve" along t and thus *foliate* spacetime, we connect each point from one hypersurface to the next along the fourvector

$$N^\mu \coloneqq \partial_t X^\mu \,. \tag{I.10}$$

Expressed in terms of the basis $\{e_i^\mu, N^\mu\}$ that we previously defined, it reads

$$N^\mu =: N n^\mu + N^i e_i^\mu \,. \tag{I.11}$$

This expression defines the *lapse function* N and the *shift function* N^i. Given eq. (I.10), we can interpret the lapse function as dictating how the proper time evolves, while the shift function indicates how a same spatial position is "shifted". For it may help to grasp the idea, it is also illustrated in fig. I.1.

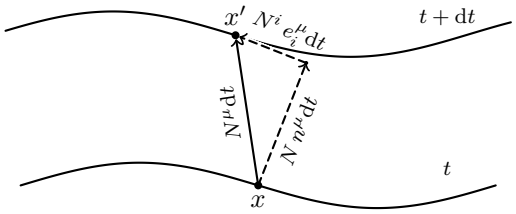

Figure I.1: Illustration of the decomposition given by eq. (I.11) [57, 58]. The two wavy curves are understood to represent schematically two hypersurfaces that are dt apart from each other.

I.2.2 The metric

Naturally, the mathematical formulation of the metric needs to be adapted accordingly. The relations given in eq. (I.9b) already reveal us some of the metric representation. The remaining ones simply define a metric γ_{ij} with signature $(+,+,+)$ as

$$\gamma_{ij} \coloneqq g_{\mu\nu} e_i^\mu e_i^\nu \tag{I.12}$$

and the overall metric is described by the line element

$$\mathrm{d}s^2 = -N^2 \mathrm{d}t^2 + \gamma_{ij} (\mathrm{d}x^i + N^i \mathrm{d}t)(\mathrm{d}x^j + N^j \mathrm{d}t) \,. \tag{I.13}$$

Note that these quantities contain $1+3+6=10$ variables, which is indeed equal to the total number of variables in the spacetime metric. From there, the volume element can be computed and reads

$$\sqrt{g}\mathrm{d}^4x \equiv N\sqrt{\gamma}\mathrm{d}^4x\ . \tag{I.14}$$

I.2.3 The Hilbert-Einstein action

To re-write the Hilbert-Einstein action within this formalism, we introduce the *extrinsic curvature* K_{ij}, which we define as

$$K_{ij} \coloneqq \frac{1}{2N}\left(\partial_t\gamma_{ij} - D_iN_j - D_jN_i\right)\ , \tag{I.15}$$

where D_i denotes the covariant derivative with respect to the metric γ on the hypersurface.

In terms of the extrinsic curvature, the Einstein-Hilbert action of eq. (I.3) is now concisely written as

$$S_{\mathrm{EH}} = \int \mathrm{d}t \int \mathrm{d}^3x\sqrt{\gamma}N\left(R_{\mathrm{3D}} + K_{ij}K^{ij} - K^2\right) \tag{I.16}$$

where the scalar curvature R_{3D} is here understood to be the three dimensional scalar curvature, in opposition to the four dimensional scalar curvature R appearing in eq. (I.3).

I.2.4 Hamiltonian formalism

In this decomposition, treating N and N^i as Lagrange multipliers and neglecting boundary contributions, the total Hamiltonian of GR can be written

$$H_{\mathrm{tot}} = \int d^3x\left[N\mathcal{H}_0(\gamma,\pi) + N^i\mathcal{H}_i(\gamma,\pi)\right], \tag{I.17}$$

in which $\mathcal{H}_0$ is the Hamiltonian constraint and $\mathcal{H}_i$ is the momentum constraint, given by

$$\mathcal{H}_0 = \frac{2}{M_{\mathrm{Pl}}^2\sqrt{\gamma}}\left(\gamma^{ik}\gamma^{lj} - \frac{1}{2}\gamma^{ij}\gamma^{kl}\right)\pi_{ij}\pi_{kl} - \frac{M_{\mathrm{Pl}}^2\sqrt{\gamma}}{2}R_{\mathrm{3D}}, \tag{I.18}$$

$$\mathcal{H}_i = -2\sqrt{\gamma}\gamma_{ik}N^kD_j\left(\frac{\pi^{ij}}{\sqrt{\gamma}}\right), \tag{I.19}$$

where π^{ij} denotes the canonical momentum of γ_{ij}, $M_{\mathrm{Pl}} = 1/\sqrt{8\pi G}$ is the reduced Planck mass (eq. (1)), G denotes Newton's gravitational constant, γ is the determinant of γ_{ij}, and R_{3D} denotes the three-dimensional Ricci scalar of γ_{ij}.

I.3 Observational successes

Most of our understanding of our Universe and cosmology stem from applications of general relativity. It is thus important to establish the foundations that GR entails. This section paints in broad strokes the history of our Universe and thus review the important successes of GR.

I.3.1 The Friedmann-Lemaître-Robertson-Walker metric

As just mentioned, eq. (I.8) can lead to system of equations difficult to deal with. However, if we are to consider the Universe at very large scales (*i.e.* $\sim 10^9$ ly), two simplifying assumptions are often made: the Universe is homogeneous and isotropic. In layman's words, we are saying that the large-scale properties of the Universe are the same anywhere (homogeneity) and in any direction (isotropy). These two hypotheses are together called the *cosmological principle*, and, while their validity may be discussed, they have overall proven robust until now [43].

Assuming the cosmological principle and using polar coordinates, the metric would accurately be described by the line element

$$\mathrm{d}s^2 = -N^2\mathrm{d}t^2 + a(t)^2\left(\frac{\mathrm{d}r}{1-k\,r^2} + r^2\mathrm{d}\Omega^2\right) \tag{I.20}$$

where a is called the scale factor and $\mathrm{d}\Omega^2$ accounts for the angular part, which, in spherical coordinates, can be expressed as

$$\mathrm{d}\Omega^2 = \mathrm{d}\theta^2 + \sin(\theta)^2\mathrm{d}\phi^2\ , \tag{I.21}$$

while k is a constant determining the type of curvature the Universe adopts

$$\begin{cases} k > 0 & \Rightarrow \text{ closed spacetime}\,, & \text{(I.22a)} \\ k = 0 & \Rightarrow \text{ flat spacetime}\,, & \text{(I.22b)} \\ k < 0 & \Rightarrow \text{ open spacetime}\ . & \text{(I.22c)} \end{cases}$$

The metric corresponding to the line element of eq. (I.20) is commonly called the *Friedmann-Lemaître-Robertson-Walker* (FLRW) metric. We have explicitly included the lapse function N here, but it is often set to 1 when working in cosmic or proper time. We shall do so in the rest of this section.

Surprisingly, as of today, cosmological observations do not allow us to confidently rule out any of these scenarios: k must be close to 0. Accordingly, this means that a flat spacetime ($k = 0$) is, in many applications, a reasonable assumption to make.

I.3.2 The Friedmann equations

For convenience, we set here $N \equiv 1$. Assuming the cosmological principle, the only non-vanishing components of the energy-momentum tensor read

$$T_{00} = \rho \tag{I.23a}$$
$$T_{ij} = a^2\,\gamma_{ij}\,p \tag{I.23b}$$

where ρ and p are *a priori* parameters of the energy-momentum tensor, but, upon closer inspection, play a role akin to an energy density and pressure of some perfect fluid filling the Universe. The ratio between the two is often defined by the equation of state, *i.e.*

$$w \coloneqq \frac{p}{\rho} \tag{I.24}$$

In these terms, the conservation eq. (I.6) now reads

$$\frac{\mathrm{d}\rho}{\mathrm{d}t} = -3H(\rho + p)\,. \tag{I.25}$$

where we introduce the Hubble expansion rate parameter H as

$$H \coloneqq \frac{\dot{a}}{N\,a}\,. \tag{I.26}$$

To keep this definition general, we have kept N explicit here only.

Using this result of eq. (I.23) and the FLRW metric, one can work out Einstein's equations eq. (I.8). In order, the temporal and the spatial equations are

$$\begin{cases} \dfrac{\dot{a}^2 + k}{a^2} = \dfrac{8}{3}\pi G\rho + \dfrac{1}{3}\Lambda\,, & \text{(I.27a)} \\ \qquad \dfrac{\ddot{a}}{a} = -\dfrac{4\pi G}{3}\,(\rho + 3\,p) + \dfrac{1}{3}\Lambda\,. & \text{(I.27b)} \end{cases}$$

In light of eq. (I.26), We can then rewrite the Friedmann equations as

$$\begin{cases} H^2 = \dfrac{8}{3}\pi G\rho + \dfrac{1}{3}\Lambda - \dfrac{k}{a^2} & \text{(I.28a)} \\ \dot{H} = -4\pi G\,(\rho + p) + \dfrac{k}{a^2}\,. & \text{(I.28b)} \end{cases}$$

The meaning of the first equation will be investigated in details soon, in section I.3.5. As for the second equation, it is now a differential equation dictating the time evolution of H in terms of ρ and p.

I.3.3 The redshift

Now that we introduce the Hubble expansion rate H, let us also define what is meant by the *redshift*. Given an observered (obs) and the original emitted (em) signals, we can define the redshift z as the quantity

$$z \coloneqq \frac{a(t_{\mathrm{obs}})}{a(t_{\mathrm{em}})} - 1 = \frac{\lambda_{\mathrm{obs}}}{\lambda_{\mathrm{em}}} - 1\,, \tag{I.29}$$

where λ_{obs} and λ_{em} are the wavelength when the signal is observed respectively emitted. As the Universe expands, the further the emission source is located, the more the observed wavelength λ_{obs} is stretched. Consequently, the redshift z increases monotonically with the distance of the emission source. By construction, $z = 0$ is here and now.

The redshift z can further be related to the Hubble parameter H, by

$$z \approx (t_{\text{obs}} - t_{\text{em}})H(t_{\text{obs}}) \,. \tag{I.30}$$

I.3.4 Conformal time

Another quantity is neatly related to the Hubble parameter as well. We define the *proper time* τ (sometimes denoted η) by

$$\mathrm{d}\tau \coloneqq \frac{\mathrm{d}t}{a(t)} \quad \Leftrightarrow \quad \tau(t) \coloneqq \int \frac{\mathrm{d}t}{a(t)} \tag{I.31}$$

Obviously, if a is constant in time t, we find $\tau a = t$.

Looking at eq. (I.13), we observe that $\mathrm{d}t$ always comes accompanied by the lapse function N. Therefore, if we "replace" the lapse by the scale factor, we can easily read out the proper time and work with it. In proper time, it is also customary to define the corresponding Hubble expansion parameter $\mathcal{H}$ (not to be confused with H of eq. (I.26)) as

$$\mathcal{H} \coloneqq \frac{\dot{a}}{a} \,. \tag{I.32}$$

If one replaces the lapse function N by the scale factor a, it is straightforward to observe that

$$\mathcal{H} = a \cdot H \,. \tag{I.33}$$

I.3.5 A short history of the cosmos

Let us now try to reason from eq. (I.28). If we define

$$\rho_\Lambda \coloneqq \frac{\Lambda}{8\pi G} \,, \tag{I.34}$$

$$\rho_k \coloneqq \frac{3}{8\pi G}\frac{-k}{a^2} \,, \tag{I.35}$$

we can consider some effective ρ_{tot} and p_{tot} to account for the cumulative effect of all contributions. Equation (I.28a) then becomes

$$\frac{3}{2}H^2 = 8\pi G \rho_{\text{tot}} \,. \tag{I.36}$$

This easily shows that, assuming a is a monomial in t, then

$$\rho_{\text{tot}} \propto t^{-2} \,. \tag{I.37}$$

Now eliminating p and subsequently ρ in eq. (I.28b) using eq. (I.24) respectively eq. (I.36) yields

$$\dot{H} = -(1+w)\frac{3}{2}H^2 \,. \tag{I.38}$$

This is a first order differential equation that can easily be solved for H first, and then for a upon substituting $H = \dot{a} \cdot a^{-1}$ (keeping $N = 1$ here). Treating independently the case where $w = -1$, we can thus express the scale factor as

$$a \propto \begin{cases} t^{\frac{2}{3(1+w)}} & \text{if } w \neq -1, \quad \text{(I.39a)} \\ \exp(t) & \text{if } w = -1. \quad \text{(I.39b)} \end{cases}$$

Therefore, as $\rho_{\text{tot}} \propto t^{-2}$ (eq. (I.37)), we also deduce $\rho_{\text{tot}} \propto a^{-3(1+w)}$ if $w \neq -1$. We see, from these last equations, that by knowing the value of w, the overall behavior of all other quantities can be approximated under the cosmological principle.

The short mathematical discussion we have had until now will now make the following discussion easier. Indeed, all main regimes driving the scale factor can be attributed a w. We can start by splitting the original ρ into the sum of a radiative component ρ_{rad} and a matter component ρ_{matter}. A detour through microphysics attributes to the former $w = \frac{1}{3}$, while the latter is modelled as a pressureless fluid, thus with

$w = 0$. If ρ_Λ is assumed to be the dominant density in eq. (I.36), then solving for a and comparing with eq. (I.39a), reveals the contribution of the cosmological constant can be interpreted as a fluid of negative pressure, *i.e.* $w = -1$. And when considering ρ_k, a similar reasoning yields $w = -\frac{1}{3}$.

Given eq. (I.39), we would expect each of these contribution to dominate turn by turn. First, the Universe is radiation-dominated, then matter-dominated. If $k \neq 0$, the spatial curvature k would then possibly dominate before the cosmological constant, again if $\Lambda \neq 0$, takes the lead thanks to its exponential behavior. This corresponds to the traditional view of the Universe's history. Later in this work, we shall consider different scenarios and diverge from this picture. For more details on the early Universe and its scenarios, we can refer the reader to refs. [61, 62, 63, 64, 65, 66].

I.3.6 The very early Universe

In the previous ever expanding Universe scenario, the oldest era of our Universe was a radiation dominated Universe, that is an era where photons would be frequently scattered, and the Universe can be seen as opaque. The transition between radiation and matter domination eras, when matter and radiation decoupled, approximately corresponds to the Universe becoming transparent to light. The photons emitted then are thus still travelling in space and can be observed. These fossil radiations constitute what is called the *cosmic microwave background* (CMB). Considering from where this fresco covering the distant sky is coming to us, we can imagine a distant expanding shell around us from where the radiation comes from. This is called the surface of last scattering.

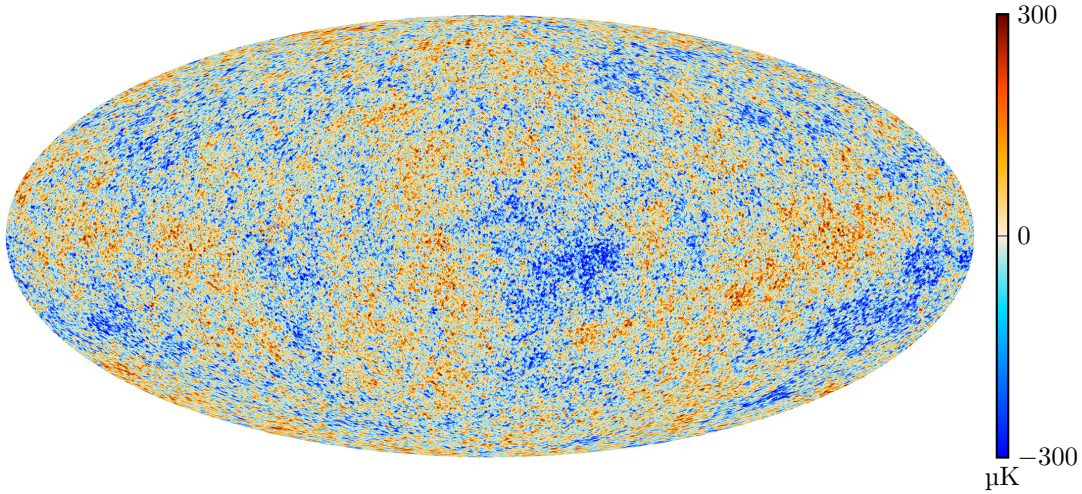

Figure I.2: Anisotropies of the cosmic microwave background as observed by ESA's Planck mission [67, 68]. The temperature indicated corresponds to the deviation, in μK, from the average temperature of about 2.726 K.

As the Universe was opaque prior to it, the CMB thus represents the furthest in the past we can probe with light. All models that try to explore beyond the CMB have thus, as their ultimate test, to match this observed relic emission. This CMB radiation is an emission of near-uniform, black body thermal energy coming from all parts of the sky.

The CMB also brings its own mysteries. A first one stems from this near uniformity. From modeling the radiation and matter decoupling, one can compute an expected spectrum for the CMB and thus how far in the past the surface of last scattering stands. Using the Friedmann equations we reviewed, it is also possible to extrapolate the Universe expansion up to its hypothetical origin. Looking at both results put side-by-side, one would observe that there is not enough time for integrality of the CMB to be causally connected. Only tiny patches of this surface are. The question thus reads: how can the CMB be uniform when there is no causal contact between its parts? This first problem is called *horizon problem* or *homogeneity problem*.

The most commonly invoked solution to this problem is to incorporate an inflationary phase prior to the CMB [69, 70, 71, 66, 61, 62]. That is a new expansion regime —inflation— would have dominated the Universe in the past and stretched the Universe so much as to freeze quantum fluctuations at cosmological scales and thus seeding the large-scale structures in the Universe.

Moreover, when extrapolating the Universe curvature in the past using the Friedmann eqs. (I.27), for it to be near-flat as it is observed today, the initial configuration of the Universe must have been incredibly fine-tuned. This is, in very short, the essence of the *flatness problem*. Inflation also serves as an explanatory mechanism for this question. Notice that one alternative to an inflationary scenario could be a *bouncing Universe*; we shall discuss it in more details in chapter VI.

While the CMB is mostly homogeneous, it does exhibit tiny inhomogeneities. These can be observed, and their spectrum is a constraining tools often referred to in order to invalidate models. Among other observations, observations show that the spectrum of scalar perturbations must be near scale-invariant [72]. Similarly, the ratio of tensor perturbations over scalar ones must be small (it has not yet been observed) [72].

For more details on what was very briefly introduced here, we would suggest to consult refs. [61, 62, 66].

I.3.7 Perturbations

As we already stated, solving the Einstein field equations in an arbitrary case represents a very difficult task, even when it is possible. To obtain the preceding results, we had to bring in the assumptions of the cosmological principle. However, how to go beyond this approximation? This is where perturbation theory comes in.

The idea is basically to Taylor expand and, since each order is linearly independent, solve order-by-order the equations at hand. While higher order may be long equations with complicated terms, often, the lower orders read as simple and understandable expressions. This approach will be repeatedly used throughout this work (see sections IV.2.2 and VI.2).

I.3.8 The null-energy condition

Let us here, make a brief parenthesis and introduce the *null energy condition* (NEC). The NEC can be formally defined by the concise expression

$$T_{\mu\nu}n^\mu n^\nu > 0 \tag{I.40}$$

where n^μ is here any null or light-like vector, *i.e.* any vector for which $g_{\mu\nu}n^\mu n^\nu = 0$ [73].

What makes the NEC interesting is twofold. On the one hand, the NEC has proven to be robust. It is fairly difficult to write a healthy theory that violate the NEC stably. More often than not, violating the NEC will either lead to a ghost or some gradient instabilities. On the other hand, if one assumes the NEC to be valid, then, under fairly broad assumptions, the Penrose theorem tells us that the Universe must possess a singularity in the distant past [74].

Getting a better grasp of what the NEC means may be easier in the context of an homogeneous and isotropic Universe. In this case, using eq. (I.23) simplifies eq. (I.40) to

$$\rho + p > 0\ . \tag{I.41}$$

Considering the second Friedmann equation, eq. (I.28b), we observe that eq. (I.41) implies $\dot{H}$ to be negative and the Hubble parameter H decreases in time. We here assumed k to be negligible (or negative). If it is positive, there are ways to circumvent this conclusion, but these are subject to restrictions. So, as a rule of thumb, breaking the NEC often amounts to modelling a contracting Universe.

I.3.9 Observational tests of general relativity

I.4 Apparent shortcomings

In spite of all its successes and its relative elegance, GR alone today appears insufficient to answer several profund problems of cosmology. In this section, we shall briefly overview three of these: the non-renormalizability of GR, the CC problem and DM. The subsequent chapters will exploit theories that try to resolve the first two, but the last, DM, will leave our focus.[1]

[1] In truth, DM will briefly come back when we'll describe Hořava-Lifshitz gravity. Indeed, while Hořava-Lifshitz was initially conceived as an answer to the non-renormalizability of GR, it rather conveniently incorporates an artifact that should behave like DM. The curious reader is invited to refer to section II.5.2 for more details.

I.4.1 Non-renormalizability

The first problem we're listing may be the most fundamental and it is a long-standing issue of GR. Simply put, GR is not renormalizable. Therefore, it does not easily play with the formalism of the quantum world. This is essentially due to Newton's constant being dimensionful (with the mass dimension $[G_N] = -2$). The non-renormalizability leads to uncontrollable *ultraviolet* (UV) divergences. Adding higher curvature terms to the Einstein-Hilbert action can make the theory renormalizable [75], or even super-renormalizable [76], but leads to massive ghosts and makes the corresponding quantum theory non-unitary in the UV. Naturally, attempts to build a quantum field theory of gravity have been encountering many serious issues.

While a hasty observer may be tempted to put this problem aside and consider the two theories having two disjointed domains of application, there are occurrences where both shall be invoked. This is most notably the case in black holes and in the distant past, both situations where high-energies flirt with small scales. More fundamentally, one may also be simply motivated to tackle this issue to, at last, obtain a cohesive and united vision of the physical forces that govern our world.

Possible answers to this problem are numerous and diverse [8, 77, 13, 12]. As it involves the reconciliation of two points of view on, one may decide to approach the issue from either high-energy and particle physics or low-energy and gravity. In the former camp, the framework probably getting the most traction nowadays are overall related to string theory [8]. Regarding the latter, this work considers HL gravity [13, 78], whose details are presented in section II.5.

I.4.2 The cosmological constant problem

The cosmological constant problem is another issue where bridging cosmological observations and quantum field theory fails. The first observations that highlighted the CC contribution to Einstein-Hilbert action used supernovae [28, 29], the cataclysmic collapse of stars upon themselves during which stars emit a tremendous amount of light. As the mechanism inside a star explaining supernovae can be reasonably described, we are able to predict that amount of emitted light. Therefore, by measuring the "brightness", *i.e.* the magnitude, of the supernova, we can fairly reasonably estimate the distance between the star and our observing position. Not only does it provide us a robust way to measure distances, it also allows us to measure distances way further other techniques are able to. To explain these observations, one could, in principle simply put some constant number, the cosmological constant Λ, in the Einstein-Hilbert action (eq. (I.3)) and *voilà*! It is therefore quite natural to consider modifying gravity at long ranges. As it is in probing these long distances that one may witness the effect of DE, it simultaneously defines the CC problem as a large-scale problem.

But what is dubbed the CC problem runs deeper than this. Indeed, observational developments in the past few decades have proven their potential to pin down cosmological parameters to high precision. Despite some recent discrepancy in the determination of the observed value of the expansion rate [79, 72, 80, 81, 82], it is now a well accepted fact that our Universe as a whole not only expands but at an accelerated rate. What causes the accelerated expansion is often dubbed *dark energy* (DE), though there is no agreed consensus about its true nature. The simplest possibility is the CC; it can be freely added to the Einstein equation with an arbitrary value at the classical level, while quantum-mechanically the zero-point energy possessed by vacuum fluctuations could contribute to it.

The discrepancy between the observed and theoretically expected values of the CC is the major source of the so-called CC problem. In the viewpoint of quantum field theory, one would sum all zero-point diagrams and thus obtain some value that is subject to UV physics, which should compose the vacuum energy. On the other hand, one might wish that the CC, written as Λ, which enters in the Einstein equations, would incorporate all the above contributions. However, if it does then the observational bounds on the CC require an enormous cancellation among different contributions. Without such a cancellation, these two numbers would not match, but more than that, they would differ by many orders of magnitude (the observational bounds being extremely smaller) [83, 84, 85]. The CC problem can thus also be seen as a bridging problem between the cosmological and the quantum worlds, and any significant progress on its resolution could eventually lead to a fundamental progress in both paradigms.

Furthermore, the CC problem, while already an issue on its own, begs yet another problem: the *coincidence problem*. It basically asks the following question: why is the small value of the vacuum energy, *i.e.* the density of DE, of the same order as that of DM today? The scaling of the DE density with respect to time is different from that of the DM, and only a few Hubble times would deviate their values by orders of magnitude. This implies that we live at a very special moment, nested at the hinge between a DM dominated and a DE dominated era. Such a coincidence requires a delicate fine tuning [86], leaving us with a speculation that there may be a physical mechanism at play to realize it.

While numerous attempts have been made to solve the CC problem, including from supersymmetry perspectives to effective modifications of gravity (see *e.g.* [83, 85] for review and references therein), none have yet provided a satisfactory and definitive answer. One may also be tempted to invoke the so-called *anthropic principle* to give a reasoning to it, *i.e.* the DE is so small and the transition occurs now, because the physical conditions to our existence are only united at this precise moment and with that physical parameter. While it might as well serve as a valid answer, and one cannot totally refute its relevance, its nature makes it difficult to test and to quantify new predictions out of it. In other words, taking it as the final answer too hastily runs into the risk of missing some more fundamental physical connection, and it therefore appears essential to further investigate a concrete mechanism to address the issue at hand. Chapter IV does precisely that and tries to bring in a CC relaxation mechanism into the early Universe.

I.4.3 Dark matter

In parallel to DE stands *dark matter* (DM), which, apart from the prefixed adjective, is seemingly unrelated to DE. Unlike the two previous discrepancies we discussed, it does not arise from invoking quantum field theory. Rather, when mapping galaxies and their properties, one quickly wonders what stars and their clustering may weight. To do so, roughly two paths can be taken and give diverging conclusions, hence the problem. On the one hand, one can measure the luminosity of the distant objects. By mathematically modelling a galaxy, the galaxy brightness can directly be related to its mass. This approach gives us a first mass estimate. On the other hand, one may consider the dynamics of the stars within the galaxy, via *e.g.* the virial theorem [15]. This gives us a second estimate, which, in practice is about four times higher than the previous one. Therefore, the difference, this missing mass in the former estimate, must not emit any light [15, 87, 16]. Hence the name *dark matter*.

The mystery does not end there: observations so far seem coincide with the existence of some large and obscure mass that affects the cosmic dynamics. At the time of this writing, there exists no unanimously agreed solution to identify the nature of dark matter. Approaches from particle physics, which have often hypothesized some kind of weakly-interacting particle have not yet been validated by any experiments [19].

From a cosmological and astrophysical perspective, this missing matter was also imagined to be *e.g.* large wandering baryonic objects or primordial black holes [88, 89], *i.e.* black holes that formed in the early ages of the Universe and that have survived until now. The former was ruled out [90, 91], while the latter, while still admissible, is being constrained more and more [20]. An alternative and less explored venue is to modify gravity (again) [92]. Modified Newtonian dynamics (MOND theories) [24, 25, 26, 23] have attempted to do so, but have so far not been able to provide a full answer to the issue at hand [93, 94, 95]. In this text, we shall talk of Hořava-Lifshitz gravity [13, 78], which could, in principle, bring an answer to the DM mystery [27]. While we give more details about this in section II.5, we work within its formalism in chapter III.

Chapter II

Beyond general relativity

As Lovelock's theorem made clear, under the broad assumptions it makes, GR is the only metric theory of gravity admissible. Therefore, naturally, to go beyond the boundaries set by GR and witness any new gravitational phenomena, one must break at least one of the theorem's hypotheses.

In this chapter, we shall quickly review different possible paths for going beyond GR and focus our attention on two in particular that we deem interesting in the subsequent two chapters. As this work explore paths to modify gravity and effectively go beyond general relativity, we consider relevant to first briefly skim through some of the common frameworks that have been and still are explored to this aim. The subsequent list is however not extensive and aims only at supporting the reader in naming points on the map of currently explored alternatives to GR. We do not, for example, describe $f(R,T)$ gravity or its more simple $f(R)$ version, nor do we talk about teleparallel gravity or supergravity [77]. Quadratic gravity, which attempts to make gravity a renormalizable theory, and the special case of Chern-Simons theories are also absent, as well as many other modified gravity theories. For more thorough reviews, we suggest: for a very wide overview, ref. [96], for massive and bi-metric gravity ref. [97], for post-Newtonian limit ref. [43] and/or for applications specifically geared towards DE and the early Universe ref. [98, 99].

II.1 Scalar-tensor theories

The most common and perhaps simple path to explore what lies beyond GR is probably the broad class of so-called *scalar-tensor theories*. As their name already suggests, scalar-tensor theory add to the metric (the tensor) a single scalar field ϕ in the formulation of their action. This mathematical simplicity has also allowed these to remain flexible, while also demonstrating a rich phenomenology, making them resilient alternatives to GR.

II.1.1 Brans-Dicke theory

The first attempts in this direction are old and could be traced back to Brans and Dicke Basing themselves on Fierz and Jordan [43], they wrote their now eponym *Brans-Dicke theory* [100]. A naive prototype scalar-tensor theory could read as

$$\int \left(\phi R - \frac{\omega(\phi)}{\phi} g^{\mu\nu} \partial_\mu \phi \, \partial_\nu \phi - U(\phi) \right) \sqrt{-g} \mathrm{d}^4 x \tag{II.1}$$

where ϕ is the new scalar field, with the potential U, and ω stands for some coupling function. The Brans-Dicke theory would be equivalent to setting the coupling amplitude ω to some constant and removing the potential U.

II.1.2 Quintessence and k-essence

Another more general model would be k-essence [101, 102, 103, 104]. Its action is often expressed as

$$\int \left(B(\phi) R + P(X, \phi) \right) \sqrt{-g} \mathrm{d}^4 x \tag{II.2}$$

where we chose to write $X = g^{\mu\nu} \partial_\mu \phi \, \partial_\nu \phi$. In the Einstein's frame, the coupling function B is often absorbed by redefining other quantities.

Provided the function can be easily decomposed as

$$P = X + V(\phi)\,, \tag{II.3}$$

we can talk of *quintessence*, rather than k-essence. While quintessence is often used to model inflation by determining an appropriate potential V, the more general k-essence also allows itself to influence the dynamics via the kinetic term X. Given their simplicity, this class of models have been ubiquitous and used to model inflatons, dilatons, curvatons, DE and many other phenomena [101, 99, 105]. We shall take advantage of them in both chapters IV and VI.

II.1.3 Horndeski theories

A more "modern" framework is found in Horndeski theories [31, 32, 33]. These were long held to be the most general scalar-tensor theories with second-order Euler-Lagrange equations (before the development of DHOST theories, see section II.1.4). While they were first exhibited by Horndeski in 1974, they passed unnoticed for a long time, before interest for these made a recent resurgence from 2011.

The action expressed by Horndeski actually turns out to be general enough to encompass several other scalar-tensor theories, including the previous two. It can also be used to describe *e.g.* galileons, k-inflation or k-essence [101]. That is why we may prefer designated Horndeski theories as a class rather than one particular theory.

To formulate the action of Horndeski's theories, we first define four "sub-Lagrangians", for convenience,

$$\mathcal{L}_2 \coloneqq K\,, \tag{II.4a}$$
$$\mathcal{L}_3 \coloneqq -G_3\Box\phi\,, \tag{II.4b}$$
$$\mathcal{L}_4 \coloneqq G_4 R + \partial_X G_4\left((\Box\phi)^2 - (\nabla_\mu\nabla_\nu\phi)^2\right)\,, \tag{II.4c}$$
$$\mathcal{L}_5 \coloneqq G_5 G_{\mu\nu}\nabla^\mu\nabla^\nu\phi - \frac{1}{6}\partial_X G_5\left((\Box\phi)^3 - 3(\Box\phi)(\nabla_\mu\nabla_\nu\phi)^2 + 2(\nabla_\mu\nabla_\nu\phi)^3\right) \tag{II.4d}$$

where K, G_3, G_4 and G_5 are arbitrary functions of both ϕ and X, and X is the standard kinetic term

$$X \coloneqq -\frac{1}{2}\partial_\mu\phi\partial^\mu\phi\,. \tag{II.5}$$

Each of the four function K, G_3, G_4 and G_5 completely define its own sub-Lagrangian, as eq. (II.4) shows, hence the decomposition. It turns out that $\mathcal{L}_4$ with $G_4 = X$ and $\mathcal{L}_5$ with $G_5 = \phi$ coincide. The same can be said up to a total derivative for $\mathcal{L}_3$ with $G_3 = f(\phi)$ and $\mathcal{L}_2$ with $K = -2X\partial_\phi f$.

It is thus now straightforward to define the action of this class of theories as

$$\int\sqrt{-g}\left(\sum_{i=2}^{5}\mathcal{L}_i\right)\mathrm{d}^4x\,. \tag{II.6}$$

Setting $G_4 = 1$ and $K = G_3 = G_5 = 0$ recovers the Einstein-Hilbert action (eq. (I.3)). As the framework offered by Horndeski theories is exploited in chapter IV. The equations of motion of eq. (II.6) for $G_5 = 0$ and $G_4 =$ constant can thus be obtained by setting $P = 0$ and rewriting φ_2 as ϕ in eq. (IV.29).

II.1.4 DHOST theories

Before going further, we wish to mention another recently developped class of theories, even more general than the Horndeski one, called *degenerate higher-order scalar-tensor* or DHOST for short [34, 35, 36, 37, 38, 39]. This framework was itself recently extended further into U-DHOST [40, 41, 42].

II.2 Vector-tensor theories

If the previous example was to add a scalar, another alternative that would now appear natural would be to add a vector U^μ instead of a scalar. Vector-tensor theories were motivated to explore violations of Lorentz invariance in gravity. The action employed in this approach reads[106, 107, 108]

$$\frac{1}{16\pi G}\int\sqrt{-g}\left((1+\omega\,U_\mu U^\mu)R - K^{\alpha\beta}{}_{\mu\nu}\nabla_\alpha U^\mu\nabla_\beta U^\nu + \lambda(U^\mu U_\mu - 1)\right) \tag{II.7}$$

where

$$K^{\alpha\beta}{}_{\mu\nu} \coloneqq c_1 g^{\alpha\beta} g_{\mu\nu} + c_2 (\delta_{\mathrm{K}})^{\alpha}_{\mu} (\delta_{\mathrm{K}})^{\beta}_{\nu} + c_3 (\delta_{\mathrm{K}})^{\alpha}_{\nu} (\delta_{\mathrm{K}})^{\beta}_{\mu} + c_4 U^{\alpha} U^{\beta} g_{\mu\nu} \tag{II.8}$$

and ω, c_1, c_2, c_3, c_4 are constants, λ is a Lagrange multiplier and δ_{K} stands for the Kronecker delta.

If the Lagrange multiplier is kept (*i.e.* $\lambda \neq 0$), the theory is called Einstein-Æther and the term in ω can be shown to be superfluous. A sub-version called *khronometric*, which restrict the vector U^{μ}, can be used to describe a low-energy limit of Hořava-Lifshitz gravity (section II.5) [109, 110]. At a Newtonian level, this amounts to an unobservable modification of the gravitational constant G. The Einstein-Æther and the khronometric versions coincide at the linear perturbations level. The theory has also been invoked to investigate a possible a Lorentz-violation of DM, for example [111, 112].

II.3 Both vector and scalar theories

Having seen both scalar-tensor theories and vector-tensor theories, the "both-worlds" option would thus naturally be to combine them all together. Indeed, There exist at least two such an approach. Tensor-vector-scalar theories, sometimes abbreviated *TeVeS*, were introduced to model the so-called modified Newtonian dynamics, or MOND, theories [23, 24, 25, 26]. More recently, scalar-vector-tensor gravity, abbreviated *SVTG* and sometimes called modified gravity, or *MOG*, was also advanced, where both a dynamical scalar and a massive vector field are incorporated [113]. While the names can be confusingly similar, and both approach were introduced to model DM, the theories are different. Both theories also seem to not match recent observations of *gravitational waves* (GWs) [95, 114]. We shall also underline that we do not refer to the scalar-vector-tensor gravity as modified gravity anywhere else in this text, as "modified gravity" is more commonly used to designate any theory of gravity different from GR.

II.4 Massive and bimetric gravity

Bimetric theories add to GR not a scalar, not a vector, but another tensor, a second metric. The first well-known such realization may be *Rosen's bimetric theory of gravity* [115] whose action reads

$$\frac{1}{64\pi G} \int \eta^{\mu\nu} g^{\alpha\beta} g^{\rho\sigma} \left((\nabla_\eta)_\mu g_{\alpha\rho} (\nabla_\eta)_\nu - \frac{1}{2} (\nabla_\eta)_\mu g_{\alpha\beta} (\nabla_\eta)_\nu g_{\rho\sigma} \right) \sqrt{-\eta} \mathrm{d}^4 x \tag{II.9}$$

where η is a flat background metric and ∇_η denotes the corresponding covariant derivative. This theory accommodates two distinct metrics. While a first $g_{\mu\nu}$ accounts describes the gravitational fields (and thus the geometry of spacetime), a second flat metric $\eta_{\mu\nu}$ is used for inertial forces. Rosen's theory incorporates extremely compact objects, but that do not have any event horizon [43]. However, despite its strong alignment with GR, the theory died with the Hulse-Taylor binary pulsar. Indeed, the theory predicts violation of the strong equivalence principle in the presence of strong gravitational events, which did not survive observational tests [43].

II.4.1 Massive gravity

Although it may not have been Einstein's intent when he penned GR, his theory can also be viewed as the unique massless spin-2 particle description [97]. This (hypothetical) particle would be called the *graviton*. To go beyond Lovelock's theorem, a physicist coming from a high-energy background may be tempted to endow the particle with a mass. Again, one could see here a possible approach to think about GR non-renormalizability, as we would model GR in a formalism much more akin to quantum field theory.

At first sight, massive gravity encounters two obstacles. Firstly, with five *degrees of freedom* (DoF) against two for GR, massive gravity may appear too exotic. The answer to this paradox is the *Vainshtein screening mechanism* [116, 117], which enable to effectively hide the extra DoF.

Secondly, naive attempts are plagued the so-called *Boulware-Deser ghost* [118]. This has been a longstanding obstacle to the development of a massive gravity. However, there has been a recent resurgence of interest in such formalism thanks to some breakthroughs. Ghost free massive gravity was indeed achieved in *e.g. de Rham-Gabadadze-Tolley (dRGT)* massive gravity [119, 120], sometimes called *new massive gravity (NMG)*. Lastly, let us mention the name of the more recent minimal massive gravity and *minimal theory of bigravity* (MTBG) [121], which exploit the construction principles of minimally modified gravity that we shall discuss in section II.6.

II.5 Hořava-Lifshitz gravity

We already mentioned that GR is non-renormalizable in section I.4.1 and why it was an issue. That is where HL gravity [13] enters. As we shall see, this quantum gravity theory is in principle power-counting renormalizable, thanks to the presence of higher-order spatial curvature terms. The action and equations of motion in HL gravity contain only terms up to second order in time derivatives and thus the theory is free from Ostrogradsky ghosts associated with higher time derivatives. The HL theory was recently proved to be perturbatively renormalizable [122, 123], and, therefore, has come to be regarded as a valid UV completion path of quantum gravity.

So how does HL gravity achieves this? The core idea is to treat space and time as physically different. This is not the same thing as the Hamiltonian and Lagrangian formalisms, where the distinction between the two concepts introduced in the former is of a mathematical nature. For the HL gravity, the differentiation intervenes via the so-called *anisotropic scaling*, or *Lifshitz scaling*. That is rescaling space by a factor b will requires to multiply time by a factor b^z, *i.e.*

$$t \to b^z t\,, \quad \vec{x} \to b\vec{x}\,, \tag{II.10}$$

where t is the time coordinate, $\vec{x}$ represents the spatial coordinates vector and z is a number called *dynamical critical exponent*. Naturally, shall z be 1, we would respect the assumption of GR and actually treat time and space on an equal footing.

Otherwise, the foliation of spacetime is here not just a choice of coordinates, but translates a physical feature of the theory. Therefore, the fundamental symmetries of HL are then foliation-preserving diffeomorphism *i.e.* either space-independent time reparametrization ($t \to t'(t)$) or time-dependent spatial diffeomorphism ($\boldsymbol{x} \to \boldsymbol{x}'(t, \boldsymbol{x})$). The theory is also assumed to be invariant under spatial parity ($\boldsymbol{x} \to -\boldsymbol{x}$) and time reflection ($t \to -t$).

In $3+1$ dimensions, an anisotropic scaling of $z = 3$ in the UV regime breaks Lorentz symmetry, but ensures renormalizability, while the usual $z = 1$ scaling is recovered in the *infrared* (IR) regime. An anisotropic scaling of $z = 3$ also handily provides a mechanism for generating scale-invariant cosmological perturbations, simultaneously solving the horizon problem [124] without inflation and providing the so-called *anisotropic instanton*, which could be an answer to the flatness problem [125]. HL could even provide mechanism to explain DM [27, 126], which we will hint in section II.5.2.

II.5.1 Framework formulation in $d+1$ dimensions

This distinction between the two concepts of time and space quite naturally invites us to write, similar to the ADM decomposition of the metric in GR [56], the $d+1$ dimensional metric as

$$\mathrm{d}s^2 = -N^2\mathrm{d}t^2 + \gamma_{ij}(\mathrm{d}x^i + N^i\mathrm{d}t)(\mathrm{d}x^j + N^j\mathrm{d}t)\,, \tag{II.11}$$

where $i = 1, \dots, d$, N is the lapse function, N^i the shift vector, and γ_{ij} is the d dimensional spatial metric with positive definite signature $(+, +, \cdots)$. The $d+1$ dimensional action S describing HL gravity is the sum of a kinetic part $\mathcal{L}_K$ and a potential part $\mathcal{L}_V$ [78]; that is

$$S_{\mathrm{HL}} \coloneqq \frac{\mathcal{M}_{\mathrm{HL}}^{d-1}}{2} \int \mathrm{d}t\, \mathrm{d}^d x N \sqrt{g}\, (\mathcal{L}_K + \mathcal{L}_V)\,, \tag{II.12}$$

where $\mathcal{M}_{\mathrm{HL}}$ sets an overall mass scale. If we define the d-dimensional extrinsic curvature K_{ij} similarly as in eq. (I.15), then the kinetic part $\mathcal{L}_K$ can be written as

$$\mathcal{L}_K = K^{ij}K_{ij} - \lambda K^2\,, \tag{II.13}$$

with λ being a coupling constant, and ∇_i the spatial covariant derivative compatible with γ_{ij}. The indices i, j run from 1 to d and the inverse of γ_{ij} is written as γ^{ij}. Accordingly, we wrote $K^{ij} \coloneqq \gamma^{ik}\gamma^{jl}K_{kl}$ and $K \coloneqq \gamma^{ij}K_{ij}$.

For simplicity, we will consider the projectable HL gravity: that we assume the lapse function depends only on time, *i.e.* $N = N(t)$. However, we shall see later on (section III.1.1) how the subsequent result can easily be extended to the non-projectable version of the theory, where the lapse depends on both time and space.

As for the potential part, it shall be built out of any possible renormalizable operators without parity violating terms, and must be expressed in terms of invariants assembled from the products of the

d-dimensional Riemann tensor (schematically denoted as Rm below) and its derivatives [127, 128]. For the highest-order potential part, denoted as $\mathcal{L}_z$, the list of possible terms is

$$\left\{(\mathrm{Rm})^d,\, (\nabla\mathrm{Rm})^2(\mathrm{Rm})^{d-3},\, (\nabla\mathrm{Rm})^4(\mathrm{Rm})^{d-6},\, (\nabla\mathrm{Rm})^6(\mathrm{Rm})^{d-9},\, \cdots\right\} . \tag{II.14}$$

Now, including lower-dimensions terms as well, we come to write

$$\mathcal{L}_V = \mathcal{L}_0 + \mathcal{L}_1 + \mathcal{L}_2 + \mathcal{L}_3 + \cdots + \mathcal{L}_{z-1} + \mathcal{L}_z \,, \tag{II.15}$$

where $\mathcal{L}_i$ denotes a collection of invariant terms with $2i$ spatial derivatives acted on the spatial metric. Here, the first two terms $\mathcal{L}_0 + \mathcal{L}_1$ are necessary to recover the $d+1$-dimensional GR in the IR limit, the third term $\mathcal{L}_2$ includes all possible quadratic and spatial curvature terms, and so on. Explicitly, the four five terms $\mathcal{L}_i$ read

$$\mathcal{L}_0 = -2\Lambda \,, \tag{II.16a}$$

$$\mathcal{L}_1 = c_g^2 \tilde{R} \,, \tag{II.16b}$$

$$\mathcal{L}_2 = c_{2,1}\tilde{R}^2 + c_{2,2}\tilde{R}^j_i\tilde{R}^i_j + c_{2,3}\tilde{R}^{ijkl}\tilde{R}_{ijkl} \,, \tag{II.16c}$$

$$\mathcal{L}_3 = c_{3,1}\tilde{R}^3 + c_{3,2}\tilde{R}\,\tilde{R}^j_i\tilde{R}^i_j + c_{3,3}\tilde{R}^j_i\tilde{R}^k_j\tilde{R}^i_k + c_{3,4}\nabla_i\tilde{R}\nabla^i\tilde{R} + c_{3,5}\nabla_i\tilde{R}_{jk}\nabla^i\tilde{R}^{jk} + \cdots \,, \tag{II.16d}$$

$$\begin{aligned}\mathcal{L}_4 = {} & c_{4,1}\tilde{R}^4 + c_{4,2}\tilde{R}^2\tilde{R}^j_i\tilde{R}^i_j + c_{4,3}\tilde{R}\,\tilde{R}^j_i\tilde{R}^k_j\tilde{R}^i_k + c_{4,4}\tilde{R}^j_i\tilde{R}^k_j\tilde{R}^l_k\tilde{R}^i_l \\ & + c_{4,5}\tilde{R}\,\nabla_i\tilde{R}\nabla^i\tilde{R} + c_{4,6}\tilde{R}\,\nabla_i\tilde{R}_{jk}\nabla^i\tilde{R}^{jk} + \cdots \,,\end{aligned} \tag{II.16e}$$

where $\tilde{R}$, $\tilde{R}_{ij}$ and $\tilde{R}_{ijkl}$ respectively denote the Ricci scalar, the Ricci tensor and the Riemann tensor, all in d spatial dimensions, and dots represent terms depending on the Riemann tensor and its derivatives. The constants Λ and c_g are the cosmological constant and the propagation speed of tensor gravitational waves, and $c_{m,n}$ are constants of appropriate dimensions. All those constants are subject to running under the *renormalization group* (RG) flow.

In the UV regime, terms with two time derivatives and those with $2z$ spatial derivatives are dominant. If $z = d$, the theory is renormalizable and if $z > d$, the theory is super-renormalizable. In the IR regime, on the other hand, higher derivative terms are subdominant and the theory naturally converges to $z = 1$. Moreover, if λ (of eq. (II.13)) goes to 1 in the IR limit, and if it does sufficiently quickly, then GR is recovered thanks to an analogue of the Vainshtein mechanism [78, 129, 130]. For simplicity, in the rest of the present chapter, we restrict our considerations to the renormalizable theory, *i.e.* $z = d$.

II.5.2 Dark matter as an integration constant

The lack of local Hamiltonian constraint also has a perhaps surprising cosmological implication. It is possible for DM to appear "naturally" as a integration constant in HL gravity[78, 27, 126].

Indeed, consider, for a start, a flat spacetime described by the FLRW (eq. (I.20)). In GR, Friedmann equations (eq. (I.27)) give four *local* constraints, since GR is invariant under four-dimensional diffeomorphism. This is not the case in the projectable version of HL gravity anymore, and we can only rely on *three* local constraints and one *global* one. In other words, a local equivalent of eq. (I.27a) does not exist and eq. (I.27b) —in HL gravity, in a flat spacetime— becomes here

$$-\frac{3\lambda - 1}{2}\left(2\dot{H} + 3H^2\right) = 8\pi G p \tag{II.17}$$

where λ is the same constant λ appearing in eq. (II.13). The equation of motion for matter reads

$$\dot{\rho} + 3H(\rho + p) = -Q \tag{II.18}$$

where Q represent some source/well term, which, at low energy, vanishes ($Q \to 0$). From thereon, one can obtain the following integral

$$\frac{3}{2}(3\lambda - 1)H^2 = 8\pi G\left(\rho + \frac{C(t)}{a^3}\right) \tag{II.19}$$

where we defined

$$C(t) \coloneqq C_0 + \int Q(\tau)a(\tau)^3 \mathrm{d}\tau \tag{II.20}$$

and C_0 is some integration constant.

As we said that Q goes to zero at low energy, this eq. (II.20) simply amounts to some constant contribution in eq. (II.19). In other words, it can represent some pressureless dust of some sort, thus effectively mimicking DM. The above discussion was carried out in a flat spacetime, but it can be extended to a more general low-energy setting. We refer the reader to the review [78] and articles [27, 126] for a more thorough discussion of this interesting venue.

II.6 Minimally modified gravity

When GR was first formulated, it showed promise by solving observational riddles that deprived physicists of their sleep at the time. Even still, GR continues to produce physically accurate predictions, e.g. the detection of GWs by LIGO/Virgo [131, 132] and the first-ever photograph of a black hole [48]. However, albeit a simple yet rigorous, elegant, and symmetrically satisfying theory, it has proven incomplete on quantum gravity scales as well as some cosmological scales, failing to explain modern observations consistently. Once more, physicists find themselves in a state of sleep deprivation.

This incentivizes us to look beyond GR. Do we need a completely new theory? Or is it possible to modify gravity in a way such that it extends down to the quantum scales, and breeds a cosmological framework that is consistent with observations? The experiments conducted at LIGO/Virgo open up the possibility of probing strongly gravitating events through GWs, such as black hole binaries and gravitational collapse. This allows for further validity testing of GR and alternative frameworks.

Several new theories of gravity have already been proposed. In the high-energy limit, supergravity and HL gravity [13] are examples of candidates for theories of quantum gravity, while massive gravity, bigravity, and various scalar-tensor theories [119, 133, 134, 135, 31] carry implications for the dark sector of the universe as well as its accelerated expansion. A common artifact when modifying gravity is accompanying degrees of freedom. On cosmological scales, these usually give rise to the phenomena we aim to explain. However, on astrophysical scales, these must be treated in order to avoid contradictions with well-established experimental data, the appearance of ghosts, and various instabilities [136]. One common method of dealing with this is to implement various screening mechanisms [137]. Alternatively, one could consider modifying gravity *minimally*, i.e. keeping the degrees of freedom at most two. Such a theory is called a *minimally modified gravity* (MMG) theory.

It was previously established in ref. [138] that all MMG theories may be divided into two types: type-I and type-II. The former are theories that are equivalent to GR, but that modify gravity due to non-trivial matter coupling, while the latter are theories simply different from GR. Formally speaking, this means type-I MMG have an Einstein frame, while type-II MMG have none (and are thus expressed in the Jordan frame) [139]. For example, the class of MMGs studied in ref. [140] were, by [141], mostly shown to be of type-I and the most generic construction of a type-I MMG is elaborated upon in subsection IV.A of [142]. Another example would be [143]. Instances of type-II MMG theories include the Cuscuton [144], the minimal theory of massive gravity [145], the previously mentioned MTBG [121], a consistent $D \to 4$ Einstein-Gauss-Bonnet gravity [146], and VCDM [139] (see also [147, 148]).

These theories do not introduce additional local physical degrees of freedom other than those in GR, while they may contain global modes called shadowy modes (or generalized instantaneous modes) [1] due to the existence of a preferred frame. Therefore, they easily avoid instabilities and constraints that could stem from extra propagating degrees of freedom that are common in other modified gravity theories, even without needing any screening mechanisms.

II.6.1 VCDM: A type-II minimally modified gravity

In chapters V and VI, we will consider the VCDM model, a specific type of MMG theory [139]. According to the classification introduced in ref. [138], the VCDM is a type-II MMG theory since it has no Einstein frame [142]. The name "VCDM" comes from promoting the cosmological constant Λ of the standard ΛCDM model to a function $V(\varphi)$ of a nondynamical, auxiliary field φ. Extending its original usage for the late-time universe, various aspects of the VCDM, including attempts to address tensions in late-time cosmology [149, 150], black holes [151], stars [152], gravitational collapse [153] and the solution space including GR solutions [154], have been explored.

The distinctive feature of VCDM is its substitution of the cosmological constant with a potential function $V(\phi)$ of a non-propagating auxiliary scalar field ϕ in the gravitational action. In order to keep the theory minimal, constraints are imposed on the field ϕ, which breaks 4D diffeomorphism invariance (although 3D spatial diffeomorphism invariance still holds). A thorough comparison with the Cuscuton has been performed in refs. [142, 154], the latter showing how any solution of VCDM is a solution of Cuscuton, while the converse need not be true. It was further shown that there exists a subset of solutions in VCDM that coincide with exact solutions in GR, given specific constraints set on the foliation of spacetime as well as the defining parameters of VCDM. Some of its implications on cosmology, including the dark sector and early Universe scenarios, have been explored in refs. [139, 149, 150], while static, spherically symmetric objects and black holes were more closely studied in refs. [152, 151].

[1] See [40, 41] for shadowy modes in the context of U-DHOST theories.

The construction of this class of theory is based on the ADM decomposition (see section I.2) and is detailed in ref. [139]. For our intents and purposes, the Lagrangian formulation of VCDM is more convenient and it reads

$$M_{\rm Pl}^2 \int dt d^3x\, N\sqrt{\gamma}\left(\frac{1}{2}\left[R_{\rm 3D}+K_{ij}K^{ij}-K^2-2V(\phi)\right]-\frac{\lambda^i_{\rm gf}}{N}\,\partial_i\phi-\frac{3}{4}\,\lambda_0^2-\lambda_0\,(K+\phi)\right)\,, \qquad \text{(II.21)}$$

where $K\equiv\gamma^{ij}K_{ij}$ for K_{ij} as defined in eq. (I.15), $R_{\rm 3D}$ is the Ricci scalar associated with γ_{ij}, the quantities λ^i and λ_0 are Lagrange multipliers, and φ is an auxiliary scalar field. As we mentioned, because of its non-trivial constraint structure, this theory contains only two propagating DoF; that is the same number as GR.

Because the theory incorporates an extra scalar field, one may be tempted to classify this theory as a scalar-tensor one. Nonetheless, in practice, the theory is often seen as in its own class, and we do so here as well.

II.7 Effective field theories

The last approach we shall mention is using effective field theories. This would perhaps qualify as the most agnostic way of doing things. The basic idea is to simply write all possible terms that may appear in the Lagrangian and weight them [155, 156]. However, because of this agnosticism, an effective field theory is almost always a computationally complicated one.

Yet, advances in this direction can sometimes be directly related to other approaches that may appear as subcases of their formalism. Effective field theories are also an interesting path to put constraints and guide the research and development of modified gravity theories. Positivity bounds obtained from assuming fundamental principles such as unitarity, locality and causality [157, 158].

Tackling cosmology's mysteries

Chapter III

The Wheeler-DeWitt equation in Hořava-Lifshitz gravity

In section I.4, we highlighted major incompatibilities problems facing GR and brought forward possible paths to modify gravity and thusly answers these concerns. In this chapter, we make concrete use of one theory —Hořava-Lifshitz gravity—, which attempts to answer to the first listed issue: the non-renormalizability of GR. We briefly reviewed its construction in section II.5 and we shall now exhibit —for the first time— the Wheeler-DeWitt equation within its context.

Although there have been numerous works on the early cosmology based on the HL gravity, the early Universe cannot be treated classically when quantum gravity is dominant, and we have to adopt a *quantum cosmology* approach. A common approach, in quantum cosmology, is to separate space and time using the ADM formalism (section I.2) and work with the Hamiltonian formulation. In this framework, the Hamiltonian constraint is interpreted as an operator equation, the *Wheeler-DeWitt* (WDW) equation [159], $\hat{H}[\gamma]\Psi[g] = 0$ where $\hat{H}[\gamma]$ is the Hamiltonian operator and $\Psi[\gamma]$ is called the *wave function of the Universe* (see [160, 161] for a review).

Whether this wave function of the Universe gives finite correlation functions of physical perturbations has a long history of debate among quantum cosmologists. In particular, in recent years, in the Lorentzian path integral formulation of the no-boundary [162] and tunneling proposals [163] —well-known boundary conditions of quantum cosmology—, it has been argued that the wave function of small perturbations around the background may take an inverse Gaussian form and become uncontrollable [164, 165]. In developments that follow, we adopt instead the so-called DeWitt boundary condition [159], which states that the wave function of the Universe should vanish at the classical big-bang singularity. In a homogeneous and isotropic Universe, the DeWitt boundary condition can be concisely expressed as $\Psi(a = 0) = 0$ and is known to successfully regularize the behavior of the wave function near the classical singularity. In a mini-superspace, where the dynamics of the Universe is parameterized only by the scale factor $a(t)$, it is easy to find an analytic expression for the *DeWitt wave function*, *i.e.* a solution to the WDW equation with the DeWitt boundary condition. However, how to generalize this result beyond this mini-superspace is not obvious.

Hereafter, we show, using the $d + 1$ dimensional framework given in section II.5.1, that the DeWitt wave function for tensor perturbations exhibits scale invariance near the classical big-bang singularity and is thus regular. We also exhibit the well-behaved DeWitt wave function for tensor perturbations numerically. This numerical demonstration for the first time illustrates the regular behavior of the DeWitt wave function for tensor perturbations in HL gravity all the way from the classical big-bang singularity to finite values of the scale factor.

In this chapter, we shall derive the DeWitt wave function for a $d+1$ dimensional Universe described by a homogeneous and isotropic background and tensor perturbations around it (section III.1.1). We further demonstrate that the wave function for the tensor perturbations is normalizable and scale-invariant on constant-a hypersurfaces near $a = 0$, where a is the scale factor (section III.2.1). This result is due to the anisotropic scaling with $z = d$. To support these conclusions, numerical results are demonstrated for $d = 3$ for concreteness (section III.2.2).

III.1 Framework continuation

In this first section, we build upon the $d + 1$ dimensional HL formulated in section II.5.1 to prepare the ground for perturbatively solving the WDW equation in section III.2. Firstly, we thus expand the tensor

perturbations in hyper-spherical harmonics and work out the action up to second order in perturbations. Secondly, we perform the canonical quantization and write the WDW equation.

III.1.1 Cosmological setup

We shall assume the d-dimensional space of the model to be the union of connected pieces Σ_α ($\alpha = 1, \dots$), each of which we shall call a *local d-dimensional Universe*. The union of all Σ_α would thus represent the Universe in its entirety. In such a configuration, while the lapse function $N = N(t)$ is common for all pieces, we have a set of a shift vector $N^i = N^i_\alpha(t,x)$ and a spatial metric $g_{ij} = g^\alpha_{ij}(t,x)$, which is different for different local Universe Σ_α. In the ADM formalism, the lapse and the shift vectors basically act as Lagrange multipliers. The variation of the projectable HL action (eq. (II.12)) with respect to N yields the following *Hamiltonian constraint*

$$\sum_\alpha \int_{\Sigma_\alpha} \mathrm{d}^d x\, \mathcal{H}_{g\perp} = 0\,, \quad \text{where} \quad \mathcal{H}_{g\perp} =: \frac{\mathcal{M}_{\rm HL}^{d-1}}{2}\sqrt{g}(\mathcal{L}_K - \mathcal{L}_V)\,. \tag{III.1}$$

It is important to stress here that in the projectable version of HL gravity, the Hamiltonian constraint is not a local equation, but a result integrated over the whole space [78]. In other words, the constraint expressed by eq. (III.1) constrains the sum of contributions from all Σ_α to vanish, but each individual contribution does not have to vanish, *i.e.*

$$\int_{\{\Sigma_\alpha\}} d^d x\, \mathcal{H}_{g\perp} =: C_\alpha\,. \tag{III.2}$$

where $\{C_\alpha\}$ are separation constants satisfying eq. (III.1): $\sum_\alpha C_\alpha = 0$. Therefore, if we are interested in one particular local Universe, *i.e.* an element of $\{\Sigma_\alpha\}$, the Hamiltonian constraint does not need to be enforced (eq. (III.2)).

For the non-projectable theory, where the lapse function depends on not only the time coordinate but also spatial coordinates as $N(t,\vec{x})$ and the action includes terms constructed from the 3-vector $\partial_i \ln N$, the Hamiltonian constraint is local, but it basically only gives 2$^{\rm nd}$-class constraints due to the lack of time diffeomorphism invariance. However, since the non-projectable theory enjoys the time reparametrization symmetry, the global Hamiltonian constraint (which is just the spatial integral of the local Hamiltonian constraint) is 1$^{\rm st}$-class. Therefore, there is only one global Wheeler-DeWitt equation that is imposed on physical states. The rest of the local Hamiltonian constraints are all 2$^{\rm nd}$-class and thus may be solved at the level of the operator equations. In the presence of more than one local universe, like here, solving those 2$^{\rm nd}$-class constraints leads to $C_\alpha = C_\beta$ for all α and β. Thus, the global Wheeler-DeWitt equation implies $C_\alpha = 0$ for all α, and the subsequent results of the present section can be directly translated to the non-projectable theory as well, by simply setting $C_\alpha = 0$.

We further assume that each connected space Σ_α is a closed universe, and that each closed universe is described by a closed Friedmann-Lemaître-Robertson-Walker (FLRW) metric and perturbations around it. Therefore, we can write

$$N^i_\alpha = 0\,, \quad g^\alpha_{ij} = a^2_\alpha(t)\left[\Omega_{ij}(\boldsymbol{x}) + h^\alpha_{ij}(t\,,\boldsymbol{x})\right]\,, \tag{III.3}$$

where Ω_{ij} is the metric of the unit d-sphere with the curvature constant set to 1, *i.e.* the Riemann curvature of Ω_{ij} is simply $\delta^i_k\delta^j_l - \delta^i_l\delta^j_k$. Given this definition, the spatial indices $i, j, \dots$ are thus raised and lowered by Ω^{ij} and Ω_{ij} respectively. The tensor perturbation h^α_{ij} must satisfy the transverse and traceless condition, *i.e.* $\Omega^{ij}h^\alpha_{ij} = \Omega^{ki}D_k h^\alpha_{ij} = 0$, where D_i is the spatial covariant derivative compatible with Ω_{ij}. Furthermore, the perturbation h^α_{ij} can be expanded in terms of the hyper-spherical harmonics [166] as

$$h^\alpha_{ij}(t,x^i) = \sum_{snlm} h^{\alpha s}_{nlm}(t) Q^{snlm}_{ij}\,, \tag{III.4}$$

where $s = \pm$ is the polarization label and the triplet (n,l,m) is comprised within the ranges $n \geq 3$, $l \in [0, n-1]$ and $m \in [-l, l]$. The tensor eigenfunctions Q^{snlm}_{ij} of the Laplacian operator $D^2[\Omega]$ on the unit d-sphere [167] satisfy

$$D^2[\Omega]\, Q^{snlm}_{ij} = -\left[n^2 + (d-3)n - d\right] Q^{snlm}_{ij}\,, \tag{III.5}$$

and are normalized via the following relation

$$\int d^d\sqrt{\Omega}\Omega^{ik}\Omega^{jl}Q^{snlm}_{ij}Q^{s'n'l'm'}_{kl} = V_d\,\delta^{ss'}\delta^{nn'}\delta^{ll'}\delta^{mm'}\,. \tag{III.6}$$

With these assumptions and the harmonic expansion (III.4), the $d+1$-dimensional HL action is expanded up to the second order in perturbations as $S = S^{(0)} + S^{(2)} + \mathcal{O}(h^3)$, where

$$S^{(0)} = \mathcal{V}\sum_\alpha \int \mathrm{d}t\, \left(N a_\alpha^d\right)\left(\frac{d(1-d\lambda)}{2}\left(\frac{\dot a_\alpha}{N a_\alpha}\right)^2 + \frac{\alpha_d}{a_\alpha^{2d}}\cdots + \frac{\alpha_3}{a_\alpha^6} + \frac{\alpha_2}{a_\alpha^4} + c_{\mathrm{g}}^2\frac{d(d-1)}{2a_\alpha^2} - \Lambda\right), \tag{III.7a}$$

$$S^{(2)} = \mathcal{V}\sum_\alpha \int \mathrm{d}t\, \left(N a_\alpha^{d-2}\right)\sum_{snlm}\left(\frac{1}{8}\left(\frac{a_\alpha}{N}\dot h_{nlm}^{\alpha s}\right)^2 + \left(\beta_1 + \frac{\beta_2}{a_\alpha^2} + \frac{\beta_3}{a_\alpha^4}\cdots + \frac{\beta_d}{a_\alpha^{2d-2}}\right)\left(h_{nlm}^{\alpha s}\right)^2\right). \tag{III.7b}$$

Here, α_i and β_i are constants that are linear combinations of coupling constants in the action, $\mathcal{V} = \mathcal{M}_{\mathrm{HL}}^{d-1}V_d$ and $V_d = \int \mathrm{d}^d x\sqrt{\Omega}$ is the volume of the unit d-sphere. For the tensor perturbations of each connected space Σ_α, in the following for simplicity we restrict our attention to the dynamics of only one mode $h_{nlm}^{\alpha s}$ with $(s,n,l,m) = (s_\alpha, n_\alpha, l_\alpha, m_\alpha)$, which we denote by h_α. With this reduction, the system is thus described by $\{a_\alpha, h_\alpha\}$.

III.1.2 Canonical quantization

Now, we turn attention to quantum cosmology, equipped with HL gravity and assuming that the dynamics of the homogeneous and isotropic Universe (including any tensor perturbations) is governed by the wave function of the WDW equation. From the HL action for perturbations (eq. (III.7)), we can compute the corresponding Hamiltonian and obtain

$$H \coloneqq \sum_{\alpha=1}\left(\Pi_{a_\alpha}\dot a_\alpha + \Pi_{h_\alpha}\dot h_\alpha\right) - \mathcal{L} \tag{III.8a}$$

$$\begin{aligned} &= \sum_{\alpha=1}\mathcal{V}\left(\frac{N}{a_\alpha^{d-2}}\right)\left(-\frac{1}{2\gamma}\Pi_{a_\alpha}^2 - \frac{\alpha_d}{a_\alpha^2}\cdots - \frac{\alpha_3}{a_\alpha^{8-2d}} - \frac{\alpha_2}{a_\alpha^{6-2d}} - c_{\mathrm{g}}^2\frac{d(d-1)}{2a_\alpha^{4-2d}} + \frac{\Lambda}{a_\alpha^{2-2d}}\right.\\ &\qquad \left. + \frac{2}{\mathcal{V}^2 a_\alpha^2}\Pi_{h_\alpha}^2 - \left(\frac{\beta_1}{a_\alpha^{4-2d}} + \frac{\beta_2}{a_\alpha^{6-2d}} + \frac{\beta_3}{a_\alpha^{8-2d}}\cdots + \frac{\beta_d}{a_\alpha^2}\right)h_\alpha^2\right), \end{aligned} \tag{III.8b}$$

where $\mathcal{L}$ is defined by $S^{(0)} + S^{(2)} =: \int \mathrm{d}t\mathcal{L}$, $\gamma \coloneqq d\,(d\lambda - 1)\,\mathcal{V}^2$ and the canonical momenta Π_{a_α} and Π_{h_α} conjugate respectively to a_α and h_α are given by

$$\Pi_{a_\alpha} \coloneqq \frac{\partial\mathcal{L}}{\partial\dot a_\alpha} = -d\,(d\lambda-1)\,\mathcal{V}\frac{a_\alpha^{d-2}}{N}\dot a_\alpha\,, \quad \Pi_{h_\alpha} \coloneqq \frac{\partial\mathcal{L}}{\partial\dot h_\alpha} = \frac{\mathcal{V}}{4}\frac{a_\alpha^d}{N}\dot h_\alpha\,. \tag{III.9}$$

We can now carry out the canonical quantization of HL gravity. This is done by transforming the canonical variables of Hamiltonian mechanics into Hermitian operators that satisfy the canonical commutation relations. The algebra generated by commutative quantities (c-numbers) becomes an algebra generated by non-commutative quantities (q-numbers) in quantum mechanics. Therefore, an ambiguity in the operator ordering here arises. In performing the canonical quantization, the canonical conjugate momenta are transformed into Hermitian operators, *i.e.*

$$\begin{aligned} \Pi_{a_\alpha} &\mapsto -i\frac{\partial}{\partial a_\alpha} \\ \Pi_{h_\alpha} &\mapsto -i\frac{\partial}{\partial h_\alpha} \end{aligned} \quad\Longrightarrow\quad \begin{aligned} \Pi_{a_\alpha}^2 &= -\frac{1}{a_\alpha^p}\frac{\partial}{\partial a_\alpha}\left(a_\alpha^p\frac{\partial}{\partial a_\alpha}\right) \\ \Pi_{h_\alpha}^2 &= -\frac{\partial^2}{\partial h_\alpha^2} \end{aligned}\,, \tag{III.10}$$

where we should take into account the operator ordering ambiguity of a_α [162]. In quantum cosmology, there exists two well-known orderings: the Laplace-Beltrami operator ordering ($p=1$) and the Vilenkin ordering ($p=-1$) [168].

Once the canonical quantization of the Hamiltonian of eq. (III.8) is realized, we obtain the WDW equation

$$\begin{aligned} \sum_\alpha \frac{1}{a_\alpha^{d-2}}\left(\frac{1}{2\gamma}\left(\frac{\partial^2}{\partial a_\alpha^2} + \frac{p}{a_\alpha}\frac{\partial}{\partial a_\alpha}\right) - \frac{\alpha_d}{a_\alpha^2} - \cdots - \frac{\alpha_2}{a_\alpha^{6-2d}} - c_{\mathrm{g}}^2\frac{d(d-1)}{2a_\alpha^{4-2d}} + \frac{\Lambda}{a_\alpha^{2-2d}}\right.\\ \left. - \frac{2}{\mathcal{V}^2 a_\alpha^2}\frac{\partial^2}{\partial h_\alpha^2} - \left(\frac{\beta_1}{a_\alpha^{4-2d}} + \frac{\beta_2}{a_\alpha^{6-2d}} + \cdots + \frac{\beta_d}{a_\alpha^2}\right)h_\alpha^2\right)\Psi\left(\{a_\alpha, h_\alpha\}\right) = 0\,, \end{aligned} \tag{III.11}$$

where $\Psi(\{a_\alpha, h_\alpha\})$ is the wave function of the entire Universe, as mentioned in introduction. By separating the variables, one can easily obtain special solutions of the form $\Psi = \prod_\alpha \Psi_\alpha(a_\alpha, h_\alpha; C_\alpha)$, where $\{C_\alpha\}$ are the separation constants satisfying $\sum_\alpha C_\alpha = 0$ (eq. (III.2)). A general solution can be then written as a linear combination of these special solutions, explicitly

$$\Psi(\{a_\alpha, h_\alpha\}) = \int \left(\prod_\beta \mathrm{d}C_\beta\right) A_{\{C_\beta\}} \prod_\alpha \Psi_\alpha(a_\alpha, h_\alpha; C_\alpha) \ . \tag{III.12}$$

where each $\Psi_\alpha(a_\alpha, h_\alpha; C_\alpha)$ represents the wave function of one local Universe Σ_α.

For notational convenience, we now redefine the variables and constants in eq. (III.11) as well as the separation constant C_α.

$$\mathfrak{h} = \frac{h_\alpha}{2\sqrt{\gamma}}\,; \qquad \mathcal{C} = \gamma C_\alpha\,;$$
$$g_d = \gamma\alpha_d\,, \quad \cdots, \quad g_2 = \gamma\alpha_2\,, \quad g_1 = \frac{\gamma c_{\mathrm{g}}^2 d(d-1)}{2}\,, \quad g_0 = \gamma\Lambda\,;$$
$$f_d = -8\gamma^2\beta_d\,, \quad \cdots, \quad f_2 = -8\gamma^2\beta_2\,, \quad f_1 = -8\gamma^2\beta_1\,;$$

Notice how the cosmological constant Λ is now incorporated into the g_0 coefficient. The WDW equation for each local universe can then be equivalently re-expressed as

$$\left(\frac{1}{2}\left(\frac{\partial^2}{\partial a^2} + \frac{p}{a}\frac{\partial}{\partial a}\right) + \left(\mathcal{C}a^{d-2} - \frac{g_d}{a^2} - \cdots - \frac{g_2}{a^{6-2d}} - \frac{g_1}{a^{4-2d}} + \frac{g_0}{a^{2-2d}}\right)\right.$$
$$\left. - \frac{1}{2\mathcal{V}^2 a^2}\frac{\partial^2}{\partial\mathfrak{h}^2} + \frac{\mathfrak{h}^2}{2}\left(\frac{f_1}{a^{4-2d}} + \frac{f_2}{a^{6-2d}} + \cdots + \frac{f_d}{a^2}\right)\right)\Psi(a,\mathfrak{h}) = 0\,, \tag{III.13}$$

where we have dropped the index α and abbreviated $\Psi_\alpha(a_\alpha, h_\alpha; C_\alpha)$ as $\Psi(a, \mathfrak{h})$.

III.2 DeWitt wave function with tensor perturbations

In this section, we compute the $d+1$-dimensional DeWitt wave function for a universe represented by a homogeneous and isotropic background and tensor perturbations around it. This extends the results of [169] to $d+1$ dimensions. In particular we show that the DeWitt wave function near the classical big-bang singularity features scale-invariant tensor perturbations due to the anisotropic scaling with $z = d$. A brief discussion of the case without tensor perturbations can be consulted in appendix B. Notice that we consider $d \geq 3$ hereafter, as in the $d = 1$ and $d = 2$ cases, talking of tensor perturbations is irrelevant.

III.2.1 Analytical estimation

In order to obtain a solution of the WDW equation (eq. (III.13)) that satisfies the DeWitt boundary condition—$\Psi(0, \mathfrak{h}) = 0$ for all $\mathfrak{h}$—, we adopt the following expansion around $a = 0$,

$$\Psi(a, \mathfrak{h}) = a^c \sum_{i=0}^{\infty} F_i(\mathfrak{h})\, a^i\,, \tag{III.14}$$

where $F_0(\mathfrak{h})$ is not identically zero and c is a positive constant to be determined. For $\Psi(a, \mathfrak{h})$ to be normalizable on constant-a hypersurfaces, we also impose the following condition on $\Psi(a, \mathfrak{h})$

$$\lim_{\mathfrak{h}\to\pm\infty} F_i(\mathfrak{h}) = 0\,. \tag{III.15}$$

If this condition (eq. (III.15)) is not satisfied, the correlation functions such as the power spectrum of $\mathfrak{h}$ on constant-a hypersurfaces would diverge. In order to determine the positive constant c, we take advantage of the this requirement, *i.e.* $F_0(\mathfrak{h})$ is a non-trivial smooth function satisfying the condition of eq. (III.15) (with $i = 0$).

In GR, it was previously demonstrated that there is no parameter set for which $F_0(\mathfrak{h})$ can satisfy the condition of eq. (III.15) (with $i = 0$) and the tensor perturbations are not smoothly suppressed [169]. In other words, no DeWitt wave function is normalizable on constant-a hypersurfaces around the classical big-bang singularity, unless higher spatial derivative terms are present, as we shall observe in what follows.

Therefore, let us turn our attention back to HL gravity. By substituting the small-a expansion (eq. (III.14)) into the WDW equation (eq. (III.13)), and solving it order by order, we can explicitly determine the functions F_i. For $i = 0, 1, 2$, we find the following three equations

$$\partial_\mathfrak{h}^2 F_0 - \mathcal{V}^2 \left[f_d \mathfrak{h}^2 + (c+p-1)c - 2g_d \right] F_0 = 0 \,, \tag{III.16a}$$

$$\partial_\mathfrak{h}^2 F_1 - \mathcal{V}^2 \left[f_d \mathfrak{h}^2 + (c+p)(c+1) - 2g_d \right] F_1 = 0 \,, \tag{III.16b}$$

$$\partial_\mathfrak{h}^2 F_2 - \mathcal{V}^2 \left[f_d \mathfrak{h}^2 + (c+p+1)(c+2) - 2g_d \right] F_2 = \mathcal{V}^2 (f_{d-1}\mathfrak{h}^2 - 2g_{d-1}) F_0 \,. \tag{III.16c}$$

As the separation constant $\mathcal{C}$ starts to appear from the order $i = d$ onwards of the expansion (see eq. (III.13)), we remark it is absent from these first three equations.

Let us first consider the first relation, *i.e.* eq. (III.16a). By requiring eq. (III.15) (with $i = 0$) and the continuity of $F_0(\mathfrak{h})$ at $\mathfrak{h} = 0$, we obtain

$$F_0(\mathfrak{h}) = \begin{cases} \frac{A}{\sqrt{\mathfrak{h}}} W_{\frac{1}{4}+N,1/4}(w) \,, & (\mathfrak{h} > 0) \\ -\frac{A}{\sqrt{-\mathfrak{h}}} W_{\frac{1}{4}+N,1/4}(w) \,, & (\mathfrak{h} < 0) \end{cases} , \tag{III.17}$$

where $W_{\mu,\nu}(w)$ is the Whittaker function, A is some constant, and w and N are defined by

$$w \coloneqq \mathcal{V}\sqrt{f_d}\mathfrak{h}^2 \,, \quad \frac{1}{4} + N \coloneqq -\frac{V}{4\sqrt{f_d}} \left[c^2(p-1)c - 2g_d \right] \,, \tag{III.18}$$

which, in turn, constrains f_d to be strictly positive. We further impose for $\partial_\mathfrak{h} F_0(\mathfrak{h})$ to be continuous as well at $\mathfrak{h} = 0$, and find

$$\lim_{\mathfrak{h}\to\pm 0} \partial_\mathfrak{h} \Psi(a, \mathfrak{h}) = \mp 2A \frac{\sqrt{\pi} f_d^{3/8} V^{3/4}}{\Gamma(N)} \,. \tag{III.19}$$

Thus, to have continuity at $\mathfrak{h} = 0$, we need N to be some non-negative integer. Therefore, imposing the latter, the definition of N (eq. (III.18)) becomes a constraint on c, at each value N.

For eq. (III.16b), we again require eq. (III.15) (with $i = 1$) and the continuity of both $F_1(\mathfrak{h})$ and $\partial_\mathfrak{h} F_1(\mathfrak{h})$ at $\mathfrak{h} = 0$. However, the latter condition, similarly to what we just did, tells us F_1 would be non-null only for non-negative integer values of $-(2c+p)V f_d^{-1/2} 4^{-1}$. As the freedom offered by c has already been used up and refraining from fine-tuning, we therefore conclude $F_1(\mathfrak{h}) \equiv 0$ as the next-to-leading order solution in a.

However, at the next-to-next-to-leading order, F_2 cannot be identically zero. Once $F_0(\mathfrak{h})$ is given, F_2 is determined by eqs. (III.15) and (III.16c) (with $i = 2$). While the computation is straightforward, the explicit expression for F_2 is fairly long. Hence, we show only its structure, for $N = 0, 1, 2$, without explicit expressions. Using the leading-order solution for different values of N, *i.e.*

$$F_0(\mathfrak{h}) = \begin{cases} A_0 \exp\left(-\frac{1}{2}w\right) \,, & (N=0) \\ (1-2w) A_1 \exp\left(-\frac{1}{2}w\right) \,, & (N=1) \\ \left(1 - 4w + \frac{4}{3}w^2\right) A_2 \exp\left(-\frac{1}{2}w\right) \,, & (N=2) \end{cases} , \tag{III.20}$$

where A_N $(N = 0, 1, 2)$ is some integration constant, the solution for F_2 takes the form

$$F_2(\mathfrak{h}) = \sum_{\tilde{N}=0}^{N+1} a_{N,\tilde{N}} w^{\tilde{N}} A_N \exp\left(-\frac{1}{2}w\right) \,. \tag{III.21}$$

Here, $a_{N,\tilde{N}}$ $(\tilde{N} = 0, \cdots, N+1)$ are constant coefficients determined by the parameters of the WDW equation (eq. (III.13)).

If $N = 0$, we obtain the ground state of the DeWitt wave function, which, in the $a \to +0$ limit, can be expressed as

$$\Psi(a, \mathfrak{h}) = A(\mathcal{V}\sqrt{f_d})^{1/4} a^c \left(e^{-\frac{\mathcal{V}\sqrt{f_d}\mathfrak{h}^2}{2}} + \mathcal{O}(a^2) \right) \,. \tag{III.22}$$

Since $f_d \propto n^{2d}$ for large n, the corresponding correlation function for the tensor perturbations then reads

$$\lim_{a\to+0} \langle \mathfrak{h}^2 \rangle = \lim_{a\to+0} \frac{\int \mathrm{d}\mathfrak{h}\, \mathfrak{h}^2 \left|\Psi(a,\mathfrak{h})\right|^2}{\int \mathrm{d}\mathfrak{h}\, \left|\Psi(a,\mathfrak{h})\right|^2} = \frac{1}{2\mathcal{V}\sqrt{f_d}} \propto n^{-d} \,, \quad \text{for large } n \text{ and } N = 0 \,. \tag{III.23}$$

This clearly shows the scale-invariance and the finiteness of the power spectrum of $\mathfrak{h}$ for $f_d > 0$ (see [169] for more details in the $d = 3$ case). Also in the general case of eq. (III.17) with general N (≥ 0), the power spectrum and other correlation functions of $\mathfrak{h}$ are scale-invariant and finite in the UV limit ($a \to +0$) as far as $f_d > 0$. In particular,

$$\mathcal{M}_{\rm HL}^{3d-3} \lim_{a\to+0} n^d \langle \mathfrak{h}^2 \rangle = \mathcal{O}(1) \times \mathcal{M}^{d-1}\,, \quad \text{for large } n \text{ and any } N \geq 0\,, \tag{III.24}$$

where $\mathcal{M}$ is the mass scale such that $\beta_d \sim n^{2d}/\mathcal{M}^{2d-2}$ (and thus $\mathcal{V}\sqrt{f_d} \sim n^d \mathcal{M}_{\rm HL}^{3d-3}/\mathcal{M}^{d-1}$) for large n. This is completely consistent with the result of ref. [124].

We have seen that eq. (III.18) and eqs. (III.16c) and (III.15) (with $i = 0$) requires $f_d > 0$. Therefore, if $f_d \leq 0$ then there is no non-trivial smooth solution satisfying eq. (III.15) (with $i = 0$). In particular, this is the case in the absence of $z = d$ terms (for which $f_d = 0$). This no-go result applies to many gravitational theories (including GR) for which the action does not contain terms with $2d$ spatial derivatives.

III.2.2 Numerical solution

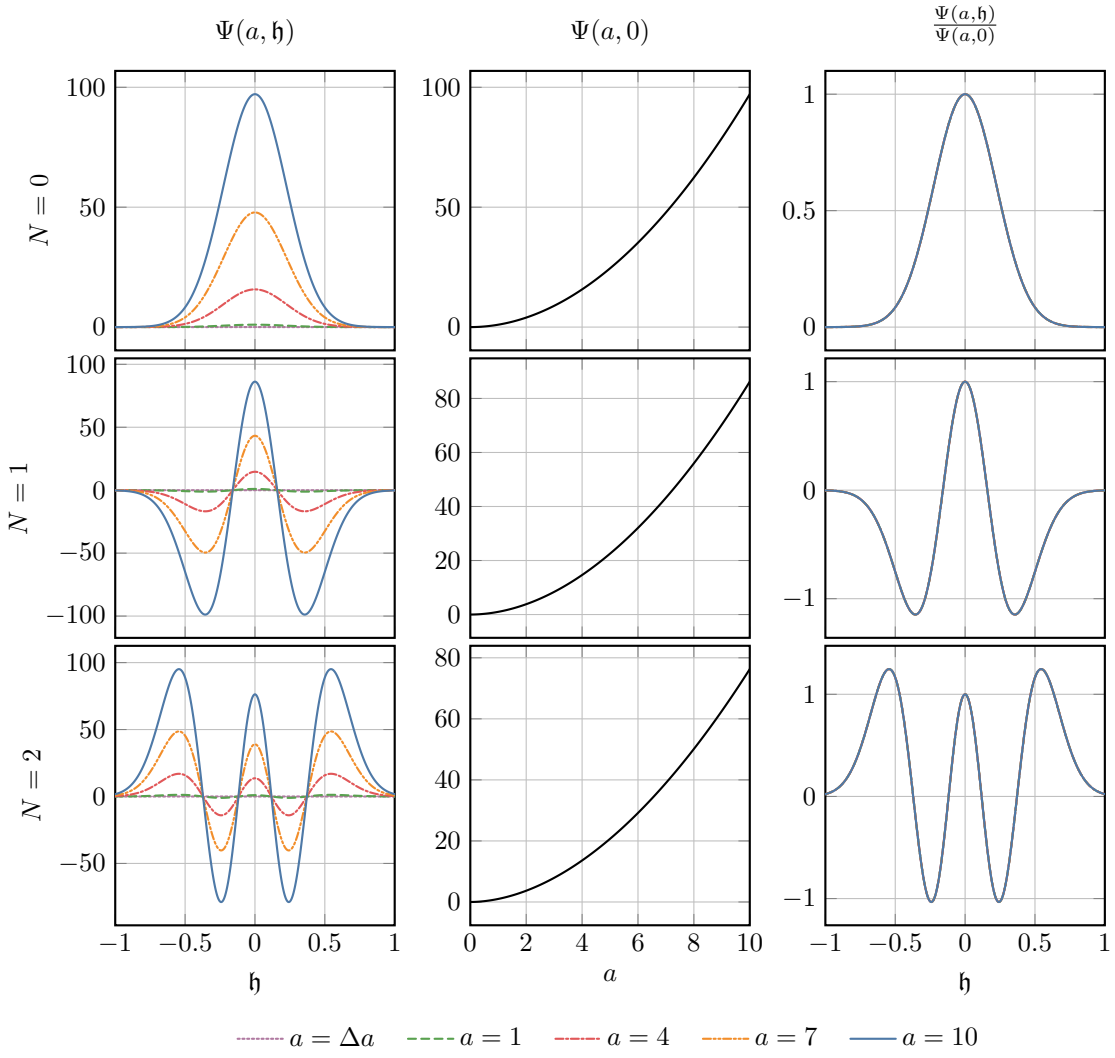

Figure III.1: Numerical integration result for the parameter set $f_2 = 0$, $\mathcal{C} = 0$, $g_0 = 0$. For any N, while the amplitude of Ψ here exponentially increases (central column) with a, the initial shape is conserved unchanged (right column).

Numerically integrating the WDW equation (eq. (III.13)) is fairly straightforward. The equation is hyperbolic, and one can use the expansion around $a = 0$ described by eq. (III.14) as the initial condition on a constant-a hypersurface, provided that the initial value of a is sufficiently small. The initial condition

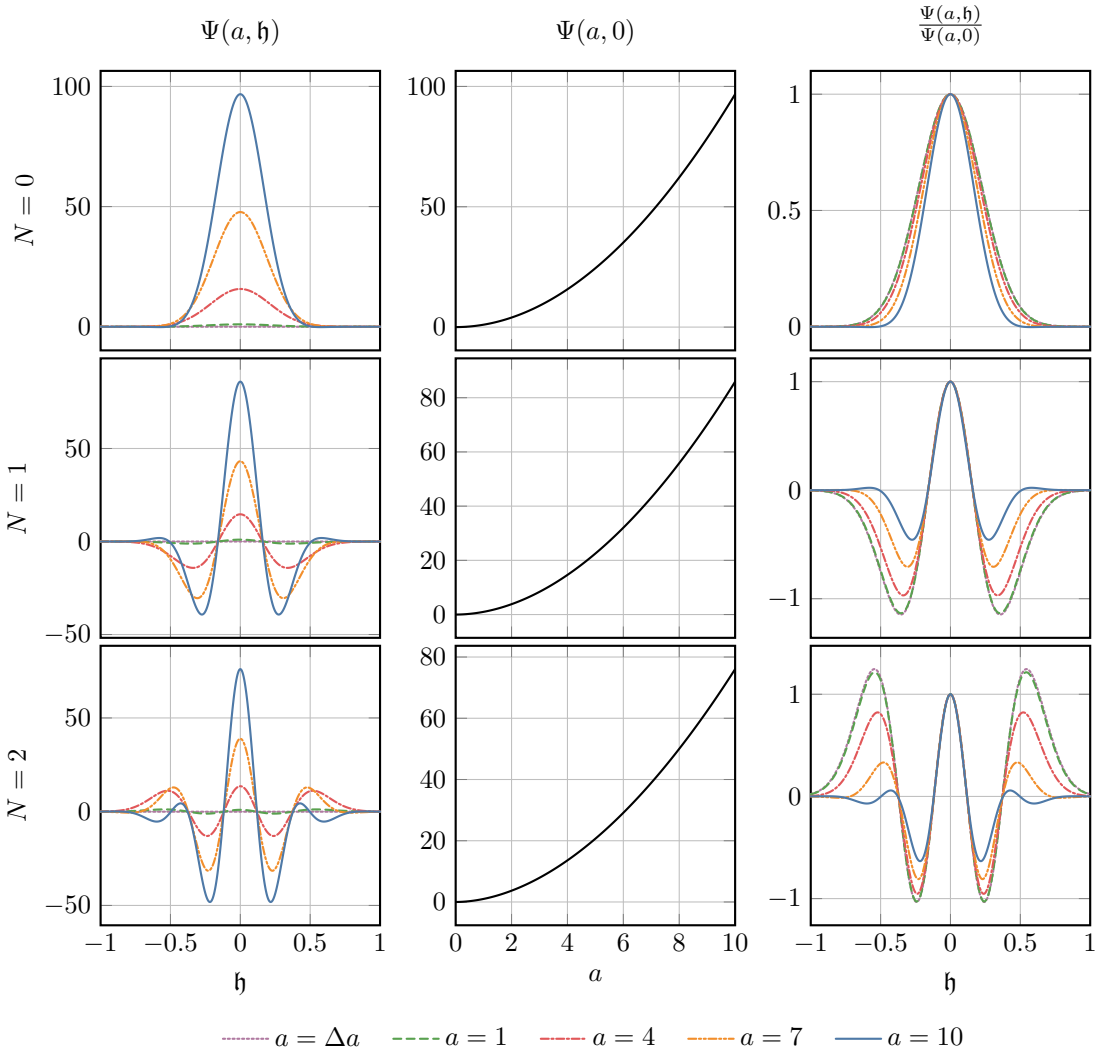

Figure III.2: Numerical integration result for the parameter set $f_2 = 1$, $\mathcal{C} = 0$, $g_0 = 0$. While overall similar, unlike the case $f_2 = \mathcal{C} = g_0 = 0$ of fig. III.1, the shape of the wave function evolves significantly through the "evolution" towards larger a, as the rightmost columns exhibits. Essentially, the amplitude's growth is slowed down the further it is from $\mathfrak{h} = 0$ (central and right columns) as f_2 actually enables a term in $\mathfrak{h}^2$ in eq. (III.26).

is uniquely specified by the non-negative integer N up to an overall amplitude. For concreteness, we fix the overall amplitude by

$$\lim_{a\to+0} a^{-c}\Psi(a,0) = 1\ . \tag{III.25}$$

This translates into $A_N = 1$ for all $N = 0, 1, 2$.

Concretely, in the numerical study, we shall only consider the $3+1$ dimensional case, employ[1] a second-order finite difference scheme for derivatives with respect to $\mathfrak{h}$, and adopt a fourth order Runge-Kutta method to evolve the system with respect to a. To this end, the "space" $\mathfrak{h}$ is sampled on a grid of 40 000 points spaced by $\Delta\mathfrak{h} = 1 \cdot 10^{-4}$. As for the "time", the range in a is discretized into 10^6 steps, each of size $\Delta a = 10^{-1} \cdot \Delta\mathfrak{h} = 1 \cdot 10^{-5}$. We start from the small initial "time" $a = a_0$ by using the solution obtained in section III.2.1—the expansion of eq. (III.14) with eqs. (III.20) and (III.21)—, which is valid for sufficiently small a_0. Here, we choose $a_0 = 10^{-1} \cdot \Delta a = 1 \cdot 10^{-6}$.

For simplicity we set $p = 1$, $g_3 = 2$, $f_3 = 1$, and g_2, g_1, f_1 and f_0 to 0 (with $d = 3$) in all simulations shown hereafter. Then, the Wheeler-DeWitt eq. (III.13) is specified by the remaining parameters f_2, $\mathcal{C}$

[1] A similar code was previously used in ref. [52]

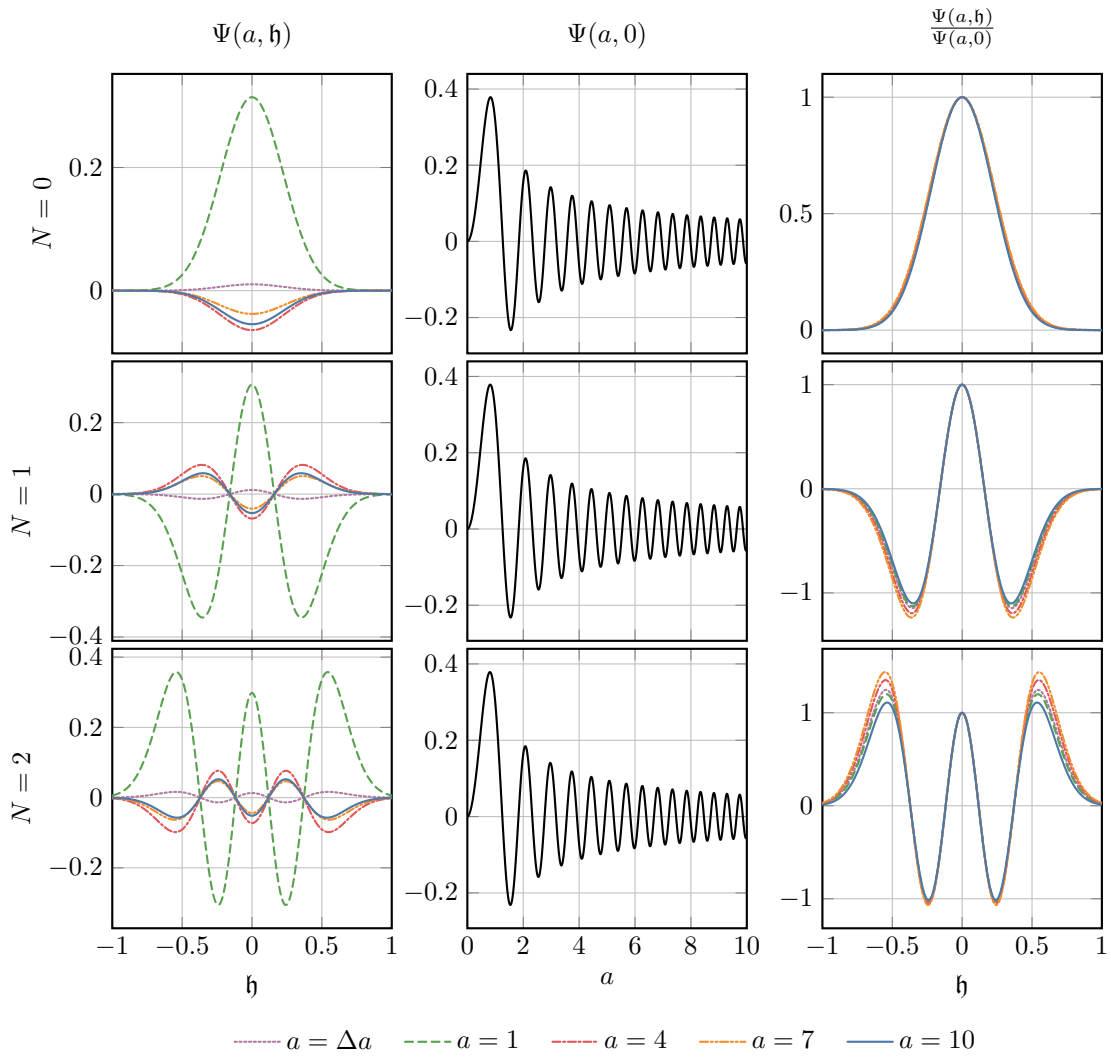

Figure III.3: Numerical integration result for the parameter set $f_2 = 1$, $\mathcal{C} = 10$, $g_0 = 0$. Now that $\mathcal{C}$ is set to 10, a term in a now enters eq. (III.26) and will quickly dominate over the previous $-a^{-2}$ term. In so doing, it brings the system in a regime of damped oscillation (central column). The effect of f_2 (see fig. III.2) remains, though now slightly muted (right column).

(dark matter) and g_0 (dark energy). It thus comes down to the compact expression

$$\left(\frac{1}{2}\left(\frac{\partial^2}{\partial a^2}+\frac{1}{a}\frac{\partial}{\partial a}\right)+\left[\mathcal{C}a-\frac{2}{a^2}+g_0a^4+\left(f_2+\frac{1}{a^2}\right)\frac{\mathfrak{h}^2}{2}\right]-\frac{1}{2\mathcal{V}^2a^2}\frac{\partial^2}{\partial\mathfrak{h}^2}\right)\Psi(a,\mathfrak{h})=0\,. \tag{III.26}$$

From thereon, we show the numerical results in figs. III.1 to III.4, and make some comments.

In the four parameter sets exhibited here, we turn on one after the other each of the three parameters we left free, *i.e.* f_2, $\mathcal{C}$ and g_0. Accordingly, we first set $f_0 = \mathcal{C} = g_0 = 0$ and there are only two non-derivative terms, both of which are proportional to a^{-2}. The result is portrayed in fig. III.1. The system in this case exhibits the exact $z = 3$ anisotropic scaling. The initial input here simply exponentially grows, without its form being altered. This is easily understood by observing the separability of eq. (III.26) with respect to $\mathfrak{h}$ and a. For $f_2 = 1$, on the other hand, a term $\propto \mathfrak{h}^2 \cdot a^0$ enters and, as seen in fig. III.2, visibly modifies the shape of the wave function.

In the next and last two figures, figs. III.3 and III.4, as we set $\mathcal{C}$, and then g_0 to 10 (*i.e.* introducing DM respectively DE), we enable, in order, terms $\propto a$ and $\propto a^4$, in eq. (III.26). They will drive the system into a damped oscillatory regime; g_0a^4 more strongly so than $\mathcal{C}a$. As these come to dominate, the effects of $f_2\mathfrak{h}^2$ and $\mathfrak{h}^2/a^2$, while remaining, are proportionately muted.

Overall, the afore-described behaviors are as expected from eq. (III.26) (or eq. (III.13)). Most importantly, the wave function is obviously well-defined and normalizable on constant-a hypersurfaces,

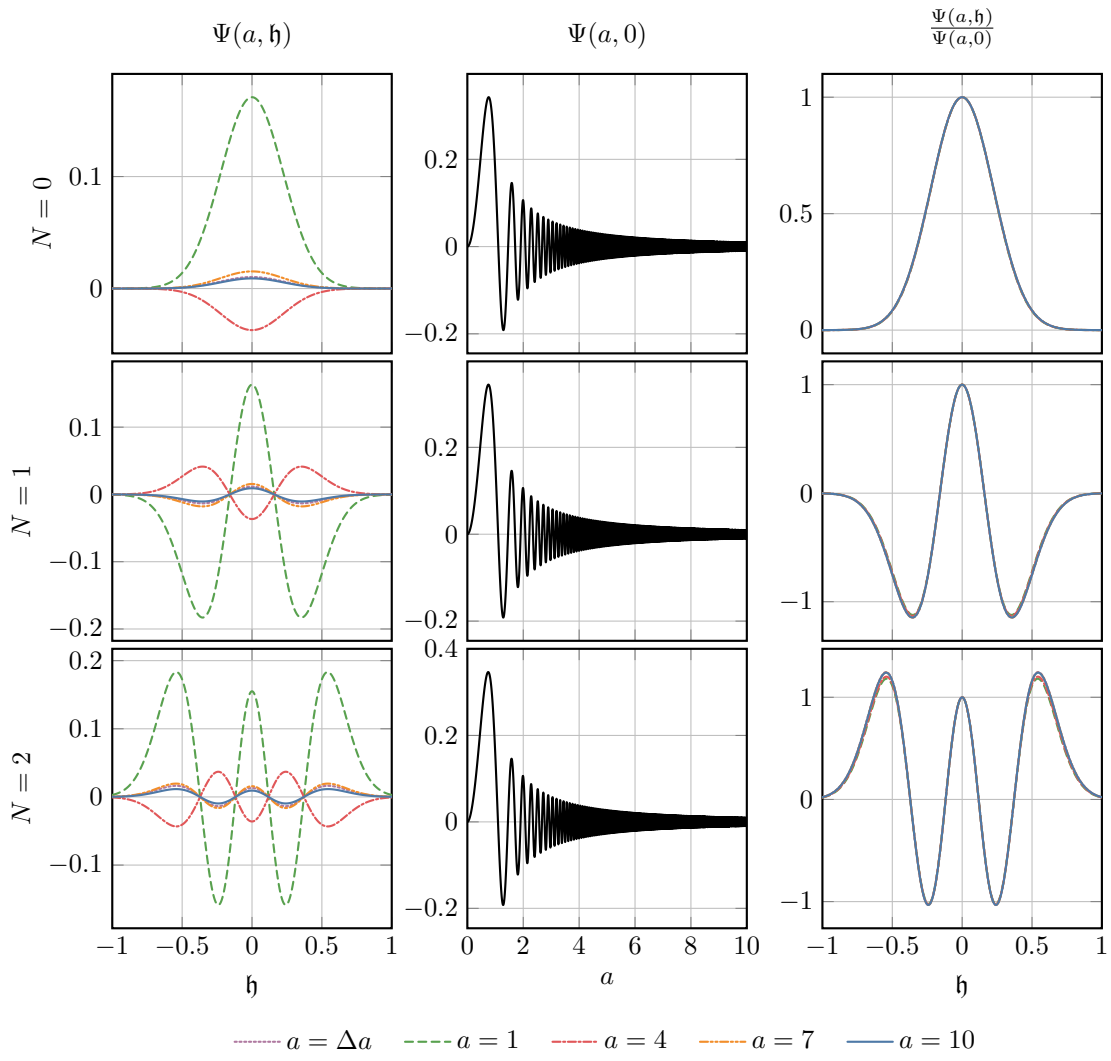

Figure III.4: Numerical integration result for the parameter set $f_2 = 1$, $\mathcal{C} = 10$, $g_0 = 10$. The g_0 coefficient now brings a a^4 term, that will eventually overcome the previous a and $-a^{-2}$ contributions, pushing the system into an even more strongly damped oscillation regime (central column). The influence of f_2 remains visible, though now barely visible (right column).

all the way from the classical big-bang singularity to finite values of a. This is precisely the "desired" behavior.

III.3 Summary

In this chapter, we have investigated the behavior of a $d+1$-dimensional Universe near the classical big-bang singularity based on the Wheeler-DeWitt equation and the DeWitt boundary condition, which amounts to a vanishing wave function of the Universe at the classical singularity. For concreteness we have studied a homogeneous and isotropic background and tensor perturbations around it described respectively by the scale factor a and the amplitude of tensor perturbations $\mathfrak{h}$ as a simple model of the Universe.

In general relativity, the DeWitt wave function for $\mathfrak{h}$ on constant-a hypersurfaces is not normalizable near $a = 0$, meaning that the perturbative expansion breaks down. On the contrary, in Hořava-Lifshitz gravity the higher dimensional operators required by the perturbative renormalizability of the theory render the wave function of the tensor perturbations normalizable, all the way from the classical big-bang singularity at $a = 0$ to finite values of a. The DeWitt wave function for $\mathfrak{h}$ on constant-a hypersurfaces is of a Gaussian shape for the ground state and a Gaussian multiplied by an even polynomial of $\mathfrak{h}$ for excited states. We have analytically proved these behaviors of the wave function near $a = 0$ for any d,

and numerically demonstrated them in a finite interval from $a = 0$ to a finite value of a, for different parameter values, including the corresponding the DM and DE constants.

The results exhibited in this chapter provide strong evidence for close connections between the regularity of the DeWitt wave function of the Universe and the renormalizability of HL gravity.

Chapter IV

Relaxing the cosmological constant

Referring back to the three shortcomings of GR that we listed in section I.4, HL gravity may answer to two. The last one is the CC problem, which is behind the mystery of the DE. Many different paths have been investigated to solve the CC problem, and this is not the first time some CC relaxation processes, as this chapter presents, have been considered. For example, one could consider to have some relaxation that unfolds during an unconventional inflationary phase [170], to work within the framework of some bouncing Universe scenario by dynamically decreasing the value of CC during a contracting phase [171], or to forbid a non-vanishing 4d curvature of a maximally symmetric 3-brane world-volume embedded in 5d spacetime [172]). Ideally, one's solution should eventually be linked to some observational signatures (*e.g.* [173]).

The approach we are about to detail hereafter does not yet expose itself to this last test and rather provides a proof of concept at this stage. It remains within the realm of effective field theories and should still be adaptable for further considerations.

References [54, 53] proposed a model that dynamically relaxes the value of the CC to a tiny one thanks to a scalar field that forever rolls down its potential [1]. The kinetic term of this field is modulated by a negative power of the Ricci scalar, and its apparent divergence in the limit of vanishing curvature is dynamically prohibited by the classical motion of the scalar background. The relaxation mechanism operates as the potential of the scalar field dominates over the kinetic term in the same limit, and yet the dynamics results in a vanishing potential, which is the future attractor of the system. Importantly, the potential can include not only that of the scalar itself but also *all the other (constant) energy contents*, that is,

$$V_{\text{total}} = V_{\text{scalar alone}} + V_{\text{c.c.}} + V_{\text{zero point}} + V_{\text{all others}} \,, \tag{IV.1}$$

and what approaches to zero is V_{total}; in a way, the scalar field dynamically fixes its potential value $V_{\text{scalar alone}}$ only to cancel the CC, the zero point energy and all the other (constant) contributions. Therefore even if large bare cosmological constant and radiative zero point energy were present, the effective vacuum energy would go as $\Lambda_{\text{eff}} \approx V_{\text{total}}/M_{\text{Pl}}^2 \to 0$ after a long time, and the spacetime geometry would anyway approach a flat one.

This relaxation mechanism partially holds a spirit similar to what Weinberg called "adjustment mechanism" in ref. [83]. The related no-go theorem [83, 174, 85] is evaded in the current mechanism thanks to the fact that, while the theorem only considers the physics at a dynamical equilibrium and thus assumes translational invariance, an essential ingredient of the mechanism considered here is the non-vanishing canonical momentum of the scalar field, rendering the mechanism considered here an exceptional case to the theorem.

However, while this process alone is a powerful mechanism to resolve the CC problem, it also effectively empties the Universe as an inevitable consequence, by eventually diluting everything away: the total energy in the Universe — which includes any radiative corrections — is constrained to asymptotically converge to a null value. To connect this empty space to our present Universe, the main purpose of this work is to implement a reheating phase after the c.c relaxation so that the standard hot big bang scenario is revived. To this aim, we not only construct a stable model that achieves the scenario, but also demonstrate it by exhibiting a concrete realization along a numerical verification.

For the reheating phase, we rely in part on the Lagrangian of the Horndeski theory [33, 31, 32], as using the latter has been shown to allow to violate the NEC in a stable manner [73, 175]. The gravitating energy elevated by the NEC violation is then transferred to another sector that eventually reheats the Universe.

[1] This scalar field corresponds to φ_1 in later sections, where the subscript number is introduced to distinguish among the three scalar fields that are involved in the different processes in our scenario.

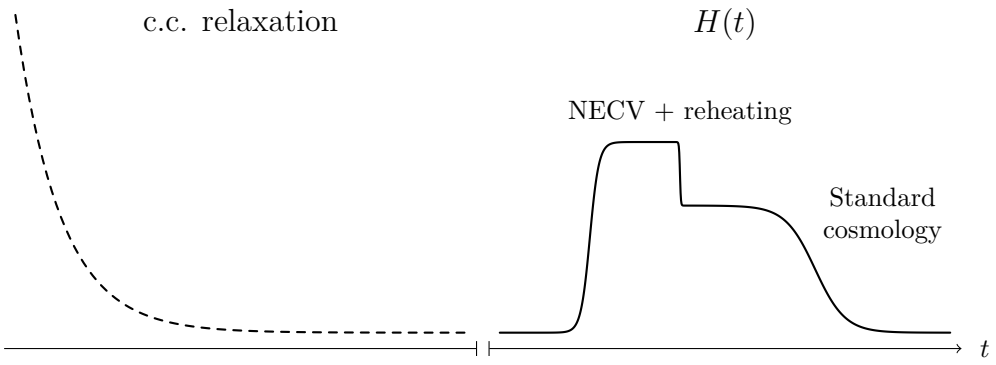

Figure IV.1: Schematic illustration of the cosmic evolution according to the scenario described in this chapter. The dashed curve on the left corresponds to the initial phase of the CC relaxation, and the solid curve on the right depicts the NEC violation and the reheating dynamics. The Universe is eventually filled with radiation and recovers the standard cosmic history. This figure is highly schematic and not to scale.

In order not to disrupt the CC relaxation mechanism, which is always in action, the NEC-violating and reheating phases must occur for sufficiently short time compared to the time scale of the relaxation. Moreover, we assume that these phases take place periodically, and our observed Universe can be the result from any one of those recurring occurrences. *In fine*, the dynamical cosmological constant relaxation described by our model would thus allow us to avoid invoking the anthropic principle to solve the CC problem, as described in section I.4.2+.

This chapter introduces a new model. To this aim, we start by describing the overall cosmic history model subsequently built aims to achieve. We also take this occasion to review the cosmological relaxation process it employs (section IV.1). The NEC-violating and the reheating sectors are then assessed from a theoretical perspective by considering their linear perturbations, explicitly providing the conditions under which we avoid having any ghost or gradient instability against the background dynamics of the desired behavior (section IV.2). We shall then focus on the reheating process, and the model and all its composing functions are now either explicitly chosen or deduced (section IV.3). Lastly, we add a numerical approach to explicitly and qualitatively witness the whole reheating process unfold (section IV.4), before concluding this chapter (section IV.5).

IV.1 Overall picture of the cosmic history

The vacuum energy that drives the accelerated cosmic expansion at the present time is, whatever its true nature is, observed to have an extremely small value, and this smallness demands an explanation. We explore a dynamical solution to this issue, and in this regard, we employ the mechanism originally proposed in refs. [54, 53]. However this mechanism alone leads to an empty universe, that is, it not only reduces the contribution from the CC but also dilutes all other contents of the Universe. In order to incorporate an additional process to eventually populate the Universe with energetic radiation, a couple of potential candidates have been sketched in ref. [176]. Our mechanism shares some aspects with their "fast violation" section but extends it further. We later provide a concrete realization of the reheating (section IV.3) and show with numerical analyses that the scenario can indeed be achieved without any instability (section IV.4).

To this end, the mechanism we propose incorporates three essential phases of cosmic history, namely and in order:

1. **Cosmological constant relaxation.** A large valued CC, together with all the other matter content, is dynamically relaxed to the small present value (section IV.1.1 for summary and [53, 54] for details).

2. **Null energy condition violation.** The Universe is energetically revived by accommodating a phase violating the NEC (section IV.1.2 for summary and section IV.3 for details).

3. **Reheating.** The Universe reheats and connects this process to the standard cosmological picture (section IV.1.2 for summary and section IV.3 for details).

This overall picture is schematically illustrated in fig. IV.1. After the relaxation, the NEC violation re-energizes the Universe, which is the first rise of H in the figure; after some time, H abruptly drops to some non-zero value, corresponding to the end of the NEC-violating phase during which a fraction of energy is transferred to the reheating sector. Eventually this sector decays to radiation, recovering the standard big bang cosmic history. We assume that the potential for the NEC-violating sector is periodic so that the sequence described above (the CC relaxation, NEC violation and reheating) repeats many times until the CC actually goes down to the observed tiny value.

The model setup can thus be described by the action

$$S = \int \mathrm{d}^4x\sqrt{-g}\left(\mathcal{L}_{\mathrm{E.H.}}[g_{\mu\nu}] + \mathcal{L}_{\mathrm{c.c.\,relax}}[\varphi_1, g_{\mu\nu}] + \mathcal{L}_{\mathrm{NECV+reh}}[\varphi_2, \varphi_3, g_{\mu\nu}]\right), \tag{IV.2}$$

where $\mathcal{L}_{\mathrm{E.H.}}$, $\mathcal{L}_{\mathrm{c.c.\,relax}}$ and $\mathcal{L}_{\mathrm{NECV+reh}}$ describe the Einstein-Hilbert part, the CC relaxation mechanism, and the combined sector of NEC violation and reheating, respectively. The fields φ_1, φ_2 and φ_3 are responsible for the CC relaxation, NEC violation and reheating, respectively, and g denotes the determinant of the spacetime metric g_{ij}. Let us note that, as we observe here and concretely show in section IV.3, the reheating sector is nontrivially coupled to the NEC-violating sector, and thus they are not separable at the level of Lagrangian. In the following subsections, we summarize the gist of the CC relaxation, NEC violation and reheating sectors individually and the requirements to achieve the desired history of the Universe.

IV.1.1 Cosmological constant relaxation

We follow [54, 53] and introduce a model that drives an initially large CC to the tiny value observed today, and this subsection serves as a brief review of its mechanism. This relaxation mechanism is driven by a scalar field φ_1 that is non-minimally coupled to gravity, and the corresponding Lagrangian $\mathcal{L}_{\mathrm{c.c.\,relax}}$ together with the Einstein-Hilbert part $\mathcal{L}_{\mathrm{E.H.}}$ introduced in eq. (IV.2) reads

$$\mathcal{L} = \overbrace{\underbrace{\frac{M_{\mathrm{Pl}}^2}{2}R}_{\mathcal{L}_{\mathrm{E.H.}}} + \underbrace{\alpha R^2 + \frac{X_1}{f(R)} - V_1(\varphi_1)}_{\mathcal{L}_{\mathrm{c.c.\,relax}}}}^{\text{gravity}}, \tag{IV.3}$$

where we hereafter denote the kinetic terms of scalar fields φ_i $(i = 1, 2, 3)$ by

$$X_i \equiv -\frac{1}{2}\, g^{\mu\nu}\partial_\mu\varphi_i\partial_\nu\varphi_i\,, \tag{IV.4}$$

and where R is the Ricci scalar associated with the spacetime metric $g_{\mu\nu}$, V_1 the potential of φ_1, and M_{Pl} and α are the (normalized) reduced Planck mass and a dimensionless constant, respectively. The curvature quadratic term αR^2 with *e.g.* $\alpha = \mathcal{O}(1)$ (> 0) is needed to tame the instability that would otherwise arise during the course of relaxation. The term is purely gravitational and thus could in principle be combined with the Einstein-Hilbert term $\mathcal{L}_{\mathrm{E.H.}}$ to together compose a gravitational action. Nevertheless, since it only affects the stability during the relaxation and becomes negligible at later stages of our scenario, we simply include it in $\mathcal{L}_{\mathrm{c.c.\,relax}}$ as expressed in eq. (IV.3) [2]. Note that any non-zero CC term, including the vacuum energy originated from the quantum fluctuations of matter fields, can be absorbed into $V_1(\varphi_1)$ without loss of generality.

A crucial part for the mechanism to work is that the coefficient of the kinetic term of φ_1 diverges in the limit of vanishing R. To this end, we demand that f vanishes at $R = 0$ as

$$f(R) \approx \left(\frac{R^2}{M_{\mathrm{Pl}}^4}\right)^m, \tag{IV.5}$$

[2] Other higher-order terms of curvature invariants such as $R_{\mu\nu}R^{\mu\nu}$ and $R_{\mu\nu\rho\sigma}R^{\mu\nu\rho\sigma}$ should arise due to quantum corrections. We can always rearrange a linear combination of R^2, $R_{\mu\nu}R^{\mu\nu}$ and $R_{\mu\nu\rho\sigma}R^{\mu\nu\rho\sigma}$ into another one of R^2, the Gauss-Bonnet term and the Weyl tensor squared. Since the Gauss-Bonnet term does not contribute to equations of motion, and the Weyl squared term is responsible for the ghost modes in UV, we call the coefficient of R^2 in this linear combination as α appearing in eq. (IV.3). Unless fine-tuned, the coefficients of those higher curvature terms are expected to be of $\mathcal{O}(1)$ in the units of M_{Pl}, and the would-be ghost modes associated with them have masses of order M_{Pl}. Therefore the higher-order terms are irrelevant at energies and momenta sufficiently below the Planck scale, with which we are concerned, and the stability only requires $\alpha > 0$ in IR.

where m is some positive number and we assume $m > 3/2$ for the reason that we explain later in this subsection. The constant $M_{\rm Pl}^4$ is introduced to make the function dimensionless, and the overall normalization of f can always be absorbed by redefining X_1. Since the kinetic term depends nonlinearly on the curvature, the system described by the Lagrangian (IV.3) contains two scalar degrees of freedom. It is straightforward to show that both scalar degrees satisfy the no-ghost condition and that the two speeds of propagation are both unity in the low-energy regime [3].

Starting with the kinetic Lagrangian of the assumed form $X_1/f(R)$, quantum corrections may generate a more general kinetic Lagrangian consisting of terms of the form $X_1^{q_i}/(R^2/M_{\rm Pl}^4)^{m_i}$ $(i = 1, 2, \cdots)$. In this case, what controls the CC relaxation is the most singular-looking term. Fortunately, the more singular-looking the dominant term is, the more robust the CC relaxation mechanism is. Therefore, less singular-looking terms generated by quantum corrections do not spoil the CC relaxation mechanism, while more singular-looking terms generated by quantum correction simply strengthen it. See [54] for some details. In the rest of the present chapter, for simplicity, we consider the simplest kinetic Lagrangian consisting of a term with $q_i = 1$ and $m_i = m > 3/2$.

Another important ingredient is that the potential $V_1(\varphi_1)$ crosses zero at some finite value of φ_1. Starting the evolution from a positive value of V_1, φ_1 rolls down the potential and approaches 0, around which V_1 can be well approximated by a linear form

$$V_1(\varphi_1) \simeq c M_{\rm Pl}^3 \, (\varphi_1 - v) \ , \tag{IV.6}$$

where v is the value of φ_1 at which the potential would cross 0 and c is some dimensionless constant. Then, on the flat Friedmann-Lemaître-Robertson-Walker (FLRW) background, the equation of motion for the homogeneous background of φ_1, denoted by $\bar{\varphi}_1$, takes the form

$$\frac{\partial \Pi_1}{\partial \mathcal{N}} + (3 + \epsilon) \, \Pi_1 + c = 0 \ , \tag{IV.7}$$

where H is the Hubble expansion rate, $\mathcal{N} \equiv \ln a$ is the number of e-folds with a being the scale factor, $\Pi_1 \equiv H^2 \partial_{\mathcal{N}} \bar{\varphi}_1 / (M_{\rm Pl}^3 f)$, and $\epsilon \equiv -\partial_{\mathcal{N}} H / H$. Eq. (IV.7) makes it evident that, for a negligible time variation of ϵ, the stationary solution is given by $\Pi_1 \simeq -c \, (3 + \epsilon)^{-1}$.

At late time the first Friedmann equation around the stationary solution takes the approximate form, that is,

$$V_1 \simeq 3 M_{\rm Pl}^2 H^2 \ . \tag{IV.8}$$

This equation, together with the aforementioned result, leads to the time variation of V_1 as

$$\frac{\partial}{\partial \mathcal{N}} \left(\frac{2 V_1}{M_{\rm Pl}^4} \right)^{2-2m} \simeq 24 \, c^2 \, (m - 1) \, \frac{(2 - \epsilon)^{2m}}{3 + \epsilon} \simeq 2^{2m+3} \, c^2 \, (m - 1) \ , \tag{IV.9}$$

where in the last equality the fact that ϵ is small during the relaxation phase is used. This result shows that, when V_1 approaches to 0, the field $\bar{\varphi}_1$ in fact stalls, and V_1 never crosses 0, namely

$$V_1 \to +0 \qquad \text{as} \quad \mathcal{N} \to +\infty \tag{IV.10}$$

is the asymptotic behavior, provided that $m > 3/2$ as we have assumed. In fact, the behavior (IV.10) only requires $m > 1$ besides the smallness of ϵ. However, if the scalar kinetic term X_1/f in eq. (IV.3) dominated over the αR^2 term at low energy ($H \ll M_{\rm Pl}$), the dynamics of the system would destabilize the stationary solution above [54]. To prevent this, we demand $X_1/f < \alpha R^2$ at low energy, which can be achieved for $m > 3/2$ and is self-consistent with the solution obtained above.

The essence of the mechanism to relax a large CC is as described above. It is worth stressing that the most important ingredient is the coefficient of X_1 in eq. (IV.3) that has a singular-looking form in the limit $R \to 0$, and this mechanism is effective as long as the most singular term among many other possible ones has the behavior described here. While quantum corrections should produce additional regular operators in the action, the motion of $\bar{\varphi}_1$ nonetheless drives the total potential to the vanishing value. On the other hand, one can show that quantum corrections do not generate a potential that is singular at $R = 0$. Singular-looking kinetic terms of the form $X_1^{q_i}/(R/M_{\rm Pl}^2)^{2m_i}$ $(i = 1, 2, \cdots)$ can be generated by quantum correction but this does not cause a problem. Actually, the more singular-looking the radiatively-corrected kinetic term is, the more robust the CC relaxation mechanism becomes.

Now, we have achieved a tiny value of the CC/vacuum energy after a sufficiently long time. However, by that same achievement, since, under the condition $m > 3/2$, the potential V_1 approaches zero more slowly than matter and radiation, the Universe would be empty after the mechanism under consideration takes place. The Universe thus needs to be "reheated" once the CC is driven to a small value. This is the subject of the subsequent subsections, and is the main purpose of our present study.

[3] See *e.g.* section V.A.4 of [177].

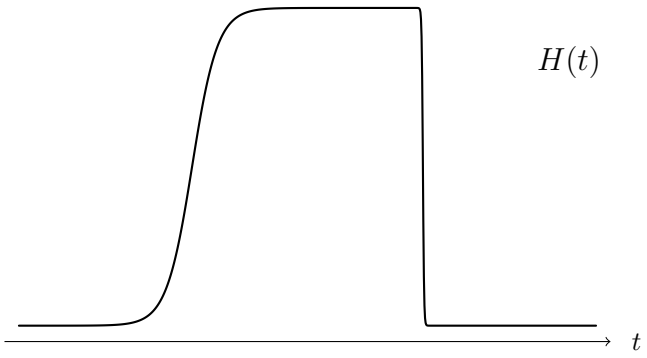

Figure IV.2: Schematic illustration for the Hubble history, with H the Hubble expansion rate. This figure is simplified in that it only extracts the behavior of the target NEC violation, with all the other sectors, including the CC relaxation and reheating sector, turned off.

IV.1.2 Null energy condition violation and reheating

After the mechanism in section IV.1.1 operates, not only the CC and vacuum energy but also all other energy contents decrease to a negligible value. In order to connect to the known cosmic thermal history, "reheating" thus needs to subsequently take place to re-populate the Universe with energetic radiation. The NEC is necessarily violated to achieve this scenario, in order for the energy required for reheating to be temporarily available. Another field that mediates the reheating process is destabilized through its coupling to the NEC-violating sector, and its acquired energy is finally transferred to radiation.

In order to stably violate the NEC we employ a subclass of the Horndeski theory [31, 32, 33], previously recalled in section II.1.3, whose scalar field is now denoted by φ_2. The reheating field φ_3 couples to this sector, and we introduce direct couplings besides the gravitational one for efficient energy transfer. A minimal setup that satisfies these requirements adopts the following form of the Lagrangian in eq. (VI.2),

$$\mathcal{L}_{\rm NECV+reh} = K(\varphi_2, X_2, \varphi_3) - G_3(\varphi_2, X_2, \varphi_3)\,\Box\varphi_2 + P(\varphi_3, X_3)\ , \tag{IV.11}$$

where φ_2 invokes the NEC violation. Here K and G_3 are some functions of φ_2, X_2 and φ_3, while P is a function of φ_3 and X_3 only. The reheating field φ_3 is implicitly coupled to radiation. For simplicity we assume that $\mathcal{L}_{\rm NECV+reh}$ is in the Einstein frame and hence the total Lagrangian that is relevant to the present mechanism is $\mathcal{L}_{\rm E.H.} + \mathcal{L}_{\rm NECV+reh}$. As far as φ_1 stays almost constant, this assumption is expected to be valid since, as explicitly shown in ref. [54] for linear perturbations, the model (IV.3) recovers general relativity at low energy. For the consistency of this treatment, we shall later clarify what we precisely mean by being "almost constant" and obtain the condition under which φ_1 stays almost constant during the NEC violation and reheating.

The CC relaxation sector discussed in section IV.1.1 is decoupled from the rest of the physics except through gravity. The relaxation mechanism continues to operate throughout the cosmic history to keep the vacuum energy from overdominating the Universe. Since it takes many (current) Hubble times to make the CC small enough, we assume that the functions K and G_3 are periodic in the NEC-violating field φ_2 so that a NEC-violating phase occurs periodically and (partial) reheating may occur several times. This is done in order to avoid invoking any miraculous fine-tuning with respect to the timing of reheating. On top of the periodicity, we assume that the functions of φ_2 enjoy an approximate shift symmetry for most of its domain and that the NEC violation (and reheating) is restricted to a short duration where this approximate shift symmetry is broken.

For the purpose of presentation, let us for the moment turn off the reheating sector φ_3 in order to focus on the NEC violation part. The Lagrangian of eq. (IV.11) is then reduced to just

$$\mathcal{L}_{\rm NECV} \equiv \mathcal{L}_{\rm NECV+reheat}\big|_{\varphi_3=0,\ P=0} = \tilde{K}(\varphi_2, X_2) - \tilde{G}_3(\varphi_2, X_2)\,\Box\varphi_2\ , \tag{IV.12}$$

where $\tilde{K} \equiv K|_{\varphi_3=0}$ and $\tilde{G}_3 \equiv G_3|_{\varphi_3=0}$. For simplicity we adopt the following ansatz for $\tilde{K}$ and G_3, keeping only terms lower-order in X_2,

$$\tilde{K} = \tilde{f}_1(\varphi_2)\,X_2 + \tilde{f}_2(\varphi_2)\,X_2^2 - \tilde{V}(\varphi_2)\ , \qquad \tilde{G}_3 = \tilde{f}(\varphi_2)\,X_2\ . \tag{IV.13}$$

The functions $\tilde{f}_1$, $\tilde{f}_2$ and $\tilde{f}$ are periodic in φ_1 with a common period and should have appropriate forms – their respective forms we consider in the present study, especially for the purpose of numerical evaluations,

are fixed according to the desired evolution of the Hubble expansion rate H and are reconstructed using the equations of motion. This procedure is discussed in detail in section IV.3.1. With these potential and kinetic structures, the motion of φ_2 accomplishes to violate the NEC and increases the value of H for some finite time. A schematic shape of the resultant evolution of H with the NEC violation is illustrated as a function of time in fig. IV.2. In this figure, all the matter contents other than the NEC-violating φ_2 are excluded. Once the reheating sector φ_3 couples to φ_2, the behavior of H is modified to the one captured in fig. IV.1.

In order to reheat the Universe, the reheating field φ_3 transfers the energy acquired during the NEC-violating period to radiation. It thus couples to φ_2, and this is realized by reintroducing the φ_3 dependence into the previous functions. Formally, we make the changes

$$\tilde{f}_{1,2}(\varphi_2) \;\to\; f_{1,2}(\varphi_2,\varphi_3)\,, \qquad \tilde{f}(\varphi_2) \;\to\; f(\varphi_2,\varphi_3)\,, \qquad \tilde{V}(\varphi_2) \;\to\; V(\varphi_2,\varphi_3)\,, \tag{IV.14}$$

and reintroduce $P(\varphi_3, X_3)$. For simplicity we assume that φ_3 is a canonically normalized scalar with a simple potential, except for its coupling to φ_2 via (IV.14). In mathematical terms, P, in eq. (IV.11), takes the form

$$P(\varphi_3, X_3) = X_3 - U(\varphi_3)\,. \tag{IV.15}$$

Thanks to these couplings in (IV.14), the effective potential of φ_3 basically changes over time with respect to the motion of φ_2. As already invoked, we assume that φ_2 enjoys approximate shift symmetry for most of its domain except for the short NEC violating period. This in particular means that the effective potential for φ_3 changes only in the vicinity of the NEC violating period. We choose the coupling between φ_2 and φ_3 so that, once the NEC violation starts operating, the effective potential forms a new local minimum in which φ_3 gets trapped. After the NEC-violating phase ends, φ_3 stays at a new minimum for a while, but, after a finite time, it eventually rolls back to the initial true minimum of the potential, around which it oscillates and thus drives the reheating. For illustration of these behaviors, we refer to fig. IV.5. These phase transitions in φ_3 triggered by φ_2 are the essential ingredient of our reheating mechanism.

Due to the approximate shift symmetry in the φ_2 direction, the system away from the NEC violation (and reheating) period realizes a phase of ghost condensation [135, 178] and the stress-energy tensor from $\mathcal{L}_{\rm NECV+reheat}$ acts as an additional contribution to the CC. Without loss of generality, this additional contribution to the CC can be absorbed into $V_1(\varphi_1)$ so that the CC away from the NEC violation (and reheating) period is precisely $V_1/M_{\rm Pl}^2$.

While this process of the NEC violation and reheating is overall decoupled from the first scalar field φ_1, one still has to be careful of the risk of overshooting. Indeed, the NEC violating and reheating eras break the simple relation (IV.8) between the potential V_1 for φ_1 and the spacetime curvature, the latter of which controls the relation between Π_1 and $\dot{\tilde{\varphi}}_1$. During the NEC violation and reheating eras, the equation (IV.7) for Π_1 is unchanged and thus $\Pi_1 = -c \times \mathcal{O}(1)$ still holds. On the other hand, $f(R)$ suddenly increases and affects the value of $\dot{\tilde{\varphi}}_1 = M_{\rm Pl}^3 H^{-1} f \Pi_1$. As a result, the field φ_1 rolls down its potential V_1 faster and may overshoot the zero of V_1. Because of this risk, the NEC-violating part should not last indefinitely; it needs to be constrained in time.

To better understand the issue at hand, let us consider the following calculations. Close to the zero of its potential V_1, the field φ_1 follows a smooth evolution. Before the NEC violation and reheating, V_1 is (virtually) locked at a height of say $V_{\rm pre} > 0$. To avoid a runaway down the potential into effectively negative CC, the potential after the NEC violation and reheating, denoted as $V_{\rm after} \equiv V_{\rm pre} + \Delta V_1$, must stay above zero. We thus require

$$|\Delta V_1| < V_{\rm pre} \tag{IV.16}$$

during the NEC violation and reheating. One can easily estimate ΔV_1 as

$$\Delta V_1 \approx c M_{\rm Pl}^3 \dot{\tilde{\varphi}}_1 \Delta t = -c^2 M_{\rm Pl}^6 \frac{f}{H}\,\Delta t \times \mathcal{O}(1) = -c^2 M_{\rm Pl}^6 \frac{f}{H}\,\frac{\Delta\varphi_2}{M^2} \times \mathcal{O}(1)\,, \tag{IV.17}$$

where Δt and $\Delta\varphi_2$ are the time duration and the corresponding field range of the NEC violating and reheating period, f is supposed to be estimated during this period, and we have assumed that the speed of φ_2 takes an approximately constant value, $\dot{\varphi}_2 \simeq M^2$. The last assumption will be explicitly confirmed by the example in section IV.3. Let us denote by V_2 ($\gg V_1$) the effective energy density of φ_2, *i.e.* $V_2 \approx 3M_{\rm Pl}^2 H^2$, during the NEC violation. Then, the condition of eq. (IV.16) translates to a condition on $\Delta\varphi_2$, *i.e.* how long the NEC violation can last in the field space, namely, neglecting order-one numerical factors,

$$\frac{\Delta\varphi_2}{M} \lesssim \frac{M}{c^2 M_{\rm Pl}} \left(\frac{M_{\rm Pl}^4}{V_2}\right)^{(4m-1)/2} \frac{V_{\rm pre}}{M_{\rm Pl}^4}\,. \tag{IV.18}$$

As the Universe experiences many sequences of the CC relaxation, NEC violation and reheating, this condition must be satisfied by every sequence all the way down to the last one before the present epoch that we live today, each time with a different (decreasing) value of $V_{\rm pre}$. Barring accidental cancellation between $V_{\rm pre}$ and ΔV_1 for the last sequence, this requirement is fulfilled if and only if

$$\frac{\Delta\varphi_2}{M} \lesssim \frac{M}{c^2 M_{\rm Pl}} \left(\frac{M_{\rm Pl}^4}{V_2}\right)^{(4m-1)/2} \frac{\Lambda_{\rm obs}}{M_{\rm Pl}^2} \,, \tag{IV.19}$$

where $\Lambda_{\rm obs}$ is the observed value of the cosmological constant, corresponding to the present value of the φ_1 potential $V_1|_{\rm now} = M_{\rm Pl}^2 \Lambda_{\rm obs}$. Recalling that the parameter m must take a value $m > 3/2$, this result says that no matter how large the NEC violation is, *i.e.* how large V_2 is, one can always achieve a sufficiently long period of it to support reheating for a sufficiently large value of m. We can thus safely pass over the overshooting problem.

IV.2 NECV and reheating sectors: background and perturbation

In this section we analyze the background system of the NEC-violating and reheating sectors and the perturbations around it, in order to find the parameter space in which it is stable against small perturbations. We do not include the CC relaxation sector φ_1 in the present analysis to avoid extra computational complexity; the φ_1 sector has supposedly decreased to a negligible amount by the time this analysis becomes relevant[4], provided that the condition (IV.19) is satisfied. Hence, the action of our interest in this section is

$$\begin{aligned} S &= \int \mathrm{d}^4x\sqrt{-g}\,(\mathcal{L}_{\rm EH} + \mathcal{L}_{\rm NECV+reheat}) \\ &= \int \mathrm{d}^4x\sqrt{-g}\left[\frac{M_{\rm Pl}^2}{2}R + K(\varphi_2, X_2, \varphi_3) - G_3(\varphi_2, X_2, \varphi_3)\,\Box\varphi_2 + P(\varphi_3, X_3)\right] \,, \end{aligned} \tag{IV.20}$$

where φ_2 and φ_3 are scalar fields for the NEC-violating and reheating sectors, respectively. We expand the two scalar fields as

$$\varphi_2(t,\boldsymbol{x}) = \bar\varphi_2(t) + \delta\varphi_2(t,\boldsymbol{x}) \,, \qquad \varphi_3(t,\boldsymbol{x}) = \bar\varphi_3(t) + \delta\varphi_3(t,\boldsymbol{x}) \,, \tag{IV.21}$$

where $\bar\varphi_2(t)$ and $\bar\varphi_3(t)$ are the homogeneous background quantities, and $\delta\varphi_2$ and $\delta\varphi_3$ are their respective perturbations. For the spacetime metric we conduct the ADM decomposition, as in section I.2,

$$\mathrm{d}s^2 = -N^2\mathrm{d}t^2 + \gamma_{ij}\left(N^i\mathrm{d}t + \mathrm{d}x^i\right)\left(N^j\mathrm{d}t + \mathrm{d}x^j\right) \,, \tag{IV.22}$$

where N and N^i are the lapse and shift functions, respectively, and γ_{ij} is the 3-D spatial metric. We decompose these variables into their background and perturbations as (we follow here the notation of *e.g.* [33])

$$N(t,\boldsymbol{x}) = \bar N(t)\,[1 + \alpha(t,\boldsymbol{x})] \,, \tag{IV.23a}$$

$$N^i(t,\boldsymbol{x}) = \frac{\bar N(t)}{a(t)}\left[\partial_i\beta(t,\boldsymbol{x}) + B^i(t,\boldsymbol{x})\right] \,, \tag{IV.23b}$$

$$\begin{aligned} \gamma_{ij}(t,\boldsymbol{x}) = a^2(t)\,\mathrm{e}^{2\zeta(t,\boldsymbol{x})}\Big[&\delta_{ij} + 2\,\partial_i\partial_j\mathcal{E}(t,\boldsymbol{x}) + 2\,\partial_{(i}E_{j)}(t,\boldsymbol{x}) \\ &+ h_{ij}(t,\boldsymbol{x}) + \frac{1}{2}\,h_{ik}(t,\boldsymbol{x})\,h_{kj}(t,\boldsymbol{x})\Big] \,, \end{aligned} \tag{IV.23c}$$

where $\bar N$ and a are the background lapse and scale factor, respectively, $\{\alpha, \beta, \zeta, \mathcal{E}\}$ are scalar modes, the vector modes $\{B_i, E_i\}$ satisfy the transverse conditions $\partial_i B_i = \partial_i E_i = 0$, and the tensor modes $\{h_{ij}\}$ are transverse and traceless: $\partial_i h_{ij} = h_{ii} = 0$. This latter condition thus brings the number of degrees of freedom of the tensor sector from 6 to 2. Under the general coordinate transformation $x^\mu \to x^\mu + \xi^\mu(t,\boldsymbol{x})$, each variable transforms as

$$\begin{aligned} &\Delta\alpha = \frac{\partial_t(\bar N\xi^0)}{\bar N} \,, \quad \Delta\beta = \frac{a^3}{\bar N}\,\partial_t\xi_L - a\bar N\xi^0 \,, \quad \Delta\zeta = H\bar N\xi^0 \,, \quad \Delta\mathcal{E} = \xi_L \,, \\ &\Delta B^i = \frac{a}{\bar N}\,\partial_t\xi_T^i \,, \quad \Delta E_i = \xi_T^i \,, \qquad\qquad \Delta h_{ij} = 0 \,, \end{aligned} \tag{IV.24}$$

[4]For the analysis on the perturbative stability of the φ_1 sector alone, we would like to direct readers to [54, 53].

and

$$\Delta\delta\varphi_2 = \partial_t\bar{\varphi}_2\,\xi^0\,, \qquad \Delta\delta\varphi_3 = \partial_t\bar{\varphi}_3\,\xi^0\,, \tag{IV.25}$$

where the decomposition $\xi^i = \delta^{ij}\partial_j\xi_L + \xi^i_T$ with $\partial_i\xi^i_T = 0$ has been used, and H is the Hubble expansion rate. Using the previous symmetry and appropriately choosing ξ^μ, we fix the gauge by setting

$$\delta\varphi_2 = \mathcal{E} = E_i = 0\,, \qquad \text{gauge fixing}\,, \tag{IV.26}$$

leaving us with no further gauge freedom. Then at the level of linear perturbations, the remaining vector modes B^i are nondynamical and fixed to null by constraints, and they can hence be omitted from our discussion altogether. Thus our system of perturbations consists of the two sectors

$$\begin{cases} \alpha\,,\ \beta\,,\ \zeta\,,\ \delta\varphi_3 & :\ \text{scalar sector}\,, \\ h_{ij} & :\ \text{tensor sector}\,. \end{cases} \tag{IV.27}$$

Among the scalar variables, α and β are nondynamical, and their values are fixed by the dynamical modes ζ and $\delta\varphi_3$. Therefore, each of the scalar and tensor sectors is a system of 2 propagating degrees of freedom. In particular, thanks to the background rotational symmetry, these sectors are decoupled at the level of the quadratic action,[5] *i.e.*

$$S^{(2)} = S_{\text{scalar}}[\alpha,\,\beta,\,\zeta,\,\delta\varphi_3] + S_{\text{tensor}}[h]\,. \tag{IV.28}$$

In the following subsections, we formally derive the background equations of this two-scalar system and the stability conditions against perturbations.[6]

IV.2.1 Background equations

The background quantities, defined in eqs. (IV.21) and (IV.23), obey their classical EoM, which are obtained by varying the action eq. (IV.20) with respect to each of them. In order to avoid crowded notations, we here take $\bar{N} = 1$ and omit the bars over background quantities in this subsection. The EoM's then read

$$\begin{aligned} 0 =& -\partial_{X_2}K\,\dot{\varphi}_2^2 - \partial_{X_3}P\,\dot{\varphi}_3^2 + \partial_{\varphi_3}G_3\,\dot{\varphi}_3\,\dot{\varphi}_2 + \partial_{\varphi_2}G_3\,\dot{\varphi}_2^2 + K + P \\ & - 3H\partial_{X_2}G_3\,\dot{\varphi}_2^3 + 3M_{\text{Pl}}^2H^2\,, \end{aligned} \tag{IV.29a}$$

$$0 = -\dot{\varphi}_2\left[\partial_{\varphi_3}G_3\,\dot{\varphi}_3 + \dot{\varphi}_2\left(\partial_{X_2}G_3\,\ddot{\varphi}_2 + \partial_{\varphi_2}G_3\right)\right] + K + P + M_{\text{Pl}}^2\left(2\dot{H} + 3H^2\right)\,, \tag{IV.29b}$$

$$\begin{aligned} 0 =& -3\,\partial_{X_2}G_3\left(\dot{H} + H^2\right)\dot{\varphi}_2^2 - 6H^2\partial_{X_2}G_3\,\dot{\varphi}_2^2 + \partial_{\varphi_2X_2}G_3\,\dot{\varphi}_2^2\ddot{\varphi}_2 + \partial_{\varphi_2\varphi_2}G_3\,\dot{\varphi}_2^2 \\ & - 3H\Big\{\dot{\varphi}_2\left[\partial_{X_2}K + \ddot{\varphi}_2\left(\partial_{X_2X_2}G_3\,\dot{\varphi}_2^2 + 2\,\partial_{X_2}G_3\right) + \partial_{\varphi_2X_2}G_3\,\dot{\varphi}_2^2 - 2\,\partial_{\varphi_2}G_3\right] \\ & + \dot{\varphi}_3\left(\partial_{X_2\varphi_3}G_3\,\dot{\varphi}_2^2 - \partial_{\varphi_3}G_3\right)\Big\} - \partial_{X_2X_2}K\,\dot{\varphi}_2^2\ddot{\varphi}_2 - \partial_{\varphi_2X_2}K\,\dot{\varphi}_2^2 - \partial_{X_2}K\,\ddot{\varphi}_2 + \partial_{\varphi_2}K \\ & + \dot{\varphi}_3\dot{\varphi}_2\left(-\partial_{X_2\varphi_3}K + \partial_{X_2\varphi_3}G_3\,\ddot{\varphi}_2 + 2\,\partial_{\varphi_2\varphi_3}G_3\right) + \partial_{\varphi_3\varphi_3}G_3\,\dot{\varphi}_3^2 + \partial_{\varphi_3}G_3\,\ddot{\varphi}_3 \\ & + 2\,\partial_{\varphi_2}G_3\,\ddot{\varphi}_2\,, \end{aligned} \tag{IV.29c}$$

$$\begin{aligned} 0 =& \partial_{\varphi_3}K - \ddot{\varphi}_3\left(\partial_{X_3X_3}P\,\dot{\varphi}_3^2 + \partial_{X_3}P\right) - \partial_{\varphi_3X_3}P\,\dot{\varphi}_3^2 + \partial_{\varphi_3}P \\ & + 3H\left(\partial_{\varphi_3}G_3\,\dot{\varphi}_2 - \partial_{X_3}P\,\dot{\varphi}_3\right) + \partial_{\varphi_3}G_3\,\ddot{\varphi}_2\,. \end{aligned} \tag{IV.29d}$$

The first eq. (IV.29a) is a constraint equation, and the remaining three equations constitute a system of second-order differential equations for φ_2, φ_3 and a that shall be numerically solved in section IV.4.

We note that, in section IV.3, we restrict our interest to seeking the solution of the NEC-violating sector that gives $X_2 =$ constant, *i.e.* $\varphi_2 \propto t$, in the absence of φ_3. This ansatz greatly simplifies the search of required forms of the functions K, G_3 and P to achieve the target cosmic history as shown in fig. IV.1 (or fig. IV.2 in the absence of φ_3). Before proceeding to the reconstruction procedure of those functions that is described in detail in section IV.3, we collect the conditions necessary to ensure our background solution to be stable against small perturbations in the following subsections.

[5] Note that the linear action only derives the background equations and gives no information about perturbations.

[6] For derivation of the equations for the background as well as perturbations, we refer to [33] for a detailed calculations of a single-field case and to [179] for a general multi-field extension.

IV.2.2 Perturbations

In this subsection we analyze the stability of the NEC violation and reheating sector against perturbations. As described at the beginning of this section, we decompose the perturbations of the fields and metric as in eqs. (IV.21) and (IV.23), respectively, and fix the gauge freedom as in eq. (IV.26). At the level of linear perturbations, the scalar, vector and tensor sectors are mutually decoupled, thanks to the background rotational symmetry, and the vector sector contains no dynamical degree of freedom. We thus need only to study the decoupled scalar and tensor perturbations as in eq. (IV.28), which is done separately hereafter.

Tensor sector The tensor sector takes the standard form, that is, the action of the type shown in eq. (IV.20) (without non-trivial G_4 or G_5 term in the Horndeski theory) leads to the same form of $S_{\rm tensor}$ as the one of General Relativity, *i.e.*

$$S_{\rm tensor} = \frac{M_{\rm Pl}^2}{8}\int \bar{N}\mathrm{d}t\, a^3 \mathrm{d}^3x \left[\frac{\partial_t h_{ij}\,\partial_t h_{ij}}{\bar{N}^2} - \frac{\partial_k h_{ij}\,\partial_k h_{ij}}{a^2}\right] , \tag{IV.30}$$

where the background lapse $\bar{N}$ is put back.[7] The tensor sector is here trivially free from ghost and gradient instabilities. Therefore, we shall simply focus on the stability conditions in the scalar perturbations.

Scalar sector The scalar sector consists of 4 variables $q \coloneqq (\alpha, \beta, \zeta, \delta\varphi_3)$, where we can choose α and β to be nondynamical and do not have their own kinetic terms, as explained around eq. (IV.27) . Fourier-transforming each variable as

$$q(t,\boldsymbol{x}) = \int \frac{\mathrm{d}^3k}{(2\pi)^{3/2}}\, \mathrm{e}^{i\boldsymbol{k}\cdot\boldsymbol{x}}\, \hat{q}(t,\boldsymbol{k}) , \tag{IV.31}$$

with hat $\hat{\ }$ denoting here Fourier-transformed quantities, the quadratic action $S_{\rm scalar}$ can be formally written in the form

$$\begin{aligned} S_{\rm scalar} = \frac{1}{2}\int \mathrm{d}t\,\mathrm{d}^3k \Big[&\partial_t\hat{\delta}^\dagger A\,\partial_t\hat{\delta} + \Big(\partial_t\hat{\delta}^\dagger B\,\hat{\delta} + \mathrm{h.c.}\Big) + \hat{\delta}^\dagger C\,\hat{\delta} \\ &+ \hat{\mathcal{N}}^\dagger D\hat{\mathcal{N}} + \Big(\hat{\mathcal{N}}^\dagger E\,\partial_t\hat{\delta} + \mathrm{h.c.}\Big) + \Big(\hat{\mathcal{N}}^\dagger F\,\hat{\delta} + \mathrm{h.c.}\Big)\Big] , \end{aligned} \tag{IV.32}$$

up to total derivatives, where $\hat{\delta} = \{\hat{\zeta}, \delta\hat{\varphi}_3\}$ and $\hat{\mathcal{N}} = \{\hat{\alpha}, \hat{\beta}\}$ are arrays grouping the dynamical and nondynamical variables, respectively. Note that the reality condition of the variables in the coordinate space is translated to $\hat{q}^\dagger(\boldsymbol{k}) = \hat{q}(-\boldsymbol{k})$ in the Fourier space. The coefficients A, B, C, D, E and F are all 2×2 square matrices whose components consist of the background quantities. These explicitly read

$$\begin{aligned} A &= \frac{a^3}{N}\begin{pmatrix} -6M_{\rm Pl}^2 & 0 \\ 0 & \mathcal{G}_\varphi \end{pmatrix} , & B &= a^3\begin{pmatrix} 0 & \frac{3}{2}c_1 \\ -\frac{3}{2}c_1 & 0 \end{pmatrix} , \\ C &= Na^3\begin{pmatrix} 2M_{\rm Pl}^2\frac{k^2}{a^2} & \frac{3}{2}c_2 \\ \frac{3}{2}c_2 & -\frac{k^2}{a^2}\left(\mathcal{G}_\varphi - 2X_3\,\partial_{X_3X_3}P\right) + c_3 \end{pmatrix} , & D &= Na^3\begin{pmatrix} 2\Sigma + \frac{c_4^2}{\mathcal{G}_\varphi} & \frac{2k^2}{a}\Theta \\ \frac{2k^2}{a}\Theta & 0 \end{pmatrix} , \\ E &= a^3\begin{pmatrix} 6\Theta & c_4 \\ -2M_{\rm Pl}^2\frac{k^2}{a} & 0 \end{pmatrix} , & F &= Na^3\begin{pmatrix} 2M_{\rm Pl}^2\frac{k^2}{a^2} & c_5 \\ 0 & \frac{k^2}{a}c_1 \end{pmatrix} , \end{aligned} \tag{IV.33}$$

where we defined

$$\mathcal{G}_\varphi \coloneqq \partial_{X_3}P + 2X_3\,\partial_{X_3X_3}P , \tag{IV.34a}$$

$$\begin{aligned} \Sigma \coloneqq -3M_{\rm Pl}^2H^2 - \frac{X_2\left(\partial_{\varphi_3}G_3\right)^2}{\mathcal{G}_\varphi} + X_2\Big(&\partial_{X_2}K + 2X_2\,\partial_{X_2X_2}K - 2\,\partial_{\varphi_2}G_3 \\ &+ 12H\frac{\dot{\varphi}_2}{N}\,\partial_{X_2}G_3 - 2X_2\,\partial_{\varphi_2X_2}G_3 + 6H\frac{\dot{\varphi}_2}{N}\,X_2\,\partial_{X_2X_2}G_3 - \frac{\dot{\varphi}_2\dot{\varphi}_3}{N^2}\,\partial_{X_2\varphi_3}G_3\Big) , \end{aligned} \tag{IV.34b}$$

[7] In deriving the expression of eq. (IV.30), the background equations are not used, which is the benefit of defining h_{ij} by adding the quadratic term of h_{ij} in eq. (IV.23c). Without it, the same form of $S_{\rm tensor}$ can be derived, but only after the background equations are imposed.

$$\Theta \coloneqq M_{\rm Pl}^2 H - \frac{\dot\varphi_2}{N}\, X_2\, \partial_{X_2} G_3 \tag{IV.34c}$$

$$c_1 \coloneqq \frac{\dot\varphi_2}{N}\, \partial_{\varphi_3} G_3 - \frac{\dot\varphi_3}{N}\, \partial_{X_3} P\,, \tag{IV.34d}$$

$$\begin{aligned} c_2 \coloneqq & -\left[\frac{1}{N}\,\partial_t\left(\frac{\dot\varphi_2}{N}\right) + 3H\,\frac{\dot\varphi_2}{N}\right]\partial_{\varphi_3} G_3 - \frac{2}{N}\,\partial_t\left(\frac{\dot\varphi_2}{N}\right) X_2 \partial_{X_2\varphi_3} G_3 - 2X_2 \partial_{\varphi_2\varphi_3} G_3 \\ & - \frac{\dot\varphi_2\dot\varphi_3}{N^2}\,\partial_{\varphi_3\varphi_3} G_3 + \left[\frac{1}{N}\,\partial_t\left(\frac{\dot\varphi_3}{N}\right) + 3H\,\frac{\dot\varphi_3}{N}\right]\partial_{X_3} P + \frac{2}{N}\,\partial_t\left(\frac{\dot\varphi_3}{N}\right) X_3 \partial_{X_3 X_3} P \\ & + 2X_3 \partial_{\varphi_3 X_3} P\,, \end{aligned} \tag{IV.34e}$$

$$\begin{aligned} c_3 \coloneqq & \partial_{\varphi_3\varphi_3} K + \left[\frac{1}{N}\,\partial_t\left(\frac{\dot\varphi_2}{N}\right) + 3H\,\frac{\dot\varphi_2}{N}\right]\partial_{\varphi_3\varphi_3} G_3 + \partial_{\varphi_3\varphi_3} P - 2X_3 \partial_{\varphi_3\varphi_3 X_3} P \\ & - \left[\frac{1}{N}\,\partial_t\left(\frac{\dot\varphi_3}{N}\right) + 3H\,\frac{\dot\varphi_3}{N}\right]\partial_{\varphi_3 X_3} P - \frac{2}{N}\,\partial_t\left(\frac{\dot\varphi_3}{N}\right) X_3 \partial_{\varphi_3 X_3 X_3} P\,, \end{aligned} \tag{IV.34f}$$

$$c_4 \coloneqq \frac{\dot\varphi_2}{N}\,\partial_{\varphi_3} G_3 - \frac{\dot\varphi_3}{N}\,\mathcal{G}_\varphi\,, \tag{IV.34g}$$

$$\begin{aligned} c_5 \coloneqq & -2X_2 \partial_{X_2\varphi_3} K - \left[\frac{1}{N}\,\partial_t\left(\frac{\dot\varphi_2}{N}\right) + 3H\,\frac{\dot\varphi_2}{N}\right]\partial_{\varphi_3} G_3 \\ & - 6H\,\frac{\dot\varphi_2}{N}\, X_2 \partial_{X_2\varphi_3} G_3 + 2X_2 \partial_{\varphi_2\varphi_3} G_3 + \frac{\dot\varphi_2\dot\varphi_3}{N^2}\,\partial_{\varphi_3\varphi_3} G_3 \\ & + \left[\frac{1}{N}\,\partial_t\left(\frac{\dot\varphi_3}{N}\right) + 3H\,\frac{\dot\varphi_3}{N}\right]\partial_{X_3} P + \frac{2}{N}\,\partial_t\left(\frac{\dot\varphi_3}{N}\right) X_3 \partial_{X_3 X_3} P\,, \end{aligned} \tag{IV.34h}$$

carefully noting that the bar $\bar{\ }$ is here omitted from the background quantities to avoid crowded notation.

By varying the action of eq. (IV.32) with respect to $\hat{\mathcal{N}}^\dagger$, we find the constraint equations that fix the nondynamical variables in terms of the dynamical ones δ, given by

$$\hat{\mathcal{N}} = -D^{-1}\left(E\,\partial_t\hat\delta + F\hat\delta\right)\,, \tag{IV.35}$$

as $\det(D) \neq 0$ in our current system. Plugging this back into eq. (IV.32), we obtain the action in terms only of the dynamical degrees of freedom,

$$S_{\rm scalar} = \frac{1}{2}\int \mathrm{d}t\,\mathrm{d}^3k\left[\partial_t\hat\delta^\dagger \tilde A\,\partial_t\hat\delta + \left(\partial_t\hat\delta^\dagger \tilde B\,\hat\delta + \text{h.c.}\right) + \hat\delta^\dagger \tilde C\,\hat\delta\right]\,, \tag{IV.36}$$

where we defined

$$\tilde A \coloneqq A - E^\dagger D^{-1} E\,, \qquad \tilde B \coloneqq B - E^\dagger D^{-1} F\,, \qquad \tilde C \coloneqq C - F^\dagger D^{-1} F\,. \tag{IV.37}$$

Notice that now the kinetic matrix $\tilde A$ is no longer diagonal. In order to diagonalize it, we can perform the following change of variables,

$$\hat\delta = M_R \hat\Delta\,, \qquad \text{with} \qquad M_R = \begin{pmatrix} 1 & 0 \\ -\dfrac{M_{\rm Pl}^2 c_4}{\mathcal{G}_\varphi \Theta} & 1 \end{pmatrix}\,, \tag{IV.38}$$

which results in the action in terms of $\hat\Delta$, instead of $\hat\delta$

$$S_{\rm scalar} = \frac{1}{2}\int \mathrm{d}t\,\mathrm{d}^3k\left[\partial_t\hat\Delta^\dagger \tilde T\,\partial_t\hat\Delta + \left(\partial_t\hat\Delta^\dagger \tilde X\,\hat\Delta + \text{h.c.}\right) - \hat\Delta^\dagger \tilde\Omega^2\,\hat\Delta\right]\,, \tag{IV.39}$$

where we defined

$$\tilde T \coloneqq M_R^\dagger \tilde A M_R\,, \tag{IV.40a}$$

$$\tilde X \coloneqq M_R^\dagger \tilde B M_R + M_R^\dagger \tilde A\,\partial_t M_R\,, \tag{IV.40b}$$

$$\tilde\Omega^2 \coloneqq -M_R^\dagger \tilde C M_R - \partial_t M_R^\dagger \tilde A\,\partial_t M_R - \partial_t M_R^\dagger \tilde B M_R - M_R^\dagger \tilde B^\dagger \partial_t M_R\,. \tag{IV.40c}$$

Finally, by adding the total derivative $-\frac{1}{4}\int \mathrm{d}t\,\mathrm{d}^3k\left(\tilde X + \tilde X^\dagger\right)$, we arrive at our final expression for the quadratic action

$$S_{\rm scalar} = \frac{1}{2}\int \mathrm{d}t\,\mathrm{d}^3k\left[\partial_t\hat\Delta^\dagger T\,\partial_t\hat\Delta + \partial_t\hat\Delta^\dagger X\,\hat\Delta - \hat\Delta^\dagger X\,\partial_t\hat\Delta - \hat\Delta^\dagger \Omega^2\,\hat\Delta\right]\,, \tag{IV.41}$$

where we accordingly now used

$$T = \tilde{T} \,, \qquad X = \frac{\tilde{X} - \tilde{X}^\dagger}{2} \,, \qquad \Omega^2 = \tilde{\Omega}^2 + \frac{\partial_t \tilde{X} + \partial_t \tilde{X}^\dagger}{2} \,. \tag{IV.42}$$

Note that T and Ω^2 are symmetric 2×2 matrices, and X is an anti-symmetric one. Now the kinetic matrix

$$T = \frac{a^3}{N} \begin{pmatrix} 2M_{\rm Pl}^2 \mathcal{G}_S & 0 \\ 0 & \mathcal{G}_\varphi \end{pmatrix} \,, \qquad \mathcal{G}_S \equiv 3 + M_{\rm Pl}^2 \frac{\Sigma}{\Theta^2} \,, \tag{IV.43}$$

is diagonal, as desired. The conditions to prohibit ghost instabilities are therefore

$$\mathcal{G}_S > 0 \,, \qquad \mathcal{G}_\varphi > 0 \,, \qquad \text{no ghost} \,, \tag{IV.44}$$

serving as part of the conditions of perturbative stability ($\mathcal{G}_\varphi$ is defined in eq. (IV.34a)).

Another instability we need to suppress is the gradient instability. We are only concerned with high-momentum catastrophic instability, as the low-momentum counterpart may be harmless at a non-linear level *à la* Jeans instability. This amounts to imposing the positivity condition for the squared sound speeds of the scalar perturbations, c_s^2, as defined hereafter. In the high-k limit, we collect the terms in the coefficient matrices of the order $T \sim \mathcal{O}(k^0)$, $X \sim \mathcal{O}(k^1)$ and $\Omega^2 \sim \mathcal{O}(k^2)$. The full expression of T is given in eq. (IV.43) and does not depend on k. The other matrices in the high-k limit read

$$X = 0 + \mathcal{O}(k^0) \,, \qquad \Omega^2 = \Omega^2_{\mathcal{O}(k^2)} + \mathcal{O}(k^0) \,, \tag{IV.45}$$

where $\Omega^2_{\mathcal{O}(k^2)}$ only contains the terms proportional to k^2 in the high-k limit. Taking the ansatz $\hat{\Delta} \propto \exp\left(i \int^t N {\rm d}t' c_s k/a\right)$ as an adiabatic solution for large k, the sound speed c_s^2 can be found by solving the characteristic equation

$$\det\left(-c_s^2 k^2 \frac{N^2}{a^2} T + \Omega^2\right) = 0 \,, \tag{IV.46}$$

leading to

$$c_s^4 - \left(c_\chi^2 + \frac{\mathcal{F}_S}{\mathcal{G}_S} + \mathcal{A} + \mathcal{B}\right) c_s^2 + c_\chi^2 \left(\frac{\mathcal{F}_S}{\mathcal{G}_S} + \mathcal{A}\right) = 0 \,, \tag{IV.47}$$

where

$$\begin{aligned} \mathcal{F}_S &\equiv \frac{M_{\rm Pl}^4}{Na} \partial_t \left(\frac{a}{\Theta}\right) - M_{\rm Pl}^2 \,, & c_\chi^2 &\equiv \frac{\partial_{X_3} P}{\partial_{X_3} P + 2X_3 \, \partial_{X_3 X_3} P} \,, \\ \mathcal{A} &\equiv -\frac{M_{\rm Pl}^4}{2\partial_{X_3} P \, \mathcal{G}_S \, \Theta^2} \left(\frac{\dot{\varphi}_2}{N} \partial_{\varphi_3} G_3 - \frac{\dot{\varphi}_3}{N} \partial_{X_3} P\right)^2 \,, & \mathcal{B} &\equiv \frac{4M_{\rm Pl}^4 X_2 X_3^2 \left(\partial_{X_3 X_3} P\right)^2 \left(\partial_{\varphi_3} G_3\right)^2}{\partial_{X_3} P \, \mathcal{G}_S \, \mathcal{G}_\varphi^2 \Theta^2} \,. \end{aligned} \tag{IV.48}$$

The values of c_s^2 are determined by the two roots of eq. (IV.47), and we impose the conditions

$$c_s^2 > 0 \,, \qquad \text{gradient stability} \,, \tag{IV.49}$$

for each value of c_s^2.

Notice from eq. (IV.47) that, in the particular cases of $\partial_{\varphi_3} G_3 = 0$ and/or $\partial_{X_3 X_3} P = 0$, we have $\mathcal{B} = 0$, and the expressions of c_s^2 vastly simplify. In our numerical examples, we indeed take

$$\partial_{\varphi_3} G_3 = 0 \qquad \& \qquad \partial_{X_3 X_3} P = 0 \,, \qquad \text{numerical examples} \,, \tag{IV.50}$$

and in this case

$$c_s^2 = c_\chi^2 \quad \text{or} \quad c_s^2 = \frac{\mathcal{F}_S}{\mathcal{G}_S} + \mathcal{A} \,, \tag{IV.51}$$

while

$$c_\chi^2 = 1 \,, \qquad \mathcal{A} = -\frac{M_{\rm Pl}^4 X_3 \, \partial_{X_3} P}{\mathcal{G}_S \, \Theta^2} \,. \tag{IV.52}$$

Therefore, in these particular examples, we only need to impose

$$\mathcal{F}_S > \frac{M_{\rm Pl}^4 X_3 \partial_{X_3} P}{\Theta^2} \,, \tag{IV.53}$$

to avoid gradient instability, as we have already imposed $\mathcal{G}_S > 0$ from the no-ghost condition. In summary, to ensure the background evolution to be stable against small perturbations, we impose the conditions in eqs. (IV.44) and (IV.49), or those in eqs. (IV.44) and (IV.53) for the particular and simpler examples, for the entire history of the Universe, and particularly during the phases of NEC violation and reheating.

IV.3 A concrete implementation

We have until now kept arbitrary the free functions $f_{1,2}(\varphi_2, \varphi_3)$, $f(\varphi_2, \varphi_3)$, $V(\varphi_2, \varphi_3)$ and $U(\varphi_3)$ in the NEC violating and reheating Lagrangian $\mathcal{L}_{\rm NECV+reh}$, eq. (IV.11), but we now choose a concrete set of functions to fully realize our desired cosmological scenario. For the purpose of the conceptual proof, we take an inverted route: we first determine a desired cosmic history we would like to achieve, which is summarized in section IV.1, and then reconstruct the functions accordingly. While we disregard the reheating field φ_3 in this procedure, we numerically verify the overall behavior of the whole system after reviving the φ_3 dependence into the reconstructed model.

IV.3.1 Reconstruction of the NEC-violating sector

We have a total of 3 independent functions, K, G_3 and P, and expand K and G_3 as polynomial functions of X_2 as in eq. (IV.13). To reconstruct them, we first consider the NEC-violating sector alone by turning off the φ_3 and disregarding $P(\varphi_3, X_3)$. On the one hand, there are 4 independent functions, $\tilde{f}_1(\varphi_2)$, $\tilde{f}_2(\varphi_2)$ and $\tilde{V}(\varphi_2)$ from $\tilde{K}$, and $\tilde{f}(\varphi_2)$ from $\tilde{G}_3$ (recall tilde denotes quantities with φ_3 dependence taken out). On the other hand, we have 2 independent background equations from eq. (IV.29) (with φ_3 turned off). Therefore, the forms of two of these functions can be fixed by the background equations, once all other arbitrary functions are chosen by hand. In the following we reconstruct these functions in the action so that the system admits the following solution,

$$H = H_{\rm necv}(\varphi_2) \,, \quad \varphi_2 = t \,, \quad \bar{N} = 1 \,, \tag{IV.54}$$

where H is the Hubble expansion rate and $H_{\rm necv}(\varphi_2)$ is a fixed function corresponding to the input Hubble expansion rate.

The NEC-violating sector is assumed to be periodic in the field value of φ_2, as discussed in section IV.1.2. Without loss of generality, we shift φ_2 such that the NEC-violating (and reheating) period is localized around $\varphi_2 = 0$. We then take the following ansatz for the forms of $\tilde{K}$ and G_3, that is,

$$\tilde{K} = M_{\rm Pl}^2 H_{\rm dip}^2 \left[F_1(\varphi_2)\, X_2 + F_2(\varphi_2)\, X_2^2 - v(\varphi_2) \right] \,, \quad v(\varphi_2) = -v_0 \exp\left(-\frac{\varphi_2^2}{2T_{\rm dip}^2} \right) \,, \tag{IV.55a}$$

$$\tilde{G}_3 = M_{\rm Pl}^2 H_{\rm necv}(\varphi_2) F_{\rm kb}(\varphi_2)\, X_2 \,, \qquad F_{\rm kb}(\varphi_2) = F_{\rm kb,0} + F_{\rm kb,1} \exp\left(-\frac{\varphi_2^2}{2T_{\rm kb}^2} \right) \,, \tag{IV.55b}$$

where $H_{\rm dip}$ is a constant of mass dimension 1, $T_{\rm dip}$ and $T_{\rm kb}$ of mass dimension -1, and v_0, $F_{\rm kb,0}$ and $F_{\rm kb,1}$ are dimensionless constants. We here normalize φ_2 so that it has mass dimension -1, and thus X_2 is dimensionless. The functions F_1, F_2 and $F_{\rm kb}$ correspond to $\tilde{f}_1$, $\tilde{f}_2$ and $\tilde{f}$ (eq. (IV.13)), respectively, that are made dimensionless. The potential v has a "dip" of depth v_0 at $\varphi_2 = 0$ so that φ_2 can be trapped to sustain a NEC-violating period. The $\tilde{G}_3$ contribution is needed to ensure the stability of the system in this period. For this reason, we use the input Hubble expansion rate $H_{\rm necv}(\varphi_2)$ as an overall factor of $\tilde{G}_3$ so that the $\tilde{G}_3$ contribution becomes prominent in the NEC violating phase.

For the actual form of $H_{\rm necv}$ that we employ, we introduce two scales to turn on and off NEC violation. There are many possible forms to achieve this, and we simply take one particular choice, *i.e.*

$$H_{\rm necv}(\varphi_2) = H_0 + H_1 \exp\left(-\frac{\varphi_2^2}{2T^2} \right) \frac{1 - \tanh\left(\frac{\varphi_2}{\tau}\right)}{2} \,, \tag{IV.56}$$

where H_0 and H_1 are constants of dimension 1, while T and τ those of dimension -1. The value of $H_{\rm necv}$ far away from the origin (*i.e.* $|\varphi_2| \gg T, \tau$) is H_0, that is during a major duration of the cosmic history, and is essentially the present value of the Hubble expansion rate if we apply this system to the last NEC

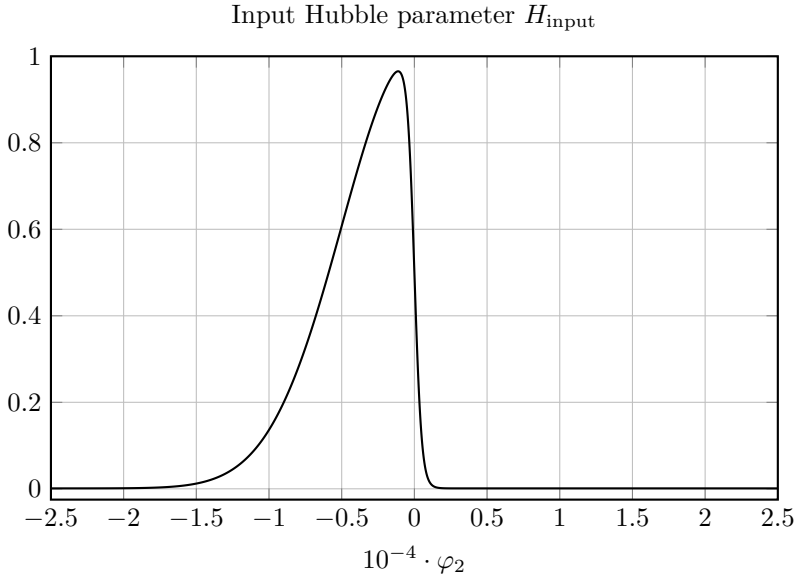

Figure IV.3: Overall shape of the input Hubble expansion rate $H_{\rm necv}$. The plot uses the numerical parameters exhibited in table IV.1.

violating phase before the present epoch of the Universe. However, during the NEC violating phase, it ascends to the maximum value $\sim H_0 + H_1$ within a time scale controlled by T, eventually going through a step-function-like drop around $\varphi_2 = 0$ to H_0 with another scale controlled by τ. The overall shape of $H_{\rm necv}$ is graphically depicted in fig. IV.3. In practice, the drop needs to be sharper than the rise ($T \gg \tau$) in order to accommodate a reheating period toward the end of the NEC violation by transferring a large portion of the energy in φ_2 abruptly enough so that the reheating field φ_3 starts oscillating using the transferred energy.

We now have all the setups for the reconstruction. In order to ensure the target cosmic history of eq. (IV.56) to be compatible with time evolution, we seek for a solution of the form eq. (IV.54). We then substitute eq. (IV.54) and eq. (IV.55) into the background equations of motion in eq. (IV.29). Only two of the equations are independent when φ_3 is turned off, and they give

$$F_1 = 4v + 3\,(F_{\rm kb} - 4)\,\frac{H_{\rm necv}^2}{H_{\rm dip}^2} + \frac{F_{\rm kb}' H_{\rm necv}}{H_{\rm dip}^2} + (F_{\rm kb} - 6)\,\frac{H_{\rm necv}'}{H_{\rm dip}^2}\ , \tag{IV.57a}$$

$$F_2 = -4v - 6\,(F_{\rm kb} - 2)\,\frac{H_{\rm necv}^2}{H_{\rm dip}^2} + \frac{4H_{\rm necv}'}{H_{\rm dip}^2}\ , \tag{IV.57b}$$

where prime denotes $\partial/\partial t = \partial/\partial\varphi_2$ under eq. (IV.54). Recovering φ_2 dependence by basically replacing $t \to \varphi_2$, these two equations fix the forms of F_1 and F_2, given the predetermined functions $H_{\rm necv}$, $F_{\rm kb}$ and v. This completes the reconstruction of the NEC-violating sector for our concrete implementation of the model.

IV.3.2 Attractor behavior of the NEC-violating dynamics

We have fixed the forms of the model functions in the φ_2 sector as eq. (IV.57) so that the NEC violation as depicted in eq. (IV.56) and eq. (IV.54) is achieved as a solution of the background equations of motion. However whether or not this particular solution is an attractor of the dynamical system is a separate issue, which we would like to address in this subsection. The analysis here concerns the background eq. (IV.29) with the reconstructed functions of eq. (IV.55) with eqs. (IV.56) and (IV.57).

We first perform a linearized analysis, and to this end we expand the background quantities as

$$\varphi_2(t) = \varphi^{(0)}(t) + \epsilon\,\varphi^{(1)}(t)\ , \qquad H(t) = H^{(0)}(t) + \epsilon\,H^{(1)}(t)\ , \tag{IV.58}$$

where $\varphi^{(0)} = t$ and $H^{(0)} = H_{\rm necv}(t)$ denote the solutions assumed for the reconstruction in the previous subsection while $\epsilon\varphi^{(1)}$ and $\epsilon H^{(1)}$ are small perturbations, and ϵ is the expansion parameter. We then expand the background eq. (IV.29) up to the linear order in ϵ. The $\mathcal{O}(\epsilon^0)$ equations are trivially satisfied,

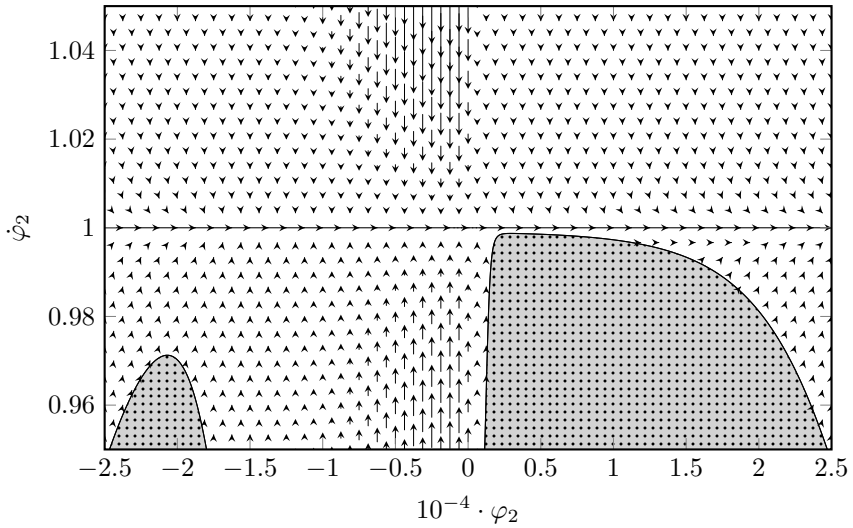

Figure IV.4: The phase portrait of φ_2 and $\dot{\varphi}_2$ as a vector field. Arrows are scaled proportionally to the gradient intensity. The above plot therefore exhibits the strong attraction to the solution $\varphi_2 \equiv t$, especially in the central area (between approximately $\varphi_2 = -5000$ and 0). The lightly shaded regions are where H takes a complex value as a solution to the constraint eq. (IV.29a), that is where a real background solution does not exist.

and the $\mathcal{O}(\epsilon^1)$ equation for $H^{(1)}$ is a constraint equation that can be solved for $H^{(1)}$ in favor of $\varphi^{(1)}(t)$ and $\partial_t \varphi^{(1)}$. As a result, the master equation of the linearized system is only in terms of $\varphi^{(1)}$ with $\mathcal{O}(\epsilon^0)$ coefficients, and reducing it to a coupled system of first-order equations gives, in a matrix form,

$$\partial_t \begin{pmatrix} \varphi^{(1)} \\ \pi_\varphi^{(1)} \end{pmatrix} = \mathcal{M} \begin{pmatrix} \varphi^{(1)} \\ \pi_\varphi^{(1)} \end{pmatrix} , \qquad \mathcal{M} = \begin{pmatrix} 0 & 1 \\ \mathcal{A} & \mathcal{B} \end{pmatrix} , \tag{IV.59}$$

where $\mathcal{A}$ and $\mathcal{B}$ are functions of the $\mathcal{O}(\epsilon^0)$ quantities. While $\mathcal{A}$ and $\mathcal{B}$ are in general of lengthy expressions, our restriction of including only up to the $\mathcal{L}_3$ terms of Horndeski theory with the EoM-consistent reconstructed functions of eq. (IV.55) conveniently sets $\mathcal{A} = 0$. Hence, the eigenvalues of the matrix $\mathcal{M}$ are 0 and $\mathcal{B}$. In order for the solutions $\varphi^{(0)} = t$ and $H^{(0)} = H_{\rm necv}(t)$ to be a local attractor of the system, we thus require these eigenvalues be non-positive, *i.e.*[8]

$$\mathcal{B} \leq 0 \, . \tag{IV.60}$$

This ensures the local stability of the solution assumed in the previous subsection.

The previous analysis is a linearized one, and in order to observe a more global behavior of the system, we resort to a numerical phase-space illustration, a representative case of which is depicted in fig. IV.4. As seen in the figure, $\varphi_2 = t$, which is our input solution for the reconstruction, is indeed the global attractor of the system. This justifies our ansatz and reconstruction of the model functions in the previous subsection, and the system is resistant against small perturbations at least in the direction of positive $\dot{\varphi}_2$. In fig. IV.4, the value of H_0, which is essentially the Hubble expansion rate at present, is taken rather close to that of H_1, which corresponds to the amount of raise in H during the NEC violating phase, for numerical ease. When the hierarchy between these values is closer to a realistic one, we note two cautions. First, the shaded complex regions approach closer to the $\dot{\varphi}_2$ line. However, they never cross it provided taking a sufficiently large value of v_0. Second, when H_0 becomes much smaller than H_1, the attractor behavior towards the input solution $\varphi_2 = t$ is rather weak away from the NEC-violating region. Indeed, in a small H_0 limit and sufficiently far from the NEC violation so that $v \approx 0$ and $F_{\rm kb} \approx F_{\rm kb,0}$, the value of $\mathcal{B}$ takes

$$\mathcal{B} \simeq -3H_0 \, , \qquad H_0 \ll H_1 \, , \tag{IV.61}$$

[8] In principle the non-positiveness condition could be imposed only on the real part of the eigenvalues. However, the components of $\mathcal{B}$ (and $\mathcal{A}$) consist of the $\mathcal{O}(\epsilon^0)$ quantities, and the only occasion in which they become complex is when the value of $H^{(0)}$ becomes complex as a solution of the constraint equation, but this only means that there is no real solution at the $\mathcal{O}(\epsilon^0)$ order. We exclude such a case.

which makes the validity of the solution $\varphi_2 = t$ somewhat worrisome. However, it is still a local attractor because $\mathcal{B} < 0$. Moreover, we are assuming a period of the NEC-preserving phase much longer than that of the NEC-violating one. Therefore, even though the attractor appears to be weak in the limit $H_0 \ll H_1$, the background system is expected to go back to the solution $\varphi_2 = t$ during the long NEC-preserving era.

IV.3.3 Recovering the reheating sector coupled to NEC violation

To realize the known big bang universe after the NEC-violating era, the reheating field φ_3 necessarily couples to φ_2 in a non-minimal manner. Our choice of the coupling amounts to making the following replacements:

$$F_1 \to \frac{1 + \alpha_{\rm kick}\, \mathrm{e}^{-\beta_{\rm kick}\varphi_3}}{1 + \alpha_{\rm kick}}\, F_1 \ , \tag{IV.62a}$$

$$F_2 \to \frac{1 + \alpha_{\rm kick}\, \mathrm{e}^{-\beta_{\rm kick}\varphi_3}}{1 + \alpha_{\rm kick}}\, F_2 \ , \tag{IV.62b}$$

$$v \to \exp\left[-\beta_{\rm dip}^2 \left(\left(\varphi_3 - 1\right)^2 - 1\right)\right] v \ , \tag{IV.62c}$$

while we reintroduce the kinetic term and bare potential of φ_3 as

$$P(\varphi_3, X_3) = M_{\rm Pl}^2 \beta_{\rm kin}^2\, X_3 - U(\varphi_3) \ , \qquad U(\varphi_3) = 3 M_{\rm Pl}^2 H_I^2 \left(1 - \mathrm{e}^{-\beta_{\rm I}\varphi_3}\right)^2 \ , \tag{IV.63}$$

where φ_3 is normalized to be dimensionless, $\alpha_{\rm kick}$, $\beta_{\rm kick}$, $\beta_{\rm dip}$, $\beta_{\rm kin}$ and $\beta_{\rm I}$ are all dimensionless parameters, and H_I is a constant of mass dimension 1. Note that setting $\varphi_3 = 0$ gives the case of the NEC-violating sector alone studied in the previous subsection.

The explicit but rather nontrivial forms of the interactions above are taken to accomplish the desired efficient energy transfer from the NEC-violating sector to reheat the Universe. One feature we aim for is to eventually yield to an oscillating reheating field φ_3 (as explained with fig. IV.5, and numerically verified in fig. IV.8). The above choices lead to the following dynamics:

- When the NEC is well preserved, φ_3 is effectively decoupled from φ_2. Then, φ_3 stays at the minimum of its Starobinsky-type bare potential U, *i.e.* $\varphi_3 = 0$ while the NEC holds.

- During the time when the NEC violation takes place, the different potentials V and U together shape the reheating potential. The potential U gives the bare potential of φ_3, while V generates an alternative local minimum for φ_3 (recall that v is negative) when φ_2 approaches to its origin. Thus φ_3 is moved to this new minimum at $\varphi_3 = 1$ during the NEC violation. This process is further discussed in section IV.3.4.

- The overall factor introduced for F_1 and F_2 in eqs. (IV.62) modulate the kinetic term of φ_2, which takes 1 for $\varphi_3 = 0$ and the smaller value $(1 + \alpha_{\rm kick})^{-1}$ for $\varphi_3 = 1$, while φ_3 is given an extra "kick" through $\beta_{\rm kick}$ around the time of NEC violation.

- The function G_3 is taken independent of φ_3 and makes important contribution only during the NEC-violating phase. It returns to a negligible value afterwards, respecting the late-time constraints [180].

To summarize everything, our total action of eq. (IV.20) consists of the functions K, G_3 and P, whose explicit forms are now

$$K = M_{\rm Pl}^2 H_{\rm dip}^2 \left[\frac{1 + \alpha_{\rm kick}\, \mathrm{e}^{-\beta_{\rm kick}\varphi_3}}{1 + \alpha_{\rm kick}} \left(F_1(\varphi_2) X_2 + F_2(\varphi_2) X_2^2\right) - \mathrm{e}^{-\beta_{\rm dip}^2\left((\varphi_3 - 1)^2 - 1\right)} v(\varphi_2)\right] \ , \tag{IV.64a}$$

$$G_3 = M_{\rm Pl}^2 H_{\rm necv}(\varphi_2)\, F_{\rm kb}(\varphi_2) X_2 \ , \tag{IV.64b}$$

$$P = M_{\rm Pl}^2 \beta_{\rm kin}^2\, X_3 - U(\varphi_3) \ , \tag{IV.64c}$$

where v and $F_{\rm kb}$ are given by eq. (IV.55), $H_{\rm necv}$ by eq. (IV.56), F_1 and F_2 by eq. (IV.57), and U by eq. (IV.63). In the following subsection, we discuss the behavior of the effective potential for φ_3 in more detail.

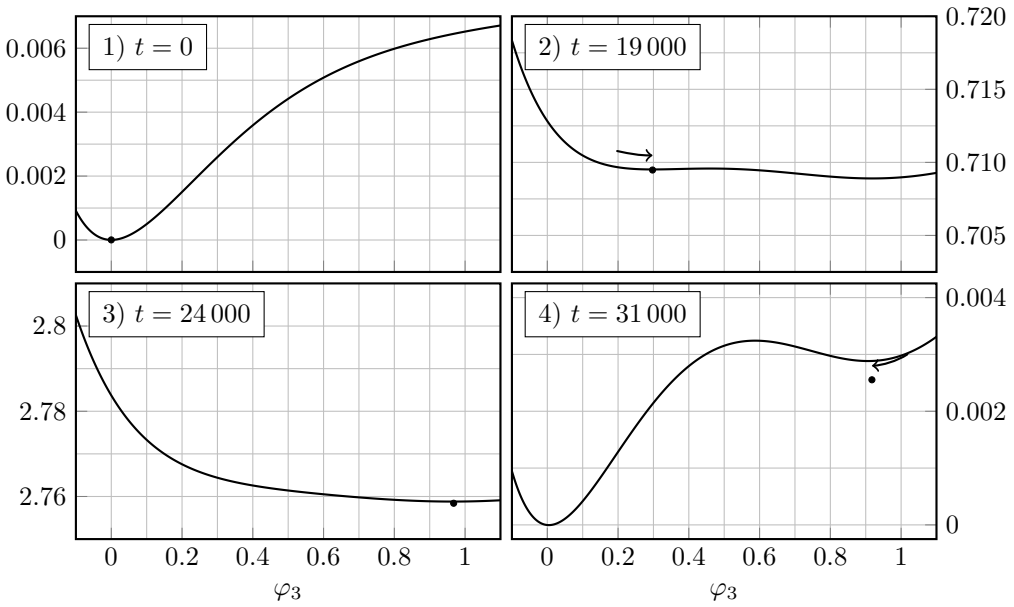

Figure IV.5: Evolution of φ_3 and the shape of its total effective potential, which is altered by φ_2. (1) The field φ_3 starts here at zero, and (2) it is then raised, until it starts rolling down to (3) a new minimum. (4) As the potential regains its previous shape, the field φ_3 falls back into (1) its original position. We also call for attention to how the vertical scale changes.

IV.3.4 The reheating potential

We have determined our full Lagrangian as in eqs. (IV.20) and (IV.64). The reconstruction procedure of section IV.3.1 is robust for the NEC-violating sector φ_2 as shown in section IV.3.2, while the reintroduction of the reheating field φ_3 is done in section IV.3.3 in a rather *ad hoc* manner. In this subsection we further describe the trajectory that φ_3 is expected to take, which shall be verified numerically in section IV.4. The reheating process operates essentially by the reheating field φ_3 rolling down to the minimum of its effective potential that is uplifted by the NEC violation. Then φ_3 starts oscillating, releasing its energy into the Universe. A coupling of φ_3 with the Standard Model particles is necessary, but implicit hereafter, and we do not specify its concrete form.

The time evolution of the effective potential of φ_3 is illustrated in fig. IV.5. The reheating procedure is essentially articulated around the evolution of φ_3 along its total potential whose shape is in turn driven by φ_2 in the following way. For most of the cosmic period in which the shift symmetry of φ_2 is well respected, the reheating field φ_3 stays at the minimum of its bare potential U. Once the NEC violation takes place by φ_2, however, the reheating field φ_3 is transported upward and rolls to a new and higher minimum. Later toward the end of the NEC-violating phase, the interaction between φ_2 and φ_3 becomes ineffective, and φ_3 is subsequently sent back to the initial minimum. On this return trajectory, the acquired kinetic energy results in oscillations around this minimum, leading to reheating of the Universe.

The shape of the bare potential $U(\varphi_3)$ is of the type of Starobinsky's inflation and is depicted in fig. IV.5 (1). The total, "effective" potential for φ_3 consists not only of $U(\varphi_3)$ but of the contributions from $K(\varphi_2, X_2, \varphi_3)$, as is given in eq. (IV.64a). A rough description of each term in K is as follows: while each term is approximately constant and takes a negligible value during the (long) NEC-preserving era, the term proportional to $F_1 X_2 + F_2 X_2^2$ is uplifted and erases the minimum around $\varphi_3 = 0$ during the NEC violation. The term proportional to v, on the other hand, arises and accommodates a new minimum at $\varphi_3 = 1$. The changing effective potential is visualized in fig. IV.5 (2) and (3). Toward the end of the NEC-violation period, the modulation by φ_2 effectively turns off, and φ_3 is drifted back to $\varphi_3 = 0$, as shown in fig. IV.5 (4).

The period during the NEC violation and before the reheating may as well accommodate inflation to produce the seeds of the structure formation. This is also an interesting possibility to realize, but is beyond the scope of our current work, and we leave it to future studies.

Function $H_{\rm necv}$		Function $F_{\rm kb}$		Function v		Reheating φ_3 modulation		Reheating φ_3 sector	
H_0	10^{-3}	$F_{\rm kb,0}$	10^{-3}	v_0	$5\cdot10^{-2}$	$\alpha_{\rm kick}$	10^{-2}	$\beta_{\rm kin}$	1
H_1	1	$F_{\rm kb,1}$	1	$T_{\rm dip}$	$2T$	$\beta_{\rm kick}$	5	$\beta_{\rm I}$	3
T	5000	$T_{\rm kb}$	$3T$	$H_{\rm dip}$	$\frac{4H_1}{10}\sqrt{\frac{\alpha_{\rm kick}}{1+\alpha_{\rm kick}}}$	$\beta_{\rm dip}$	2	H_I	$\frac{5H_1}{10}\sqrt{\frac{\alpha_{\rm kick}}{1+\alpha_{\rm kick}}}$
τ	500								

Table IV.1: Compilation of all the numerical parameters used in the numerical computations.

IV.4 Numerical validation

Now that we have constructed all the ingredients to achieve the scenario of our interest, we proceed to its numerical verification in this section. Our goals are two-fold: to provide a concrete example in which our model can indeed violate the NEC in a stable manner, and to demonstrate that a successful reheating follows the NEC-violating period. We focus on the NEC-violating-reheating transitions for this discussion and do not include the cosmological constant relaxation sector φ_1 in our numerical computation, whose time scale is much longer than the former eras and would thus be computationally rather impractical. As far as the relaxation sector is concerned, we impose the condition of eq. (IV.19) to ensure that the domination of φ_2 would not lead the motion of φ_1 to overshoot.

Before going further ahead, we make a brief note that a known robust no-go result for stable NEC violation exists in the cases of Genesis scenario and non-singular bounce [181, 182]. However, the crucial assumption for the no-go is that the scale factor either approaches to a non-zero constant value in the asymptotic past or starts with a contracting initial condition. Our present model, on the other hand, is different from either of the cases in that the Hubble expansion rate never vanishes, and thus the no-go theorem does not apply. Our model also differs from the "rolling background" model that must obeys other constraints [73].

IV.4.1 Implementation details

To execute the numerical integration of our model, we solve simultaneously the three equations of motion, *i.e.* eqs. (IV.29b) to (IV.29d). We use the constraint equation, eq. (IV.29a), to monitor the numerical convergence, as it must be compatible with the time evolution of the system. The second derivatives enter the equations only linearly and are hence single-valued at a given time, and the system can be numerically solved using any standard integration algorithm.

The functions K, G_3 and P, appearing in the equations of motion, are substituted by eq. (IV.64) together with v, $F_{\rm kb}$, $H_{\rm necv}$ and U in eqs. (IV.55a), (IV.55b), (IV.56) and (IV.63), respectively, and F_1 and F_2 reconstructed as in eq. (IV.57). In order to fix a reasonable set of model parameters, we choose the values compiled in table IV.1 for our numerical integration. The duration of the NEC-violating period relates to a few parameters, *i.e.* T, $T_{\rm kb}$ and $T_{\rm dip}$, and we thus take them at roughly the same order of magnitude. The ending time of the NEC violation is controlled by τ, and since we demand the reheating field φ_3 transit back to its true potential minimum quickly enough to start oscillating, the value of τ is taken smaller than T. The parameter H_1 approximately normalizes the value of the Hubble expansion rate at the NEC-violating era, and we use it as the units for inverse time t^{-1}, amounting to fixing $H_1 = 1$. In seeking a solution of the approximate form $\partial_t\varphi_2 \sim 1$, we also measure φ_2 in the units of H_1^{-1}. In order for φ_2 to kinetically dominate the energy density during the NEC-violation, we take the values of $H_{\rm dip}$ and H_I smaller than H_1. During the NEC violation the φ_2 field receives a small "kick" associated with $\alpha_{\rm kick}$ by the change of φ_3. The value of H_0 is that of the Hubble expansion rate during the long-lasting NEC-preserving era, which is to our concern essentially the present Hubble value. It is thus supposed to be extremely small; however, such a huge hierarchy is rather difficult to handle in numerical computations, and we here take a relatively large (but much smaller than H_1) value $H_0 = 10^{-3}$ for the purpose of demonstration. Values of order unity are chosen for other parameters. The reduced Planck mass $M_{\rm Pl}$ does not affect the dynamics. Let us emphasize that this set of parameters is chosen to support a proof-of-concept, and other choices can show behaviors similar to the current study.

We take the initial time of the numerical integration well before the onset of the NEC violation. We choose to set the initial conditions as

$$\varphi_2 = -5T\,, \qquad \dot\varphi_2 = 1\,, \qquad \varphi_3 = 0\,, \qquad \dot\varphi_3 = 0\,. \tag{IV.65}$$

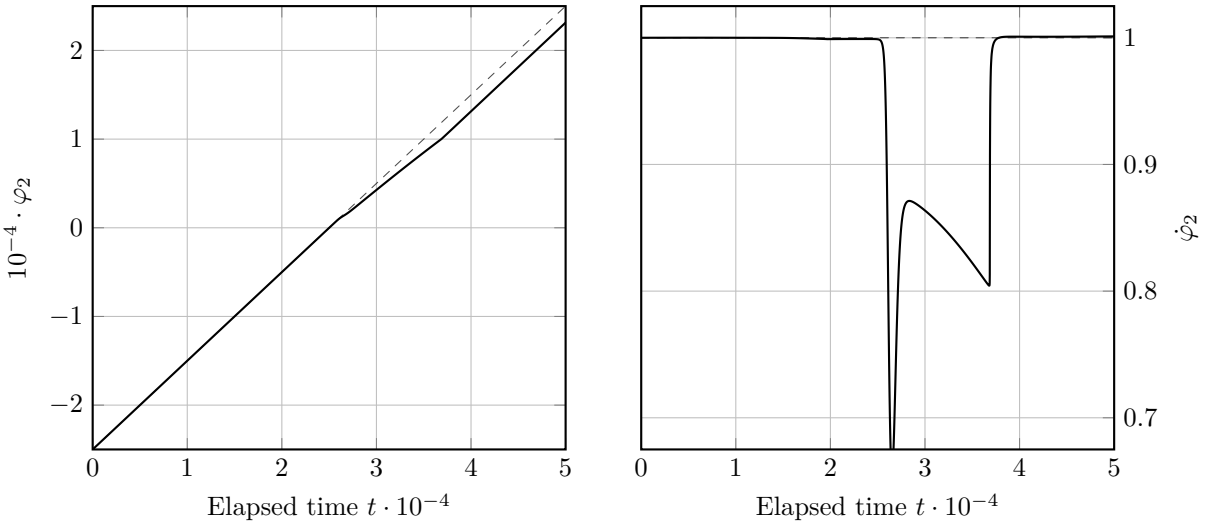

Figure IV.6: Time evolution of the NEC-violating field φ_2 on the left panel, and its time derivative $\dot{\varphi}_2$ on the right. The dashed line on the left corresponds to $\varphi_2 = t$, which would be the solution in the absence of φ_3.

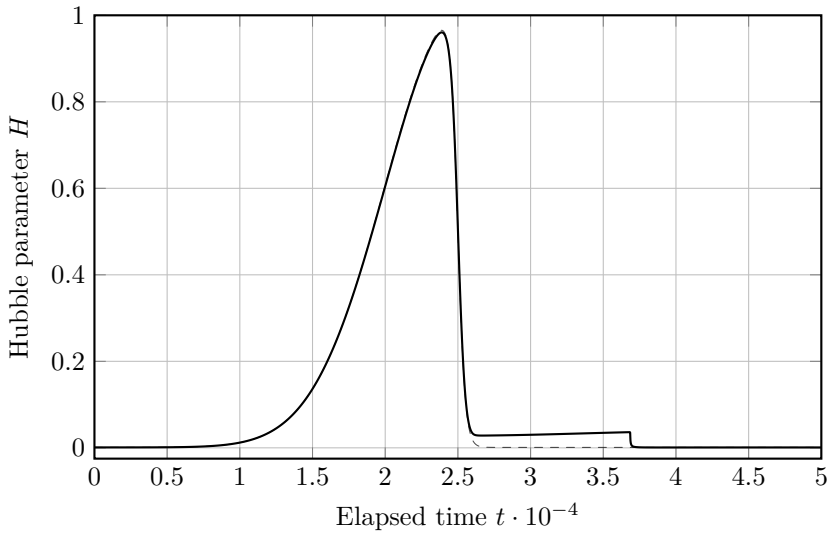

Figure IV.7: Time evolution of the Hubble expansion rate H. Notice the overall bell shape as well as the small drop at later times. The input shape H_{necv} (fig. IV.3) is here reminded by the dashed line, which would be the behavior of H in the absence of φ_3.

That is, the NEC-violation field φ_2 is assumed to be on its attractor solution, and our choice of φ_3 potential sets the minimum of φ_3 at the origin during the period of conserved NEC. Now all the ingredients are ready to perform the numerical computation.

IV.4.2 Numerical results

We show the result plots in figs. IV.6 to IV.8. The first, fig. IV.6, depicts the trajectories for φ_2 and its time derivative $\dot{\varphi}_2$. As can be observed, the overall behavior is close to $\varphi_2 = t$, in accordance to the input eq. (IV.54) of the reconstruction process, with a transient deviation during the NEC-violating phase. This indicates that φ_2 stays closely in the attractor regime discussed in section IV.3.2, despite the additional ingredient for reheating, which is φ_3. This justifies our separate treatment of the NEC-violation and reheating sectors in section IV.3 and confirms the validity of our scenario.

The evolution of the Hubble expansion rate, shown in fig. IV.7, also verifies the desired behavior by

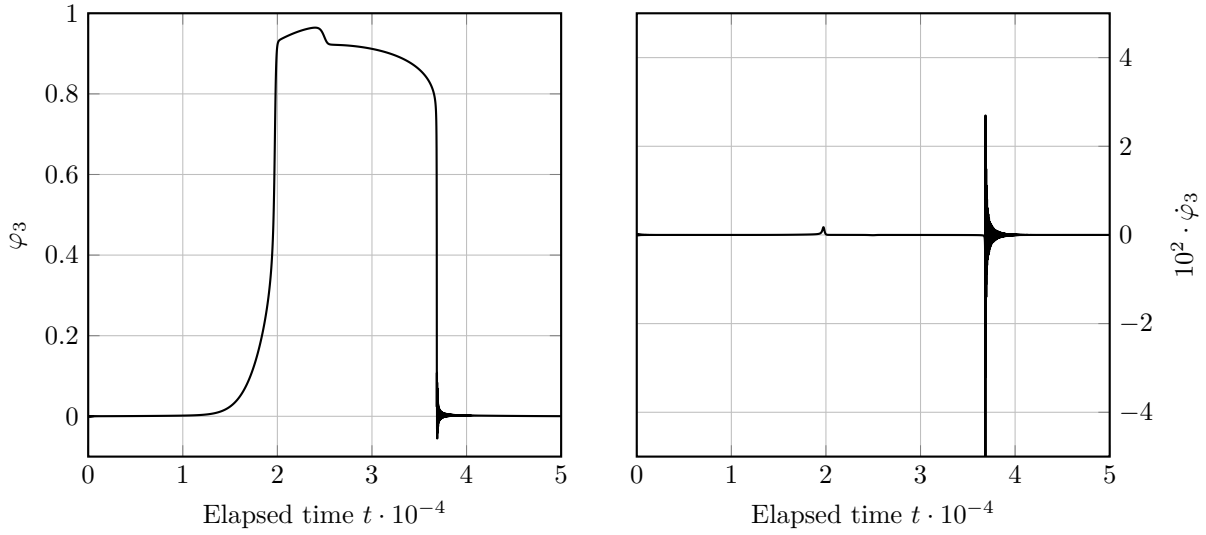

Figure IV.8: Time evolution of the reheating field φ_3 on the left, and its time derivative $\dot{\varphi}_3$ on the right. One can refer to fig. IV.5 to observe that φ_3 overall follows the target trajectory, and ends up oscillating on its return to the true minimum of the reheating potential. The latter oscillation is also clearly visible in the time derivative of φ_3, as well as the comparatively small initial move to the temporary equilibrium position.

violating the NEC violation for a finite duration. While the value of H drops toward the end of the NEC violating period around $t \approx 2.5 \cdot 10^4$, it does not reach its final value immediately, but instead it stays at a larger value for some time until finally dropping to the NEC-preserving value H_0. This is due to the contribution from the reheating field φ_3, which is trapped at the local minimum of its effective potential as illustrated in the bottom panels of fig. IV.5. Except for this small modulation, the overall behavior mimics the shape of the predetermined $H_{\rm necv}$ in eq. (IV.56), which is co-drawn as a dashed curve in fig. IV.7.

Thanks to the NEC violation, φ_2 effectively stores energy, and the field φ_3 that is coupled to it in turn acquires part of the energy to reheat the Universe. For successful reheating and efficient energy release, it is essential for φ_3 to actually roll down at the end of the NEC violation and start oscillating around its true potential minimum. This is the dynamics indeed observed in the numerical evolution as in fig. IV.8. As seen, the initially stabilized φ_3 at $\varphi_3 = 0$ is displaced at the beginning of the NEC-violating phase through its interaction with φ_2. When H drops around $t \approx 2.5 \cdot 10^4$, φ_3 is left at the same local minimum, though its value slightly changes due to the drop. It stays there for some time, during which its effective potential regains the true minimum at the origin as illustrated in the bottom right panel of fig. IV.5. Eventually φ_3 drops toward the minimum and starts the oscillation, which is the moment reheating occurs. This concludes the concrete demonstration of the reheating mechanism of the Universe that would otherwise be empty after the relaxation phase of the cosmological constant.

A few consistency checks are in order. First, we ensure that the presence of the NEC violation should not mess up the relaxation mechanism, namely the condition for no overshooting, eq. (IV.19), needs to be imposed. Under the current parametrization of the numerics, $\partial_t \varphi_2 \equiv M^2 \approx 1$, and t is measured in the units of H_1^{-1}, and so is φ_2, where H_1 is approximately equal to the value of the Hubble expansion rate during the NEC violation. Then the condition of eq. (IV.19) translates to

$$\frac{\Delta\varphi_2}{H_1^{-1}} \lesssim \left(\frac{M_{\rm Pl}}{\sqrt{3}\,H_1}\right)^{4m-2} \frac{H_0^2}{M_{\rm Pl}^2}\,. \tag{IV.66}$$

In our example numerical computation, $\Delta\varphi_2$ for the NEC violation is about a few times 10^4 in the units of H_1^{-1}, and if we take $H_1 \sim 10^{12}\,\text{GeV} \sim 10^{-6} M_{\rm Pl}$, assuming a high NEC violating energy scale, we have $H_0 = 10^{-3} H_1 \sim 10^{-9} M_{\rm Pl}$. Then the above condition of eq. (IV.66) is satisfied for $m \gtrsim 1.45$, which is weaker than the theoretical constraint $m > 3/2$ already imposed (see after eq. (IV.10)). Note that the realistic value of H_0 is much smaller than that taken in our numerical example, and nonetheless the condition can be met for a larger value of m without difficulty.

Moreover, we can easily verify that the stability conditions against small perturbations are also fulfilled in our result. Among the no-ghost conditions summarized in eq. (IV.44), the second one, $\mathcal{G}_\varphi > 0$, is trivially

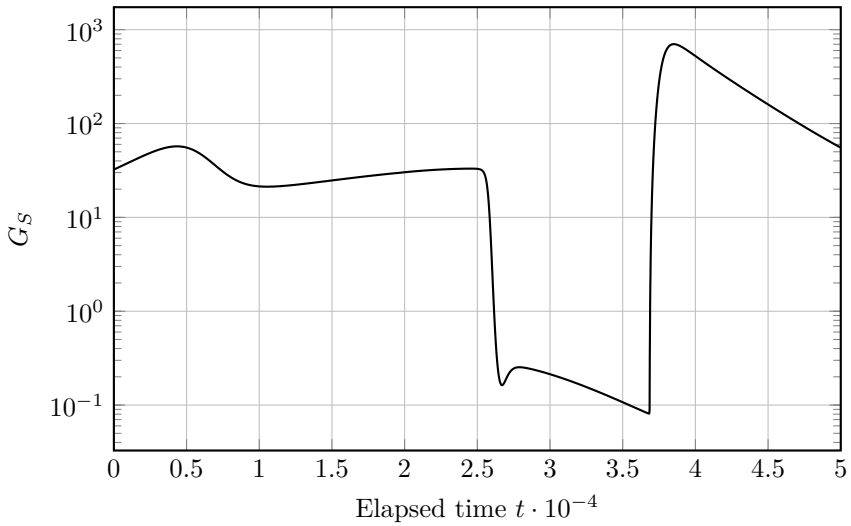

Figure IV.9: Time evolution of the no-ghost condition $\mathcal{G}_S$, defined in eq. (IV.43). Its value is observed to remain positive, satisfying the first no-ghost condition in eq. (IV.44). Note that the other no-ghost condition is trivially satisfied, see the main text.

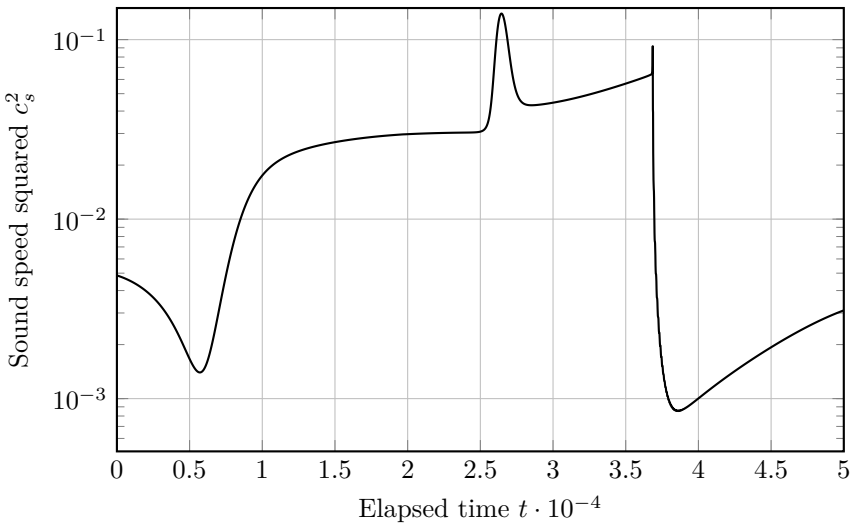

Figure IV.10: The square of the speed of sound, c_s^2, remains strictly positive and below unity during the whole cosmic history, showing the absence of gradient instability and superluminality. The other sound speed is trivially 1 in our present case.

satisfied with our choice $P \propto X_3$ (*i.e.* $\mathcal{G}_\varphi = M_{\rm Pl}^2 \beta_{\rm kin}^2$), and the first one, $\mathcal{G}_S > 0$, is numerically confirmed in fig. IV.9. On the other hand, the squared sound speeds c_s^2 obtained in eq. (IV.51) do not invoke any instabilities. One of the values is trivially unity, $c_\chi^2 = 1$, in our case, and the other, $c_s^2 = \mathcal{F}_S/\mathcal{G}_S + \mathcal{A}$, is shown to be bounded by $0 < c_s^2 < 1$ in fig. IV.10 for the entire duration of the computation, and thus neither gradient instability nor superluminality is present.

The above results therefore show the realization of our target scenario: while φ_1 operates the relaxation mechanism of cosmological constant, reviewed in section IV.1.1, the field φ_2 stably violates the NEC, and the reheating field φ_3 moves to a new minimum, before oscillating on its way back to its true minimum and eventually reheating the Universe.

IV.5 Summary and discussion

This section exhibits a concrete model that both answers to the cosmological constant problem by dynamically relaxing the CC, and subsequently reheats the Universe (section IV.1). It builds upon two previous works, [53, 54] and [176], and extends the studies on stability and potential overshooting issues with numerical confirmation. This work provides a conceptual proof of a system that resolves the CC problem without fine-tuning.

The model built here is the stable assembly of three components. Firstly, it introduces a scalar field φ_1 [53, 54] equipped with an atypical kinetic term modulated by an inverse power of the spacetime curvature invariant, which effectively lets the field φ_1 roll down and eventually has its potential converge to a tiny, but positive value. This final value becomes an effective CC. This dynamical relaxation process "feels" the value of any existing contributions to the CC, including quantum vacuum energy, and fixes the classical vacuum expectation value of φ_1 such that it cancels out the CC. The mechanism is not vulnerable to radiative corrections to curvature either, thus enjoying the advantage of avoiding known fine-tuning issues associated with CC. However, it also effectively empties the Universe, by diluting its contents such as radiation and matter by the cosmic expansion. This is by construction an inevitable consequence from the φ_1 sector alone, and an additional ingredient is in need for successful cosmology.

Secondly, to resolve this newly introduced issue, two other scalar fields φ_2 and φ_3 work together to violate the null-energy condition and repopulate our Universe. The former field φ_2 goes through the dynamics that effectively raises the value of the Hubble expansion rate for transient periods, thus breaking the null-energy condition. In order to ensure that the NEC violation does not destroy the CC relaxation mechanism of φ_1, we impose the condition of eq. (IV.19) to avoid the case in which φ_2's motion irreversibly lets φ_1 overshoot the zero of the effective CC. We also require the time scale of the former be much shorter than that of the latter, giving sufficient time for the CC relaxation to operate, and that φ_2 respects (approximate) shift symmetry in the regions where the NEC is preserved. Moreover, for the sake of naturalness with respect to the timing of NEC violation, the field space of φ_2 is assumed to be periodic with a period much longer than the duration of a single NEC violation phase. This way our Universe goes through this phase multiple times and our current Universe merely occurs after many cycles of them. The field φ_3 acts as a reheating field that extracts the energy from the NEC violation sector, starts oscillating after it, and eventually reheats the Universe.

Thirdly, the last component of our model is the gravity sector. It has non-minimal couplings to φ_1 and φ_2, as already described. As the metric-only part, together with the standard Einstein-Hilbert term, our action includes the quadratic term of the Ricci scalar, which stabilizes the CC relaxation sector [53, 54]. These three ingredients together achieve our complete cosmological scenario of CC relaxation, NEC violation, and reheating, in a stable manner.

In order to concretely realize the desired cosmological history, the model functions need to be fixed, and we proceed to their reconstruction in section IV.3. While we determine the φ_2 sector in an unambiguous manner, the way φ_3 is included is rather *ad hoc*. Nevertheless we conduct numerical integration for the entire system of φ_2 and φ_3 (but without φ_1, for numerical ease) in section IV.4, thus justifying our methodology and confirming the realization of NEC violation followed by a reheating phase. The stability conditions against small perturbations are also shown to be respected.

In our numerical example, the energy used for reheating is roughly one order of magnitude smaller than the energy acquired by the NEC violation in the units of H, as seen in figs. IV.7 and IV.8. This is basically the limitation due of the concrete implementation we have chosen, and we leave to future studies the possibility of more efficient energy transfer and higher reheating scale. Moreover, our current choice of parameters does not accommodate an inflationary phase and thus has no implications (for now) for the structure formation and cosmic microwave background anisotropies. The connection to these observables

is beyond the scope of our present work, as satisfying all the stability conditions simultaneously is already a non-trivial task in the minimal scenario. We would like to return to this issue in the future work.

The current model is based on the Horndeski class of theories to violate the NEC. As an another possibility, the so-called minimally modified gravity theories [140, 183, 139] could be an interesting candidate. While this class of theory contains only two degrees of freedom and consequently avoids instabilities with no difficulty, it nonetheless allows a large freedom for background evolution, not limited by energy conditions. Our conceptual scenario may thus provide a fertile ground for model buildings.

The concrete model considered in these last sections is an effective theory. Linking it to some more fundamental UV theory could also lead to an interesting path to explore. That would accomplish a complete, self-containing solution to the long-standing CC problem. We wish our present study gives one step forward in healing this conceptual pathology.

Applying minimally modified gravity

Chapter V

Spherical gravitational collapse

As the first of the two applications of VCDM presented in this work, we will investigate numerically the gravitational collapse of a massless scalar field in VCDM. For the introduction of VCDM, we refer to the previous section II.6.1.

It is well-established that GR generates black holes following gravitational collapse. In fact, it is even a possible test for candidate alternative theories of gravity: can the candidate theory accommodate a *black hole* (BH), or at the very least include an object that imitates closely BH. By virtue of its aforementioned overlap with GR solutions, one may already expect VCDM to admit BH from gravitational collapse as well, at least in specific foliations of spacetime. On the other hand, unlike GR, the fundamental symmetry of VCDM is no the 4D diffeomorphism invariance, but the invariance under the foliation-preserving diffeomorphism (like for HL gravity, which we saw in chapter III). Thusly, one cannot change the time slicing that is preferred by the theory. In VCDM, different time foliations represent physically different solutions and, whether or not the *apparent horizon* (AH) appears before a singularity and a breakdown of the time foliation carries great importance. A collapsing cloud of dust was recently subject to a numerical study in ref. [153] and did indeed demonstrate the formation of a black hole, its solution coinciding with a particular foliation of the Oppenheimer-Snyder collapse in which the AH forms prior to the singularity and the breakdown of the foliation.

This chapter is articulated around two parts. Firstly, in section V.1, we derive the equations of motion after assuming a spherically symmetric ansatz. These are simplified by demanding an asymptotically flat spacetime, allowing us to integrate out the instantaneous shadowy mode and acquire a constant ϕ and traceless extrinsic curvature. After specifying relevant boundary conditions and initial conditions, the equations of motion are integrated. Secondly, we complete our investigation with a numerical study of our system. The numerical setup, as well as the simulation results, are presented in section V.2. We confirm the simulation convergence is well-behaved, the appearance of an AH, and the lapse evolution inside the AH towards zero. Section V.3 ends this chapter with a summary and a discussion of the results obtained.

V.1 Setup

As a matter source, we consider a canonical massless scalar field ψ described by the action

$$\frac{M_{\rm Pl}^2}{2}\int dtd^3xN\sqrt{\gamma}\left[(\partial_\perp\psi)^2-\gamma^{ij}\partial_i\psi\partial_j\psi\right]\,,\quad \partial_\perp\equiv\frac{1}{N}(\partial_t-N^i\partial_i)\,. \tag{V.1}$$

Combining eq. (II.21) and eq. (V.1) produces the total action. We shall now start by deriving the EoM in a spherically symmetric case before defining the setup that will enable us to numerically evolve the system in section V.2.

V.1.1 Basic equations

In its simplest form, a BH is traditionally expected to respect a spherical symmetry, as the Schwarzschild metric in GR bears witness. Naturally, we then decide to adopt a spherically symmetric ansatz. In mathematical terms, this translates as

$$N=\alpha(t,r)\,,\quad N_idx^i=\beta(t,r)dr\,,\quad \gamma_{ij}dx^idx^j=dr^2+\Phi(t,r)^2d\Omega_2^2\,,\quad \psi=\psi(t,r)\,, \tag{V.2}$$

where α and β now relate to the lapse and the shift, respectively, and Φ is the *areal radius*. In parallel, we also write

$$\phi=\phi(t,r)\,,\quad \lambda=\lambda(t,r)\,,\quad \lambda^i_{\rm gf}\partial_i=\tilde{\lambda}(t,r)\partial_r\,, \tag{V.3}$$

where $d\Omega_2^2$ is the metric of the unit 2-sphere. In order to simplify the equations of motion, we introduce trace of the extrinsic curvature K_{ij}, which now reads

$$K = 2\partial_\perp \ln\Phi - \frac{1}{\alpha}\partial_r\beta\,, \tag{V.4}$$

where $\partial_\perp = (1/\alpha)(\partial_t - \beta\partial_r)$, as well as the following variables

$$Q \coloneqq K_r^r - \frac{1}{3}K = -\frac{2}{3}\left(\partial_\perp \ln\Phi + \frac{1}{\alpha}\partial_r\beta\right)\,, \quad P \coloneqq \partial_\perp\psi\,, \quad a \coloneqq \partial_r \ln\alpha\,, \tag{V.5}$$

where K_j^i is obtained by using the spatial metric, *i.e.* $K_j^i = \gamma^{ik}K_{kj}$.

Given this ansatz, the position of an AH, $r = r_{\rm AH}$, can be found by solving[1]

$$g^{\Phi\Phi}\big|_{r=r_{\rm AH}} = 0\,, \tag{V.6}$$

where

$$g^{\Phi\Phi} \equiv -(\partial_\perp\Phi)^2 + (\partial_r\Phi)^2 = -\frac{1}{4}Q^2\Phi^2 + (\partial_r\Phi)^2\,. \tag{V.7}$$

Equations (V.6) and (V.7) represent a known result that is explained again in appendix A. The EoM entirely determine the Lagrange constraints λ and $\bar\lambda$, and we can thus formulate the in the subsequent EoM. These can be categorized into different types. There are three nondynamical equations, which read

$$\frac{\partial_r^2\Phi}{\Phi} = \frac{1-(\partial_r\Phi)^2}{2\Phi^2} - \frac{3}{8}Q^2 - \frac{1}{4}P^2 - \frac{1}{4}(\partial_r\psi)^2 - \frac{1}{2}V(\phi) + \frac{1}{6}\phi^2\,, \tag{V.8a}$$

$$\partial_r Q = -3Q\partial_r\ln\Phi + P\partial_r\psi\,, \tag{V.8b}$$

$$\partial_r\phi = 0\,, \tag{V.8c}$$

and the five the dynamical equations are

$$\partial_t\psi = \alpha P + \beta\partial_r\psi\,, \tag{V.9a}$$

$$\partial_t P = \alpha\left(-KP + \partial_r^2\psi + (a + 2\partial_r\ln\Phi)\partial_r\psi\right) + \beta\partial_r P\,, \tag{V.9b}$$

$$\partial_t\Phi = \alpha\left(\frac{1}{3}K - \frac{1}{2}Q\right)\Phi + \beta\partial_r\Phi\,, \tag{V.9c}$$

$$\begin{aligned}\partial_t Q = \alpha\Bigg(&-KQ - \frac{1}{4}Q^2 + \frac{2}{3}(a^2 + \partial_r a - a\partial_r\ln\Phi) + \frac{1-(\partial_r\Phi)^2}{\Phi^2} - \frac{1}{6}P^2 + \frac{1}{2}(\partial_r\psi)^2\\ &+\frac{1}{9}\phi^2 - \frac{1}{3}V(\phi)\Bigg) + \beta(P\partial_r\psi - 3Q\partial_r\ln\Phi)\,,\end{aligned} \tag{V.9d}$$

$$\partial_t\phi = \alpha\left(-a^2 - \partial_r a - 2a\partial_r\ln\Phi + \frac{3}{2}Q^2 + P^2 + \frac{1}{3}\phi^2 - V(\phi)\right)\,. \tag{V.9e}$$

Two of the nondynamical equations are derived from the definitions of (a, Q, K) and give the first spatial derivative of the lapse and the shift as

$$\partial_r\ln\alpha = a\,, \tag{V.10}$$

$$\partial_r\beta = -\alpha\left(Q + \frac{1}{3}K\right)\,. \tag{V.11}$$

Two extra nondynamical equations are obtained by requiring that the time derivative of the constraints be consistent with spatial derivatives of the dynamical equations as

$$\begin{aligned}\partial_r^2 K = &-2(a + \partial_r\ln\Phi)\partial_r K\\ &-\left(a^2 + \partial_r a + 2a\partial_r\ln\Phi - \frac{3}{2}Q^2 - P^2 - \frac{1}{3}\phi^2 + V(\phi)\right)\left(K + \phi - \frac{3}{2}V'(\phi)\right)\,,\end{aligned} \tag{V.12}$$

$$\begin{aligned}\partial_r^2 a = &-3a\partial_r a + a\left(\frac{(\partial_r\Phi)^2 - 1}{\Phi^2} + \frac{9}{4}Q^2 + \frac{3}{2}P^2 + \frac{1}{2}(\partial_r\psi)^2\right) - 2a^2\partial_r\ln\Phi - a^3\\ &+ P(3Q\partial_r\psi + 2\partial_r P) - 9Q^2\partial_r\ln\Phi + 2(a\partial_r\ln\Phi - \partial_r a)\partial_r\ln\Phi\,.\end{aligned} \tag{V.13}$$

[1] For more details on this, consult subsection III B in [153] and/or subchapters 2.4 and 5.1.7 in [184].

Finally, the extra equations that determine the Lagrange multipliers λ and $\tilde{\lambda}$, and which we can make use to remove any depedence in these, are

$$\lambda = -\frac{2}{3}(K+\phi)\,, \quad \partial_r\tilde{\lambda} + 2\tilde{\lambda}\partial_r \ln\Phi = -\left(\frac{2}{3}(K+\phi) - V'(\phi)\right)\alpha\,. \tag{V.14a}$$

We are interested in evolving the nine variables ψ, P, Φ, Q, ϕ, α, β, K and a. The two Lagrange multipliers λ and $\tilde{\lambda}$ do not appear in any of the eqs. (V.8a) and (V.13). Hence, we shall not consider them anymore.

V.1.2 Integrating out shadowy mode

In actual numerical studies, we restrict our considerations to the situation where the solution far from the center approaches a flat spacetime in the standard Minkowski slicing without excitations of the scalar field ψ. In vacuum (or for $\psi = $ const.), the theory admits a flat spacetime in the standard Minkowski slicing without spontaneous breaking of the spatial diffeomorphism invariance (and thus with $\tilde{\lambda} = 0$) if and only if $\phi = \phi_0$, where ϕ_0 is a constant that simultaneously satisfies

$$V'(\phi_0) = \frac{2}{3}\phi_0\,, \tag{V.15}$$

$$V(\phi_0) = \frac{1}{3}\phi_0^2\,. \tag{V.16}$$

One can see eq. (V.15) as the definition of ϕ_0 and eq. (V.16) as the condition setting the effective cosmological constant to zero. The latter can be achieved by tuning a constant in $V(\phi)$. Since eq. (V.8c) says that ϕ is independent of r, the assumed asymptotic condition that the solution should approach the flat spacetime far from the center implies that $\phi = \phi_0$ everywhere, where ϕ_0 is defined through eq. (V.15), and that the effective cosmological constant should be set to zero as in eq. (V.16).

In this case, eqs. (V.9e) and (V.12) are greatly simplified and respectively become

$$\partial_r a = -a^2 - 2a\partial_r \ln\Phi + \frac{3}{2}Q^2 + P^2 \tag{V.17}$$

$$\partial_r^2 K = -2(a + \partial_r \ln\Phi)\partial_r K\,. \tag{V.18}$$

As ϕ is no longer dynamical, the previously dynamical eq. (V.9e) for ϕ has been downgraded to a nondynamical eq. (V.17) for a. Because of this, eq. (V.13) will no longer be listed; it simply follows from the other equations.

The equation eq. (V.18) for K can be integrated once to give

$$\partial_r K(t,r) = \frac{f_1(t)}{\alpha(t,r)\Phi(t,r)}\,, \tag{V.19}$$

where $f_1(t)$ is an arbitrary function of t. The regularity of the solution at $r = 0$, where $\Phi(t, r=0) = 0$, requires that $\alpha(t, r=0) \neq 0$ and that $\partial_r K(t, r=0) = 0$. Therefore, the regularity of the center $r = 0$ sets $f_1(t) = 0$ and thus $\partial_r K(t,r) = 0$ and $K(t,r) = f_0(t)$, where $f_0(t)$ is an arbitrary function of t. As already stated, we assume that the solution far from the center approaches a flat spacetime in the standard Minkowski slicing without excitations of the scalar field ψ. This implies that $K(t,r)$ should vanish at the spatial infinity, meaning that $f_0(t) = 0$ and $K(t,r) = 0$. This way, we have successfully integrated out the so-called shadowy mode, avoiding the corresponding boundary value problem.

V.1.3 Nondynamical Q

Integrating out the shadowy mode simplifies the EoM. For practical reasons—and we shall do so in the subsequent numerical computations of section V.2— one can downgrade Q from a dynamical variable to a nondynamical one by abandoning eq. (V.9d) and instead using eq. (V.8b) to determine the evolution of Q. In this case, the dynamical equations, with the shadowy mode removed, are thus reduced to

$$\partial_t\psi = \alpha P + \beta\partial_r\psi\,, \tag{V.20a}$$

$$\partial_t P = \alpha\left(\partial_r^2\psi + (a + 2\partial_r \ln\Phi)\partial_r\psi\right) + \beta\partial_r P\,, \tag{V.20b}$$

$$\partial_t\Phi = -\frac{1}{2}\alpha Q\Phi + \beta\partial_r\Phi\,,\,, \tag{V.20c}$$

and the nondynamical equations, with eq. (V.8b) now incorporated, become

$$\partial_r Q = -3Q\partial_r \ln\Phi + P\partial_r\psi \,, \tag{V.21a}$$
$$\partial_r \ln\alpha = a \,, \tag{V.21b}$$
$$\partial_r \beta = -\alpha Q \,, \tag{V.21c}$$
$$\partial_r a = -a^2 - 2a\partial_r \ln\Phi + \frac{3}{2}Q^2 + P^2 \,. \tag{V.21d}$$

After downgrading eq. (V.8b), we only keep eq. (V.8a). It now reads

$$\frac{\partial_r^2\Phi}{\Phi} = \frac{1-(\partial_r\Phi)^2}{2\Phi^2} - \frac{3}{8}Q^2 - \frac{1}{4}P^2 - \frac{1}{4}(\partial_r\psi)^2 \,. \tag{V.22}$$

For convenience, we can reformulate this constraint and define the derived quantity $\mathcal{C}$ as

$$\mathcal{C} \coloneqq \partial_r^2\Phi + \frac{(\partial_r\Phi)^2-1}{2\Phi} + \left(\frac{3}{8}Q^2 + \frac{1}{4}P^2 + \frac{1}{4}(\partial_r\psi)^2\right)\Phi \,. \tag{V.23}$$

Therefore, if the constraint of eq. (V.22) is respected, $\mathcal{C}$ must remain identically zero. Deviations from zero will later enable us to observe and quantify the numerical convergence.

Moreover, as K has now reduced to a constant (actually 0), it follows from eq. (V.14a) that λ also does so. Accordingly, the solutions to eqs. (V.20) to (V.22) will, in fact, be exact GR solutions. We are interested in whether or not an AH appears, and if it does, before or after breakdown of the time foliation and formation of a singularity. We reiterate that in GR, a change of the spacetime foliation could reverse the order of these events. However, different foliations in VCDM correspond to physically different solutions. Any singularity or breakdown of the time foliation, once appeared in VCDM, cannot be circumvented by a change of the time slicing.

V.1.4 Boundary conditions

We need to be careful about the boundary condition at the center of spherical symmetry, where $\Phi = 0$. By redefinition of the radial coordinate r, we set

$$\Phi(t, r=0) = 0 \,, \tag{V.24a}$$
$$\Phi(t, r>0) > 0 \tag{V.24b}$$

so that the center of spherical symmetry is at $r = 0$ and that we consider the region $r \geq 0$. For the regularity of the center we require ψ, P, Q, α to be even functions of r and Φ, β and a to be odd functions of r. Furthermore, eq. (V.22) implies that

$$\partial_r\Phi(t, r=0) = 1 \tag{V.25}$$

and eq. (V.21a) implies that

$$Q(t, r=0) = 0 \,. \tag{V.26}$$

Then, once ψ, P, Φ, Q, α, β and a are Taylor expanded with respect to r, the right hand sides of all relevant eqs. (V.20a) to (V.20c), (V.21) and (V.22) are well-defined in the limit $r \to +0$ and can also be Taylor expanded with respect to r. As a consistency check, one can show that the right hand sides of eqs. (V.20a), (V.20b), (V.21c), (V.21d) and (V.22) are even functions of r and that the right hand sides of eqs. (V.20c), (V.21a) and (V.21b) are odd functions of r. Similarly as before, by using the $r \to +0$ limits of eqs. (V.21c) and (V.22), respectively, one can also show that the first r-derivative of the right hand side of eq. (V.20c) vanishes at $r = 0$.

We now introduce an outer boundary at $r = r_\mathrm{b}$ and hereafter consider the region $0 \leq r \leq r_\mathrm{b}$. In order to evolve (ψ, P, Φ) by using the dynamical eqs. (V.20a) to (V.20c), we need to impose appropriate boundary conditions on the outer boundary at $r = r_\mathrm{b}$. If r_b is large enough then we can demand

$$\psi(t, r_\mathrm{b}) = 0 \,, \tag{V.27}$$
$$P(t, r_\mathrm{b}) = 0 \,, \tag{V.28}$$
$$\partial_r^2\Phi(t, r_\mathrm{b}) = 0 \,. \tag{V.29}$$

Up to now, the overall normalization of α is not fixed, correspondingly to the fact that the theory enjoys the time reparametrization symmetry. We fix it by imposing on the lapse

$$\alpha(t, r = r_{\mathrm{b}}) = 1 \tag{V.30}$$

so that the time t agrees with the proper time measured by an observer at the outer boundary. Equations (V.21c) and (V.21d) for the shift and the acceleration a do not require additional boundary conditions since the fact that β and a are odd functions of r already imposes $\beta(t, r = 0) = 0 = a(t, r = 0)$.

V.1.5 Initial condition

We consider the following initial condition at the initial time $t = t_0$:

$$P(t_0, r) = 0\,, \quad Q(t_0, r) = 0\,, \quad \alpha(t_0, r) = 1\,, \quad \beta(t_0, r) = 0\,, \quad a(t_0, r) = 0\,, \tag{V.31}$$

and

$$\psi(t_0, r) = \psi_0(r)\,, \quad \Phi(t_0, r) = \Phi_0(r)\,. \tag{V.32}$$

We localize the initial scalar field $\psi(t_0, r) =: \psi_0$ at some fixed r_0 (effectively forming a "shell"), and we choose to practically model this as

$$\psi_0(r) = A \exp\left(-\frac{(r^2 - r_0^2)^2}{s^4}\right)\,. \tag{V.33}$$

The constants A, r_0 and s determine the amplitude, starting position, and width of the initial wave packet respectively. Having defined ψ_0, the constraint of eq. (V.22) implies that $\Phi_0(r)$ is the solution to

$$\frac{\partial_r^2 \Phi_0}{\Phi_0} = \frac{1 - (\partial_r \Phi_0)^2}{2\Phi_0^2} - \frac{1}{4}(\partial_r \psi_0)^2 \tag{V.34}$$

with the boundary conditions

$$\Phi_0(r = 0) = 0\,, \quad \partial_r \Phi_0(r = 0) = 1\,. \tag{V.35}$$

V.2 Numerical integration

This section now gives the results from numerically integrating the system we have just described. It begins by explaining the schematics of the integration and stating the parameter choice for the initial conditions. We then go on by presenting the simulation results and confirm the creation of an AH. Finally, we make a short parenthesis to explore varying the initial conditions.

V.2.1 Setting up the computations

The dynamics of the collapse are fully described by three dynamical equations for ψ, P and Φ and four nondynamical ones for α, β, a and Q. We solve the system of equations defined by eqs. (V.20a) to (V.20c), (V.21) and (V.22) with the boundary conditions and initial conditions formulated in sections V.1.4 and V.1.5. In order to remain consistent, the nondynamical equations must be solved at every time evaluation. Starting from the initial time $t = t_0$, the initial condition must satisfy the eq. (V.22) and the nondynamical eqs. (V.21) and (V.21a). We then evolve ψ, P and Φ to the next time step $t = t_1$ by using the dynamical eqs. (V.20a) to (V.20c). In order to obtain α, β, a and Q at $t = t_1$, we integrate the nondynamical eqs. (V.21) and (V.21a) on the time slice $t = t_1$. At this point, the numerical accuracy of the solution may be gauged by checking how well the data on the time slice $t = t_1$ satisfies the constraint (eq. (V.22)). The numerical scheme can then be advanced to the next time step by repeating the same procedure.

Unless stated otherwise, the initial field ψ is given by an even Gaussian wave packet of height $A = 0.15$ and a width characterized by $s = 4$ positioned at $r_0 = 10$. An outer boundary r_{b} of the system is placed far from the origin $r = 0$ and the initial wave packet, to prevent it from disturbing the collapsing process and to best simulate an asymptotically flat spacetime. In our case, $r_{\mathrm{b}} = 80$ was used. Larger or slightly smaller values yield equivalent results. Space and time are uniformly discretized into intervals of size Δr and Δt, respectively. We decide here to keep the ratio $\Delta t/\Delta r = 0.2$ constant. A smaller ratio would also have been acceptable, but if Δt is too large relative to Δr, the system may become unstable.

To prevent instabilities from jeopardizing the computations, we also adopt two additional safety measures. Firstly —and most importantly— we use a series expansion near 0 to approximate the first integration points of the nondynamical fields (see also section V.1.4). This significantly helps in taming down numerical errors that are prone to appear near the origin. Secondly, we also include a Kreiss-Oliger dissipation term [185], to mitigate high-frequency instabilities. As is standard, it is chosen to be two orders higher than the convergence order of the spatial numerical derivatives.

The simulation was executed with different integration schemes with consistent result. As an extra sanity check the quantity $\mathcal{C}$, defined in eq. (V.23), was continuously and carefully surveilled to ensure it remained sufficiently small throughout the simulation. A more quantitative examination of $\mathcal{C}$ was also carried out, as demonstrated by fig. V.1. While the overall shape of $\mathcal{C}$ remains unchanged (left plot), the amplitude of $\mathcal{C}$ is inversely proportional to the square of the time step Δt or, equivalently, the spatial gap Δr (right plot). The quadratic convergence is expected as the code uses Heun's method, a second-order method, to integrate the nondynamical equations in space. A fourth-order method was used to compute spatial derivatives and integrate in time. At the time, the same code was used satisfactorily in previous works [186, 49].

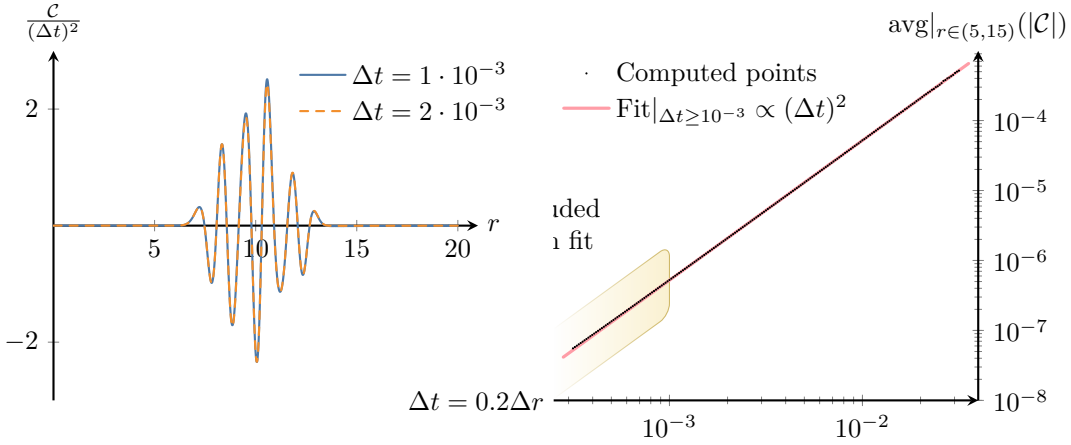

Figure V.1: The left plot displays the constraint $\mathcal{C}$, as defined in eq. (V.23), divided by the square of the time step Δt, versus the radius r, for two different values of Δt. We reiterate that $\Delta t = 0.2\Delta r$. As the shape remains unchanged for the two values of Δt, we conclude that $\mathcal{C} \propto (\Delta t)^2$ and that the numerical convergence is of quadratic order as expected. The right plot portrays the average absolute value of $\mathcal{C}$ for $5 \leq r \leq 15$ (the region in the left plot for which $\mathcal{C}$ clearly is non-zero) against Δt. A simple linear fit neatly illustrates the quadratic convergence order. The fit is here restricted to $\Delta t \geq 10^{-3}$ values in order to avoid the small numerical noise that starts seeping in at lower step sizes (the excluded points are highlighted above). Both plots are generated at time $t = 2$. Albeit early after the numerical resolution is engaged, choosing different times t does not affect the convergence order.

V.2.2 Simulation results

We now turn to the physical quantities thus obtained. Figure V.2 shows the areal radius Φ as a function of r for some selected times t. Notice that one of the displayed times, in this figure and the subsequent ones, is $t \approx 14.1$. As we shall explain in section V.2.3, this corresponds to the AH formation time. At $t = 0$, we observe that $\Phi \approx r$. As time proceeds, it only retains this behavior near $r = 0$, in accordance with eq. (V.24), falling and settling down into a plateau elsewhere. Henceforth, we shall employ Φ as an effective radial coordinate to display how the other quantities behave. Henceforth, we shall use Φ as an "effective radius". The height of its plateau, $\Phi_{\text{pl.}} \approx 0.65$, echoes in the other quantities, as the subsequent figures show.

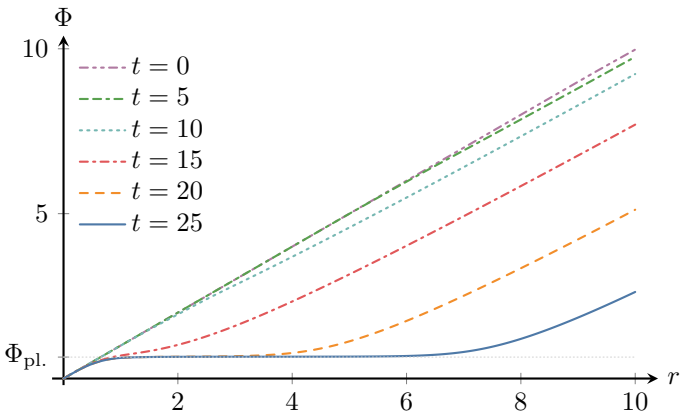

Figure V.2: The areal radius Φ plotted against the proper distance r from the center, at different times t. One may observe the boundary conditions established in section V.1.4 in the shape of Φ. Following the fall of the right side of Φ, a plateau forms around $\Phi_{\text{pl.}} \approx 0.65$.

The other two dynamical quantities ψ and P are given for different times in fig. V.3. For the initial conditions prescribed, the auxiliary scalar field ψ starts by splitting into two parts. One moves out to $r = \infty$ and vanishes, while the other falls to the origin $r = 0$ under its self-gravity and eventually settles near $r = 0$. Naturally, this foreshadows an AH formation (see section V.2.3). Similar behavior is observed for the related variable P ($:= \partial_\perp \psi$, as defined in eq. (V.5)).

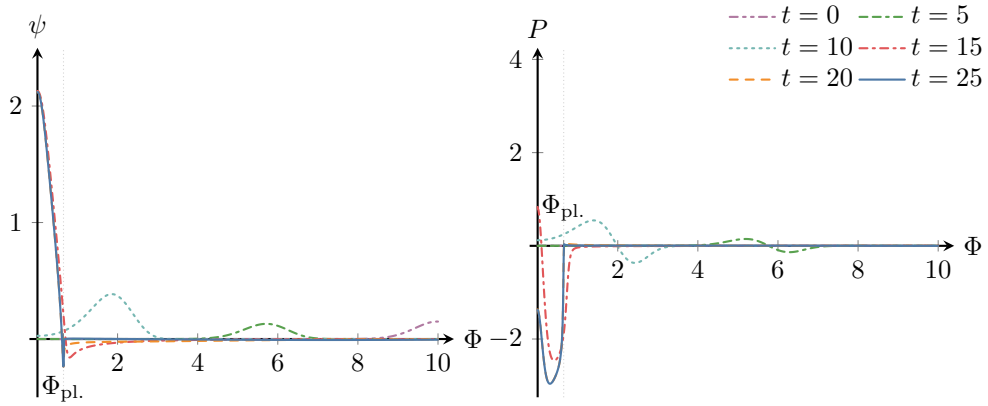

Figure V.3: The auxiliary field ψ (left) and P (right) against the areal radius Φ for different values of time t. The two sharo changes seen at $t = 25$ — the dip under zero for ψ and the sharp turn for P — are located around $\Phi = \Phi_{\text{pl.}}$. For the chosen range in Φ, the split of ψ is not explicitly observable (as $r_0 = 10$).

In parallel, the results for the nondynamical fields are given in fig. V.4. One can observe how the lapse α and the shift β collapse to zero below the threshold value of $\Phi_{\text{pl.}}$. Far from the origin, an asymptotically flat value is manifestly recovered for both quantities. The variables a and Q simultaneously spike around the same threshold value of $\Phi_{\text{pl.}}$.

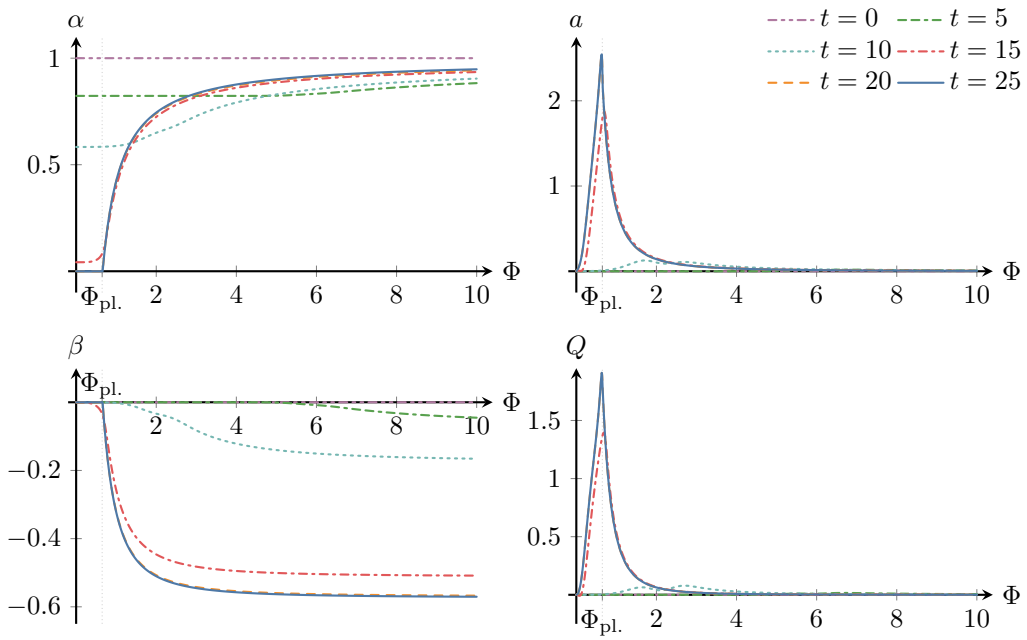

Figure V.4: All four nondynamical fields α, a, β and Q, here plotted against the areal radius Φ at different times t.

V.2.3 Apparent horizon formation

The quantity $g^{\Phi\Phi}$ (defined in eq. (V.7)) is shown for different times in the left plot of fig. V.5. As the behavior of ψ already suggested (see fig. V.3), the collapse does in fact yield an AH, which occurs when $g^{\Phi\Phi}$ crosses zero. This condition is satisfied at $t \approx 14.1$, as the right plot of fig. V.5 shows. Furthermore, in fig. V.4, one can deduce that α and β have not yet collapsed down to 0 at the time of the crossing, implying that the AH indeed forms before any singularity does. Eventually, as the lapse and shift inside the AH evolve towards zero, $g^{\Phi\Phi}$ settles with a minimum around $\Phi_{\text{pl.}} \approx 0.65$ and an outermost crossing of zero near $\Phi \approx 0.88$. This constitutes the main achievement of this work, namely that the gravitational collapse of a massless scalar field in VCDM results in the manifestation of an AH before the breakdown of the time foliation. The final stage of the collapse appears to be a static and stationary black hole.

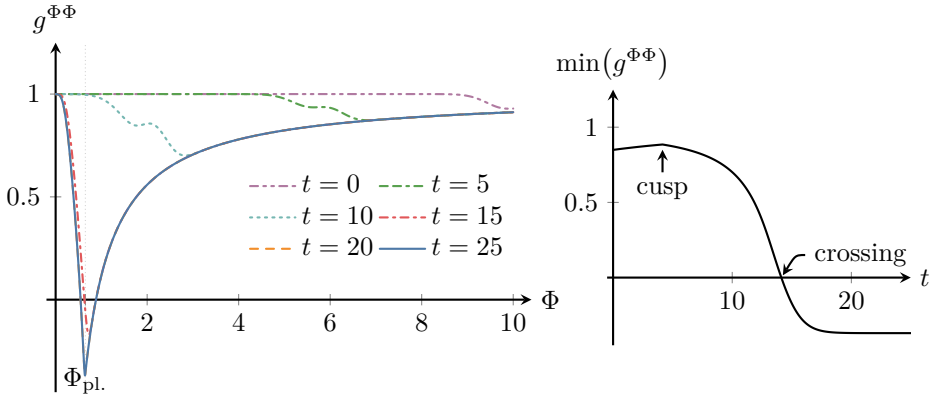

Figure V.5: The left panel gives $g^{\Phi\Phi}$ at different times and demonstrates the creation of an AH eq. (V.6). At late time, $g^{\Phi\Phi}$ settles with a minimum around $\Phi_{\text{pl.}}$ and an outermost crossing near $\Phi \approx 0.88$. The right panel details the minimum of $g^{\Phi\Phi}$ as a function of time and portrays how the horizon forms at $t \approx 14.1$, at the "crossing". A careful reader may wonder about the small cusp near $t \approx 4.1$: it is a consequence of ψ splitting into two at the beginning.

V.2.4 Parameter variation

Until now, we have fixed the initial scalar field parameters of ψ_0 as defined in eq. (V.33) to $A = 0.15$ and $s = 4$. However, depending on the values assigned to these two parameters, an AH may or may not form. The parameter space where an AH does appear is illustrated in fig. V.6. A decrease in A and/or an increase of s may both "dilute" the scalar field enough to allow it to bounce back around the origin before any AH appears or the time slicing breaks down. The scalar field in such a situation is illustrated in the left plot of fig. V.7 for $s = 8$. The right plot of the same figure makes the AH non-formation evident: $g^{\Phi\Phi}$ never crosses zero.

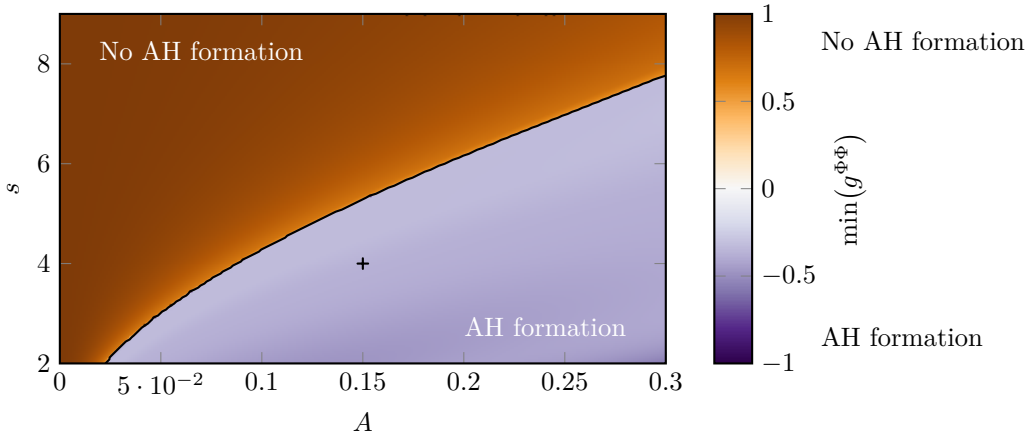

Figure V.6: The minimal value (in time and space) that $g^{\Phi\Phi}$ reaches before $t = 30$, which, given that the initial wave packet ψ is placed at $r_0 = 10$, is enough time to determine whether a horizon forms or not (See eq. (V.6)). The black cross indicates the $A = 0.15$ and $s = 4$ parameter pair that was previously used, while the black line approximately delimits $\min(g^{\Phi\Phi}) = 0$. The range in A was uniformly sampled in 301 points from 0.0 to 0.3, while the values in s were sampled in 176 points uniformly spread from 2.0 to 9.0.

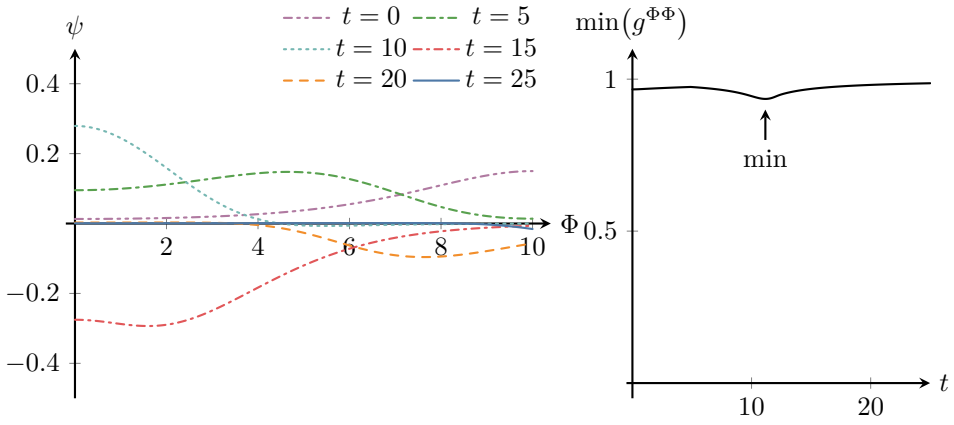

Figure V.7: Evolution of the scalar field ψ for $A = 0.15$ and $s = 8$ on the left. Observe how the packet moves toward the origin before bouncing back. At $t = 25$, the bulk is mostly out of the represented range. The right plot gives $\min(g^{\Phi\Phi})$ for the same configuration. Naturally, no AH forms (*i.e.* $\forall t : g^{\Phi\Phi} > 0$)

V.3 Summary and discussion

As is well-known, a gravitational collapse in the framework of GR leads to the formation of a black hole, a trapped region of spacetime bounded by a marginally outer trapped surface, called the apparent horizon. Deviations from this picture may lead to contradictions with various observations such as GWs and BH shadows. So, whether an alternative theory of gravity admits black holes or not is often used as a litmus test for its validity. It has been previously shown in ref. [154] that a subset of the solutions of VCDM coincides exactly with solutions in GR when the 3+1-decomposition admits a constant trace of

the extrinsic curvature. This subset of VCDM solutions consists of those for which the auxiliary field ϕ and Lagrange multiplier λ are constant. Reassuringly, [153] shows that the spherical gravitational collapse of a homogeneous cloud of dust in VCDM coincides with a foliation of the Oppenheimer-Snyder collapse in GR for which indeed the aforementioned criteria are satisfied.

In the continuation of [153], we have numerically investigating the collapse of a massless scalar field in VCDM, in hopes of observing the formation of a black hole and whether its horizon appears before or after any singularity or foliation breakdown. Starting from a spherically symmetric ansatz of the metric and other relevant quantities in the total action (eq. (VI.2)), we derive the equations of motion. By requiring vacuum flat spacetime in the standard Minkowski time slicing at infinity, regularity at $r = 0$, it has been shown that ϕ to be constant and the trace of the extrinsic curvature to vanish. Equation (V.14a) then further implies a constant λ. Hence, the sufficient conditions are satisfied for solutions of this system to coincide with ones in GR in the specified time foliation.

The equations of motion reduce to a constraint eq. (V.22), three dynamical ones, eqs. (V.20a) to (V.20c), and four nondynamical ones, eqs. (V.21) and (V.21a). These were integrated with the boundary conditions in section V.1.4 and initial conditions in section V.1.5. Furthermore, the quantity $\mathcal{C}$ of eq. (V.23) was used for assessing the numerical accuracy of the integration. The production of an AH was deduced by observing $g^{\Phi\Phi}$ as defined in eq. (V.7) and solving eq. (V.6). For stability purposes, the meshing in time and space was chosen such that $\Delta t/\Delta r = 0.2$. Moreover, possible short-distance instabilities were tamed by implementing Taylor expansions near the origin and the Kreiss-Oliger dissipation term.

First and foremost, as a second-order method —Heun's method— was employed in space, it is reassuring that fig. V.1 portrays a quadratic convergence of the error. Secondly, as seen in fig. V.5, the solutions to eqs. (V.20a) to (V.20c) and (V.21a) to (V.21d) indeed lead to the formation of an AH. Concurrently considering fig. V.4, the lapse α and shift β are everywhere non-zero at the time of the AH formation, meaning the foliation preferred by the theory fully describes spacetime inside the black hole at the time of its formation. As the simulation proceeds, α and β evolve towards zero in a finite region inside (but not up to) the AH. The proper time in this region proceeds slower and slower than that measured by an observer far away at infinity as the universe evolves, eventually standing still. In other words, the breakdown of the time foliation inside the AH is in the process, though from the perspective of an observer outside the AH, it will take infinitely long for it to actually happen. This is by all means not an issue, as there is also an infinite amount of time for the universe to evolve in VCDM. It does however imply that a UV-completion of the theory is needed to fully describe the inside of the black hole.

As previously mentioned, [154] tested the corresponding Oppenheimer-Snyder case; this paper proceeded with studying a collapsing massless scalar field. We have observed the creation of a black hole, its AH forming prior to breakdown of the time foliation and the formation of the singularity. There would be many possible future research paths. In the future, one could consider a collapsing star made up of more realistic matter, such as a fluid, or adding further layers of properties, such as charge or angular momentum. However, this would drastically complicate the dynamics of the collapse. Any form of non-symmetrical dynamics — rotating black holes, black hole and neutron star binaries, GWs — may prevent ϕ from being constant in time. This would yield non-GR solutions of VCDM, which necessarily need to be studied if the theory is to be fully explored.

Chapter VI

Bouncing Universe

As previously described (section I.3.6), inflation [69, 70, 71] has proven to be a very successful framework to simultaneously answer several major cosmological questions, *e.g.* the horizon problem, the flatness problem and the origin of primordial fluctuations. Its paradigm is robust enough to pass high-precision observational tests such as the one presented by the cosmological microwave background (CMB) [72]. However, while phenomenologically satisfying, inflation also leaves us with a set of unanswered questions like the initial singularity [187, 188, 74] and the trans-Planckian problem [63, 65].

A popular alternative approach is the bouncing universe. That is a scenario of the universe where the cosmic expansion we are now observing was preceded by a contracting phase. The turning point between the two dynamics being called the "bounce". In this case, the cosmic history is extended further in the past and gives a natural explanation for causal-connectedness. By introducing this pre-bounce history, the smoothness and flatness problems, as well as the horizon problem, are thus non-issues [65, 189, 190, 191, 64]. Therefore, a bouncing universe does not suffer from the aforementioned issues of inflation, while answering the same concerns the inflationary approach was built to address.

Noticeably, general relativity (GR) does not admit any bouncing solution under the NEC (section I.3.8). Therefore, if the Universe has to undergo a bounce, it must be described by an extended theory of gravity or by a non standard matter content. Several attempts have been made, within different frameworks to invoke such a cosmic history, in *e.g.* $f(T)$ gravity [192], DHOST [193, 194] or Hořava-Lifshitz gravity [195], using a quintom matter field [196], a Cuscuton field [197, 198], and others.

However, constructing viable bouncing models is a challenge. First, due to the violation of the NEC, these models tend to suffer commonly from ghost or gradient instabilities. Within the Horndeski framework [32, 31, 33], that has led to a no-go theorem [181, 182], and a similar result [199] holds in k-essence models [102, 103] as well. Nevertheless, these limitations have not prevented the development of a healthy bounce without ghost or gradient instability near the bounce [200, 201] [1].

Alternatively, these issues can be avoided by working within more general frameworks like ghost condensation [204, 205] and beyond Horndeski/DHOST models [206, 207], as also suggested by the effective field theory of cosmological perturbations [208, 209]. Another issue is the anisotropic stress, or the Belinski-Khalatnikov-Lifshitz (BKL) instability [210]. Besides the conceptual problems the current observations set strict constraints on the scalar spectral index, $n_s \approx 0.96$, while the tensor-to-scalar ratio must respect the bounds of $r_{0.05} < 0.036$ (95% CL) [211]. Naturally, a healthy bouncing scenario must account for these observations. However, while for instance the matter bounce is successful in obtaining an almost scale invariant power spectrum [212, 213], it breaks the bounds on the tensor-to-scalar ratio. Indeed, a conjectured no-go theorem [214, 215, 216] forbids a naive single scalar-field (k-essence CITE) matter bounce to simultaneously satisfy the requirement of a nearly scale-invariant scalar power spectrum, and the tensor-to-scalar ratio bounds, without producing excessive non-Gaussianities. Introducing additional scalar fields can reconcile the matter bounce via the curvaton mechanism [196].

In the present chapter, we build and exhibit a full and concrete model of a bouncing universe scenario, conceived within the formalism of the minimally modified gravity (MMG) [140, 183, 139].

When applied to the very early universe, the VCDM model has the advantage, by construction, to provide the freedom to realize this bouncing scenario as well as safely return to GR after the bounce. It evades the aforementioned no-go theorems, yet provides just enough of a framework to violate the null energy condition, similarly to what was shown recently with Cuscuton [197]. As recently demonstrated in ref. [154], any solutions of the Cuscuton model [144] are solutions of the VCDM model. However, as shown in the same paper [154], the VCDM also admits other solutions, such as GR solutions. Furthermore,

[1] Another model based on the cubic Galileon action was also put forward [202] with limitations [203] however.

the framework of VCDM greatly simplifies the reconstruction of the potential in the Lagrangian from background cosmological histories, as already shown in ref. [139] for general expanding backgrounds. Within the present study, we shall consider whether the scalar power spectrum is (almost) scale invariant at superhorizon scales, as well as investigate the tensor-to-scalar ratio, so that these observables are indeed compatible with the observations.

This chapter is organized as follows. The general formulations of the background and linear perturbations of the tensor, vector and scalar modes in VCDM (model introduced in section II.6.1) are derived in sections VI.1 and VI.2, respectively. In section VI.3, a concrete bouncing dynamics is implemented in the model, and the predictions of the scalar and tensor power spectra are computed. Section VI.4 is devoted to discussions and conclusions of this chapter.

VI.1 Background bouncing solutions

We consider the action of VCDM given in eq. (II.21) to which we add a matter field that evolves on the background. This field is here modelized by a (shift-symmetric) k-essence type of field, explicitly

$$S_{\rm matter} = M_{\rm Pl}^2 \int \mathrm{d}^4x N\sqrt{\gamma}\, P(X)\ , \qquad X \equiv -\frac{1}{2}\, g^{\mu\nu}\partial_\mu\chi\,\partial_\nu\chi = \frac{1}{2}\left[(\partial_\perp\chi)^2 - \gamma^{ij}\partial_i\chi\,\partial_j\chi\right]\ , \tag{VI.1}$$

where $\partial_\perp\chi \equiv n^\mu\partial_\mu\chi$. We have chosen here to normalize the matter sector such that $M_{\rm Pl}^2$ multiplies the entire matter action. The total action is thus

$$S = S_{\rm VCDM} + S_{\rm matter}\ . \tag{VI.2}$$

Since the VCDM alone has only 2 (tensor) DoF, the introduction of the matter sector is essential to generate scalar perturbations, which eventually seed the structure formation in the universe.

By considering a homogeneous and isotropic background, we can write the background quantities as

$$\begin{aligned} &N = \bar{N}(t)\ , \quad N^i = 0\ , \qquad \gamma_{ij} = a^2(t)\,\delta_{ij}\ , \quad \varphi = \phi(t)\ , \\ &\lambda^i = 0\ , \qquad \lambda_0 = \bar{\lambda}(t)\ , \qquad \chi = \bar{\chi}(t)\ . \end{aligned} \tag{VI.3}$$

Then the variations of the action (VI.2) with respect to $\bar{N}$, $\bar{\lambda}$, ϕ, a, $\bar{\chi}$ lead, respectively, to

$$3H^2 = V + \phi\bar{\lambda} + \frac{3}{4}\,\bar{\lambda}^2 + 2XP_X - P\ , \tag{VI.4a}$$

$$0 = 3H + \phi + \frac{3}{2}\,\bar{\lambda}\ , \tag{VI.4b}$$

$$0 = \bar{\lambda} + V_\varphi\ , \tag{VI.4c}$$

$$2\,\frac{\partial_t H}{\bar{N}} + 3H^2 = V + \phi\bar{\lambda} + \frac{3}{4}\,\bar{\lambda}^2 - \frac{\partial_t\bar{\lambda}}{\bar{N}} - P\ , \tag{VI.4d}$$

$$0 = (P_X + 2XP_{XX})\,\frac{1}{\bar{N}}\,\partial_t\left(\frac{\partial_t\bar{\chi}}{\bar{N}}\right) + 3HP_X\,\frac{\partial_t\bar{\chi}}{\bar{N}}\ , \tag{VI.4e}$$

where H is the Hubble expansion rate of eq. (I.26), and V, X and P (and their derivatives) are all evaluated at the background values. After some manipulations, the above equations, they can be rewritten in a more convenient form as

$$0 = V - \frac{\phi^2}{3} + \rho_\chi\ , \qquad \rho_\chi \coloneqq 2XP_X - P\ , \tag{VI.5a}$$

$$0 = 3H + \phi - \frac{3}{2}\,V_\varphi\ , \tag{VI.5b}$$

$$0 = \bar{\lambda} + V_\varphi\ , \tag{VI.5c}$$

$$2\,\frac{\partial_t H}{\bar{N}} = V_{\varphi\varphi}\,\frac{\partial_t\phi}{\bar{N}} - (\rho_\chi + P)\ , \tag{VI.5d}$$

$$0 = \frac{1}{\bar{N}}\,\partial_t\left(\frac{\partial_t\bar{\chi}}{\bar{N}}\right) + 3c_s^2 H\,\frac{\partial_t\bar{\chi}}{\bar{N}}\ , \qquad c_s^2 \coloneqq \frac{P_X}{P_X + 2XP_{XX}}\ , \tag{VI.5e}$$

provided that $P_X + 2XP_{XX} \neq 0$.

Combining the time derivative of eqs. (VI.5b) and (VI.5d) in the above expressions, we find

$$\frac{\partial_t \phi}{\bar{N}} = 3P_X X = \frac{3}{2}\left(\rho_\chi + P\right) \ . \tag{VI.6}$$

Also note that, as standard, eq. (VI.5e) can be rewritten as

$$\frac{\partial_t \rho_\chi}{\bar{N}} + 3H\left(\rho_\chi + P\right) = 0 \ . \tag{VI.7}$$

Combining these last two expressions, eqs. (VI.6) and (VI.7), one can formally write

$$\phi = \frac{3}{2}\int^t \bar{N}\mathrm{d}t'\left(\rho_\chi + P\right) = -\frac{1}{2}\int^t \mathrm{d}t'\,\frac{\partial_{t'}\rho_\chi}{H} \ . \tag{VI.8}$$

For our purpose, we consider from now on a matter species with a constant equation of state $w \coloneqq P/\rho_\chi = \text{const.}$. This can be realized by choosing $P(X)$ as

$$P = P_0\, X^{\frac{1+w}{2w}} = P_0\, X^{\frac{\gamma}{2(\gamma-3)}} \ , \qquad \gamma \coloneqq 3(1+w) \ , \tag{VI.9}$$

where P_0 is some constant. Then we observe the energy density of χ behaves as a matter with equation of state w, *i.e.*,

$$\rho_\chi = \rho_0 \left(\frac{a_0}{a}\right)^\gamma \ , \tag{VI.10}$$

where subscript 0 denotes values at some fiducial time.

VI.2 Linear perturbations

We now consider perturbations around the background eq. (VI.3). We expand the lapse, shift and 3-D metric as

$$N = \bar{N}(t)\left(1+\nu\right) \ , \qquad N^i = \frac{\bar{N}(t)}{a(t)}\left(\partial_i\beta + B_i\right) \ , \qquad \gamma_{ij} = a^2(t)\,\mathrm{e}^{2\zeta}\left[\delta_{ij} + 2\partial_i\partial_j E + 2\partial_{(i}E_{j)} + h_{ij} + \frac{1}{2}\,h_{ik}h_{kj}\right] \ , \tag{VI.11}$$

where $\{\nu, \beta, \zeta, E\}$ are scalar perturbations, $\{B_i, E_i\}$ are vectors ($\partial_i B_i = \partial_i E_i = 0$), and $\{h_{ij}\}$ are tensors ($\partial_i h_{ij} = h_{[ij]} = h_{ii} = 0$), and they all depend on both time and space coordinates. We also expand the auxiliary fields $\{\varphi, \lambda_0, \lambda^i\}$ and the matter field χ as

$$\varphi = \phi(t) + \delta\varphi(t,\boldsymbol{x}) \ , \qquad \lambda_0 = \bar{\lambda}(t) + \delta\lambda_0(t,\boldsymbol{x}) \ , \qquad \lambda^i = \frac{1}{a^2}\left[\partial_i\delta\lambda_s(t,\boldsymbol{x}) + \delta\lambda_i(t,\boldsymbol{x})\right] \ , \qquad \chi = \bar{\chi}(t) + \delta\chi(t,\boldsymbol{x}) \ , \tag{VI.12}$$

where $\partial_i\delta\lambda_i = 0$. The theory eq. (VI.2) under consideration does not respect the symmetry under the temporal coordinate transformation but still preserves the spatial diffeomorphism. Under the transformation

$$x^i \to x^i + \xi^i(\boldsymbol{x}) \ , \tag{VI.13}$$

each variable transforms by the amount, at the linear order,

$$\begin{gathered} \Delta E = a^2\xi_L \ , \qquad \Delta E_i = a^2\xi^i_T \ , \\ \Delta\nu = \Delta\beta = \Delta\zeta = \Delta B_i = \Delta h_{ij} = \Delta\delta\varphi = \Delta\delta\lambda_0 = \Delta\delta\lambda_s = \Delta\delta\lambda_i = \Delta\delta\chi = 0 \ , \end{gathered} \tag{VI.14}$$

where ξ^i has been expanded as

$$\xi^i = \partial_i\xi_L + \xi^i_T \ , \qquad \partial_i\xi^i_T = 0 \ . \tag{VI.15}$$

As can be seen, the h_{ij} components are gauge-invariant, as in GR. Additionally, ν and ζ are also independent of the 3-D spatial gauge choice.[2] We now use the freedom of ξ_L and ξ^i_T to fix the gauge by setting

$$E = E_i = 0 \ , \qquad \text{gauge choice} \ . \tag{VI.17}$$

[2]For 4-D transformation $x^\mu \to x^\mu + \xi^\mu$, writing $\xi_0 \coloneqq \bar{N}\xi^0$, the variables transform as

$$\Delta\nu = \frac{\partial_t\xi_0}{\bar{N}} \ , \quad \Delta\beta = \frac{a}{\bar{N}}\,\partial_t\xi_L - \xi_0 \ , \quad \Delta\zeta = H\xi_0 \ , \quad \Delta E = a^2\xi_L \ , \quad \Delta B_i = \frac{a}{\bar{N}}\,\partial_t\xi^i_T \ , \quad \Delta E_i = a^2\xi^i_T \ , \quad \Delta h_{ij} = 0 \ , \quad \Delta\delta\chi = \frac{\partial_t\bar{\chi}}{\bar{N}}\,\xi_0 \ . \tag{VI.16}$$

Then, we work through the calculations for the following variables:

$$\begin{aligned}&\text{Scalar modes: } \nu,\, \beta,\, \zeta,\, \delta\varphi,\, \delta\lambda_0,\, \delta\lambda_s,\, \delta\chi\ ,\\ &\text{Vector modes: } B_i,\, \delta\lambda_i\ ,\\ &\text{Tensor modes: } h_{ij}\ ,\end{aligned}$$

among which all scalar modes, but one, and all vector modes are nondynamical modes (*i.e.* they appear in the action without time derivatives, up to total derivatives). On top of that, due to the peculiar constraint structure of MMG, one of the remaining scalar degrees of freedom is also nondynamical. Therefore, at the end of the day, we have the following number of propagating (dynamical) degrees of freedom:

$$\begin{aligned}&\text{Scalar: } 1 \text{ DoF}\ ,\\ &\text{Vector: } 0 \text{ DoF (all nondynamical)}\ ,\\ &\text{Tensor: } 2 \text{ DoF}\ .\end{aligned}$$

This counting is the same as in GR (+ one matter DoF). Subsequently, we perform the perturbative analysis of the quadratic action for each sector separately.

VI.2.1 Tensor sector

In what follows, we use the conformal time τ (akin to setting $\bar{N} = a$, see section I.3.4). The tensor sector $\{h_{ij}\}$ is essentially the same as GR. Decomposing h_{ij} into polarization modes in the Fourier space, it reads

$$h_{ij}(\tau, \boldsymbol{x}) = \sum_\sigma \int \frac{\mathrm{d}^3 k}{(2\pi)^{3/2}}\, \mathrm{e}^{i\boldsymbol{k}\cdot\boldsymbol{x}}\, \Pi^\sigma_{ij}\big(\hat{k}\big)\, h_\sigma(\tau, \boldsymbol{k})\ , \tag{VI.18}$$

where we now used the conformal time τ, and where Π^σ_{ij} is the polarization tensor for the 2 polarization modes, satisfying

$$\delta^{ij}\Pi^\sigma_{ij}\big(\hat{k}\big) = \hat{k}^i \Pi^\sigma_{ij}\big(\hat{k}\big) = 0\ , \qquad \Pi^\sigma_{ij}\big(\hat{k}\big)\, \Pi^{\sigma'\,*}_{ij}\big(\hat{k}\big) = \delta^{\sigma\sigma'}\ , \qquad \Pi^{\sigma\,*}_{ij}\big(\hat{k}\big) = \Pi^\sigma_{ij}\big(-\hat{k}\big)\ , \tag{VI.19}$$

and these modes are decoupled at the linear order. Thanks to these properties and the reality condition of $h_{ij}(t, \boldsymbol{x})$, we see $h^\dagger_\sigma(\boldsymbol{k}) = h_\sigma(-\boldsymbol{k})$. Then the quadratic action for $h_\sigma(\tau, \boldsymbol{k})$ reads

$$S^{(2)}_T = \frac{M^2_{\mathrm{Pl}}}{8} \sum_\sigma \int \mathrm{d}\tau\, \mathrm{d}^3 k\, a^2 \left[|h'_\sigma|^2 - k^2\, |h_\sigma|^2\right]\ . \tag{VI.20}$$

where the prime ($'$) denotes a derivative with respect to conformal time. To obtain this, there is no use of background equations. The tensor sector is as standard as GR.

VI.2.2 Vector sector

The vector sector $\{B_i, \delta\lambda_i\}$ is as trivial as in GR. In fact $\delta\lambda_i$ simply does not appear in the quadratic action. We thus decompose B_i into polarizations in the Fourier space,

$$B_i(t, \boldsymbol{x}) = \sum_s \int \frac{\mathrm{d}^3 k}{(2\pi)^{3/2}}\, \mathrm{e}^{i\boldsymbol{k}\cdot\boldsymbol{x}}\, \epsilon^s_i\big(\hat{k}\big)\, B_s(\tau, \boldsymbol{k})\ , \tag{VI.21}$$

where ϵ^s_i is the polarization vector satisfying

$$\hat{k}^i \epsilon^s_i\big(\hat{k}\big) = 0\ , \qquad \epsilon^s_i\big(\hat{k}\big)\, \epsilon^{s'\,*}_i\big(\hat{k}\big) = \delta^{ss'}\ , \qquad \epsilon^{s\,*}_i\big(\hat{k}\big) = \epsilon^s_i\big(-\hat{k}\big)\ , \tag{VI.22}$$

and the reality condition of $B_i(\tau, \boldsymbol{x})$ results in $B^\dagger_s(\boldsymbol{k}) = B_s(-\boldsymbol{k})$. The quadratic action for the vector sector then reads

$$S^{(2)}_V = \frac{M^2_{\mathrm{Pl}}}{4} \int \mathrm{d}\tau\, \mathrm{d}^3 k\, a^2 k^2\, |B_s|^2\ . \tag{VI.23}$$

Therefore there is no dynamical vector mode, just like in GR.

VI.2.3 Scalar sector

The scalar sector $\{\nu, \beta, \delta\varphi, \delta\lambda_0, \delta\lambda_s, \zeta, \delta\chi\}$ is the non-trivial one. Let us first Fourier-decompose each variable as

$$\delta(t, \boldsymbol{x}) = \int \frac{\mathrm{d}^3 k}{(2\pi)^{3/2}} \, \mathrm{e}^{i\boldsymbol{k}\cdot\boldsymbol{x}} \, \delta(\tau, \boldsymbol{k}) \, , \tag{VI.24}$$

where $\delta = \{\nu, \beta, \delta\varphi, \delta\lambda_0, \delta\lambda_s, \zeta, \delta\chi\}$. Note the reality condition imposes $\delta^\dagger(\boldsymbol{k}) = \delta(-\boldsymbol{k})$. In order to eliminate the nondynamical variables in favor of the dynamical ones, we employ the Faddeev-Jackiw method [217]. Due to the non-trivial structure of the theory, we need to impose the background equations before integrating out the nondynamical variables, in order to obtain all the constraint equations. As counted at the beginning of this section, there is only 1 dynamical degree of freedom. We have some freedom to choose the variable we wish to work with. It is convenient to choose the comoving curvature perturbation, defined as

$$\mathcal{R}_k \coloneqq \zeta_k - \frac{\mathcal{H}}{\bar{\chi}'} \delta\chi_k \tag{VI.25}$$

with the conformal Hubble expansion rate $\mathcal{H} \coloneqq aH$ (see section I.3.4). Since this definition does not contain any time derivatives of perturbation variables, this change of variable from the original variables (eq. (VI.25)) amounts to a trivial canonical transformation. After eliminating all the other (nondynamical) variables, we find the quadratic action for $\mathcal{R}_k$ as

$$S_S^{(2)} = \frac{M_{\mathrm{Pl}}^2}{2} \int \mathrm{d}\tau \, \mathrm{d}^3 k \, z^2 \left(|\mathcal{R}_k'|^2 - c_{\mathcal{R}}^2 k^2 |\mathcal{R}_k|^2 \right) \, , \tag{VI.26}$$

where

$$z^2 = a^2 \alpha (1+w) \, \frac{k^2 + \frac{3}{2}(1+w)\alpha\mathcal{H}^2}{c_s^2 \left(k^2 + \frac{3}{2}(1+w)\alpha\mathcal{H}^2 \right) + \frac{1+w}{2}\alpha\mathcal{H}^2 \left(\frac{1+w}{2}\alpha - \epsilon \right)} \, , \tag{VI.27a}$$

$$c_{\mathcal{R}}^2 = \frac{c_s^4 (1+w)^2 k^4 + B_1 \mathcal{H}^2 k^2 + B_2 \mathcal{H}^4}{c_s^2 (1+w)^2 k^4 + A_1 \mathcal{H}^2 k^2 + A_2 \mathcal{H}^4} \tag{VI.27b}$$

with

$$A_1 = \frac{1}{4}(1+w)^3 \alpha (12 c_s^2 + (1+w)\alpha - 2\epsilon) \, , \tag{VI.28a}$$

$$A_2 = \frac{3}{8}(1+w)^4 \alpha^2 (6 c_s^2 + (1+w)\alpha - 2\epsilon) \, , \tag{VI.28b}$$

$$B_1 = \frac{1}{4} c_s^2 (1+w)^2 \left((1+w)^2 \alpha^2 + 6(1+w)\alpha(1 + 3c_s^2 - \epsilon) + 4\epsilon\eta \right) \, , \tag{VI.28c}$$

$$B_2 = \frac{1}{8}(1+w)^3 \alpha \big(-(1+w)^2 \alpha^2 + 2(1+w)\alpha(6c_s^2 + 9c_s^4 + (2 - 3c_s^2)\epsilon) \tag{VI.28d}$$

$$+ 4\epsilon(-(1+3c_s^2)\epsilon + 3c_s^2(1 + 3c_s^2 + \eta))\big) \tag{VI.28e}$$

and

$$\alpha = \frac{\rho_\chi a^2}{\mathcal{H}^2} \, , \qquad \epsilon = 1 - \frac{\mathcal{H}'}{\mathcal{H}^2} \, , \qquad \eta = \frac{\epsilon'}{\epsilon \mathcal{H}} \, . \tag{VI.29}$$

The equation of motion is then simply given by

$$v_k'' + \left(c_{\mathcal{R}}^2 k^2 - \frac{z''}{z} \right) v_k = 0 \, , \tag{VI.30}$$

where we have introduced the Mukhanov-Sasaki-type variable $v_k = z\mathcal{R}_k$. We note that the structure of z and $c_{\mathcal{R}}$ appears to include non-local terms. However, in the ultraviolet limit $k \to \infty$ and with finite $\mathcal{H}$ as well as in the regime of GR at the background level, *i.e.* $\alpha(1+w) = 2\epsilon$ and $\eta = -3(1+w) + 2\epsilon$, for all k, we recover the usual equations of motion from GR.

VI.3 Bouncing scenario

VI.3.1 Set-up

In order to search for a viable parameter space in which the scalar power spectrum is almost scale invariant, we first note that in the regime where the modified gravity from the potential $V(\phi)$ dominates,

i.e. $\alpha\mathcal{H}^2/k^2 \ll 1$, the form of z^2 and $c_{\mathcal{R}}$ simplifies to

$$z^2 \approx a^2\alpha\frac{(1+w)}{c_s^2}\,, \qquad c_{\mathcal{R}}^2 \approx c_s^2\,. \tag{VI.31}$$

Therefore, in that regime we can solve eq. (VI.30) approximately. Supposing that the scale factor behaves as $a \propto (\tau^2)^{n/2}$ we obtain

$$\frac{\mathrm{d}^2 v_k}{\mathrm{d}x^2} + \left(c_s^2\kappa^2 - \frac{n(3w-1)(-2+n(3w-1))}{4x^2}\right)v_k \approx 0\,, \tag{VI.32}$$

where we have introduced $x = \tau/\tau_B$ and $\kappa = k\tau_B$ with $\tau_B > 0$ the bouncing time scale. Therefore, at that regime the independent solutions are as usual given by the Hankel functions, provided w and c_s^2 are constant. Assuming that the regime $\alpha \ll 1$ holds up to horizon crossing for the cosmological microwave background (CMB) scales we can estimate that the spectral index is given via

$$n(3w-1)(-2+n(3w-1)) = 15 - 8n_s + n_s^2\,, \tag{VI.33}$$

which yields the following two solutions for n

$$\frac{5-n_s}{3w-1} \quad \text{and} \quad \frac{n_s-3}{3w-1}\,. \tag{VI.34}$$

In order to have a valid bouncing solution we require that $n > 0$. Therefore, the first solution is valid for $w \gtrapprox 1/3$ and the second one for $w \lessapprox 1/3$, since $n_s \approx 0.96$ [72].

However, an equation of state $w \lessapprox 1/3$ can lead to issues since the anisotropies then grow faster than the energy density of the scalar field in the contracting phase [210]. That is why we shall focus on the first case with $w \geq 1$. Note that this corresponds to $z \propto \tau^{(-3+n_s)/2}$. For $n_s < 3$, which is the case for the primordial curvature perturbation of our universe, z increases in time during the contraction phase and, therefore, $\mathcal{R}_k$ has a decreasing and constant mode in contrast to common bouncing scenarios.

After the bounce we want to recover the usual evolution from GR. This can be achieved either by considering a non-constant equation of state or a transition of the scale factor. We consider the latter case so that

$$\lim_{\tau\to\infty} a \propto \tau^{\frac{2}{3w+1}}\,. \tag{VI.35}$$

In order to match the background after the bounce with GR we have to further ensure that

$$\lim_{\tau\to\infty} \frac{3\mathcal{H}^2}{\rho_\chi a^2} = 1\,, \tag{VI.36}$$

which fixes the normalization ρ_0 of ρ_χ. To combine both ends and include the bounce we write the ansatz

$$a(\tau) = a_0\left(\frac{\tau^2}{\tau_e^2}\right)^{\frac{n}{2}}\Theta(\tau_e-\tau) + a_1\left[1+\left(\frac{\tau}{\tau_B}\right)^2\right]^{\frac{1}{3w+1}}\Theta(\tau-\tau_e)\,, \tag{VI.37}$$

where

$$a_1 = a_0\left(1+\left(\frac{tau_e}{\tau_B}\right)^2\right)^{\frac{-1}{3w+1}} \tag{VI.38}$$

to ensure continuity and the step function is operationally defined as

$$\Theta(x) = \lim_{m\to\infty}\frac{1}{1+e^{-mx}}\,. \tag{VI.39}$$

In these choices, the time τ_e locates the transition between the two different regimes, which we place before the bounce, *i.e.* $\tau_e < 0$. For numerical purposes we have to choose a finite m. The bigger m the sharper the transition, but this may also lead to numerical issues, since the derivatives start to diverge. Later on, we will actually choose rather small values of m.

Furthermore, depending on n, finite m may again bring other numerical issues around $\tau = 0$, at the bounce. That is why it may be convenient to slightly detune the relation by introducing a small τ_a/τ_e shift. Explicitly, the ansatz of eq. (VI.37) is modified to

$$a(\tau) = a_0\left[\left(\frac{\tau}{\tau_e}\right)^2 + \left(\frac{\tau_a}{\tau_e}\right)^2\right]^{\frac{n}{2}}\Theta(\tau_e-\tau) + a_1\left[1+\left(\frac{\tau}{\tau_B}\right)^2\right]^{\frac{1}{3w+1}}\Theta(\tau-\tau_e) \tag{VI.40}$$

with

$$a_1 = a_0 \left(1 + \left(\frac{\tau_a}{\tau_e}\right)^2\right)^{\frac{n}{2}} \left(1 + \left(\frac{\tau_e}{\tau_B}\right)^2\right)^{\frac{-1}{3w+1}} , \tag{VI.41}$$

where $|\tau_a| \ll |\tau_e|$. The role of τ_a is only to regulate the behavior of (the derivatives of) a at the bounce, and we shall later check that the choice of τ_a with $|\tau_a| \ll |\tau_e|$ does not impact the final result.

VI.3.2 Reconstruction of the potential V

Using the background equation of motion (eq. (VI.6)), we can solve ϕ in terms of the conformal time as

$$\phi = \frac{3}{2} \int \mathrm{d}\tau' a(1+w)\rho_\chi + \phi_0 , \tag{VI.42}$$

where ϕ_0 is an integration constant. If we are to consider the full period, this equation can be solved numerically. Before doing so, let us first have a look at the two different regimes separately.

On one hand, deep in the contraction phase, where $-\tau \gg |\tau_e|$ the scale factor is well approximated by

$$a(\tau) \approx a_0 \left(\frac{\tau}{\tau_e}\right)^n , \tag{VI.43}$$

in which ϕ becomes a function of time as,

$$\phi(\tau) \approx \frac{3}{2} \frac{(1+w)\, a_0\, \rho_0}{1 - n\,(2+3w)} \left(\frac{\tau}{\tau_e}\right)^{-n\,(2+3w)} \tau + \phi_0 . \tag{VI.44}$$

The scalar field ϕ asymptotically approaches ϕ_0 for $\tau \to -\infty$ and then grows monotonically in the contraction phase before the transition period. Using eq. (VI.5a), the potential can then be reconstructed as

$$V(\tau) = \frac{1}{3} \left(\frac{3}{2} \frac{(1+w)\, a_0\, \rho_0}{1 - n\,(2+3w)} \left(\frac{\tau}{\tau_e}\right)^{-n\,(2+3w)} \tau + \phi_0 \right)^2 - \rho_0 \left(\frac{\tau}{\tau_e}\right)^{-3n\,(w+1)} . \tag{VI.45}$$

Since during this phase ϕ is monotonically increasing in time we can invert the relation (VI.44) to express τ in terms of ϕ and V in terms of ϕ.

On the other hand, after the transition, but before the bounce, for large $m \gg 1$, the scale factor acts as

$$a(\tau) \approx a_1 \left(1 + \frac{\tau^2}{\tau_B^2}\right)^{\frac{1}{3w+1}} , \tag{VI.46}$$

which leads to

$$\phi(x) \approx \phi_0 + \frac{3}{2} \left(\frac{a_0}{a_1}\right)^{3(1+w)} (1+w)\, a_1 \tau_B \rho_0 x\, {}_2F_1\left(\frac{1}{2}, \frac{2+3w}{1+3w}, \frac{3}{2}, -x^2\right) , \tag{VI.47}$$

where ${}_2F_1$ denotes the hypergeometric function. Similarly as before, the potential then reads

$$\begin{aligned} V(x) \approx \frac{1}{3} & \left(\phi_0 + \frac{3}{2} \left(\frac{a_0}{a_1}\right)^{3(1+w)} (1+w)\, a_1 \tau_B \rho_0 x\, {}_2F_1\left(\frac{1}{2}, \frac{2+3w}{1+3w}, \frac{3}{2}, -x^2\right) \right)^2 \\ & - \rho_0 \left(\frac{a_0}{a_1}\right)^{3(1+w)} (1+x)^{-\frac{3(1+w)}{1+3w}} . \end{aligned} \tag{VI.48}$$

In fig. VI.1, we give the result obtained by the numerical simulation of $\phi(x)$ and $V(\phi)$, across the bounce. The left-hand side plot shows the evolution of the scalar field $\phi(x)$ for the case where $w = 1$, $n = 2.02$, $m = 1$, $\tau_e = -300\tau_B$ and $\tau_a = 0$ (corresponding to $n_s = 0.96$). We there observe that the scalar field is indeed monotonically growing. Therefore, we can invert $\phi(x) \to x(\phi)$ to reconstruct the potential $V(\phi)$ which is given in the right-hand side plot of fig. VI.1. We choose the integration constant ϕ_0 such that ϕ goes to 0 in the limit $x \to \infty$, and then we see $V \to 0$ in the same limit. Before the bounce but after the transition, *i.e.* $-300 (= \tau_e/\tau_B) \ll x \ll -1$, the potential approaches a linear trend. This is expected since for $V(\phi) \propto \phi$, VCDM recovers GR. For $x \ll -300 (= \tau_e/\tau_B)$ the potential (eq. (VI.45)) models the impact of matter and is therefore expected to deviate from the linear trend. However, since the scalar field is roughly constant in that regime the deviation is not visible anymore on this particular plot.

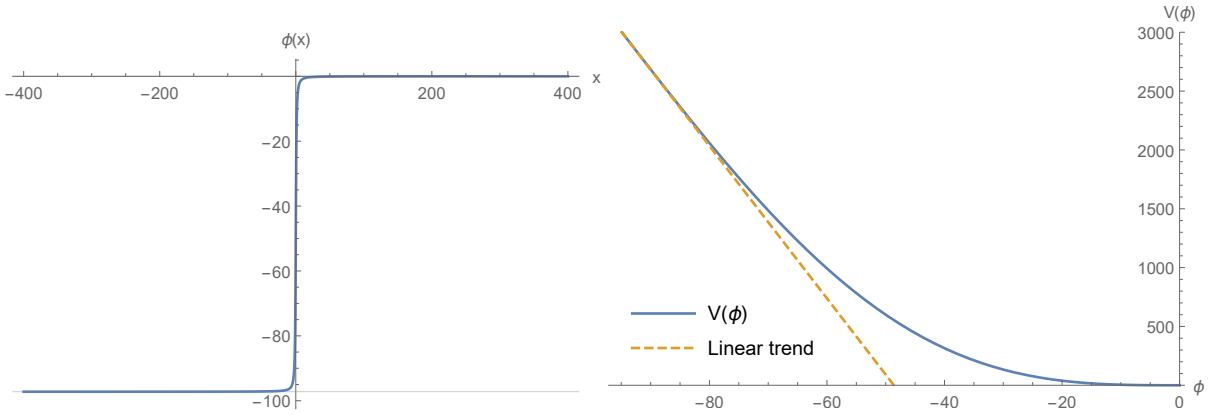

Figure VI.1: The form of the reconstructed potential for $w = 1$, $n = 2.02$, $m = 1$, $\tau_e = -300\tau_B$ and $\tau_a = 0$ (right) and the evolution of the scalar field $\phi(x)$ for the same parameter set (left), where $x = \tau/\tau_B$. Notice that the linear trend indicated (right) is here simply built from the tangent at the minimum of ϕ.

VI.3.3 Power spectrum

Scalar part

We first consider the scalar part and solve the equation of motion (VI.30) numerically. In the present study, we fix the transition time scale $\tau_e = -300\tau_B$ and choose a slow transition with rather small values of m for computational ease. Note that in our convention the bouncing time scale τ_B is taken to be strictly positive.

In fig. VI.2, we plot the sound speed square $c_{\mathcal{R}}^2$ and z, for $n = 2.02$ and $w = 1$ (following eq. (VI.34)) for different values of $\kappa = k\tau_B$ and m. We can observe that z remains positive throughout the evolution and, as expected, it remains independent of m and κ both at very early times and after the bounce. However, in the regime around the transition, at $x = -300$, z depends both on m and κ. In particular for very small values of κ, the value of z starts to deviate earlier from the approximated behavior $z^2 \approx a^2\alpha(1+w)/c_s^2$. This can be easily understood: the approximation is only valid for a large ratio of $k^2 = \kappa^2/\tau_B^2$ to $\alpha\mathcal{H}^2$.

The behavior of $c_{\mathcal{R}}^2$, which is defined in eqs. (VI.26) and (VI.27b), is similar. It deviates only around the transition regime, *i.e.* when the dependency of m actually manifests itself. Again, the dependency on κ depends on the ratio $k^2/(\alpha\mathcal{H}^2)$. Note that for $\kappa \ll 1$ the sound speed square $c_{\mathcal{R}}^2$ can become negative around the transition regime. However, this does not correspond to the standard gradient instability with the exponentially fast growth in the ultraviolet (UV), since in the UV limit ($\kappa \gg 1$) the sound speed squared given in eq. (VI.27b) is positive-definite. On the other hand, in the infrared (IR) or at large scales ($\kappa \ll 1$), where $c_{\mathcal{R}}^2 < 0$, the frequency is still positive-definite since $|z''/z| \gg |c_{\mathcal{R}}^2 k^2|$ (and $z''/z < 0$) so that $\omega^2 \equiv c_{\mathcal{R}}^2 k^2 - z''/z > 0$. Therefore, the model is not plagued by either UV or IR instabilities during the transition phase. Furthermore, the model should be free from the strong coupling, which is usually [3] signaled by vanishing of the UV/subhorizon (*i.e.* $\kappa \gg 1$) sound speed and which is insensitive to the dispersion relation in the intermediate/IR scales. Each mode remains within the regime of validity of the perturbative expansion and smoothly evolves from the initial time to the final time.

In order to numerically obtain the scalar power spectrum, we fix the initial conditions to the standard adiabatic vacuum so that

$$\frac{v_k(x = x_i)}{\sqrt{\tau_B}} = \frac{\sqrt{\pi}}{2}\sqrt{-x_i}H^{(1)}_{\frac{4-n_s}{2}}(-c_s\kappa x_i) \tag{VI.49}$$

and similarly for its derivative. Firstly, we check that our initial conditions for $x \ll -300$ are indeed valid. In fig. VI.3 we plot the normalized error ΔEOM of the initial conditions for different values of κ or m, that is the quantity

$$\Delta\text{EOM} = \left|\frac{1}{v_k}\frac{\mathrm{d}^2 v_k(x)}{\mathrm{d}x^2}\left(c_{\mathcal{R}}^2\kappa^2 - \frac{1}{z}\frac{\mathrm{d}^2 z}{\mathrm{d}x^2}\right)^{-1} + 1\right|. \tag{VI.50}$$

We verify that far away from the transition regime where $\alpha\mathcal{H}^2/k^2 \ll 1$ the error is negligibly small. It only starts to increase during the contraction phase, just as expected. For smaller values of κ, the impact of the scale-dependent mass and sound speed starts to matter earlier since the approximation depends on

[3] This is indeed the case *e.g.* in the framework of EFT of single-field inflation/DE, see *e.g.* [218].

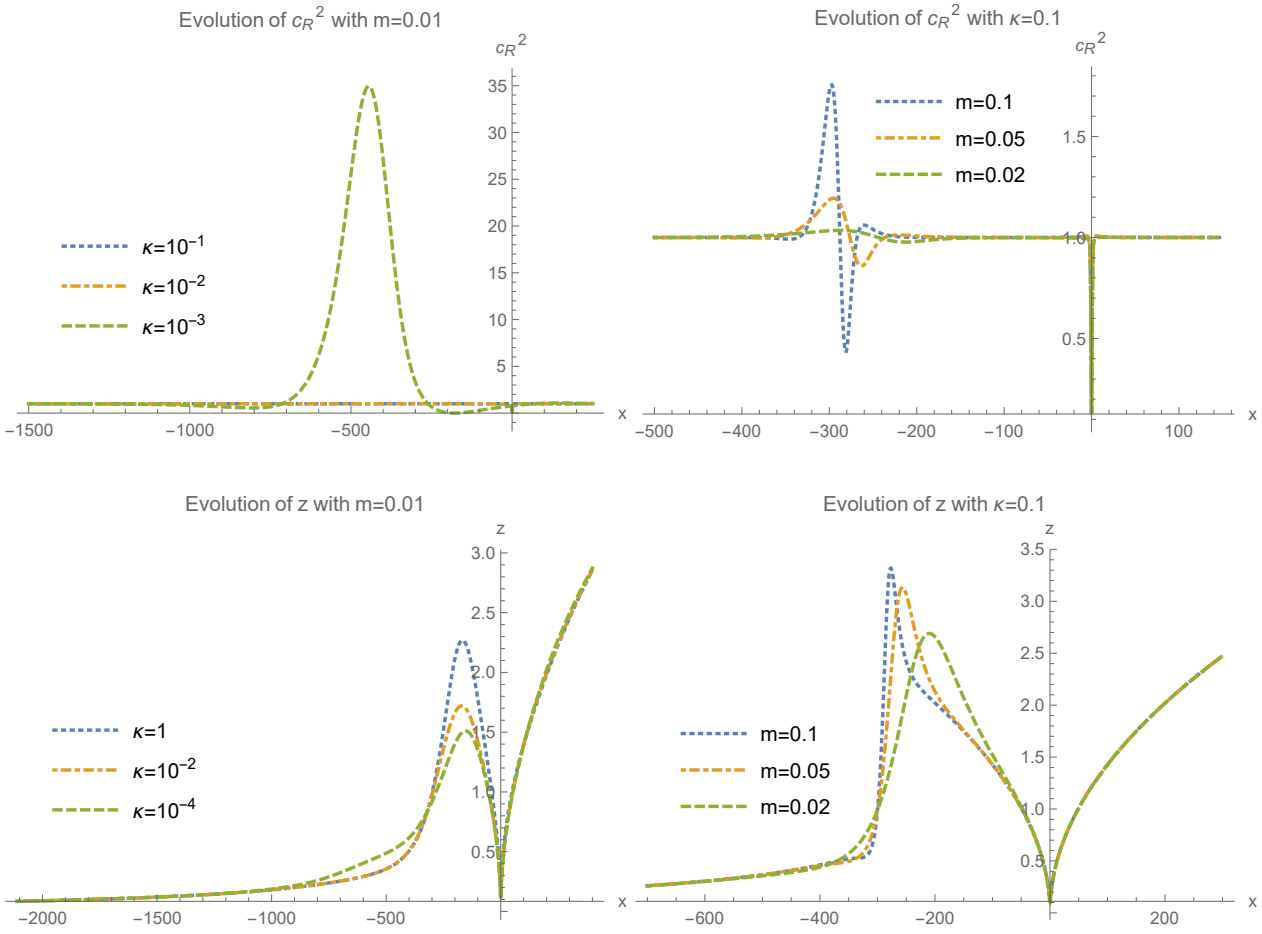

Figure VI.2: In the upper panels we plot the sound speed square for different values of κ (top left) and m (top right). In the lower panels, we plot z for, again, different values of κ (bottom left) and m (bottom right). For these plots we consider the case of $n = 2.02$ and $w = 1$.

the ratio of $\alpha\mathcal{H}^2$ to $k^2 = \kappa^2/\tau_B^2$. On the other hand, changing the value of m does not have any impact at early times. Thanks to the good agreement at $x \leq -10^6$, we do not need to start evolving the EOM from inside the horizon. We can instead start outside the horizon using the analytic approximation. In the following we will fix the starting point for our numerical solution at $x = -5 \cdot 10^6$ for $10^{-11} \leq \kappa \leq 10^{-7}$. Different starting values do not affect the conclusions of this work. From thereon, we shall use $m = 0.01$.

In fig. VI.4, we exhibit the real part and the absolute value of $\kappa^{3/2}\mathcal{R}_k$ for different values of κ. We see that neither at the transition regime nor at the bounce, do we obtain any instability. In fact, neither the transition nor the bounce has any significant impact on the curvature perturbation modes which are already far outside the horizon. For large κ the comoving curvature perturbation is oscillating, while for small κ the curvature perturbation is frozen. However, we still have to be careful. Our analytic approximation holds as long as $\alpha\mathcal{H}^2 \ll k^2$ $(= \kappa^2/\tau_B^2)$. In fig. VI.5, the left-hand side plot shows the ratio for small values of κ. For small values of κ, the approximation here breaks down outside the horizon but still far away from the bouncing regime. The right-hand side plot shows the normalized absolute value of the curvature perturbation (similarly to the right-hand side of fig. VI.4). As expected, the curvature perturbation is frozen before the breakdown of our analytic approximation. During the regime where $\alpha\mathcal{H}^2/k^2 \approx 1$ the curvature perturbation falls down before freezing again. Therefore, the curvature power spectrum after leaving the horizon does not coincide with the one after the bounce.

In fig. VI.6, the power spectrum is given before (at $x = -10^6$) and after the bounce (at $x = 300$) for different combinations of w and n (compatible with $n_s = 0.96$), along with their fit by a spectral index of the form $A \cdot \kappa^{n_s-1}$, where A is the amplitude of $P_\mathcal{R} := k^3|\mathcal{R}_k|^2/(2\pi^2)$. The power spectrum $P_\mathcal{R}$ is indeed slightly red-tilted with the correct spectral index of $n_s = 0.96$ for the three different combination of w and n, for small values of κ. The overall amplitude is slightly different for the curvature power spectrum, while the spectral shape is the same before and after the bounce, because of the aforementioned fall and

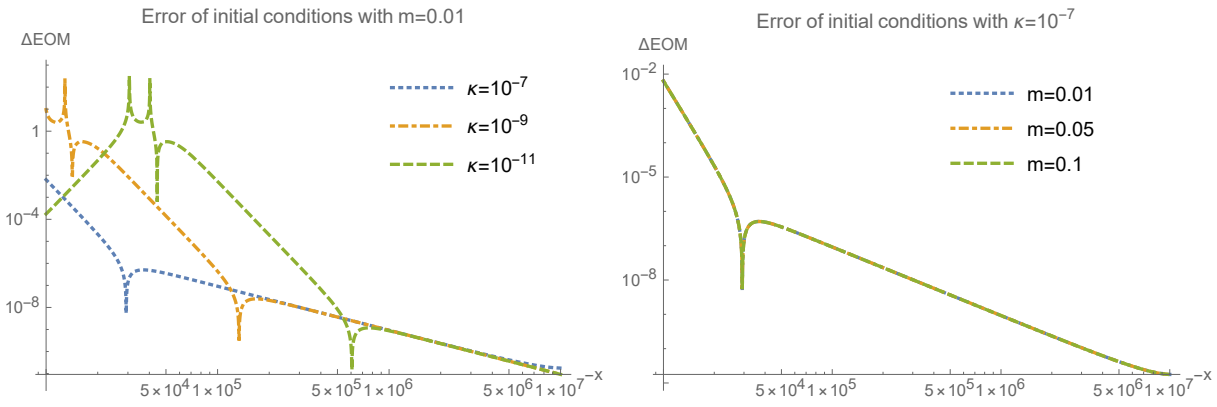

Figure VI.3: The normalized error of the analytical solution for $n = 2.02$ and $w = 1$, for different values of κ with $m = 0.01$ (left) and for different values of m with $\kappa = 10^{-7}$ (right).

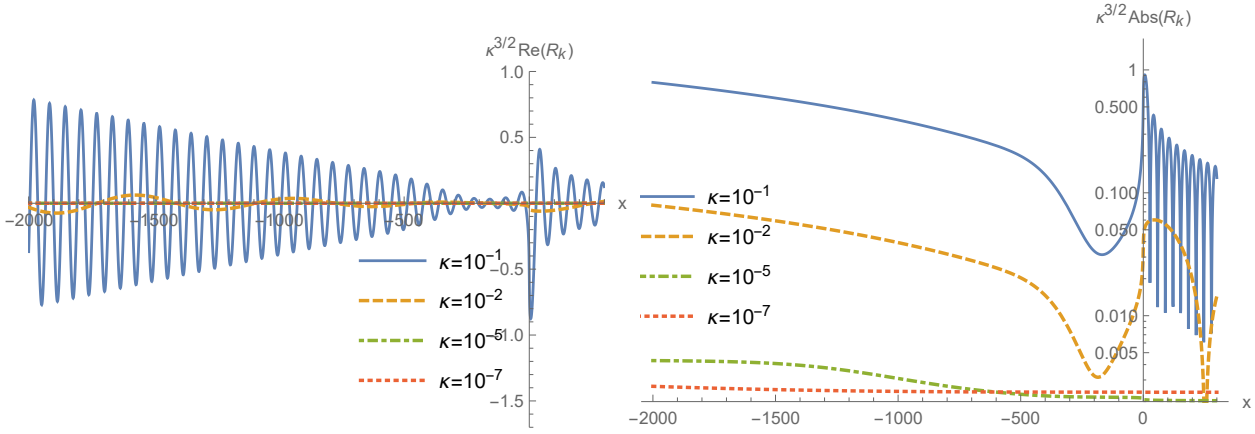

Figure VI.4: The real part (left) and the absolute value (right) of the normalized evolution of the curvature perturbation modes for $n = 2.02$ and $w = 1$, for different values of κ.

freezing behavior.

Tensor part

The tensor perturbations are the same as in GR and are governed by the equation

$$\frac{\mathrm{d}^2 u_k}{\mathrm{d}x^2} + \left(\kappa^2 - \frac{1}{a}\frac{\mathrm{d}^2 a(x)}{\mathrm{d}x^2}\right) u_k = 0 \,. \tag{VI.51}$$

Therefore, it only depends on the specific form of the scale factor a. Before the transition period the scale factor is given by $a \propto (-x)^n$. Therefore, for $n \neq 1$, the solutions are given by the Hankel functions

$$\frac{u_k}{\sqrt{\tau_B}} = \frac{\sqrt{\pi}}{2}\sqrt{-x}H_\nu^{(1)}(-\kappa x) \,, \quad \text{where} \quad \nu = \frac{2n-1}{2} \,. \tag{VI.52}$$

The tensor power spectrum for the cosmological scales will explicitly depend on n and is not anymore always almost scale invariant, but instead we have

$$n_t = 4 - 2n \tag{VI.53}$$

for $n > 1/2$, at horizon crossing in the contracting phase. Here n_t is the spectral index of the tensor power spectrum $P_h := \sum_\sigma k^3 |h_\sigma|^2/(2\pi^2) = A_h k^{n_t}$, with A_h being its amplitude. Therefore, among the three different cases considered for the scalar part with $n = 2.02$, $n = 1.01$ and $n = 101/150 \approx 0.67333\cdots$, only the first case leads to an almost scale invariant power spectrum. The other ones are blue tilted.

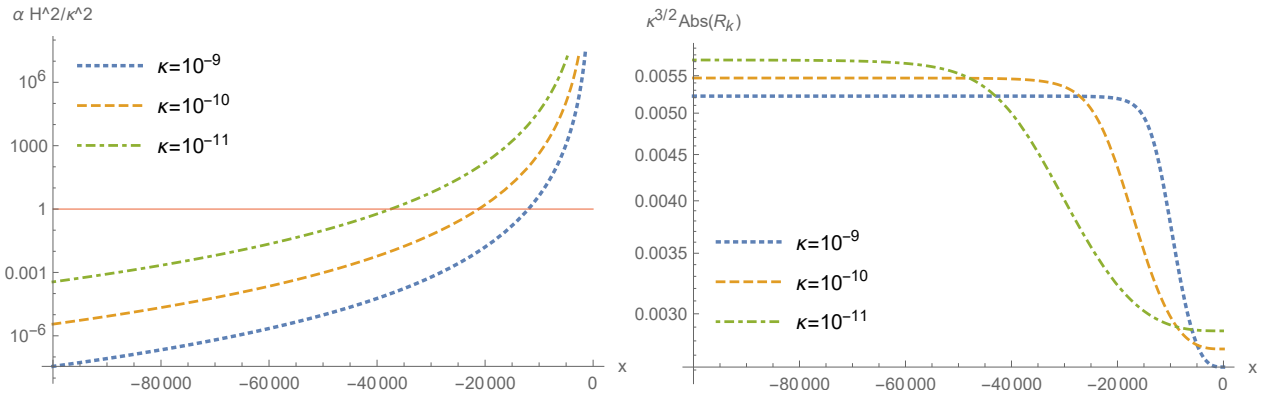

Figure VI.5: The left-hand side displays the ratio $\alpha\mathcal{H}^2/k^2$, and the right-hand side shows the normalized absolute value of the curvature perturbation for $n = 2.02$ and $w = 1$.

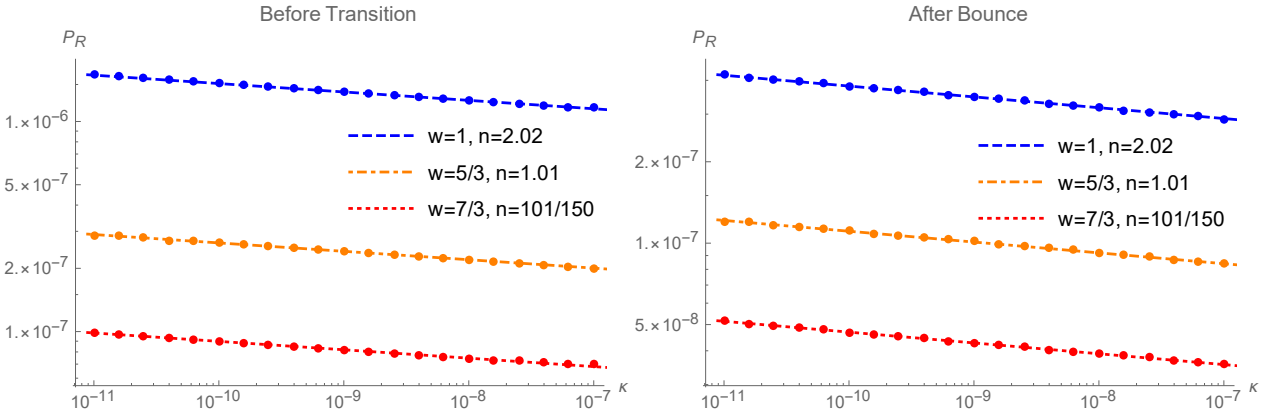

Figure VI.6: The scalar power spectrum before (left) the transition period and after the bounce (right) for different combinations of w and n, *i.e.* $w = 1$ & $n = 2.02$, $w = 5/3$ & $n = 1.01$ and $w = 7/3$ & $n = 101/150$.

The scale factor is decreasing in the contracting phase and, therefore, outside the horizon the tensor modes are either frozen or growing, in contrast to the scalar modes. The time evolutions of the tensor modes for $n = 2.02$ are given in fig. VI.7 and we observe that on superhorizon scales the modes are indeed growing. However, as for the scalar modes, neither the bounce nor the transition period impacts the scale dependency of the tensor power spectrum, as fig. VI.8 demonstrates. Instead, it only leads to an overall amplification factor coming from the superhorizon growth in the contracting phase. Only for $n = 2.02$ do we recover the almost scale invariant power spectrum. In fact, the spectral index of the tensor and scalar modes are the same in this case, which renders the comparison straightforward.

However, in that case, the tensor-to-scalar ratio, *i.e.* $r \coloneqq P_h/P_{\mathcal{R}}$, is extremely large ($r \gg 1$), making this option unviable. This is apparent when comparing the scales of figs. VI.6 and VI.8. On the other hand, for $n < 2$ the tensor spectrum is blue tilted and the tensor-to-scalar ratio becomes scale dependent. Indeed, one can write the tensor-to-scalar ratio as

$$r = r_0 \kappa^{n_t - n_s + 1} \,. \tag{VI.54}$$

Assuming $n_s \approx 0.96$ and using eq. (VI.53), the same conclusion is easily drawn. Numerically, it translates as $r \propto \kappa^{1.94}$ for $n = 1.01$ or $r \propto \kappa^{2.61333\cdots}$ for $n = 101/150$. In these two cases, on cosmological scales, the tensor power spectrum is significantly lower than the scalar one $r|_{k=k_{CMB}} \ll 1$ as long as the time scale of the bounce is significantly shorter than the scale at the CMB, *i.e.* $\kappa_{\rm CMB} = k_{\rm CMB}\tau_B \ll 1$. Practically, this latter assumption should be easily satisfied.

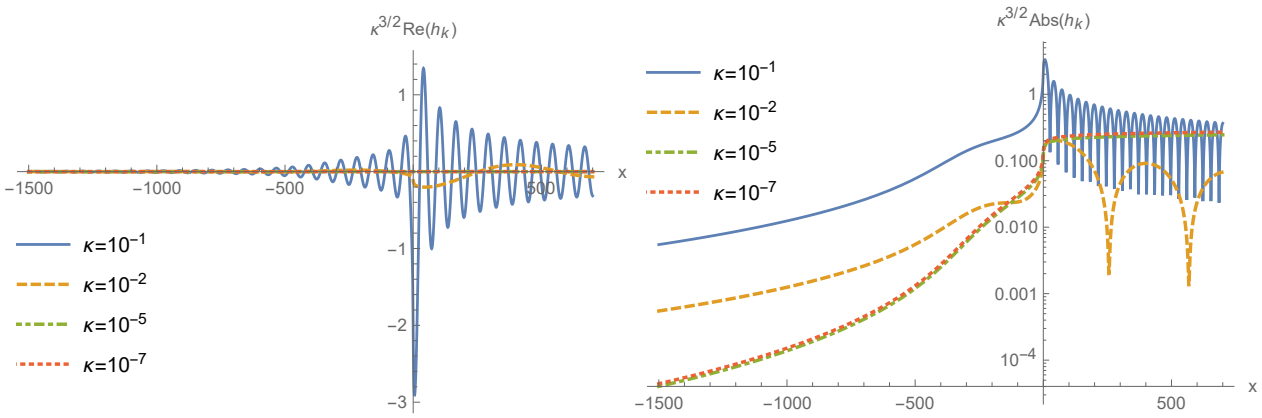

Figure VI.7: The real part (left) and the absolute value (right) of the tensor modes are plotted for $n = 2.02$, $w = 1$ and different values of κ.

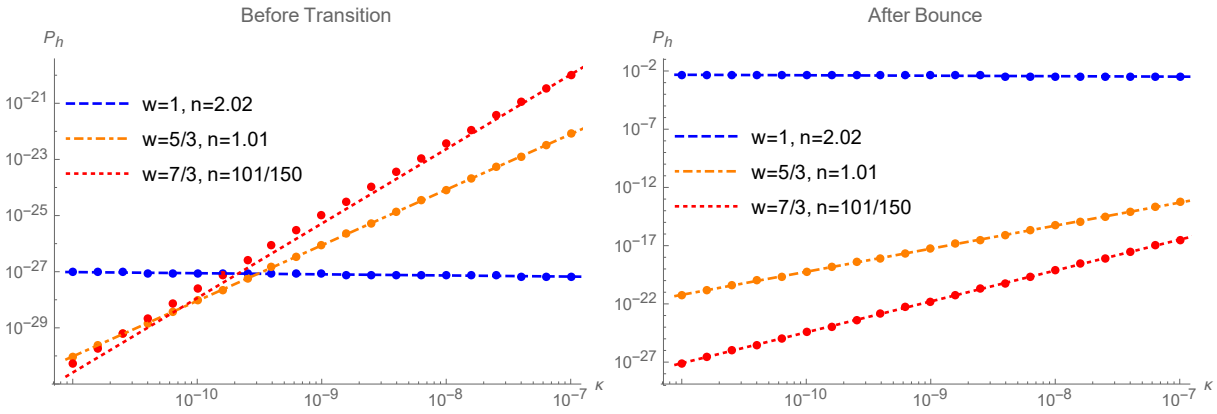

Figure VI.8: Tensor power spectra evaluated at $x = -3000$ before the transition (left) and at $x = 300$ after the bounce (right) are plotted for different combinations of w and n, *i.e.* $w = 1$ & $n = 2.02$, $w = 5/3$ & $n = 1.01$ and $w = 7/3$ & $n = 101/150$.

VI.4 Summary and discussion

In this chapter, we introduced an explicit and testable bouncing universe scenario, built within the framework of minimally modified gravity theories, specifically the class of so-called VCDM models. The proposed model successfully passes the first tests a bounce scenario has to face. It does not suffer from ghost or gradient instabilities coming from the NEC violation and there are no issues related to the anisotropic stress or the BKL instability thanks to the ekpyrotic ($w \geq 1$) equation of state. From the observational side, the scalar power spectrum can be adapted by the choice of the equation of state and the form of the potential leading to a nearly scale-invariant power spectrum with a spectral index of $n_s \approx 0.96$ in accordance of the results of the Planck collaboration [72]. Moreover, the tensor power spectrum scales, in general, differently from the scalar one. An equation of state $w > 1$ leads to a blue tensor spectrum. It is, therefore, possible to obtain a small tensor-to-scalar ratio within the observational bounds at cosmological scales, while potentially detectable at much smaller scales such as those of the gravitational-wave interferometers. To meet all these goals, the current model relies on a simple asymmetric bounce with the minimal number of propagating DoF (1 scalar + 2 tensors), unlike previous works based on Cuscuton [197, 198], in which case the authors introduced an additional scalar field to fulfill the experimental constraints. This is a key part of this work: we have built our model based on the VCDM, which can accommodate both modified gravity behavior and GR behavior, and have reconstructed the potential in the Lagrangian from the background dynamics we chose.

Future work could investigate how sensitive to the bounce details (*e.g.* shape, duration, etc...) these tests are. *A priori*, we argue that the conclusion of this work should prove relatively robust in this regard.

Another crucial aspect to consider would be non-Gaussianities, and evading the no-go theorem associated with it [216, 215]. However, since the curvature perturbations are frozen outside the horizon, non-Gaussianities are generated inside the horizon when the kinetic energy of the scalar field is subdominant. Naively, this should lead to small non-Gaussianities [219]. Otherwise, one may also worry of seeing a superluminal sound speed in the matter sector (k-essence field). A standard ekpyrotic scalar field may sooth this, but would require a more complicated, and probably more numerically involved, approach to handle.

Conclusion

Chapter VII

Conclusion

Motivated by the natural curiosity into puzzles —and what puzzling and quizzical puzzles the Universe has laid ahead of us!— this work has explored diverse alternative theories of gravity to the highly successful, but possibly incomplete general relativity. In so doing, we also approached some fundamental and deep-seated mysteries currently debated in modern cosmology. The variety of frameworks and unresolved enigmas we touched here could be seen as both a strength and a possible weakness. Indeed, in so doing, we never extensively explored any single framework, but we believe that sweeping across the landscape of cosmology constitutes a wise choice in order to gather original perspectives and enrich one's dictionary of skills. Incidentally, virtually all the directions taken here have exploited some numerical studies as supporting arguments.

This work presents several original contributions, in different domains. Firstly, we exhibited a sane Wheeler-DeWitt equation within Hořava-Lifshitz gravity in chapter III and demonstrated that the corresponding DeWitt wave function for tensor perturbations is well-defined around the classical Big Bang singularity. This enabled us to introduce and describe the recently proposed Hořava-Lifshitz gravity that aims at tackling the longstanding issue of non-renormalizability intrinsic to general relativity, as well as to distantly touch on the nature of dark matter. Secondly, we turned our our attention to an early Universe reheating scenario bolted onto a cosmological constant relaxing mechanism in chapter IV. The latter had the inconvenient side-effect of virtually emptying the Universe content. That why we conceived a proof-of-concept reheating machinery to subsequently repopulate the Universe and connect the scenario to standard cosmology. This model also gave us to talk of yet another popular modified gravity class of theories: Horndeski theories. At this stage already, taken together, these two chapters already touch all three shortcomings initially listed in section I.4.

In a kind of parallel way, all within a type-II theory of minimally modified gravity dubbed VCDM, we then carry out a sanity check and imagine another early Universe scenario. Minimally modified gravity theories aim at going beyond general relativity without introducing any extra propagating degrees of freedom; as general relativity, it has only two tensor modes. To achieve this, and differentiate itself from general relativity, it treats on unequal footing time and space, just as Hořava-Lifshitz gravity does. This class of theories thus breaks the full spacetime diffeomorphism invariance that general relativity enjoys. As a third contribution, and within this framework, we numerically investigated the spherical collapse of a scalar field in chapter V, and demonstrated that an apparent horizon healthily forms, and hinted at its conditional parameter dependence. Fourthly and lastly, we turned towards the early Universe in chapter VI where we produced a bouncing Universe scenario. The latter respects current observational constraints by exhibiting a near scale invariant scalar perturbation power spectrum as well as the ability to accommodate a small tensor-to-scalar ratio. As a consequence of that latter constraint, the model also offers itself to potential observational tests as it predicts a blue-tilted tensor perturbation power spectrum.

The number of research angles adopted in this text naturally allows sprawling into a wide panel of possible continuations. We shall refer the invested reader to the discussions of outlooks given at the end of each chapter. Nonetheless, let us here review the perhaps most promising paths laid out, as well as the direction this work taken all together may suggest.

In regard to the Wheeler-DeWitt equation and the corresponding wave function that were exhibited, possible future studies could investigate the addition of matter fields or attempt to get a finer interpretation of the cosmic wave function.

In parallel, we looked at the early Universe via two different scenarios, and both have room for improvement. Regarding the cosmological constant relaxation mechanism along the reheating mechanism developed in this text, this setup is not yet connected to the standard picture drawn in cosmology. As, at this stage, the model remains merely a proof-of-concept, the future developments should probably aim at more concretely connecting it to some observational signature. Incorporating yet another phase akin to inflation subsequent to this reheating may be the shortest route to do so. Whether the observational signature it shall entail are have some discriminating power remains to be seen.

In contrast, the bouncing Universe scenario may benefit from shorter path to observations. Actually, the blue-tilted tensor power spectrum is already a potentially observable signature. Next, and they will surely be the topic of a subsequent work, one can consider non-Gaussianities [219, 220]. This would bring another test against observations for the scenario, but the investigation could also uncover new specific features of the model. Preliminary computations are being carried out just as this works concludes.

Furthermore, a bouncing Universe is not the only singularity-free alternative to inflation. A perhaps harder approach could be to devise what is called a *genesis* scenario, again in the formalism set by minimally modified gravity. Genesis is a scenario where, instead of starting from a singularity, we start from a flat Minkowski spacetime and an expanding Universe spontaneously emerge from it [221].

Notice also that VCDM is one instance of type-II minimally modified gravity theories. It would also be enriching to remain at a more agnostic level and derive these results, for example, for an arbitrary (type-II) minimally modified gravity or within the sister-theory of MTBG, and determine the conditions under which the previously explored scenarios are possible. In that vein, the same kind of study as the one on the spherical collapse of chapter V could be carried out within either a different theory, such as MTBG, or with assuming a more realistic setup like with a non-pressureless fluid or some non-zero angular momentum. As a black hole formation is often seen as a simple litmus test a theory must pass, this kind of simple analysis is crucial to complete. Of course, doing so adds layers of complexity and it would probably require a more involved mathematical treatment. However, Occam's razor is, while a reasonable principle, just a principle, not an absolute rule. No one knows (yet) which paths are the more fruitful...

Appendices

Appendix A

Apparent horizon

We want to derive eqs. (V.6) and (V.7), in a spherical symmetry, as it is considered in chapter V, *i.e.*

$$g_{\mu\nu}dx^\mu dx^\nu = -(\alpha^2 - \beta^2)dt^2 + 2\beta dt dr + dr^2 + \Phi^2 d\Omega^2 \,, \tag{A.1}$$

where α and β are positive functions of t and r, and $\Phi = \Phi(t, r)$ is non-negative. Let us first consider the two radial null vector fields $k_\pm$ defined by

$$k_\pm^\mu \partial_\mu = \partial_t \pm (\alpha \mp \beta)\partial_r \,. \tag{A.2}$$

The vector field k_+ is tangent to a congruence of radially outgoing null curves, and similarly k_- is tangent to a congruence of radially ingoing ones. We note the relations

$$k_\pm^\mu k_{\pm,\mu} = 0, \quad k_+^\mu k_{-,\mu} = k_-^\mu k_{+,\mu} = -2\alpha^2 < 0 \,. \tag{A.3}$$

It is further necessary for us to define a transverse metric to the two null vector fields. Such a metric is given by

$$h^{\mu\nu} = g^{\mu\nu} + \frac{k_+^\mu k_-^\nu + k_-^\mu k_+^\nu}{-k_+^\mu k_{-,\mu}} \,, \tag{A.4}$$

for which $h^{tt} = h^{tr} = h^{rt} = h^{rr} = 0$. The AH radius $r = r_{\rm AH}$ is found by solving for a marginally outer trapped surface, i.e. demanding that the expansion scalar θ_+ of k_+ at $r = r_{\rm AH}$ be 0, which is given by the transverse projection of the covariant derivative of k_+:

$$\theta_+ \equiv h^{\mu\nu}\nabla_\nu k_{+,\mu} = 2\alpha \frac{\partial_\perp \Phi + \partial_r \Phi}{\Phi} \,. \tag{A.5}$$

If we now set $\theta_+|_{r=r_{\rm AH}} = 0$, eq. (A.5) implies that

$$(\partial_\perp \Phi)^2\big|_{r=r_{\rm AH}} = (\partial_r \Phi)^2\big|_{r=r_{\rm AH}} \,, \tag{A.6}$$

The latter can now simply be reformulated to conclude eq. (A.8). Indeed, using $\Phi(t, r)$ instead of r as the radial coordinate, the metric component $g^{\Phi\Phi}$ then reads

$$\begin{aligned} g^{\Phi\Phi} &= \frac{\partial\Phi}{\partial x^\mu}\frac{\partial\Phi}{\partial x^\mu} g^{\mu\nu} \\ &= -(\partial_\perp \Phi)^2 + (\partial_r \Phi)^2 \,, \end{aligned} \tag{A.7}$$

where $\partial_\perp = 1/(\alpha(\partial_t - \beta\partial_r))$. Therefore, in terms of eq. (A.7), the condition of eq. (A.6) can now be conveniently rewritten as

$$g^{\Phi\Phi}\big|_{r=r_{\rm AH}} = 0 \,. \tag{A.8}$$

Consequently, one of the solutions to eq. (A.8) will correspond to the AH. It is then simply a matter of substitution using eq. (V.5) to arrive at the right-hand side expression seen of eq. (V.7).

Appendix B

Hořava-Lifshitz DeWitt wave function without tensor perturbations

We review quantum cosmology based on the HL gravity and consider the DeWitt wave function in the WDW equation (eq. (III.13)) for a homogeneous and isotropic universe without any perturbations. For only a in $3+1$ dimensions, the HL DeWitt wave function has already been investigated in previous works *e.g.* refs.. [222, 223, 224]. However, the HL gravity introduces an extra component that behaves like a pressure-less dust and that is called DM as an integration constant [27, 126, 78]. The new DM component was derived in the classical cosmology. Correspondingly, when one considers the WDW equation, the HL gravity naturally introduces a DM as a separation constant (instead of an integration constant) into the local universe [169].

Hereafter, we will consider the evolution of the early universe in the HL quantum cosmology. In the anisotropic scaling regime, the HL term of g_3 dominates and the solution of the WDW equation (eq. (III.13) with $\partial/\partial h$ and h removed) approximately takes the from $\Psi(a) = \mathcal{A}_1 a^{\tilde{c}}$, where $\mathcal{A}_1$ is a normalization constant [222] and $\tilde{c}$ is a constant determined by $\tilde{c}(\tilde{c}-1)+p\tilde{c}-2g_3=0$, *i.e.*

$$\tilde{c} = \frac{1}{2}\left(1-p+\sqrt{(1-p)^2+8g_3}\right) , \tag{B.1}$$

where we must impose $g_3 > -(1-p)^2/8$ to ensure the regularity of the solution. Recalling that the DeWitt wave function is regular at the classical big-bang singularity, the wave function describes a universe that has emerged from the initial singularity to the anisotropic scaling regime.

In order to highlight the effects of the DM as an integration constant (or as a separation constant), *i.e.* the $\mathcal{C}$ term, we set $g_2 = g_1 = g_0 = 0$. In this case the WDW equation (eq. (III.13) with $\partial/\partial h$ and h removed) reads,

$$\left\{\frac{1}{2}\left(\frac{\partial^2}{\partial a^2}+\frac{p}{a}\frac{\partial}{\partial a}\right)+\mathcal{C}a-\frac{g_3}{a^2}\right\}\Psi(a) = 0 . \tag{B.2}$$

Thus, imposing the DeWitt boundary condition on the wave function and using the asymptotic form of $J_\nu(z)$, we can get the following wave function

$$\Psi(a) = \mathcal{A}_2\, 3^{\frac{p-1}{3}} a^{\frac{1-p}{2}} (2\mathcal{C})^{\frac{1-p}{6}} \Gamma\left(1+\frac{1}{3}\sqrt{(1-p)^2+8g_3}\right) J_{\frac{1}{3}\sqrt{(1-p)^2+8g_3}}\left(\frac{2}{3}a^{3/2}\sqrt{2\mathcal{C}}\right) , \tag{B.3}$$

whose asymptotic forms are given by

$$\begin{aligned} &\Psi(a \ll 1) \sim \mathcal{A}_2\,(\mathcal{C}a)^{\frac{1-p+\sqrt{(1-p)^2+8g_3}}{6}}, \\ &\Psi(a \gg 1) \sim \mathcal{A}_2\, a^{-\frac{1+2p}{4}} (2\mathcal{C})^{-\frac{1+2p}{12}} \cos\left(\frac{2}{3}a^{3/2}\sqrt{2\mathcal{C}} - \frac{1+\frac{2}{3}\sqrt{(1-p)^2+8g_3}}{4}\pi\right) . \end{aligned} \tag{B.4}$$

Here, $\mathcal{A}_2$ is a normalization constant. These expressions show that the DeWitt wave function is suppressed and oscillates, respectively, in the anisotropic scaling regime and the dark-matter dominated regime. After the Universe emerges through the classical big-bang singularity and the anisotropic scaling regime, the DM as an integration constant (or as a separation constant) represented by the parameter $\mathcal{C}$ dominates the energy density of the universe. Subsequently, in such a local universe, the DM component may eventually decay into ordinary matter and radiation [125], and in this case the cosmological evolution would be smoothly connected to the usual big-bang cosmology.

Bibliography

[1] Albert Einstein. "The foundation of the general theory of relativity." In: *Annalen Phys.* 49.7 (1916). Ed. by Jong-Ping Hsu and D. Fine, pp. 769–822. DOI: 10.1002/andp.19163540702.

[2] Albert Einstein. "Explanation of the Perihelion Motion of Mercury from the General Theory of Relativity". In: *Sitzungsber. Preuss. Akad. Wiss. Berlin (Math. Phys.)* 1915 (1915), pp. 831–839.

[3] F. W. Dyson, A. S. Eddington, and C. Davidson. "A Determination of the Deflection of Light by the Sun's Gravitational Field, from Observations Made at the Total Eclipse of May 29, 1919". In: *Phil. Trans. Roy. Soc. Lond. A* 220 (1920), pp. 291–333. DOI: 10.1098/rsta.1920.0009.

[4] Daniel M. Popper. "Red Shift in the Spectrum of 40 Eridani B." In: *ApJ* 120 (Sept. 1954), p. 316. DOI: 10.1086/145916.

[5] Marc H. Goroff and Augusto Sagnotti. "Quantum gravity at two loops". In: *Phys. Lett. B* 160 (1985), pp. 81–86. DOI: 10.1016/0370-2693(85)91470-4.

[6] Marc H. Goroff and Augusto Sagnotti. "The Ultraviolet Behavior of Einstein Gravity". In: *Nucl. Phys. B* 266 (1986), pp. 709–736. DOI: 10.1016/0550-3213(86)90193-8.

[7] K. Becker, M. Becker, and J. H. Schwarz. *String theory and M-theory: A modern introduction*. Cambridge University Press, Dec. 2006. ISBN: 978-0-511-25486-4, 978-0-521-86069-7, 978-0-511-81608-6. DOI: 10.1017/CBO9780511816086.

[8] Eran Palti. "The Swampland: Introduction and Review". In: *Fortsch. Phys.* 67.6 (2019), p. 1900037. DOI: 10.1002/prop.201900037. arXiv: 1903.06239 [hep-th].

[9] J. Polchinski. *String theory. Vol. 1: An introduction to the bosonic string*. Cambridge Monographs on Mathematical Physics. Cambridge University Press, Dec. 2007. ISBN: 978-0-511-25227-3, 978-0-521-67227-6, 978-0-521-63303-1. DOI: 10.1017/CBO9780511816079.

[10] J. Polchinski. *String theory. Vol. 2: Superstring theory and beyond*. Cambridge Monographs on Mathematical Physics. Cambridge University Press, Dec. 2007. ISBN: 978-0-511-25228-0, 978-0-521-63304-8, 978-0-521-67228-3. DOI: 10.1017/CBO9780511618123.

[11] Carlo Rovelli. "Loop quantum gravity". In: *Living Rev. Rel.* 1 (1998), p. 1. DOI: 10.12942/lrr-1998-1. arXiv: gr-qc/9710008.

[12] Carlo Rovelli and Francesca Vidotto. *Covariant Loop Quantum Gravity: An Elementary Introduction to Quantum Gravity and Spinfoam Theory*. Cambridge Monographs on Mathematical Physics. Cambridge University Press, Nov. 2014. ISBN: 978-1-107-06962-6, 978-1-316-14729-0.

[13] Petr Horava. "Quantum Gravity at a Lifshitz Point". In: *Phys. Rev. D* 79 (2009), p. 084008. DOI: 10.1103/PhysRevD.79.084008. arXiv: 0901.3775 [hep-th].

[14] Vera C. Rubin and Jr. Ford W. Kent. "Rotation of the Andromeda Nebula from a Spectroscopic Survey of Emission Regions". In: *ApJ* 159 (Feb. 1970), p. 379. DOI: 10.1086/150317.

[15] F. Zwicky. "Die Rotverschiebung von extragalaktischen Nebeln". In: *Helv. Phys. Acta* 6 (1933), pp. 110–127. DOI: 10.1007/s10714-008-0707-4.

[16] Anne M. Green. "Dark matter in astrophysics/cosmology". In: *SciPost Phys. Lect. Notes* 37 (2022), p. 1. DOI: 10.21468/SciPostPhysLectNotes.37. arXiv: 2109.05854 [hep-ph].

[17] Constantinos Skordis and Tom Zlosnik. "New Relativistic Theory for Modified Newtonian Dynamics". In: *Phys. Rev. Lett.* 127.16 (2021), p. 161302. DOI: 10.1103/PhysRevLett.127.161302. arXiv: 2007.00082 [astro-ph.CO].

[18] Lasha Berezhiani, Benoit Famaey, and Justin Khoury. "Phenomenological consequences of superfluid dark matter with baryon-phonon coupling". In: *JCAP* 09 (2018), p. 021. DOI: 10.1088/1475-7516/2018/09/021. arXiv: 1711.05748 [astro-ph.CO].

[19] P. A. Zyla et al. "Review of Particle Physics". In: *PTEP* 2020.8 (2020), p. 083C01. DOI: 10.1093/ptep/ptaa104.

[20] Bernard Carr, Kazunori Kohri, Yuuiti Sendouda, and Jun'ichi Yokoyama. "Constraints on primordial black holes". In: *Rept. Prog. Phys.* 84.11 (2021), p. 116902. DOI: 10.1088/1361-6633/ac1e31. arXiv: 2002.12778 [astro-ph.CO].

[21] Jodi Cooley. "Dark Matter direct detection of classical WIMPs". In: *SciPost Phys. Lect. Notes* 55 (2022), p. 1. DOI: 10.21468/SciPostPhysLectNotes.55. arXiv: 2110.02359 [hep-ph].

[22] Tracy R. Slatyer. "Les Houches Lectures on Indirect Detection of Dark Matter". In: *SciPost Phys. Lect. Notes* 53 (2022), p. 1. DOI: 10.21468/SciPostPhysLectNotes.53. arXiv: 2109.02696 [hep-ph].

[23] J. Bekenstein and Mordehai Milgrom. "Does the missing mass problem signal the breakdown of Newtonian gravity?" In: *Astrophys. J.* 286 (1984), pp. 7–14. DOI: 10.1086/162570.

[24] M. Milgrom. "A Modification of the Newtonian dynamics as a possible alternative to the hidden mass hypothesis". In: *Astrophys. J.* 270 (1983), pp. 365–370. DOI: 10.1086/161130.

[25] M. Milgrom. "A Modification of the Newtonian dynamics: Implications for galaxies". In: *Astrophys. J.* 270 (1983), pp. 371–383. DOI: 10.1086/161131.

[26] M. Milgrom. "A modification of the Newtonian dynamics: implications for galaxy systems". In: *Astrophys. J.* 270 (1983), pp. 384–389. DOI: 10.1086/161132.

[27] Shinji Mukohyama. "Dark matter as integration constant in Horava-Lifshitz gravity". In: *Phys. Rev. D* 80 (2009), p. 064005. DOI: 10.1103/PhysRevD.80.064005. arXiv: 0905.3563 [hep-th].

[28] Adam G. Riess et al. "Observational evidence from supernovae for an accelerating universe and a cosmological constant". In: *Astron. J.* 116 (1998), pp. 1009–1038. DOI: 10.1086/300499. arXiv: astro-ph/9805201.

[29] S. Perlmutter et al. "Measurements of Ω and Λ from 42 high redshift supernovae". In: *Astrophys. J.* 517 (1999), pp. 565–586. DOI: 10.1086/307221. arXiv: astro-ph/9812133.

[30] D. Lovelock. "The four-dimensionality of space and the einstein tensor". In: *J. Math. Phys.* 13 (1972), pp. 874–876. DOI: 10.1063/1.1666069.

[31] Gregory Walter Horndeski. "Second-order scalar-tensor field equations in a four-dimensional space". In: *Int. J. Theor. Phys.* 10 (1974), pp. 363–384. DOI: 10.1007/BF01807638.

[32] C. Deffayet, Xian Gao, D. A. Steer, and G. Zahariade. "From K-Essence to Generalised Galileons". In: *Physical Review D: Particles and Fields* 84 (2011), p. 064039. DOI: 10.1103/PhysRevD.84.064039. arXiv: 1103.3260 [hep-th].

[33] Tsutomu Kobayashi, Masahide Yamaguchi, and Jun'ichi Yokoyama. "Generalized G-Inflation: Inflation with the Most General Second-Order Field Equations". In: *Progress of Theoretical Physics* 126 (2011), pp. 511–529. DOI: 10.1143/PTP.126.511. arXiv: 1105.5723 [hep-th].

[34] Hayato Motohashi and Teruaki Suyama. "Third order equations of motion and the Ostrogradsky instability". In: *Phys. Rev. D* 91.8 (2015), p. 085009. DOI: 10.1103/PhysRevD.91.085009. arXiv: 1411.3721 [physics.class-ph].

[35] David Langlois and Karim Noui. "Degenerate higher derivative theories beyond Horndeski: evading the Ostrogradski instability". In: *JCAP* 02 (2016), p. 034. DOI: 10.1088/1475-7516/2016/02/034. arXiv: 1510.06930 [gr-qc].

[36] Remko Klein and Diederik Roest. "Exorcising the Ostrogradsky ghost in coupled systems". In: *JHEP* 07 (2016), p. 130. DOI: 10.1007/JHEP07(2016)130. arXiv: 1604.01719 [hep-th].

[37] Hayato Motohashi, Karim Noui, Teruaki Suyama, Masahide Yamaguchi, and David Langlois. "Healthy degenerate theories with higher derivatives". In: *JCAP* 07 (2016), p. 033. DOI: 10.1088/1475-7516/2016/07/033. arXiv: 1603.09355 [hep-th].

[38] Hayato Motohashi, Teruaki Suyama, and Masahide Yamaguchi. "Ghost-free theory with third-order time derivatives". In: *J. Phys. Soc. Jap.* 87.6 (2018), p. 063401. DOI: 10.7566/JPSJ.87.063401. arXiv: 1711.08125 [hep-th].

[39] Hayato Motohashi, Teruaki Suyama, and Masahide Yamaguchi. "Ghost-free theories with arbitrary higher-order time derivatives". In: *JHEP* 06 (2018), p. 133. DOI: 10.1007/JHEP06(2018)133. arXiv: 1804.07990 [hep-th].

[40] Antonio De Felice, David Langlois, Shinji Mukohyama, Karim Noui, and Anzhong Wang. "Generalized instantaneous modes in higher-order scalar-tensor theories". In: *Phys. Rev. D* 98.8 (2018), p. 084024. DOI: 10.1103/PhysRevD.98.084024. arXiv: 1803.06241 [hep-th].

[41] Antonio De Felice, Shinji Mukohyama, and Kazufumi Takahashi. "Nonlinear definition of the shadowy mode in higher-order scalar-tensor theories". In: *JCAP* 12.12 (2021), p. 020. DOI: 10.1088/1475-7516/2021/12/020. arXiv: 2110.03194 [gr-qc].

[42] Antonio De Felice, Shinji Mukohyama, and Kazufumi Takahashi. "Avoidance of Strong Coupling in General Relativity Solutions with a Timelike Scalar Profile in a Class of Ghost-Free Scalar-Tensor Theories". In: *Phys. Rev. Lett.* 129.3 (2022), p. 031103. DOI: 10.1103/PhysRevLett.129.031103. arXiv: 2204.02032 [gr-qc].

[43] Clifford M. Will. *Theory and Experiment in Gravitational Physics*. 2nd ed. Cambridge University Press, 2018. DOI: 10.1017/9781316338612.

[44] M. Hazumi et al. "LiteBIRD: A Satellite for the Studies of B-Mode Polarization and Inflation from Cosmic Background Radiation Detection". In: *J. Low Temp. Phys.* 194.5-6 (2019), pp. 443–452. DOI: 10.1007/s10909-019-02150-5.

[45] T. Matsumura et al. "Mission design of LiteBIRD". In: *J. Low Temp. Phys.* 176 (2014), p. 733. DOI: 10.1007/s10909-013-0996-1. arXiv: 1311.2847 [astro-ph.IM].

[46] Kentaro Somiya. "Detector configuration of KAGRA: The Japanese cryogenic gravitational-wave detector". In: *Class. Quant. Grav.* 29 (2012). Ed. by Mark Hannam, Patrick Sutton, Stefan Hild, and Chris van den Broeck, p. 124007. DOI: 10.1088/0264-9381/29/12/124007. arXiv: 1111.7185 [gr-qc].

[47] Pau Amaro-Seoane et al. "Laser Interferometer Space Antenna". In: (Feb. 2017). arXiv: 1702.00786 [astro-ph.IM].

[48] Kazunori Akiyama et al. "First M87 Event Horizon Telescope Results. I. The Shadow of the Supermassive Black Hole". In: *Astrophys. J. Lett.* 875 (2019), p. L1. DOI: 10.3847/2041-8213/ab0ec7. arXiv: 1906.11238 [astro-ph.GA].

[49] Paul Martens, Hiroki Matsui, and Shinji Mukohyama. "DeWitt wave function in Hořava-Lifshitz cosmology with tensor perturbation". In: *JCAP* 11 (2022), p. 031. DOI: 10.1088/1475-7516/2022/11/031. arXiv: 2205.11746 [gr-qc].

[50] Paul Martens, Shinji Mukohyama, and Ryo Namba. "Reheating after relaxation of large cosmological constant". In: *JCAP* 11 (2022), p. 047. DOI: 10.1088/1475-7516/2022/11/047. arXiv: 2205.11754 [hep-th].

[51] Alexander Ganz, Paul Martens, Shinji Mukohyama, and Ryo Namba. "Bouncing cosmology in VCDM". In: *JCAP* 04 (2023), p. 060. DOI: 10.1088/1475-7516/2023/04/060. arXiv: 2212.13561 [gr-qc].

[52] Emanuele Berti, Vitor Cardoso, Mark Ho-Yeuk Cheung, Francesco Di Filippo, Francisco Duque, Paul Martens, and Shinji Mukohyama. "Stability of the Fundamental Quasinormal Mode in Time-Domain Observations: The Elephant and the Flea Redux". In: (May 2022). arXiv: 2205.08547 [gr-qc].

[53] Shinji Mukohyama and Lisa Randall. "A Dynamical Approach to the Cosmological Constant". In: *Physical Review Letters* 92 (2004), p. 211302. DOI: 10.1103/PhysRevLett.92.211302. arXiv: hep-th/0306108.

[54] Shinji Mukohyama. "Gravity in the Dynamical Approach to the Cosmological Constant". In: *Physical Review D* 70 (2004), p. 063505. DOI: 10.1103/PhysRevD.70.063505. arXiv: hep-th/0306208.

[55] D. Lovelock. "The Einstein tensor and its generalizations". In: *J. Math. Phys.* 12 (1971), pp. 498–501. DOI: 10.1063/1.1665613.

[56] Richard L. Arnowitt, Stanley Deser, and Charles W. Misner. "The Dynamics of general relativity". In: *Gen. Rel. Grav.* 40 (2008), pp. 1997–2027. DOI: 10.1007/s10714-008-0661-1. arXiv: gr-qc/0405109.

[57] Roman Scoccimarro. "Cosmology course, Scalar-vector-tensor decomposition 1". Spring University Lecture. 2019. URL: https://cosmo.nyu.edu/roman/courses/cosmology_2019/SVT_1.pdf.

[58] R.M. Wald. *General Relativity*. University of Chicago Press, 2010. ISBN: 9780226870373. URL: https://books.google.co.jp/books?id=9S-hzg6-moYC.

[59] Alejandro Corichi and Dario Núñez. "Introduction to the ADM formalism". In: *Rev. Mex. Fis.* 37 (1991), pp. 720–747. arXiv: 2210.10103 [gr-qc].

[60] Rishabh Jha. "Introduction to Hamiltonian Formulation of General Relativity and Homogeneous Cosmologies". In: Apr. 2022. arXiv: 2204.03537 [gr-qc].

[61] Dmitry S Gorbunov and Valery A Rubakov. *Introduction to the Theory of the Early Universe*. World Scientific Publishing Company, 2011. DOI: 10.1142/7874. eprint: https://www.worldscientific.com/doi/pdf/10.1142/7874. URL: https://www.worldscientific.com/doi/abs/10.1142/7874.

[62] Valery A Rubakov and Dmitry S Gorbunov. *Introduction to the Theory of the Early Universe*. 2nd. WORLD SCIENTIFIC, 2017. DOI: 10.1142/10447. eprint: https://www.worldscientific.com/doi/pdf/10.1142/10447. URL: https://www.worldscientific.com/doi/abs/10.1142/10447.

[63] Robert Brandenberger. "Do we have a Theory of Early Universe Cosmology?" In: *Stud. Hist. Phil. Sci. B* 46 (2014), pp. 109–121. DOI: 10.1016/j.shpsb.2013.09.008. arXiv: 1204.6108 [astro-ph.CO].

[64] Robert H. Brandenberger. "The Matter Bounce Alternative to Inflationary Cosmology". In: (June 2012). arXiv: 1206.4196 [astro-ph.CO].

[65] Robert Brandenberger and Patrick Peter. "Bouncing Cosmologies: Progress and Problems". In: *Found. Phys.* 47.6 (2017), pp. 797–850. DOI: 10.1007/s10701-016-0057-0. arXiv: 1603.05834 [hep-th].

[66] Daniel Baumann. "Inflation". In: *Theoretical Advanced Study Institute in Elementary Particle Physics: Physics of the Large and the Small*. 2011, pp. 523–686. DOI: 10.1142/9789814327183_0010. arXiv: 0907.5424 [hep-th].

[67] N. Aghanim et al. "Planck 2018 results. I. Overview and the cosmological legacy of Planck". In: *Astron. Astrophys.* 641 (2020), A1. DOI: 10.1051/0004-6361/201833880. arXiv: 1807.06205 [astro-ph.CO].

[68] European Space Agency (ESA). *Planck's view of the cosmic microwave background*. 2018. URL: https://www.esa.int/ESA_Multimedia/Images/2018/07/Planck_s_view_of_the_cosmic_microwave_background (visited on 07/17/2018).

[69] Alan H. Guth. "The Inflationary Universe: A Possible Solution to the Horizon and Flatness Problems". In: *Phys. Rev. D* 23 (1981). Ed. by Li-Zhi Fang and R. Ruffini, pp. 347–356. DOI: 10.1103/PhysRevD.23.347.

[70] K. Sato. "First Order Phase Transition of a Vacuum and Expansion of the Universe". In: *Mon. Not. Roy. Astron. Soc.* 195 (1981), pp. 467–479.

[71] Alexei A. Starobinsky. "A New Type of Isotropic Cosmological Models Without Singularity". In: *Phys. Lett. B* 91 (1980). Ed. by I. M. Khalatnikov and V. P. Mineev, pp. 99–102. DOI: 10.1016/0370-2693(80)90670-X.

[72] N. Aghanim et al. "Planck 2018 results. VI. Cosmological parameters". In: *Astron. Astrophys.* 641 (2020). [Erratum: Astron.Astrophys. 652, C4 (2021)], A6. DOI: 10.1051/0004-6361/201833910. arXiv: 1807.06209 [astro-ph.CO].

[73] V. A. Rubakov. "The Null Energy Condition and Its Violation". In: *Physics-Uspekhi* 57 (2014), pp. 128–142. DOI: 10.3367/UFNe.0184.201402b.0137. arXiv: 1401.4024 [hep-th].

[74] Roger Penrose. "Gravitational collapse and space-time singularities". In: *Phys. Rev. Lett.* 14 (1965), pp. 57–59. DOI: 10.1103/PhysRevLett.14.57.

[75] K. S. Stelle. "Renormalization of Higher Derivative Quantum Gravity". In: *Phys. Rev. D* 16 (1977), pp. 953–969. DOI: 10.1103/PhysRevD.16.953.

[76] M. Asorey, J. L. Lopez, and I. L. Shapiro. "Some remarks on high derivative quantum gravity". In: *Int. J. Mod. Phys. A* 12 (1997), pp. 5711–5734. DOI: 10.1142/S0217751X97002991. arXiv: hep-th/9610006.

[77] Daniel Z. Freedman and Antoine Van Proeyen. *Supergravity*. Cambridge University Press, 2012. DOI: 10.1017/CBO9781139026833.

[78] Shinji Mukohyama. "Horava-Lifshitz Cosmology: A Review". In: *Class. Quant. Grav.* 27 (2010), p. 223101. DOI: 10.1088/0264-9381/27/22/223101. arXiv: 1007.5199 [hep-th].

[79] Adam G. Riess et al. "A 3% Solution: Determination of the Hubble Constant with the Hubble Space Telescope and Wide Field Camera 3". In: *The Astrophysical Journal* 730.2 (Mar. 2011), p. 119. ISSN: 1538-4357. DOI: 10.1088/0004-637x/730/2/119. URL: http://dx.doi.org/10.1088/0004-637X/730/2/119.

[80] V. Bonvin et al. "H0LiCOW – V. New COSMOGRAIL time delays of HE 0435−1223: H_0 to 3.8 per cent precision from strong lensing in a flat ΛCDM model". In: *Mon. Not. Roy. Astron. Soc.* 465.4 (2017), pp. 4914–4930. DOI: 10.1093/mnras/stw3006. arXiv: 1607.01790 [astro-ph.CO].

[81] Jose Luis Bernal, Licia Verde, and Adam G. Riess. "The trouble with H_0". In: *JCAP* 10 (2016), p. 019. DOI: 10.1088/1475-7516/2016/10/019. arXiv: 1607.05617 [astro-ph.CO].

[82] Adam G. Riess et al. "A Comprehensive Measurement of the Local Value of the Hubble Constant with 1 km/s/Mpc Uncertainty from the Hubble Space Telescope and the SH0ES Team". In: (Dec. 2021). arXiv: 2112.04510 [astro-ph.CO].

[83] Steven Weinberg. "The Cosmological Constant Problem". In: *Rev. Mod. Phys.* 61 (1989). Ed. by Jong-Ping Hsu and D. Fine, pp. 1–23. DOI: 10.1103/RevModPhys.61.1.

[84] Jerome Martin. "Everything You Always Wanted To Know About The Cosmological Constant Problem (But Were Afraid To Ask)". In: *Comptes Rendus Physique* 13 (2012), pp. 566–665. DOI: 10.1016/j.crhy.2012.04.008. arXiv: 1205.3365 [astro-ph.CO].

[85] Antonio Padilla. "Lectures on the Cosmological Constant Problem". In: (Feb. 2015). arXiv: 1502.05296 [hep-th].

[86] H. E. S. Velten, R. F. vom Marttens, and W. Zimdahl. "Aspects of the cosmological "coincidence problem"". In: *Eur. Phys. J. C* 74.11 (2014), p. 3160. DOI: 10.1140/epjc/s10052-014-3160-4. arXiv: 1410.2509 [astro-ph.CO].

[87] Vera C. Rubin and W. Kent Ford Jr. "Rotation of the Andromeda Nebula from a Spectroscopic Survey of Emission Regions". In: *Astrophys. J.* 159 (1970), pp. 379–403. DOI: 10.1086/150317.

[88] Stephen Hawking. "Gravitationally collapsed objects of very low mass". In: *Mon. Not. Roy. Astron. Soc.* 152 (1971), p. 75. DOI: 10.1093/mnras/152.1.75.

[89] Ya. B. Zel'dovich and I. D. Novikov. "The Hypothesis of Cores Retarded during Expansion and the Hot Cosmological Model". In: *Soviet Astron. AJ (Engl. Transl.),* 10 (1967), p. 602.

[90] P. Tisserand et al. "Limits on the Macho Content of the Galactic Halo from the EROS-2 Survey of the Magellanic Clouds". In: *Astron. Astrophys.* 469 (2007), pp. 387–404. DOI: 10.1051/0004-6361:20066017. arXiv: astro-ph/0607207.

[91] C. Alcock et al. "The MACHO project: Microlensing results from 5.7 years of LMC observations". In: *Astrophys. J.* 542 (2000), pp. 281–307. DOI: 10.1086/309512. arXiv: astro-ph/0001272.

[92] T. G Zlosnik, P. G Ferreira, and G. D Starkman. "Modifying gravity with the Aether: An alternative to Dark Matter". In: *Phys. Rev. D* 75 (2007), p. 044017. DOI: 10.1103/PhysRevD.75.044017. arXiv: astro-ph/0607411.

[93] Stacy S. McGaugh. "A tale of two paradigms: the mutual incommensurability of ΛCDM and MOND". In: *Can. J. Phys.* 93.2 (2015), pp. 250–259. DOI: 10.1139/cjp-2014-0203. arXiv: 1404.7525 [astro-ph.CO].

[94] Douglas Clowe, Marusa Bradac, Anthony H. Gonzalez, Maxim Markevitch, Scott W. Randall, Christine Jones, and Dennis Zaritsky. "A direct empirical proof of the existence of dark matter". In: *Astrophys. J. Lett.* 648 (2006), pp. L109–L113. DOI: 10.1086/508162. arXiv: astro-ph/0608407.

[95] S. Boran, S. Desai, E. O. Kahya, and R. P. Woodard. "GW170817 Falsifies Dark Matter Emulators". In: *Phys. Rev. D* 97.4 (2018), p. 041501. DOI: 10.1103/PhysRevD.97.041501. arXiv: 1710.06168 [astro-ph.HE].

[96] Timothy Clifton, Pedro G. Ferreira, Antonio Padilla, and Constantinos Skordis. "Modified Gravity and Cosmology". In: *Phys. Rept.* 513 (2012), pp. 1–189. DOI: 10.1016/j.physrep.2012.01.001. arXiv: 1106.2476 [astro-ph.CO].

[97] Claudia de Rham. "Massive Gravity". In: *Living Rev. Rel.* 17 (2014), p. 7. DOI: 10.12942/lrr-2014-7. arXiv: 1401.4173 [hep-th].

[98] S. Nojiri, S. D. Odintsov, and V. K. Oikonomou. "Modified Gravity Theories on a Nutshell: Inflation, Bounce and Late-time Evolution". In: *Phys. Rept.* 692 (2017), pp. 1–104. DOI: 10.1016/j.physrep.2017.06.001. arXiv: 1705.11098 [gr-qc].

[99] Edmund J. Copeland, M. Sami, and Shinji Tsujikawa. "Dynamics of dark energy". In: *Int. J. Mod. Phys. D* 15 (2006), pp. 1753–1936. DOI: 10.1142/S021827180600942X. arXiv: hep-th/0603057.

[100] C. Brans and R. H. Dicke. "Mach's Principle and a Relativistic Theory of Gravitation". In: *Phys. Rev.* 124 (3 Nov. 1961), pp. 925–935. DOI: 10.1103/PhysRev.124.925. URL: https://link.aps.org/doi/10.1103/PhysRev.124.925.

[101] C. Armendariz-Picon, T. Damour, and Viatcheslav F. Mukhanov. "k - inflation". In: *Phys. Lett. B* 458 (1999), pp. 209–218. DOI: 10.1016/S0370-2693(99)00603-6. arXiv: hep-th/9904075.

[102] C. Armendariz-Picon, Viatcheslav F. Mukhanov, and Paul J. Steinhardt. "A Dynamical solution to the problem of a small cosmological constant and late time cosmic acceleration". In: *Phys. Rev. Lett.* 85 (2000), pp. 4438–4441. DOI: 10.1103/PhysRevLett.85.4438. arXiv: astro-ph/0004134.

[103] C. Armendariz-Picon, Viatcheslav F. Mukhanov, and Paul J. Steinhardt. "Essentials of k essence". In: *Phys. Rev. D* 63 (2001), p. 103510. DOI: 10.1103/PhysRevD.63.103510. arXiv: astro-ph/0006373.

[104] Takeshi Chiba, Takahiro Okabe, and Masahide Yamaguchi. "Kinetically driven quintessence". In: *Phys. Rev. D* 62 (2000), p. 023511. DOI: 10.1103/PhysRevD.62.023511. arXiv: astro-ph/9912463.

[105] Shin'ichi Nojiri and Sergei D. Odintsov. "Mimetic $F(R)$ gravity: inflation, dark energy and bounce". In: (Aug. 2014). [Erratum: Mod.Phys.Lett.A 29, 1450211 (2014)]. DOI: 10.1142/S0217732314502113. arXiv: 1408.3561 [hep-th].

[106] Ted Jacobson and David Mattingly. "Gravity with a dynamical preferred frame". In: *Phys. Rev. D* 64 (2001), p. 024028. DOI: 10.1103/PhysRevD.64.024028. arXiv: gr-qc/0007031.

[107] Christopher Eling, Ted Jacobson, and David Mattingly. "Einstein-Aether theory". In: *Deserfest: A Celebration of the Life and Works of Stanley Deser*. Oct. 2004, pp. 163–179. arXiv: gr-qc/0410001.

[108] T. Jacobson and D. Mattingly. "Einstein-Aether waves". In: *Phys. Rev. D* 70 (2004), p. 024003. DOI: 10.1103/PhysRevD.70.024003. arXiv: gr-qc/0402005.

[109] D. Blas, O. Pujolas, and S. Sibiryakov. "Consistent Extension of Horava Gravity". In: *Phys. Rev. Lett.* 104 (2010), p. 181302. DOI: 10.1103/PhysRevLett.104.181302. arXiv: 0909.3525 [hep-th].

[110] Diego Blas, Oriol Pujolas, and Sergey Sibiryakov. "Models of non-relativistic quantum gravity: The Good, the bad and the healthy". In: *JHEP* 04 (2011), p. 018. DOI: 10.1007/JHEP04(2011)018. arXiv: 1007.3503 [hep-th].

[111] Diego Blas, Mikhail M. Ivanov, and Sergey Sibiryakov. "Testing Lorentz invariance of dark matter". In: *JCAP* 10 (2012), p. 057. DOI: 10.1088/1475-7516/2012/10/057. arXiv: 1209.0464 [astro-ph.CO].

[112] Dario Bettoni, Adi Nusser, Diego Blas, and Sergey Sibiryakov. "Testing Lorentz invariance of dark matter with satellite galaxies". In: *JCAP* 05 (2017), p. 024. DOI: 10.1088/1475-7516/2017/05/024. arXiv: 1702.07726 [astro-ph.CO].

[113] J. W. Moffat. "Scalar-tensor-vector gravity theory". In: *JCAP* 03 (2006), p. 004. DOI: 10.1088/1475-7516/2006/03/004. arXiv: gr-qc/0506021.

[114] Jose María Ezquiaga and Miguel Zumalacárregui. "Dark Energy After GW170817: Dead Ends and the Road Ahead". In: *Phys. Rev. Lett.* 119.25 (2017), p. 251304. DOI: 10.1103/PhysRevLett.119.251304. arXiv: 1710.05901 [astro-ph.CO].

[115] N. Rosen. "A theory of gravitation". In: *Annals Phys.* 84 (1974), pp. 455–473. DOI: 10.1016/0003-4916(74)90311-X.

[116] A. I. Vainshtein. "To the problem of nonvanishing gravitation mass". In: *Phys. Lett. B* 39 (1972), pp. 393–394. DOI: 10.1016/0370-2693(72)90147-5.

[117] Eugeny Babichev and Cédric Deffayet. "An introduction to the Vainshtein mechanism". In: *Class. Quant. Grav.* 30 (2013), p. 184001. DOI: 10.1088/0264-9381/30/18/184001. arXiv: 1304.7240 [gr-qc].

[118] D. G. Boulware and Stanley Deser. "Can gravitation have a finite range?" In: *Phys. Rev. D* 6 (1972), pp. 3368–3382. DOI: 10.1103/PhysRevD.6.3368.

[119] Claudia de Rham, Gregory Gabadadze, and Andrew J. Tolley. "Resummation of Massive Gravity". In: *Phys. Rev. Lett.* 106 (2011), p. 231101. DOI: 10.1103/PhysRevLett.106.231101. arXiv: 1011.1232 [hep-th].

[120] Claudia de Rham and Gregory Gabadadze. "Generalization of the Fierz-Pauli Action". In: *Phys. Rev. D* 82 (2010), p. 044020. DOI: 10.1103/PhysRevD.82.044020. arXiv: 1007.0443 [hep-th].

[121] Antonio De Felice, François Larrouturou, Shinji Mukohyama, and Michele Oliosi. "Minimal Theory of Bigravity: construction and cosmology". In: *JCAP* 04 (2021), p. 015. DOI: 10.1088/1475-7516/2021/04/015. arXiv: 2012.01073 [gr-qc].

[122] Andrei O. Barvinsky, Diego Blas, Mario Herrero-Valea, Sergey M. Sibiryakov, and Christian F. Steinwachs. "Renormalization of Hořava gravity". In: *Phys. Rev. D* 93.6 (2016), p. 064022. DOI: 10.1103/PhysRevD.93.064022. arXiv: 1512.02250 [hep-th].

[123] Andrei O. Barvinsky, Diego Blas, Mario Herrero-Valea, Sergey M. Sibiryakov, and Christian F. Steinwachs. "Renormalization of gauge theories in the background-field approach". In: *JHEP* 07 (2018), p. 035. DOI: 10.1007/JHEP07(2018)035. arXiv: 1705.03480 [hep-th].

[124] Shinji Mukohyama. "Scale-invariant cosmological perturbations from Horava-Lifshitz gravity without inflation". In: *JCAP* 06 (2009), p. 001. DOI: 10.1088/1475-7516/2009/06/001. arXiv: 0904.2190 [hep-th].

[125] Sebastian F. Bramberger, Andrew Coates, João Magueijo, Shinji Mukohyama, Ryo Namba, and Yota Watanabe. "Solving the flatness problem with an anisotropic instanton in Hořava-Lifshitz gravity". In: *Phys. Rev. D* 97.4 (2018), p. 043512. DOI: 10.1103/PhysRevD.97.043512. arXiv: 1709.07084 [hep-th].

[126] Shinji Mukohyama. "Caustic avoidance in Horava-Lifshitz gravity". In: *JCAP* 09 (2009), p. 005. DOI: 10.1088/1475-7516/2009/09/005. arXiv: 0906.5069 [hep-th].

[127] Thomas P. Sotiriou, Matt Visser, and Silke Weinfurtner. "Phenomenologically viable Lorentz-violating quantum gravity". In: *Phys. Rev. Lett.* 102 (2009), p. 251601. DOI: 10.1103/PhysRevLett.102.251601. arXiv: 0904.4464 [hep-th].

[128] Thomas P. Sotiriou, Matt Visser, and Silke Weinfurtner. "Quantum gravity without Lorentz invariance". In: *JHEP* 10 (2009), p. 033. DOI: 10.1088/1126-6708/2009/10/033. arXiv: 0905.2798 [hep-th].

[129] Keisuke Izumi and Shinji Mukohyama. "Nonlinear superhorizon perturbations in Horava-Lifshitz gravity". In: *Phys. Rev. D* 84 (2011), p. 064025. DOI: 10.1103/PhysRevD.84.064025. arXiv: 1105.0246 [hep-th].

[130] A. Emir Gumrukcuoglu, Shinji Mukohyama, and Anzhong Wang. "General relativity limit of Horava-Lifshitz gravity with a scalar field in gradient expansion". In: *Phys. Rev. D* 85 (2012), p. 064042. DOI: 10.1103/PhysRevD.85.064042. arXiv: 1109.2609 [hep-th].

[131] B. P. Abbott et al. "Observation of Gravitational Waves from a Binary Black Hole Merger". In: *Phys. Rev. Lett.* 116.6 (2016), p. 061102. DOI: 10.1103/PhysRevLett.116.061102. arXiv: 1602.03837 [gr-qc].

[132] R. Abbott et al. "Observation of Gravitational Waves from Two Neutron Star–Black Hole Coalescences". In: *Astrophys. J. Lett.* 915.1 (2021), p. L5. DOI: 10.3847/2041-8213/ac082e. arXiv: 2106.15163 [astro-ph.HE].

[133] Angnis Schmidt-May and Mikael von Strauss. "Recent developments in bimetric theory". In: *J. Phys. A* 49.18 (2016), p. 183001. DOI: 10.1088/1751-8113/49/18/183001. arXiv: 1512.00021 [hep-th].

[134] Ratra, Bharat and Peebles, P. J. E. "Cosmological consequences of a rolling homogeneous scalar field". In: *Phys. Rev. D* 37 (12 June 1988), pp. 3406–3427. DOI: 10.1103/PhysRevD.37.3406. URL: https://link.aps.org/doi/10.1103/PhysRevD.37.3406.

[135] Nima Arkani-Hamed, Hsin-Chia Cheng, Markus A. Luty, and Shinji Mukohyama. "Ghost condensation and a consistent infrared modification of gravity". In: *JHEP* 05 (2004), p. 074. DOI: 10.1088/1126-6708/2004/05/074. arXiv: hep-th/0312099.

[136] Antonio De Felice, Mark Hindmarsh, and Mark Trodden. "Ghosts, Instabilities, and Superluminal Propagation in Modified Gravity Models". In: *JCAP* 08 (2006), p. 005. DOI: 10.1088/1475-7516/2006/08/005. arXiv: astro-ph/0604154.

[137] Lotte ter Haar, Miguel Bezares, Marco Crisostomi, Enrico Barausse, and Carlos Palenzuela. "Dynamics of Screening in Modified Gravity". In: *Phys. Rev. Lett.* 126 (2021), p. 091102. DOI: 10.1103/PhysRevLett.126.091102. arXiv: 2009.03354 [gr-qc].

[138] Katsuki Aoki, Antonio De Felice, Chunshan Lin, Shinji Mukohyama, and Michele Oliosi. "Phenomenology in type-I minimally modified gravity". In: *JCAP* 01 (2019), p. 017. DOI: 10.1088/1475-7516/2019/01/017. arXiv: 1810.01047 [gr-qc].

[139] Antonio De Felice, Andreas Doll, and Shinji Mukohyama. "A theory of type-II minimally modified gravity". In: *JCAP* 09 (2020), p. 034. DOI: 10.1088/1475-7516/2020/09/034. arXiv: 2004.12549 [gr-qc].

[140] Chunshan Lin and Shinji Mukohyama. "A Class of Minimally Modified Gravity Theories". In: *JCAP* 10 (2017), p. 033. DOI: 10.1088/1475-7516/2017/10/033. arXiv: 1708.03757 [gr-qc].

[141] Raúl Carballo-Rubio, Francesco Di Filippo, and Stefano Liberati. "Minimally modified theories of gravity: a playground for testing the uniqueness of general relativity". In: *JCAP* 06 (2018). [Erratum: JCAP 11, E02 (2018)], p. 026. DOI: 10.1088/1475-7516/2018/06/026. arXiv: 1802.02537 [gr-qc].

[142] Katsuki Aoki, Francesco Di Filippo, and Shinji Mukohyama. "Non-uniqueness of massless transverse-traceless graviton". In: *JCAP* 05 (2021), p. 071. DOI: 10.1088/1475-7516/2021/05/071. arXiv: 2103.15044 [gr-qc].

[143] Justin C. Feng and Sante Carloni. "New class of generalized coupling theories". In: *Phys. Rev. D* 101.6 (2020), p. 064002. DOI: 10.1103/PhysRevD.101.064002. arXiv: 1910.06978 [gr-qc].

[144] Niayesh Afshordi, Daniel J. H. Chung, and Ghazal Geshnizjani. "Cuscuton: A Causal Field Theory with an Infinite Speed of Sound". In: *Phys. Rev. D* 75 (2007), p. 083513. DOI: 10.1103/PhysRevD.75.083513. arXiv: hep-th/0609150.

[145] Antonio De Felice and Shinji Mukohyama. "Minimal theory of massive gravity". In: *Phys. Lett. B* 752 (2016), pp. 302–305. DOI: 10.1016/j.physletb.2015.11.050. arXiv: 1506.01594 [hep-th].

[146] Katsuki Aoki, Mohammad Ali Gorji, and Shinji Mukohyama. "A consistent theory of $D \to 4$ Einstein-Gauss-Bonnet gravity". In: *Phys. Lett. B* 810 (2020), p. 135843. DOI: 10.1016/j.physletb.2020.135843. arXiv: 2005.03859 [gr-qc].

[147] Zhi-Bang Yao, Michele Oliosi, Xian Gao, and Shinji Mukohyama. "Minimally modified gravity with an auxiliary constraint: A Hamiltonian construction". In: *Phys. Rev. D* 103.2 (2021), p. 024032. DOI: 10.1103/PhysRevD.103.024032. arXiv: 2011.00805 [gr-qc].

[148] Zhi-Bang Yao, Michele Oliosi, Xian Gao, and Shinji Mukohyama. "Minimally modified gravity with auxiliary constraints formalism". In: *Phys. Rev. D* 107.10 (2023), p. 104052. DOI: 10.1103/PhysRevD.107.104052. arXiv: 2302.02090 [gr-qc].

[149] Antonio De Felice, Shinji Mukohyama, and Masroor C. Pookkillath. "Addressing H_0 tension by means of VCDM". In: *Phys. Lett. B* 816 (2021). [Erratum: Phys.Lett.B 818, 136364 (2021)], p. 136201. DOI: 10.1016/j.physletb.2021.136201. arXiv: 2009.08718 [astro-ph.CO].

[150] Antonio De Felice and Shinji Mukohyama. "Weakening gravity for dark matter in a type-II minimally modified gravity". In: *JCAP* 04 (2021), p. 018. DOI: 10.1088/1475-7516/2021/04/018. arXiv: 2011.04188 [astro-ph.CO].

[151] Antonio De Felice, Andreas Doll, François Larrouturou, and Shinji Mukohyama. "Black holes in a type-II minimally modified gravity". In: *JCAP* 03 (2021), p. 004. DOI: 10.1088/1475-7516/2021/03/004. arXiv: 2010.13067 [gr-qc].

[152] Antonio De Felice, Shinji Mukohyama, and Masroor C. Pookkillath. "Static, spherically symmetric objects in type-II minimally modified gravity". In: *Phys. Rev. D* 105.10 (2022), p. 104013. DOI: 10.1103/PhysRevD.105.104013. arXiv: 2110.14496 [gr-qc].

[153] Antonio De Felice, Kei-ichi Maeda, Shinji Mukohyama, and Masroor C. Pookkillath. "Gravitational collapse and formation of a black hole in a type II minimally modified gravity theory". In: (Nov. 2022). arXiv: 2211.14760 [gr-qc].

[154] Antonio De Felice, Kei-ichi Maeda, Shinji Mukohyama, and Masroor C. Pookkillath. "Comparison of two theories of Type-IIa minimally modified gravity". In: *Phys. Rev. D* 106.2 (2022), p. 024028. DOI: 10.1103/PhysRevD.106.024028. arXiv: 2204.08294 [gr-qc].

[155] C. P. Burgess. *Introduction to Effective Field Theory: Thinking Effectively about Hierarchies of Scale*. Cambridge University Press, 2020. DOI: 10.1017/9781139048040.

[156] Giulia Gubitosi, Federico Piazza, and Filippo Vernizzi. "The Effective Field Theory of Dark Energy". In: *JCAP* 02 (2013), p. 032. DOI: 10.1088/1475-7516/2013/02/032. arXiv: 1210.0201 [hep-th].

[157] Claudia de Rham, Scott Melville, Andrew J. Tolley, and Shuang-Yong Zhou. "Positivity bounds for scalar field theories". In: *Phys. Rev. D* 96.8 (2017), p. 081702. DOI: 10.1103/PhysRevD.96.081702. arXiv: 1702.06134 [hep-th].

[158] Claudia de Rham, Laura Engelbrecht, Lavinia Heisenberg, and Alice Lüscher. "Positivity bounds in vector theories". In: *JHEP* 12 (2022), p. 086. DOI: 10.1007/JHEP12(2022)086. arXiv: 2208.12631 [hep-th].

[159] Bryce S. DeWitt. "Quantum Theory of Gravity. 1. The Canonical Theory". In: *Phys. Rev.* 160 (1967). Ed. by Li-Zhi Fang and R. Ruffini, pp. 1113–1148. DOI: 10.1103/PhysRev.160.1113.

[160] Jonathan J. Halliwell. "INTRODUCTORY LECTURES ON QUANTUM COSMOLOGY". In: *7th Jerusalem Winter School for Theoretical Physics: Quantum Cosmology and Baby Universes*. 1989. arXiv: 0909.2566 [gr-qc].

[161] David L. Wiltshire. "An Introduction to quantum cosmology". In: *8th Physics Summer School on Cosmology: The Physics of the Universe*. Jan. 1995, pp. 473–531. arXiv: gr-qc/0101003.

[162] J. B. Hartle and S. W. Hawking. "Wave Function of the Universe". In: *Phys. Rev. D* 28 (1983). Ed. by Li-Zhi Fang and R. Ruffini, pp. 2960–2975. DOI: 10.1103/PhysRevD.28.2960.

[163] A. Vilenkin. "Quantum Creation of Universes". In: *Phys. Rev. D* 30 (1984), pp. 509–511. DOI: 10.1103/PhysRevD.30.509.

[164] Job Feldbrugge, Jean-Luc Lehners, and Neil Turok. "No smooth beginning for spacetime". In: *Phys. Rev. Lett.* 119.17 (2017), p. 171301. DOI: 10.1103/PhysRevLett.119.171301. arXiv: 1705.00192 [hep-th].

[165] Job Feldbrugge, Jean-Luc Lehners, and Neil Turok. "No rescue for the no boundary proposal: Pointers to the future of quantum cosmology". In: *Phys. Rev. D* 97.2 (2018), p. 023509. DOI: 10.1103/PhysRevD.97.023509. arXiv: 1708.05104 [hep-th].

[166] U. H. Gerlach and U. K. Sengupta. "Homogeneous Collapsing Star: Tensor and Vector Harmonics for Matter and Field Asymmetries". In: *Phys. Rev. D* 18 (1978), pp. 1773–1784. DOI: 10.1103/PhysRevD.18.1773.

[167] Atsushi Higuchi. "Symmetric Tensor Spherical Harmonics on the N Sphere and Their Application to the De Sitter Group SO(N,1)". In: *J. Math. Phys.* 28 (1987). [Erratum: J.Math.Phys. 43, 6385 (2002)], p. 1553. DOI: 10.1063/1.527513.

[168] Roman Steigl and Franz Hinterleitner. "Factor ordering in standard quantum cosmology". In: *Class. Quant. Grav.* 23 (2006), pp. 3879–3894. DOI: 10.1088/0264-9381/23/11/013. arXiv: gr-qc/0511149.

[169] Hiroki Matsui, Shinji Mukohyama, and Atsushi Naruko. "DeWitt boundary condition is consistent in Hořava-Lifshitz quantum gravity". In: (Oct. 2021). arXiv: 2111.00665 [gr-qc].

[170] V. A. Rubakov. "Relaxation of the cosmological constant at inflation?" In: *Phys. Rev. D* 61 (2000), p. 061501. DOI: 10.1103/PhysRevD.61.061501. arXiv: hep-ph/9911305.

[171] Peter W. Graham, David E. Kaplan, and Surjeet Rajendran. "Relaxation of the Cosmological Constant". In: *Physical Review D* 100.1 (2019), p. 015048. DOI: 10.1103/PhysRevD.100.015048. arXiv: 1902.06793 [hep-ph].

[172] Nima Arkani-Hamed, Savas Dimopoulos, Nemanja Kaloper, and Raman Sundrum. "A Small cosmological constant from a large extra dimension". In: *Phys. Lett. B* 480 (2000), pp. 193–199. DOI: 10.1016/S0370-2693(00)00359-2. arXiv: hep-th/0001197.

[173] Oleg Evnin, Victor Massart, and Kévin Nguyen. "Robustness of the Cosmological Constant Damping Mechanism through Matter Eras". In: (Oct. 2020). arXiv: 2010.05927 [gr-qc].

[174] Ichiro Oda. "Scale Symmetry and Weinberg's No-go Theorem in the Cosmological Constant Problem". In: *Adv. Stud. Theor. Phys.* 13 (2019), pp. 195–214. DOI: 10.12988/astp.2019.9520. arXiv: 1812.09864 [hep-th].

[175] Sakine Nishi and Tsutomu Kobayashi. "Reheating and Primordial Gravitational Waves in Generalized Galilean Genesis". In: *JCAP* 04 (2016), p. 018. DOI: 10.1088/1475-7516/2016/04/018. arXiv: 1601.06561 [hep-th].

[176] Lasma Alberte, Paolo Creminelli, Andrei Khmelnitsky, David Pirtskhalava, and Enrico Trincherini. "Relaxing the Cosmological Constant: A Proof of Concept". In: *JHEP* 12 (2016), p. 022. DOI: 10.1007/JHEP12(2016)022. arXiv: 1608.05715 [hep-th].

[177] Antonio De Felice, Shinji Mukohyama, and Shinji Tsujikawa. "Density perturbations in general modified gravitational theories". In: *Phys. Rev. D* 82 (2010), p. 023524. DOI: 10.1103/PhysRevD.82.023524. arXiv: 1006.0281 [astro-ph.CO].

[178] Nima Arkani-Hamed, Paolo Creminelli, Shinji Mukohyama, and Matias Zaldarriaga. "Ghost inflation". In: *JCAP* 04 (2004), p. 001. DOI: 10.1088/1475-7516/2004/04/001. arXiv: hep-th/0312100.

[179] Tsutomu Kobayashi, Norihiro Tanahashi, and Masahide Yamaguchi. "Multifield extension of G inflation". In: *Phys. Rev. D* 88.8 (2013), p. 083504. DOI: 10.1103/PhysRevD.88.083504. arXiv: 1308.4798 [hep-th].

[180] Paolo Creminelli, Giovanni Tambalo, Filippo Vernizzi, and Vicharit Yingcharoenrat. "Dark-Energy Instabilities induced by Gravitational Waves". In: *JCAP* 05 (2020), p. 002. DOI: 10.1088/1475-7516/2020/05/002. arXiv: 1910.14035 [gr-qc].

[181] Tsutomu Kobayashi. "Generic instabilities of nonsingular cosmologies in Horndeski theory: A no-go theorem". In: *Phys. Rev. D* 94.4 (2016), p. 043511. DOI: 10.1103/PhysRevD.94.043511. arXiv: 1606.05831 [hep-th].

[182] M. Libanov, S. Mironov, and V. Rubakov. "Generalized Galileons: instabilities of bouncing and Genesis cosmologies and modified Genesis". In: *JCAP* 08 (2016), p. 037. DOI: 10.1088/1475-7516/2016/08/037. arXiv: 1605.05992 [hep-th].

[183] Shinji Mukohyama and Karim Noui. "Minimally Modified Gravity: a Hamiltonian Construction". In: *JCAP* 07 (2019), p. 049. DOI: 10.1088/1475-7516/2019/07/049. arXiv: 1905.02000 [gr-qc].

[184] Eric Poisson. *A Relativist's Toolkit: The Mathematics of Black-Hole Mechanics*. Cambridge University Press, Dec. 2009. DOI: 10.1017/CBO9780511606601.

[185] Bertil Gustafsson, Heinz-Otto Kreiss, and Joseph Oliger. *Stability and Convergence for Difference Methods*. John Wiley & Sons, Ltd, 2013. ISBN: 9781118548448. DOI: DOI:10.1002/9781118548448. eprint: https://onlinelibrary.wiley.com/doi/pdf/10.1002/9781118548448. URL: https://onlinelibrary.wiley.com/doi/abs/10.1002/9781118548448.

[186] Emanuele Berti, Vitor Cardoso, Mark Ho-Yeuk Cheung, Francesco Di Filippo, Francisco Duque, Paul Martens, and Shinji Mukohyama. "Stability of the fundamental quasinormal mode in time-domain observations against small perturbations". In: *Phys. Rev. D* 106.8 (2022), p. 084011. DOI: 10.1103/PhysRevD.106.084011. arXiv: 2205.08547 [gr-qc].

[187] Arvind Borde and Alexander Vilenkin. "Singularities in inflationary cosmology: A Review". In: *Int. J. Mod. Phys. D* 5 (1996). Ed. by V. A. Berezin, V. A. Rubakov, and D. V. Semikoz, pp. 813–824. DOI: 10.1142/S0218271896000497. arXiv: gr-qc/9612036.

[188] Arvind Borde and Alexander Vilenkin. "Eternal inflation and the initial singularity". In: *Phys. Rev. Lett.* 72 (1994), pp. 3305–3309. DOI: 10.1103/PhysRevLett.72.3305. arXiv: gr-qc/9312022.

[189] D. Battefeld and Patrick Peter. "A Critical Review of Classical Bouncing Cosmologies". In: *Phys. Rept.* 571 (2015), pp. 1–66. DOI: 10.1016/j.physrep.2014.12.004. arXiv: 1406.2790 [astro-ph.CO].

[190] Yi-Fu Cai. "Exploring Bouncing Cosmologies with Cosmological Surveys". In: *Sci. China Phys. Mech. Astron.* 57 (2014), pp. 1414–1430. DOI: 10.1007/s11433-014-5512-3. arXiv: 1405.1369 [hep-th].

[191] Anna Ijjas and Paul J. Steinhardt. "Bouncing Cosmology made simple". In: *Class. Quant. Grav.* 35.13 (2018), p. 135004. DOI: 10.1088/1361-6382/aac482. arXiv: 1803.01961 [astro-ph.CO].

[192] Yi-Fu Cai, Shih-Hung Chen, James B. Dent, Sourish Dutta, and Emmanuel N. Saridakis. "Matter Bounce Cosmology with the f(T) Gravity". In: *Class. Quant. Grav.* 28 (2011), p. 215011. DOI: 10.1088/0264-9381/28/21/215011. arXiv: 1104.4349 [astro-ph.CO].

[193] Mian Zhu, Amara Ilyas, Yunlong Zheng, Yi-Fu Cai, and Emmanuel N. Saridakis. "Scalar and tensor perturbations in DHOST bounce cosmology". In: *JCAP* 11.11 (2021), p. 045. DOI: 10.1088/1475-7516/2021/11/045. arXiv: 2108.01339 [gr-qc].

[194] Amara Ilyas, Mian Zhu, Yunlong Zheng, Yi-Fu Cai, and Emmanuel N. Saridakis. "DHOST Bounce". In: *JCAP* 09 (2020), p. 002. DOI: 10.1088/1475-7516/2020/09/002. arXiv: 2002.08269 [gr-qc].

[195] Robert Brandenberger. "Matter Bounce in Horava-Lifshitz Cosmology". In: *Phys. Rev. D* 80 (2009), p. 043516. DOI: 10.1103/PhysRevD.80.043516. arXiv: 0904.2835 [hep-th].

[196] Yi-Fu Cai, Robert Brandenberger, and Xinmin Zhang. "The Matter Bounce Curvaton Scenario". In: *JCAP* 03 (2011), p. 003. DOI: 10.1088/1475-7516/2011/03/003. arXiv: 1101.0822 [hep-th].

[197] Supranta S. Boruah, Hyung J. Kim, Michael Rouben, and Ghazal Geshnizjani. "Cuscuton bounce". In: *JCAP* 08 (2018), p. 031. DOI: 10.1088/1475-7516/2018/08/031. arXiv: 1802.06818 [gr-qc].

[198] J. Leo Kim and Ghazal Geshnizjani. "Spectrum of Cuscuton Bounce". In: *JCAP* 03 (2021), p. 104. DOI: 10.1088/1475-7516/2021/03/104. arXiv: 2010.06645 [gr-qc].

[199] Alexander Vikman. "Can dark energy evolve to the phantom?" In: *Phys. Rev. D* 71 (2005), p. 023515. DOI: 10.1103/PhysRevD.71.023515. arXiv: astro-ph/0407107.

[200] Damien A. Easson, Ignacy Sawicki, and Alexander Vikman. "G-Bounce". In: *JCAP* 11 (2011), p. 021. DOI: 10.1088/1475-7516/2011/11/021. arXiv: 1109.1047 [hep-th].

[201] Yi-Fu Cai, Damien A. Easson, and Robert Brandenberger. "Towards a Nonsingular Bouncing Cosmology". In: *JCAP* 08 (2012), p. 020. DOI: 10.1088/1475-7516/2012/08/020. arXiv: 1206.2382 [hep-th].

[202] Anna Ijjas and Paul J. Steinhardt. "Classically stable nonsingular cosmological bounces". In: *Phys. Rev. Lett.* 117.12 (2016), p. 121304. DOI: 10.1103/PhysRevLett.117.121304. arXiv: 1606.08880 [gr-qc].

[203] David A. Dobre, Andrei V. Frolov, José T. Gálvez Ghersi, Sabir Ramazanov, and Alexander Vikman. "Unbraiding the Bounce: Superluminality around the Corner". In: *JCAP* 03 (2018), p. 020. DOI: 10.1088/1475-7516/2018/03/020. arXiv: 1712.10272 [gr-qc].

[204] Paolo Creminelli, Markus A. Luty, Alberto Nicolis, and Leonardo Senatore. "Starting the Universe: Stable Violation of the Null Energy Condition and Non-standard Cosmologies". In: *JHEP* 12 (2006), p. 080. DOI: 10.1088/1126-6708/2006/12/080. arXiv: hep-th/0606090.

[205] Chunshan Lin, Robert H. Brandenberger, and Laurence Perreault Levasseur. "A Matter Bounce By Means of Ghost Condensation". In: *JCAP* 04 (2011), p. 019. DOI: 10.1088/1475-7516/2011/04/019. arXiv: 1007.2654 [hep-th].

[206] Yong Cai and Yun-Song Piao. "A covariant Lagrangian for stable nonsingular bounce". In: *JHEP* 09 (2017), p. 027. DOI: 10.1007/JHEP09(2017)027. arXiv: 1705.03401 [gr-qc].

[207] R. Kolevatov, S. Mironov, N. Sukhov, and V. Volkova. "Cosmological bounce and Genesis beyond Horndeski". In: *JCAP* 08 (2017), p. 038. DOI: 10.1088/1475-7516/2017/08/038. arXiv: 1705.06626 [hep-th].

[208] Yong Cai, Youping Wan, Hai-Guang Li, Taotao Qiu, and Yun-Song Piao. "The Effective Field Theory of nonsingular cosmology". In: *JHEP* 01 (2017), p. 090. DOI: 10.1007/JHEP01(2017)090. arXiv: 1610.03400 [gr-qc].

[209] Yong Cai, Hai-Guang Li, Taotao Qiu, and Yun-Song Piao. "The Effective Field Theory of nonsingular cosmology: II". In: *Eur. Phys. J. C* 77.6 (2017), p. 369. DOI: 10.1140/epjc/s10052-017-4938-y. arXiv: 1701.04330 [gr-qc].

[210] V.A. Belinskii, I.M. Khalatnikov, and E.M. Lifshitz. "41 - Oscillatory approach to a singular point in relativistic cosmology Reprinted with permission from Advances in Physics 19, Part 80, 525, 1970." In: *Perspectives in Theoretical Physics*. Ed. by L.P. Pitaevski. Amsterdam: Pergamon, 1992, pp. 609–658. ISBN: 978-0-08-036364-6. DOI: https://doi.org/10.1016/B978-0-08-036364-6.50046-6. URL: https://www.sciencedirect.com/science/article/pii/B9780080363646500466.

[211] P. A. R. Ade et al. "Improved Constraints on Primordial Gravitational Waves using Planck, WMAP, and BICEP/Keck Observations through the 2018 Observing Season". In: *Phys. Rev. Lett.* 127.15 (2021), p. 151301. DOI: 10.1103/PhysRevLett.127.151301. arXiv: 2110.00483 [astro-ph.CO].

[212] David Wands. "Duality invariance of cosmological perturbation spectra". In: *Phys. Rev. D* 60 (1999), p. 023507. DOI: 10.1103/PhysRevD.60.023507. arXiv: gr-qc/9809062.

[213] Fabio Finelli and Robert Brandenberger. "On the generation of a scale invariant spectrum of adiabatic fluctuations in cosmological models with a contracting phase". In: *Phys. Rev. D* 65 (2002), p. 103522. DOI: 10.1103/PhysRevD.65.103522. arXiv: hep-th/0112249.

[214] Jerome Quintin, Zeinab Sherkatghanad, Yi-Fu Cai, and Robert H. Brandenberger. "Evolution of cosmological perturbations and the production of non-Gaussianities through a nonsingular bounce: Indications for a no-go theorem in single field matter bounce cosmologies". In: *Phys. Rev. D* 92.6 (2015), p. 063532. DOI: 10.1103/PhysRevD.92.063532. arXiv: 1508.04141 [hep-th].

[215] Yu-Bin Li, Jerome Quintin, Dong-Gang Wang, and Yi-Fu Cai. "Matter bounce cosmology with a generalized single field: non-Gaussianity and an extended no-go theorem". In: *JCAP* 03 (2017), p. 031. DOI: 10.1088/1475-7516/2017/03/031. arXiv: 1612.02036 [hep-th].

[216] Shingo Akama, Shin'ichi Hirano, and Tsutomu Kobayashi. "Primordial non-Gaussianities of scalar and tensor perturbations in general bounce cosmology: Evading the no-go theorem". In: *Phys. Rev. D* 101.4 (2020), p. 043529. DOI: 10.1103/PhysRevD.101.043529. arXiv: 1908.10663 [gr-qc].

[217] L. D. Faddeev and R. Jackiw. "Hamiltonian Reduction of Unconstrained and Constrained Systems". In: *Phys. Rev. Lett.* 60 (1988), pp. 1692–1694. DOI: 10.1103/PhysRevLett.60.1692.

[218] Clifford Cheung, Paolo Creminelli, A. Liam Fitzpatrick, Jared Kaplan, and Leonardo Senatore. "The Effective Field Theory of Inflation". In: *JHEP* 03 (2008), p. 014. DOI: 10.1088/1126-6708/2008/03/014. arXiv: 0709.0293 [hep-th].

[219] Nicola Bartolo, Alexander Ganz, and Sabino Matarrese. "Cuscuton inflation". In: *JCAP* 05.05 (2022), p. 008. DOI: 10.1088/1475-7516/2022/05/008. arXiv: 2111.06794 [gr-qc].

[220] Yi-Fu Cai, Wei Xue, Robert Brandenberger, and Xinmin Zhang. "Non-Gaussianity in a Matter Bounce". In: *JCAP* 05 (2009), p. 011. DOI: 10.1088/1475-7516/2009/05/011. arXiv: 0903.0631 [astro-ph.CO].

[221] Paolo Creminelli, Alberto Nicolis, and Enrico Trincherini. "Galilean Genesis: An Alternative to Inflation". In: *JCAP* 11 (2010), p. 021. DOI: 10.1088/1475-7516/2010/11/021. arXiv: 1007.0027 [hep-th].

[222] Orfeu Bertolami and Carlos A. D. Zarro. "Hořava-Lifshitz Quantum Cosmology". In: *Phys. Rev. D* 84 (2011), p. 044042. DOI: 10.1103/PhysRevD.84.044042. arXiv: 1106.0126 [hep-th].

[223] Amna Ali, Sourish Dutta, Emmanuel N. Saridakis, and Anjan A. Sen. "Horava-Lifshitz cosmology with generalized Chaplygin gas". In: *Gen. Rel. Grav.* 44 (2012), pp. 657–683. DOI: 10.1007/s10714-011-1298-z. arXiv: 1004.2474 [astro-ph.CO].

[224] B. Vakili and V. Kord. "Classical and quantum Hořava-Lifshitz cosmology in a minisuperspace perspective". In: *Gen. Rel. Grav.* 45 (2013), pp. 1313–1331. DOI: 10.1007/s10714-013-1527-8. arXiv: 1301.0809 [gr-qc].